

**Characterisation of the Raf protein kinases  
by gene targeting**

Thesis submitted for the degree of  
Doctor of Philosophy  
at the University of Leicester

by

Jahan Nurany Hussain (B.Sc. Hons. Liverpool)  
Department of Biochemistry  
University of Leicester

November 2005

UMI Number: U212829

All rights reserved

INFORMATION TO ALL USERS

The quality of this reproduction is dependent upon the quality of the copy submitted.

In the unlikely event that the author did not send a complete manuscript and there are missing pages, these will be noted. Also, if material had to be removed, a note will indicate the deletion.



UMI U212829

Published by ProQuest LLC 2013. Copyright in the Dissertation held by the Author.  
Microform Edition © ProQuest LLC.

All rights reserved. This work is protected against  
unauthorized copying under Title 17, United States Code.



ProQuest LLC  
789 East Eisenhower Parkway  
P.O. Box 1346  
Ann Arbor, MI 48106-1346

## ABSTRACT

### Characterisation of Raf protein kinases by gene targeting

Jahan Hussain

Transfection of constructs expressing various human mutants of C-RAF into *C-raf*<sup>-/-</sup> MEFs confirmed the MEK kinase activity of C-Raf is not required for its role in cell survival and suggested this role is also independent of C-Raf kinase activity, but Ras-dependent.

The role of B-Raf in cell growth and survival was investigated using primary MEFs lacking B-Raf. Cell growth and proliferation were found to be reduced and this coincided with alterations in the expression levels of various proteins involved in the G1 to S phase of the cell cycle. Analysis of *B-raf*<sup>-/-</sup> cells upon serum withdrawal-induced apoptosis showed this was associated with decreased phosphorylation levels of phospho-T125-caspase 9.

A *B-raf* allele containing a conditional kinase inactivating D594A mutation was generated. This was produced by designing a vector containing loxP sites flanking exons 15-18 of *B-raf* upstream of a second *B-raf* exon 15 containing the mutation. Upon gene targeting homologous recombination was successfully achieved for three ES clones and these were used to generate chimeric mice. Two of these targeted ES clones led to successful germline transmission. Mice carrying the mutation were mated with Cre-expressing mice, allowing the generation of mice heterozygous for the D594A mutation, *B-raf*<sup>+/*Lox*-D594A</sup>. These mice were shown to have neoplasia due to splenomegaly and this was attributed to the elevated phospho-ERK levels observed.

Intercrossing of *B-raf*<sup>+/*Lox*-D594A</sup> mice did not generate any viable *B-raf*<sup>*Lox*-D594A/*Lox*-D594A</sup> mice, suggesting the D594A mutation was embryonic lethal. Analysis of *B-raf*<sup>*Lox*-D594A/*Lox*-D594A</sup> primary MEFs showed their phenotype differed from *B-raf*<sup>-/-</sup> cells. In *B-raf*<sup>*Lox*-D594A/*Lox*-D594A</sup> MEFs, phospho-MEK and phospho-ERK levels were significantly elevated. This was attributed to increased C-Raf kinase activity observed within these cells. Further analysis indicated increased survival and increased cell growth and proliferation in these cells, suggesting the mutation was acting as an oncogene as observed for some B-Raf D594 mutations in human cancers.

# CONTENTS

<b>Title page</b>	<b>i</b>
<b>Abstract</b>	<b>ii</b>
<b>Contents</b>	<b>iii</b>
<b>Abbreviations</b>	<b>xii</b>
<b>Acknowledgements</b>	<b>xvii</b>

---

<b>1. INTRODUCTION .....</b>	<b>1</b>
<b>1.1 Cell signalling.....</b>	<b>1</b>
<i>1.1.1 Mitogen-activated protein kinase (MAPK) cascades .....</i>	<i>1</i>
<i>1.1.2 The various mammalian MAPK pathways .....</i>	<i>1</i>
<b>1.2 The Raf protein kinases .....</b>	<b>5</b>
<i>1.2.1 Discovery of the Raf proteins .....</i>	<i>5</i>
<i>1.2.2 raf homologues in other organisms .....</i>	<i>5</i>
<i>1.2.3 Expression of the three raf isoforms in mammals .....</i>	<i>6</i>
<i>1.2.4 Structural comparisons of the three Raf isoforms .....</i>	<i>6</i>
<i>1.2.5 Crystal structure of B-Raf.....</i>	<i>7</i>
<i>1.2.6 Differential splicing of B-Raf .....</i>	<i>9</i>
<b>1.3 Activation of the Raf protein kinases.....</b>	<b>11</b>
<i>1.3.1 Signalling through receptor tyrosine kinases .....</i>	<i>11</i>
<i>1.3.2 Ras family of proteins .....</i>	<i>13</i>
<i>1.3.3 Downstream of Ras .....</i>	<i>14</i>
<i>1.3.4 Interaction of Ras with Raf.....</i>	<i>14</i>
<i>1.3.5 Ras is required to recruit C-Raf to the plasma membrane .....</i>	<i>15</i>
<i>1.3.6 Interaction of Raf with other Ras family members .....</i>	<i>16</i>
<b>1.4 Phosphorylation events of C-Raf.....</b>	<b>16</b>
<i>1.4.1 Phosphorylation of tyrosine 341 .....</i>	<i>17</i>
<i>1.4.2 Phosphorylation of Serine 338 .....</i>	<i>18</i>
<i>1.4.3 Negative regulation by phosphorylation of residues 43, 259 and 621 .....</i>	<i>20</i>
<i>1.4.4 C-Raf regulation by feedback phosphorylation of numerous serine residues .....</i>	<i>22</i>

---

1.4.5 Other potential phosphorylation sites of C-Raf.....	23
1.4.6 B-Raf specific phosphorylation sites .....	23
1.4.7 Autoregulation of the Raf protein kinases .....	24
<b>1.5 Chaperones .....</b>	<b>25</b>
1.5.1 14-3-3.....	25
1.5.2 Hsp90 and p50.....	28
1.5.3 Sur-8 .....	29
1.5.4 KSR .....	29
1.5.5 RKIP .....	30
<b>1.6 Downstream of the Raf protein kinases.....</b>	<b>30</b>
1.6.1 MEKs and ERKs .....	30
1.6.2 Other Raf protein binding partners .....	32
1.6.3 Downstream of ERKs.....	32
1.6.4 Cytoplasmic substrates of ERKs.....	33
1.6.5 Nuclear substrates of ERKs.....	35
<b>1.7 Proliferation .....</b>	<b>36</b>
1.7.1 The Raf/MEK/ERK cascade and proliferation .....	38
1.7.2 Raf protein kinases and proliferation.....	39
<b>1.8 Apoptosis .....</b>	<b>41</b>
1.8.1 Death receptor-mediated apoptosis pathway .....	42
1.8.2 Mitochondria-mediated apoptosis pathway .....	43
1.8.3 Linkage of the death receptor & mitochondria mediated apoptosis pathways .....	43
1.8.4 The Bcl-2 family of proteins .....	45
1.8.5 ERK-dependent role for Raf proteins in apoptosis suppression.....	45
1.8.6 Bim.....	46
1.8.7 p90 <sup>RSK</sup> .....	47
1.8.8 Caspase 9.....	47
1.8.9 ERK-independent roles for Raf proteins in apoptosis suppression.....	48
1.8.10 Bcl-2 family members .....	48
1.8.11 Bag-1 .....	49

---

1.8.12 <i>NF-<math>\kappa</math>B</i> .....	49
1.8.13 <i>ASK1</i> .....	51
1.8.14 <i>PI3-K/Akt and cell survival</i> .....	53
<b>1.9 Cellular Transformation</b> .....	<b>54</b>
1.9.1 <i>Mutations of B-RAF in human cancers</i> .....	55
1.9.2 <i>Relating structure to B-RAF mutations in human cancer</i> .....	57
1.9.3 <i>The role of V600 mutated B-RAF in human cancer</i> .....	59
<b>1.10 Manipulating the mouse genome</b> .....	<b>60</b>
1.10.1 <i>Embryonic stem cells</i> .....	60
1.10.2 <i>Gene targeting in ES cells</i> .....	61
1.10.3 <i>Generation of transgenic mice</i> .....	63
<b>1.11 Ras/Raf/MEK/ERK knockouts/knockins in mice</b> .....	<b>64</b>
1.11.1 <i>Ras knockout and knockin mice</i> .....	64
1.11.2 <i>Raf knockout and knockin mice</i> .....	67
1.11.3 <i>MEK knockout mice</i> .....	69
1.11.4 <i>ERK knockout mice</i> .....	70
<b>1.12 Aims</b> .....	<b>70</b>
<b>2. MATERIALS AND METHODS</b> .....	<b>71</b>
<b>2.1. Molecular Biology</b> .....	<b>71</b>
2.1.1 <i>Plasmids</i> .....	71
2.1.2 <i>Ethanol Precipitation</i> .....	73
2.1.3 <i>Agarose gel electrophoresis</i> .....	73
2.1.4 <i>Production of competent DH5<math>\alpha</math></i> .....	73
2.1.5 <i>Transformation of competent DH5<math>\alpha</math></i> .....	74
2.1.6 <i>Minipreparation of plasmid DNA from bacteria</i> .....	74
2.1.7 <i>Midipreparation of plasmid DNA from bacteria</i> .....	74
2.1.8 <i>Caesium chloride preparation of plasmid DNA from bacteria</i> .....	75
2.1.9 <i>Restriction digest of plasmid DNA</i> .....	75
2.1.10 <i>Removal of 5' phosphate groups from linearised DNA</i> .....	75
2.1.11 <i>Purification of gel fragments</i> .....	76
2.1.12 <i>Ligation of DNA fragments</i> .....	76
2.1.13 <i>Primer synthesis and DNA sequencing</i> .....	76

---

2.1.14 Lysis of cells to extract genomic DNA .....	76
2.1.15 Lysis of cells to extract RNA .....	76
2.1.16 Synthesis of cDNA from total RNA .....	77
2.1.17 Lysis of mouse tail samples .....	77
2.1.18 Lysis of mouse tail samples for long range Polymerase Chain Reaction ...	77
2.1.19 Polymerase Chain Reaction .....	77
2.1.20 B-raf long range PCR.....	78
2.1.21 Southern blot analysis .....	79
2.1.22 Probe radio-labelling and hybridisation .....	79
<b>2.2. Cell culture .....</b>	<b>80</b>
2.2.1 Production of primary mouse embryonic fibroblasts (MEFs) from E12.5 mouse embryos .....	80
2.2.2 Maintenance of MEFs .....	80
2.2.3 Freezing down stocks of cell lines .....	81
2.2.4 Transfection of tsSV40T transfected MEFs with lipofectamine™.....	81
2.2.5 Selection of resistant MEF clones .....	81
2.2.6 Transfection of MEFs via Nucleofector™ technology.....	82
2.2.7 Mitomycin C treatment of primary MEFs .....	82
2.2.8 Maintenance of embryonic stem (ES) cells.....	82
2.2.9 Electroporation of ES cells.....	83
2.2.10 Selection of resistant ES cell .....	84
2.2.11 Freezing down and seeding for DNA analysis of ES cell/MEF clones .....	84
2.2.12 Generation of transgenic mice .....	84
2.2.13 Cre transfection of ES cells .....	85
<b>2.3. MEF analysis.....</b>	<b>85</b>
2.3.1 Annexin V FITC staining of cells.....	85
2.3.2 Cell growth curves .....	86
2.3.3 DNA staining .....	86
2.3.4 Immunofluorescence of cells .....	86
2.3.5 5-Bromo-2'-deoxy-uridine (BrdU) cell analysis.....	87
<b>2.4. Protein analysis .....</b>	<b>87</b>
2.4.1 Production of cell lysates cells for protein analysis.....	87

2.4.2 Stimulation of cells and production of clear cell lysates for protein analysis .....	88
2.4.3 Stimulation of cells and production of clear cell lysates for protein analysis .....	89
2.4.4 Bicinchoninic acid (BCA) protein analysis .....	89
2.4.5 Immunoprecipitation assay.....	89
2.4.6 Sodium dodecyl sulfate polyacrylamide gel electrophoresis (SDS-PAGE)...	89
2.4.7 Western blot analysis.....	90
<b>2.5. Statistical analysis.....</b>	<b>92</b>

### **3. CHARACTERISATION OF THE ROLE OF C-Raf IN CELL SURVIVAL USING *C-raf*<sup>-/-</sup> MOUSE EMBRYONIC**

<b>FIBROBLASTS.....</b>	<b>93</b>
<b>3.1 Introduction .....</b>	<b>93</b>
3.1.1 Investigation of the role of C-Raf in apoptosis .....	93
<b>3.2 Aims .....</b>	<b>98</b>
<b>3.3 Results.....</b>	<b>98</b>
3.3.1 Reproduction of the apoptotic phenotype of tsSV40T transformed <i>C-raf</i> <sup>+/+</sup> and <i>C-raf</i> <sup>-/-</sup> MEFs .....	98
3.3.2 Transfection of tsSV40T transformed <i>C-raf</i> <sup>-/-</sup> MEFs with expression vectors containing various human C-RAF cDNAs .....	104
3.3.3 Characterisation of the apoptotic phenotype of tsSV40T transformed <i>C-raf</i> <sup>-/-</sup> MEFs transfected with various human C-RAF cDNAs .....	110
3.3.4 Transient transfection of tsSV40T transformed <i>C-raf</i> <sup>-/-</sup> MEFs with expression vectors containing various human C-RAF cDNAs .....	119
3.3.5 Characterisation of the apoptotic phenotype of <i>C-raf</i> <sup>-/-</sup> immortalised MEFs transiently transfected with various human C-RAF cDNAs upon $\alpha$ -CD95 antibody induction .....	120
3.3.6 Analysis of p38-MAPK phosphorylation upon $\alpha$ -CD95 induced apoptosis of <i>C-Raf</i> primary MEFs .....	122
<b>3.4 Conclusions.....</b>	<b>122</b>

<b>4. CHARACTERISATION OF GROWTH, PROLIFERATION AND APOPTOSIS IN <i>B-raf</i><sup>-/-</sup> MEFs</b> .....	<b>129</b>
<b>4.1 Introduction</b> .....	<b>129</b>
4.1.1 <i>B-Raf knock out studies</i> .....	129
4.1.2 <i>Role of B-Raf in proliferation</i> .....	130
4.1.3 <i>Role of B-Raf in the suppression of apoptosis</i> .....	131
<b>4.2 Aims</b> .....	<b>132</b>
<b>4.3 Results</b> .....	<b>133</b>
4.3.1 <i>Derivation of <i>B-raf</i><sup>-/-</sup> primary MEFs</i> .....	133
4.3.2 <i>Analysis of ERK phosphorylation in <i>B-raf</i><sup>-/-</sup> primary MEFs</i> .....	133
4.3.3 <i>Analysis of the growth characteristics of <i>B-raf</i> primary MEFs</i> .....	136
4.3.4 <i>Analysis of proliferation of <i>B-raf</i> primary MEFs</i> .....	139
4.3.5 <i>Analysis of proteins involved in the G1 to S phase of the cell cycle in <i>B-raf</i> primary MEFs</i> .....	141
4.3.6 <i>Analysis of the apoptotic phenotype of <i>B-raf</i><sup>-/-</sup> and <i>B-raf</i><sup>+/+</sup> MEFs upon <math>\alpha</math>-CD95 antibody induction</i> .....	142
4.3.7 <i>Analysis of the apoptotic phenotype of <i>B-raf</i><sup>-/-</sup> and <i>B-raf</i><sup>+/+</sup> MEFs upon serum withdrawal</i> .....	146
4.3.8 <i>Analysis of MEK and ERK phosphorylation upon induction of apoptosis in <i>B-raf</i> primary MEFs</i> .....	146
4.3.9 <i>Analysis of Bim expression levels upon serum withdrawal induced apoptosis of <i>B-raf</i> primary MEFs</i> .....	148
4.3.10 <i>Analysis of phospho-Akt levels upon serum withdrawal induced apoptosis of <i>B-raf</i> primary MEFs</i> .....	150
4.3.11 <i>Analysis of phospho-p90<sup>RSK</sup> levels upon serum withdrawal induced apoptosis of <i>B-raf</i> primary MEFs</i> .....	152
4.3.12 <i>Analysis of T125-phospho-specific caspase 9 levels upon serum withdrawal induced apoptosis of <i>B-raf</i> primary MEFs</i> .....	152
<b>4.4 Conclusions</b> .....	<b>154</b>
<b>5. GENERATION OF A CONDITIONAL B-RAF KINASE INACTIVE MOUSE</b> .....	<b>160</b>

<b>5.1 Introduction .....</b>	<b>160</b>
5.1.1 <i>The kinase domain of B-Raf</i> .....	160
5.1.2 <i>Cre/loxP technology</i> .....	161
5.1.3 <i>Reported uses of the Cre/loxP recombination system</i> .....	162
<b>5.2 Aims .....</b>	<b>164</b>
<b>5.3 Results.....</b>	<b>165</b>
5.3.1 <i>Construction of the right arm of the targeting vector</i> .....	165
5.3.2 <i>Generation of the final targeting vector</i> .....	167
5.3.3 <i>Electroporation of B-raf<sup>LSL-D594A</sup> targeting construct into ES cells</i> .....	167
5.3.4 <i>Detection of homologous recombination with B-raf<sup>LSL-D594A</sup> by PCR</i> .....	172
5.3.5 <i>Confirmation of homologous recombination with B-raf<sup>LSL-D594A</sup> targeting vector by Southern blot analysis</i> .....	172
5.3.6 <i>Further analysis of B-raf<sup>LSL-D594A</sup> targeted ES cell clones 71, 111, 166, 184 and 214</i> .....	175
5.3.7 <i>Generation of mice from B-Raf<sup>LSL-D594A</sup> targeted ES cell clones</i> .....	181
5.3.8 <i>Screening of mice for the presence of the targeting event</i> .....	181
5.3.9 <i>Maintenance of a mouse colony expressing the B-raf targeted event</i> .....	183
5.3.10 <i>Intercrossing of mice with the B-Raf<sup>LSL-D594A</sup> allele</i> .....	183
5.3.11 <i>Generation of embryos homozygous for the B-raf<sup>LSL-D594A</sup> targeted event</i> ..	187
5.3.12 <i>In vitro Cre-mediated deletion of the B-raf<sup>LSL-D594A</sup> allele</i> .....	188
<b>5.4 Conclusions.....</b>	<b>192</b>
<b>6. CHARACTERISATION OF B-raf KINASE INACTIVE MICE AND MEFs .....</b>	<b>195</b>
<b>6.1 Introduction .....</b>	<b>195</b>
6.1.1 <i>B-Raf kinase activity</i> .....	195
<b>6.2 Aims .....</b>	<b>196</b>
<b>6.3 Results.....</b>	<b>197</b>
6.3.1 <i>Generation of B-raf<sup>+ /Lox-D594A</sup> mice</i> .....	197
6.3.2 <i>Preliminary evaluation of B-raf<sup>+ /LSL-D594A</sup> + Cre mice</i> .....	197
6.3.3 <i>Intercrosses of B-raf<sup>+ /Lox-D594A</sup> mice</i> .....	203
6.3.4 <i>Phenotype of B-raf<sup>Lox-D594A /Lox-D594A</sup> embryos</i> .....	203
6.3.5 <i>Derivation of B-raf<sup>Lox-D594A /Lox-D594A</sup> primary MEFs</i> .....	205

6.3.6 Analysis of Raf protein expression levels in <i>B-Raf</i> <sup>Lox-D594A/Lox-D594A</sup> primary MEFs .....	205
6.3.7 Analysis of MEK and ERK phosphorylation in <i>B-Raf</i> <sup>Lox-D594A/Lox-D594A</sup> primary MEFs.....	205
6.3.8 Analysis of <i>B-raf</i> <sup>+/Lox-D594A</sup> primary MEFs .....	208
6.3.9 Analysis of the growth characteristics of <i>B-raf</i> <sup>Lox-D594A/Lox-D594A</sup> primary MEFs .....	209
6.3.10 Analysis of ERK phosphorylation upon serum stimulation for 20 hours in <i>B-Raf</i> <sup>Lox-D594A/Lox-D594A</sup> primary MEFs.....	209
6.3.11 Analysis of proteins involved in the G1 to S phase of the cell cycle in <i>B-Raf</i> <sup>Lox-D594A/Lox-D594A</sup> primary MEFs .....	212
6.3.12 Analysis of the apoptotic phenotype of <i>B-raf</i> <sup>Lox-D594A/Lox-D594A</sup> primary MEFs upon $\alpha$ -CD95 induction.....	214
6.3.13 Analysis of the apoptotic phenotype of <i>B-raf</i> <sup>Lox-D594A/Lox-D594A</sup> and <i>B-raf</i> <sup>+/+</sup> primary MEFs upon serum withdrawal.....	214
6.3.14 Analysis of MEK and ERK phosphorylation of <i>B-raf</i> <sup>Lox-D594A/Lox-D594A</sup> primary MEFs upon induction of apoptosis by serum withdrawal .....	216
6.3.15 Analysis of Thr125-phospho-specific caspase 9 levels upon EGF stimulation of <i>B-Raf</i> <sup>Lox-D594A/Lox-D594A</sup> primary MEFs .....	216
<b>6.4 Conclusions.....</b>	<b>218</b>
<b>7. SUMMARY AND DISCUSSION.....</b>	<b>224</b>
<b>7.1 Characterisation of the role of C-Raf in the suppression of <math>\alpha</math>-CD95 antibody-induced apoptosis .....</b>	<b>224</b>
<b>7.2 Characterisation of cell growth, proliferation and apoptosis in <i>B-raf</i><sup>-/-</sup> primary MEFs.....</b>	<b>225</b>
<b>7.3 Generation of a floxed <i>B-raf</i> kinase inactive allele by homologous recombination and the subsequent generation of <i>B-raf</i><sup>+/Lox-D594A</sup> mice expressing the <i>B-raf</i> kinase inactive mutation .....</b>	<b>226</b>
<b>7.4 Production and characterisation of <i>B-raf</i><sup>+/Lox-D594A</sup> MEFs expressing the <i>B-raf</i> kinase inactive mutation.....</b>	<b>227</b>

<b>7.5 Conclusion .....</b>	<b>227</b>
<b>RERERENCES.....</b>	<b>229</b>
<b>APPENDIX.....</b>	<b>273</b>

**ABBREVIATIONS**

AEBSF	4-(2-aminoethyl) benzenesulphonyl fluoride
<i>amp</i> <sup>R</sup>	ampicillin resistance
AP-1	activating protein-1
ATF-2	activating transcription factor-2
Apaf-1	apoptotic protease activating factor-1
ASK1	apoptosis signal regulating kinase 1
Asp	aspartic acid
bp	base pairs
BH	Bcl-2 homology
BrdU	bromo-2'-deoxy-uridine
BSA	bovine serum albumin
CREB	cAMP response element
CK2	casein kinase 2
CKI	cdk inhibitor
CIP	cdk-interacting protein
cDNA	complementary DNA
CR	conserved region
cAMP	cyclic AMP
CIP	cyclin dependent kinase-interacting protein
cPLA <sub>2</sub>	cytoplasmic phospholipase A <sub>2</sub>
CRD	cysteine-rich domain
DISC	death-inducing signalling complex
DNA	deoxyribonucleic acid
DMSO	dimethyl sulphoxide
DDT	dithiothreitol
DMEM	Dulbecco's modified Eagle's medium
EDTA	diaminoethane-tetra acetic acid
E	embryonic day
ES cell	embryonic stem cell
EGF	epidermal growth factor
eIF-4E	eukaryotic initiation factor 4E

---

ERK	extracellular signal-regulated kinases
FADD	Fas-associated death domain
FACS	fluorescence activated cell sorting
FITC	fluorescein isothiocyanate
FCS	foetal calf serum
GLB	Glo lysis buffer
Grb-2	growth factor receptor-bound protein 2
GEF	guanine nucleotide-exchange factor
GAP	Ras GTPase activating protein
Hsp90	heat-shock protein of 90KDa
HSV- <i>tk</i>	herpes simplex virus thymidine kinase
hbER	hormone-binding domain of the estrogen receptor
h	hours
<i>hprt</i>	hypoxanthine phosphoribosyl transferase
IKK	I $\kappa$ B-kinase complex
IEG	immediate early gene
IP	immunoprecipitation
IAP	inhibitor of apoptosis
INK4	inhibitor of cyclin-dependent kinase 4
IL-1	interleukin-1
JNK	c-Jun N terminal protein kinase
Kb	kilobase(s)
KDa	kiloDalton
KIP	kinase-interacting protein
KSR	kinase suppressor of Ras
LIF	leukeamia inhibitory factor
LB	Luria Bertani
MBP	myelin basic protein
MEF	mouse embryonic fibroblast
MST2	mammalian sterile 20-like kinase
MEK	MAPK/ERK kinase
MNK	MAP kinase interacting kinase
MH2	Mill Hill no. 2

---

min	minute(s)
MAPK	mitogen activated protein kinase
MKK	mitogen activated protein kinase kinase
MKKK	mitogen activated protein kinase kinase kinase
MSK	mitogen and stress activated kinase
MLK	mixed lineage protein kinase
MLCK	myosin light chain kinase
<i>neo</i> <sup>R</sup>	neomycin resistance
NFκB	nuclear factor κB
NGF	nerve growth factor
PKA	cAMP-dependent kinase
Pak3	p21-activated kinase 3
p90 <sup>RSK</sup>	p90 ribosomal S6 kinases
PFA	paraformaldehyde
PBS	phosphate buffered saline
PtdIns	phosphoinositides
PI3-K	phosphoinositide 3-kinase
PDK1	3-phosphoinositide-dependent protein kinase 1
PTB	phosphotyrosine binding
PDGF	platelet derived growth factor
PA	polyadenylation
PCD	programmed cell death
PKB	protein kinase B
PKC	protein kinase C
PP2A	protein phosphatase 2A
<i>puro</i> <sup>R</sup>	puromycin resistance
RKIP	Raf kinase inhibitor protein
RBD	Ras binding domain
RTK	receptor tyrosine kinase
Rb	retinoblastoma protein
RXRα	retinoid X receptor α
rpm	revolutions per minute
RNase	ribonuclease

---

RNA	ribonucleic acid
s	second(s)
Ser	serine
SGK	serum and glucocorticoid-inducible kinase
SRE	serum response element
SRF	serum response factor
Sos	Son of Sevenless
SSC	sodium chloride-sodium citrate
SDS-PAGE	sodium dodecyl sulphate-polyacrylamide gel electrophoresis
SA	Splice acceptor
SD	Splice donor
SH	Src homology
Sur-8	suppressor of Ras-8
tau	microtubule-associated protein
TPA	12-O-tetradecanoyl-phorbol-13-acetate
tsSV40T	temperature sensitive Simian Virus 40 large T antigen
TCF	ternary complex factors
TEMED	tetramethyl-ethylenediamine
Thr	threonine
TRADD	TNFR-associated death domain
TAK1	transforming growth factor $\beta$ -activated kinase 1
Tris	Tris (hydroxymethyl) aminomethane
TAE	Tris-acetate-EDTA
TBS	Tris-buffered saline
TE	Tris-EDTA
TNF	tumour necrosis factor
TNFR	tumour necrosis factor receptor
Tpl-2	tumour progression locus-2
Tyr	tyrosine
UV	ultraviolet
v-Src	Rous sarcoma virus
VDAC	voltage dependent anion channel
V	volts

v/v	volume to volume
w/v	weight to volume
WT	wild type

## ACKNOWLEDGEMENTS

I would like to sincerely thank my supervisor Catrin for all her help, guidance and support during my PhD. I would also like to thank Kathryn for her help, as well as past and present members of Lab. 205. Additional thanks go to Jane and Anthony for their micromanipulation expertise and to Lin for assisting in the breeding. I would also like to say thank you to my family and friends for their support, in particular a special thank you to my husband Sid; I could not have done this without you. Thank you for everything.

# 1. INTRODUCTION

## 1.1 Cell signalling

Cells contain all the structures and molecular constituents required for life. Cells can perceive changes in the extracellular environment and mount an appropriate response to maintain correct functioning of the multicellular organism. Cell signalling is a key process via which cells are able to respond to extracellular stimuli and regulate cellular events. Extracellular signalling molecules can interact with cell surface receptors leading to the transduction of the signal across the plasma membrane. These signals can then influence cytosolic and/or nuclear events. Signal transduction cascades can regulate many events including proliferation, differentiation, cell shape and motility and programmed cell death.

### *1.1.1 Mitogen-activated protein kinase (MAPK) cascades*

One group of cascades activated by cell surface receptors and found to be evolutionarily highly conserved from yeast to mammals are the mitogen-activated protein kinase cascades. The structure and organisation of these cascades is highly conserved. They consist of a module of three cytoplasmic kinases: a mitogen-activated protein kinase kinase kinase (MKKK or MEKK), a mitogen-activated protein kinase kinase (MKK or MEK) and a MAPK. The module conveys a signal in the form of phosphorylation events, and is designed to allow the cytoplasmic kinases to be finely regulated and the opportunity of amplification of the initial signal.

In yeast the most well studied MAPK cascades are those of the budding yeast *Saccharomyces cerevisiae*. This organism has 5 different MAPKs which are required to respond to environmental changes such as high osmolarity, cell integrity, starvation and filamentous growth, and used to regulate mating and sporulation.

### *1.1.2 The various mammalian MAPK pathways*

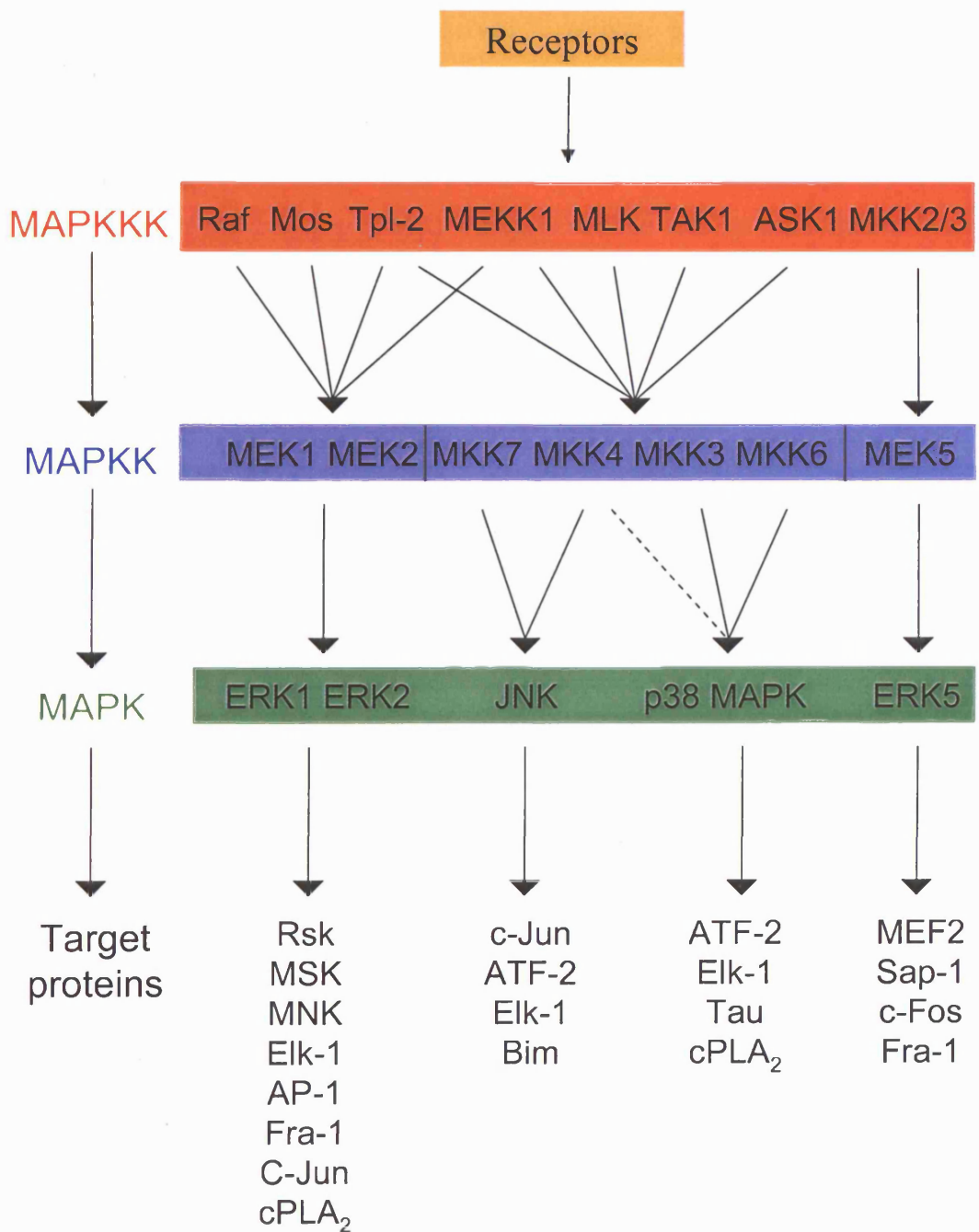
In mammals 4 different sub-groups of MAPKs are known to exist, namely ERK1/2, JNK/SAPK, p38-MAPK and ERK5. Each is involved in a different MAPK cascade (Figure 1.1). Each signalling pathway is very complex, involving many proteins such as

adapter, scaffold and anchor proteins. Together the proteins can form large multi-protein signalling complexes to aid the signalling processes.

The extracellular signal-regulated kinases; ERK 1 (p44 MAPK) and ERK2 (p42 MAPK) are phosphorylated and activated by the MKK's MAPK/ERK kinase (MEK)1 and 2 (Seger *et al.*, 1992; Zheng and Guan 1993), which in turn are activated by a number of upstream regulators, namely Raf (Kyriakis *et al.*, 1992; Dent *et al.*, 1992; Howe *et al.*, 1992), MEK Kinase (MEKK) (Lange-Carter *et al.*, 1993), Mos (Pham *et al.*, 1995) and tumor progression locus-2 (Tpl-2) (Salmeron *et al.*, 1996). Activation of the ERK MAPK cascade is mainly via mitogenic stimuli. Upon activation, ERK1/2 can target a number of substrates including cytoplasmic, membrane, cytoskeletal and nuclear proteins. These include p90 ribosomal S6 kinases (p90<sup>RSK</sup>) (Sturgill *et al.*, 1988), Mnk2 (Waskiewicz *et al.*, 1997), cytoplasmic phospholipase A2 (cPLA<sub>2</sub>) (Lin *et al.*, 1993) and transcription factors such as c-Myc (Alvarez *et al.*, 1991; Gupta *et al.*, 1993), Elk-1 (Gille *et al.*, 1992; Marais *et al.*, 1993; Gille *et al.*, 1995), c-Fos (Chen *et al.*, 1993; Chen *et al.*, 1996) and ATF-2 (Abdel-Hafiz *et al.*, 1992).

The mammalian c-Jun N terminal protein kinases (JNKs) family consists of three members, namely JNK1, JNK2 and JNK3. Each *Jnk* gene can be alternatively spliced, giving rise to at least 10 different JNK proteins (Gupta *et al.*, 1996). JNKs are activated in response to stress stimuli, such as ultraviolet radiation (Dérillard *et al.*, 1994), changes in temperature and osmolarity, (Galcheva-Gargova *et al.*, 1994) or via inflammatory cytokines such as tumour necrosis factor- $\alpha$  (TNF- $\alpha$ ) (Sluss *et al.*, 1994) and interleukin-1 (IL-1) (Bird *et al.*, 1994). The upstream activators of JNKs are MKK4 and MKK7 (Sanchez *et al.*, 1994; Derillard *et al.*, 1995; Lin *et al.*, 1995; Gerwins *et al.*, 1997). MKK4 and 7 are in turn activated by MEKK1 (Yan *et al.*, 1994), Tpl-2 (Salmeron *et al.*, 1996), mixed lineage protein kinase (MLK) (Rana *et al.*, 1996), apoptosis signal regulating kinase 1 (ASK1) (Ichijo *et al.*, 1997) and transforming growth factor  $\beta$ -activated kinase 1 (TAK1) (Wang *et al.*, 2001). Downstream targets of the JNKs include nuclear targets such as the transcription factors c-Jun, ATF2, Elk-1, and p53 (Kyriakis *et al.*, 1995; Gupta *et al.*, 1995; Cavigelli *et al.*, 1995; Buschmann *et al.*, 2001). JNKs have also been shown to play a role in UV stimulated apoptosis by the phosphorylation of the BH3-only proteins Bim and Bmf (Lei *et al.*, 2002; Lei and Davis, 2003).

**Figure 1.1** The numerous mammalian MAPK kinase cascades. The signalling pathways consist of three tiers linking cell surface receptors to cytoplasmic and nuclear events.



The p38-MAPK mammalian family of protein kinases consists of four members produced by alternative splicing. These are p38 $\alpha$ , p38 $\beta$ , p38 $\gamma$  (ERK6, SAPK3) and p38 $\delta$  (SAPK4). Activation of p38-MAPK occurs in response to extracellular stimuli including UV light, heat, osmotic shock, inflammatory cytokines (TNF and IL-1) and hemopoietic growth factors (Rouse *et al.*, 1994; Han *et al.*, 1994; Freshney *et al.*, 1994; Foltz *et al.*, 1997). The major upstream activators of p38-MAPKs are MKK3 and MKK6. MKK4, the upstream activator of JNKs, has also been observed to activate p38-MAPKs in some cell types (Derijard *et al.*, 1995; Han *et al.* 1996; Moriguchi *et al.*, 1996). MKK3 and MKK6 share the same upstream activators as MKK4 and MKK7, namely MKK1 (Yan *et al.*, 1994), Tpl-2 (Salmeron *et al.*, 1996), MLK (Rana *et al.*, 1996), ASK1 (Ichijo *et al.*, 1997) and TAK1 (Wang *et al.*, 2001). p38-MAPK targets include various transcription factors such as ATF2 (Raugeaud *et al.*, 1996; Jiang *et al.*, 1996), Elk-1, and Sap-1 (Price *et al.*, 1996; Whitmarsh *et al.*, 1997). Cytoskeletal and cytosolic protein targets of p38-MAPK include the microtubule-associated protein (tau) (Reynolds *et al.*, 1997) and cPLA<sub>2</sub> (Kramer *et al.*, 1996).

Extracellular signal-regulated kinase 5 (also known as big MAP kinase 1 (BMK1)), is the least studied member of the mammalian MAPKs. This protein kinase is larger than the other MAPKs and has a distinct C-terminal and loop-12 domain (Lee *et al.*, 1995a). It is activated by MKK5 (Zhou *et al.*, 1995; English *et al.*, 1995; Kato *et al.*, 1997). Recent studies have shown MKK5 $\alpha$  but not MKK5 $\beta$  activates ERK5 (Cameron *et al.*, 2004). MKK5 is activated by MEKK2 and MEKK3 (Sun *et al.*, 2001; Chao *et al.*, 1999). ERK5 activity increases in response to oxidative stress, hyperosmolarity and several growth factors including epidermal growth factor and nerve growth factor (Abe *et al.*, 1996; Kato *et al.*, 1997; Kamakura *et al.*, 1999; Fukuhara *et al.*, 2000). Substrates of ERK5 include members of the myocyte enhancer factor 2 (MEF2) family (Kato *et al.*, 1997; Chao *et al.*, 1999) and the transcription factors Sap1a (Kamakura *et al.*, 1999), c-Fos and Fra-1 (Kamakura *et al.*, 1999; Terasawa *et al.*, 2003). ERK5 has been implicated in angiogenesis, as homozygous deletion of ERK5 resulted in embryonic lethality showing vascular and cardiovascular defects (Regan *et al.*, 2002; Sohn *et al.*, 2002).

A well studied MAPK signal transduction cascade is the Ras/Raf/MEK/ERK pathway. Members of this cascade are the focus of this thesis. The various proteins of this pathway are discussed subsequently within this chapter.

## 1.2 The Raf protein kinases

### 1.2.1 Discovery of the Raf proteins

There are three members of the mammalian Raf protein kinase family, namely C-Raf (also known as Raf-1), A-Raf and B-Raf. All were discovered for their ability to oncogenically transform cells. C-Raf was the first isotype to be discovered. *v-raf* was initially identified as the oncogene of the 3611 murine sarcoma virus and shown to transform cells *in vitro* (Fukui *et al.*, 1985; Rapp *et al.*, 1983) and induces fibrosarcomas and erythroleukaemias in newborn mice (Rapp *et al.*, 1985). The cellular homologue of *v-raf* was found to be mammalian C-Raf (Rapp *et al.*, 1983, Bonner *et al.*, 1985). Hybridisation analysis showed that the oncogene of the Mill Hill no. 2 (MH2) carcinoma virus, *v-Rmil*, was the avian retroviral homologue of *v-raf*, and both oncogenes were found to be expressed as gag-fusion proteins (Sutrave *et al.*, 1984). A-Raf was subsequently identified from screening a murine spleen cDNA library against a *v-raf* specific probe (Huleihel *et al.*, 1986). *B-raf* was initially discovered, but not characterised, as a novel transforming gene from human Ewing sarcoma DNA (Fukui *et al.*, 1985). The *B-raf* gene was also identified by homology to the avian homologue *v-Rmil* (Marx *et al.*, 1988). Further studies suggested substitution of the amino-terminal part of the gene was involved in the transforming activity of the *raf* genes (Ikawa *et al.*, 1988).

### 1.2.2 *raf* homologues in other organisms

Raf genes are evolutionarily conserved. Although there have not been any *raf* homologues found in yeast to date, they are present in higher and lower eukaryotes. In *Caenorhabditis elegans* the *raf* homologue *lin-45* is essential for larval viability, fertility and the induction of cell fates (Hsu *et al.*, 2002). It also promotes muscle degradation in differentiated muscle (Szewczyk *et al.*, 2002). The *Drosophila melanogaster raf* homologue is *Draf* (Mark *et al.*, 1987). It is important in the induction of terminal development of the larva (Ambrosio *et al.*, 1989), can induce R7 photoreceptor cell development of the *Drosophila* eye (Dickson *et al.*, 1992) and may have other roles in the eye (Melnick *et al.*, 1993). Probing the *Xenopus laevis* genome led to the discovery of a *raf* homologue (Le Guellec *et*

*al.*, 1991). It is required for fibroblast growth factor induced differentiation of the mesoderm (MacNicol *et al.*, 1993). Raf therefore plays a role in cell differentiation in a number of organisms.

### ***1.2.3 Expression of the three raf isoforms in mammals***

The C-Raf protein is expressed ubiquitously at high levels in most cell types and tissues (Storm *et al.*, 1990). A-Raf is also widely expressed, with the highest levels found in tissues that comprise the urogenital system (Storm *et al.*, 1990; Luckett *et al.*, 2000). B-Raf mRNA transcripts are present in most tissues. However, it was originally thought the B-Raf protein was not widely expressed. High levels were detected in neuronal tissue such as the brain and the spinal cord, as well as in the testis and spleen, but at extremely low levels in all other cell types and tissues (Barnier *et al.*, 1995). However, this analysis was complicated due to the lack of a good antibody against B-Raf. This problem has been overcome; studies now show B-Raf is in fact widely expressed, although it is expressed at its highest levels in the brain, testis and spleen (personal communication, C. Pritchard).

### ***1.2.4 Structural comparisons of the three Raf isoforms***

The three mammalian Raf protein kinases share a high degree of sequence homology. The initial identification of the *raf* genes as oncogenes occurred in the absence of the non-catalytic N-terminus of the protein. This region has since been confirmed as a regulatory region and shown to repress C-Raf activity (Cutler *et al.*, 1998), thus explaining the transforming potential of the truncated *raf* genes. The Raf protein kinases are composed of three highly conserved regions; CR1 and CR2 in the N terminus, and CR3 in the C terminus (Figure 1.2). Between these conserved regions are variable regions that allow the proteins to be distinct. Within C-Raf, CR1 consists of amino acid residues 61-194 and contains two regions that bind to Ras-GTP. The Ras binding domain (RBD), spanning residues 51-131 of C-Raf, is one such region (Vojtek *et al.*, 1993; Scheffler *et al.*, 1994), the majority of which lies within CR1 (Figure 1.2). The second region is the cysteine-rich domain (CRD) that spans residues 139-184 of C-Raf (Mott *et al.*, 1996). CR1 also contains a putative zinc binding domain (Beck *et al.*, 1987; Ghosh *et al.*, 1994). CR2 is a region covering 14 amino acid residues, 254-269, of C-Raf. It is a serine and threonine-rich region that contains sites of regulatory phosphorylation. CR3 of C-Raf contains the kinase domain and encompasses residues 335-627. This domain contains the highest degree of

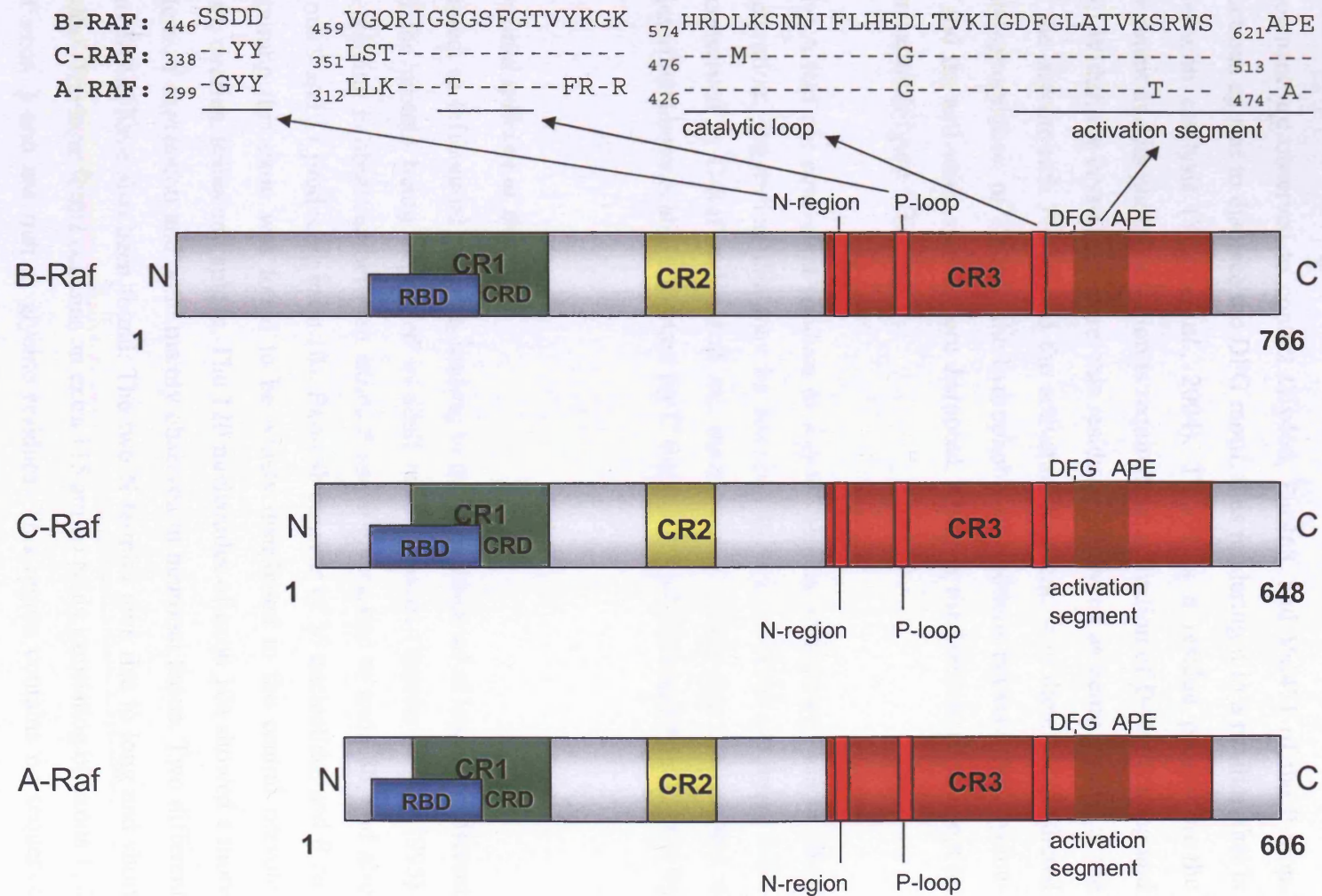
homology between the three Raf proteins (Daum *et al.*, 1994). Overall, A-Raf and B-Raf are very similar to C-Raf in these CR domains, although B-Raf has the greatest number of differing amino acids in the conserved regions when compared to C-Raf and A-Raf (Mercer *et al.*, 2003). (The amino acid numbering for B-Raf has changed in recent years. B-Raf is described in the current project using numbers corresponding to the correct amino acid sequence (see Appendix)).

### ***1.2.5 Crystal structure of B-Raf***

Many attempts have been made to obtain the crystal structure of C-Raf. However, as C-Raf binds to a number of chaperones, obtaining crystals of C-Raf that were suitable for subsequent analysis has proven to be unsuccessful. Until recently, all information obtained on the core structure of the Raf proteins has been via comparison to the crystal structure of other protein kinases. Wan *et al* (2004) originally produced crystals of a C-terminal truncated form of B-Raf, containing the kinase domain of B-Raf. However, they also found that these crystals were unsuitable for crystallography studies. They overcame this problem by expressing the truncated kinase form of B-Raf in the presence of the Raf inhibitor BAY43-9006, leading to the production of crystals suitable for further analysis. Crystals were also produced of BAY43-9006 attached to a mutated form of B-Raf, namely B-Raf V600E, in which a glutamate is substituted for valine 600. By studying the two crystal structures they suggested a number of structure-activity relationships.

The overall structure of the B-Raf kinase domain is well ordered, except from two regions; one in the N terminus (Gln433-Ser447), and residues Lys601-Gln612 of CR3. The kinase domain consists of C and N lobes, an  $\alpha$ -E helix, an  $\alpha$ -C helix and three regions in the CR3, known as the N-region, the glycine-rich P-loop and the activation segment (Figure 1.2). The activation segment contains the DFG motif, which is a conserved region in protein kinases and important for the activation of the protein. The D of the DFG motif is a highly conserved residue in all protein kinases and involved in binding an ATP chelating metal (Johnson *et al.*, 1998). Mutations in this region can cause the protein to be inactive (Wan *et al.*, 2004). Looking at the interactions of the inhibitor BAY43-9006 with B-Raf, an indication of the interactions that maintain B-Raf in its inactive conformation have been obtained (Wan *et al.*, 2004).

**Figure 1.2** Domain structures of the three mammalian Raf family members. The three conserved regions (CR1, CR2 and CR3) are highlighted. The N-region, P-loop, catalytic loop and activation segments are also shown. Abbreviations; RBD = Ras binding domain; CRD = cysteine rich domain



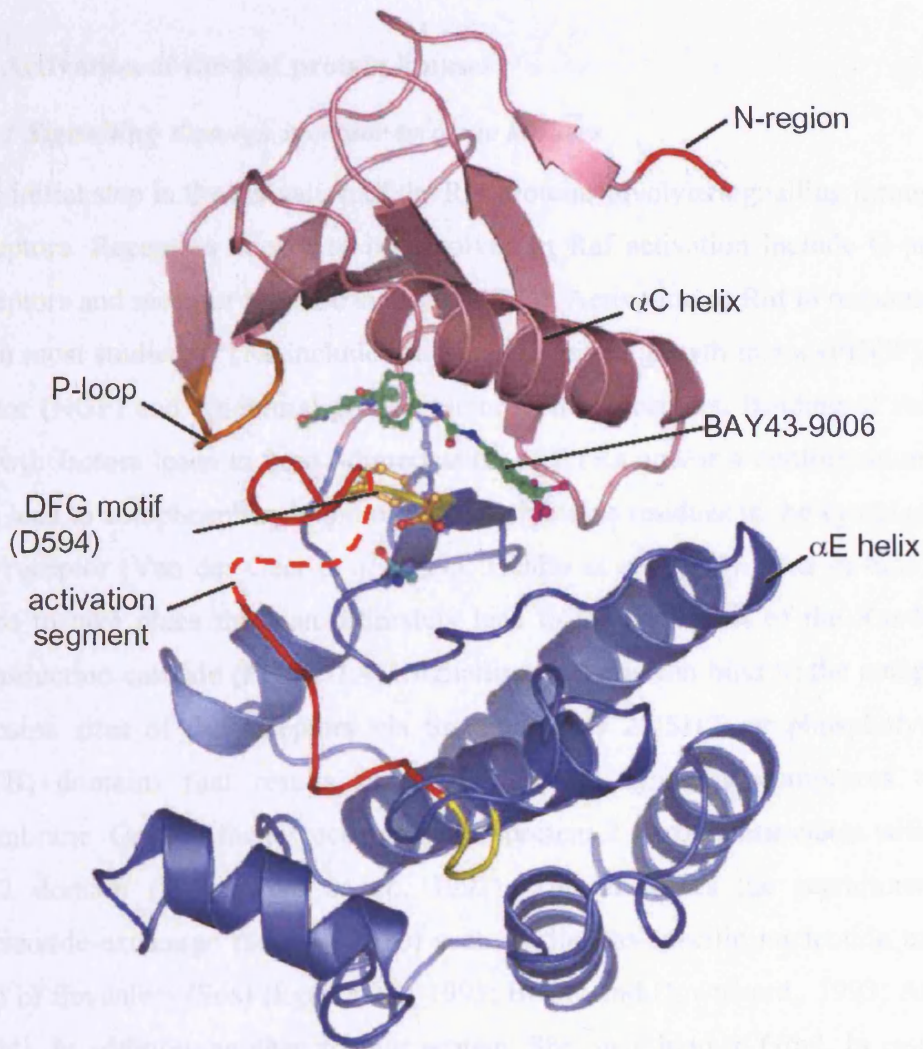
The overall structure adopted is typical of an active kinase, involving a small and a large lobe, separated by a catalytic cleft. The N region aspartic acid at position 448 helps to stabilise the small lobe. There are distinctive hydrophobic interactions between the glycine rich P-loop and the activation segment. The side chains of Leu597 and Val600 of the activation segment are observed to contact Gly466, Phe468, and Val471 of the P-loop. These interactions appear to displace the DFG motif, thus rendering it in a position that is incompatible with catalysis (Wan *et al.*, 2004). Thr599 is a residue present in the activation segment and its phosphorylation is required for activation of B-Raf (Zhang and Guan, 2000). Within the crystal structure, this residue is observed as being located at the interface of the glycine-rich P-loop and the activation segment. It is therefore predicted that upon phosphorylation of Thr599, the hydrophobic interactions between the glycine-rich P-loop and the activation segment are disrupted, allowing the DFG motif to adopt an active confirmation (Figure 1.3)

In C-Raf and A-Raf the equivalent residues to Asp448 require phosphorylation to allow their full activation, suggesting this may be required to help stabilise the small lobe. Thr599 is conserved in C-Raf and A-Raf and therefore it is likely that the method of activation described above is also important for C-Raf and A-Raf, although this is yet to be proven.

### ***1.2.6 Differential splicing of B-Raf***

B-Raf is subject to differential splicing, leading to the production of at least 10 different isoforms of the protein being expressed in adult mouse tissues (Barnier *et al.*, 1995). Alternative splicing is observed between exons 8 and 9 giving rise to exon 8b, and also between exons 9 and 11 producing exon 10a. Exon 8b consists of 36 nucleotides and *B-raf* cDNA containing this exon was found to be widely distributed in the central nervous system, heart, ovaries, testes and spleen. The 120 nucleotides of exon 10a showed a more limited pattern of expression and were mainly observed in neuronal tissue. Two different N termini of B-Raf have also been found. The two N termini give rise to long and short forms of *B-Raf*. The long forms contains an extra 115 amino acids, consisting of exons 1, 2 and part of exon 3 and are rich in glycine residues. This region contains no sequence homology with either C-Raf or A-Raf. The role of this extra N terminal domain is

**Figure 1.3** Crystal structure of the B-Raf kinase domain bound to the BAY43-9006 inhibitor, with various catalytic and structural features highlighted. (Taken from Wan *et al.*, 2004. For clarity, the amino acid number has been altered to reflect the updated B-Raf amino acid sequence).



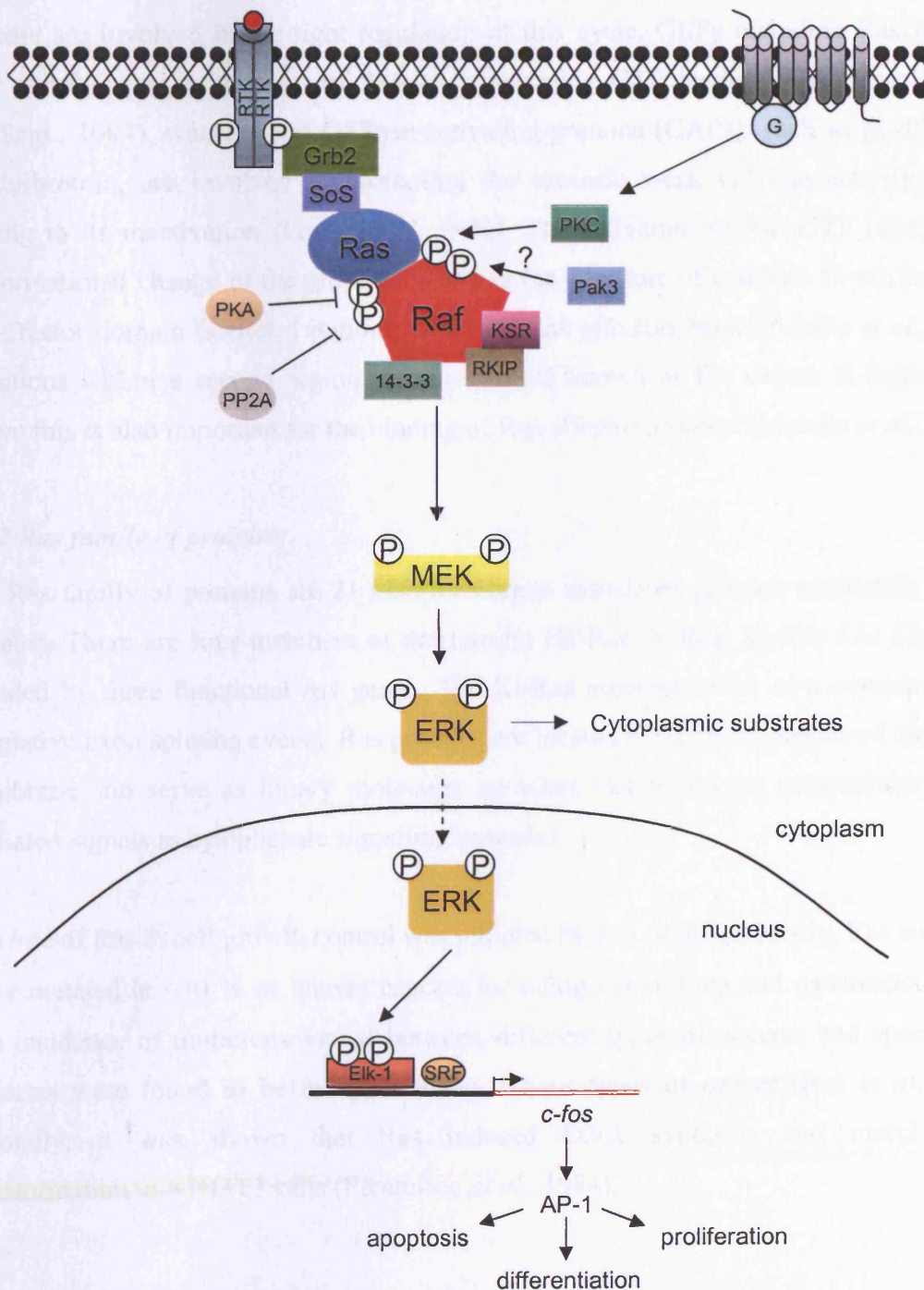
currently unknown. The differential splicing of B-Raf gives rise to a variety of proteins that range from 67 to 99 kDa (Barnier *et al.*, 1995). A-Raf is the smallest isoform at 68 kDa and C-Raf is 72-74 kDa (Storm *et al.*, 1990). The differential splicing of B-Raf has been shown to affect its activity. The presence of exon 10a leads to increased affinity and basal kinase activity towards MEK, whilst the presence of exon 8b has been observed to have the opposite effect.

### **1.3 Activation of the Raf protein kinases**

#### ***1.3.1 Signalling through receptor tyrosine kinases***

The initial step in the activation of the Raf proteins involves signalling through cell surface receptors. Receptors known to be involved in Raf activation include G-protein coupled receptors and receptor tyrosine kinases (RTKs). Activation of Raf in response to RTKs has been most studied. RTKs include the platelet derived growth factor (PDGF), nerve growth factor (NGF) and epidermal growth factor (EGF) receptors. Binding of receptor specific growth factors leads to homo-dimerisation of RTKs and/or a conformational change that can lead to autophosphorylation of multiple tyrosine residues in the cytoplasmic portion of the receptor (Van der Geer *et al.*, 1995; Heldin *et al.*, 1995). This in turn allows several steps to take place that can ultimately lead to the activation of the Ras/Raf/MEK/ERK transduction cascade (Figure 1.4). Signalling proteins can bind to the autophosphorylated tyrosine sites of the receptors via Src homology 2 (SH2) or phosphotyrosine binding (PTB) domains that results in recruitment of signalling complexes to the plasma membrane. Growth factor receptor-bound protein 2 (Grb-2) associates with RTKs via its SH2 domain (Lowenstein *et al.*, 1992). This mediates the recruitment of guanine nucleotide-exchange factors (GEFs) such as the Ras-specific nucleotide exchange factor Son of Sevenless (Sos) (Egan *et al.*, 1993; Buday and Downward., 1993; Aronheim *et al.*, 1994). In addition, another adaptor protein, Shc, may bind to Grb2. In resting cells Sos1 forms a stable interaction with the Src homology 3 (SH3) domain of Grb2. Upon receptor stimulation, the Grb2-Sos complex is recruited to the plasma membrane, allowing it to be in close proximity to membrane-bound Ras. Sos forms a complex with Ras that results in the expulsion of nucleotides that are otherwise bound tightly to Ras (Nimnual and Barsagi., 2002; Boriack-Sjodin *et al.*, 1998). In its basal state, Ras exists in a GDP-bound form (Ras-GDP). Upon interaction with Sos, Sos is able to stimulate the exchange of GDP

**Figure 1.4** The role of the Raf family of protein kinases in the Ras/Raf/MEK/ERK pathway, from transduction of signals at the plasma membrane from receptors, to the induction of altered patterns of gene expression in the nucleus that can effect cell fate.



for GTP, leading to an activated GTP-bound form of Ras (Ras-GTP). The catalytic region of Sos contains the CDC25 homology domain and this interacts directly with Ras. Binding of the CDC25 homology domain to Ras induces the structural changes necessary for Sos catalyzed nucleotide dissociation (Boriack-Sjodin *et al.*, 1998). The activity of Ras is controlled by a regulated GDP/GTP cycle. Ras cycles between an inactive GDP-bound form and an activated GTP-bound form (Bourne *et al.*; 1990). Two types of regulatory proteins are involved in the tight regulation of this cycle. GEFs including RasGRF and SOS promote the active form of Ras by accelerating GTP loading (Orita *et al.*, 1993; Bar-Sagi., 1994), whereas Ras GTPase activating proteins (GAPs), such as p120<sup>GAP</sup> and neurofibromin, are involved in promoting the intrinsic weak GTPase activity of Ras leading to its inactivation (Lowy *et al.*; 1991). The activation of Ras-GTP involves the conformational change of the protein leading to the exposure of residues 32-40, known as the effector domain (switch I region), to which Ras effectors bind (Polakis *et al.*, 1993). Mutations within a second region, residues 60-72 known as the switch II region, have shown this is also important for the binding of Ras effector proteins (Moodie *et al.*, 1995).

### ***1.3.2 Ras family of proteins***

The Ras family of proteins are 21 kDa membrane associated guanine nucleotide binding proteins. There are four members of the family; Ha-Ras, N-Ras, Ki-Ras 4A, Ki-Ras 4B encoded by three functional *ras* genes. The Ki-Ras members arise as a consequence of alternative exon splicing events. Ras proteins are located at the inner surface of the plasma membrane and serve as binary molecular switches that transduce extracellular ligand-mediated signals to cytoplasmic signalling cascades.

The role of Ras in cell growth control was initiated by two findings. Firstly, Ras was found to be mutated in ~30 % of human cancers including colon, lung and pancreatic cancers. The incidence of mutations varied between different types of cancers and specific Ras isoforms were found to be mutated in the various types of cancer (Bos *et al.*, 1989). Secondly, it was shown that Ras induced DNA synthesis and morphological transformation in NIH3T3 cells (Feramisco *et al.*, 1984).

### 1.3.3 Downstream of Ras

Ras has a diverse range of effector targets that transduce signals via a number of pathways. The most well characterised target is C-Raf, although Ras also targets the other isoforms of Raf; A-Raf and B-Raf. Other targets of Ras include class I phosphoinositide 3-kinases (PI3-K) (Rodriguez-Viciano *et al.*, 1994) and members of the Ral guanine nucleotide exchange factor (RalGEF) family (Wolthuis *et al.*, 1998). Ras interacts with the p110 catalytic subunit of PI3-K to stimulate its activity. PI3-K in turn phosphorylates the D3 position of phosphoinositides-4,5-P<sub>2</sub> (PtdIns-4,5-P<sub>2</sub>) to yield PtdIns-3,4,5-P<sub>3</sub>. PtdIns-3,4,5-P<sub>3</sub> is involved in a wide range of cellular responses. One well established target of PI3-K mediated production of PtdIns-3,4,5-P<sub>3</sub> is Akt/PKB, which has been shown to play a role in cell survival (Khwaja *et al.*, 1997). Activated Ras promotes RalGEF (RalGDS, Rgl, Rlf) activation of the RalA and RalB Ras-related small GTPases (Urano *et al.*, 1996; Murai *et al.*, 1997; Wolthuis *et al.*, 1997). RalA activates phospholipase D and is an important mediator of transformation and tumourigenesis *in vivo*.

### 1.3.4 Interaction of Ras with Raf

Initial interactions of Ras with Raf were shown using C-Raf. Studies showed that using dominant negative mutations of C-Raf and C-Raf antisense, proliferation and transformation induced by activated Ki-Ras and Ha-Ras could be blocked (Kolch *et al.*, 1991). Other studies to suggest a link between the two proteins showed hyperphosphorylation of C-Raf in cells that were treated with agonists known to activate Ras (Morrison *et al.*, 1988) and also in cells expressing oncogenic Ras (Wood *et al.*, 1992). A direct physical interaction between the proteins was subsequently shown by various groups via *in vitro* binding assays and the *in vivo* yeast two-hybrid system (Vojtek *et al.*, 1993; Koide *et al.*, 1993; Van Aelst *et al.*, 1993; Warne *et al.*, 1993; Zhang *et al.*, 1993). Co-immunoprecipitation of Ras and C-Raf was observed in stimulated but not unstimulated mammalian cells (Hallberg *et al.*, 1994). Ras has subsequently been shown to interact with C-Raf specifically in two domains of the N-terminal of C-Raf. It interacts with the Ras binding domain (RBD; amino acids 51-131) and the cysteine-rich domain (CRD; amino acids 139-184) which forms a zinc finger structure (Brtva *et al.*, 1995; Hu *et al.*, 1995). The strength of the Ras interactions with the two domains of C-Raf varies. The strongest interaction occurs between Ras-GTP and the RBD region of C-Raf and has been shown to be essential for C-Raf activity (Chuang *et al.*, 1994). Binding to the CRD of C-

Raf occurs at a lower affinity than to the RBD, nevertheless, this interaction has also been shown to be required for the activation of C-Raf (Hu *et al.*, 1995; Drugan *et al.*, 1996; Luo *et al.*, 1997; Mineo *et al.*, 1997; Roy *et al.*, 1997). All four isoforms of Ras interact with Raf proteins although the efficiency of binding varies between the four isoforms (Voice *et al.*, 1999). The two forms of K-Ras are the most efficient, followed by N-Ras, which is more efficient than Ha-Ras.

### ***1.3.5 Ras is required to recruit C-Raf to the plasma membrane***

Upon interaction of Ras with C-Raf, it has been shown that Ras localises C-Raf to the plasma membrane. Examining the structure of C-Raf showed that in its inactive state C-Raf is found in the cytosol as part of a multi-subunit complex (Wartmann and Davis, 1994). *In vitro* studies showed that Ras-GTP was unable to activate C-Raf unless it was membrane bound (Traverse *et al.*, 1993; Dent and Sturgill, 1994; Stokoe and McCormick, 1997). Furthermore, it was suggested that the role of Ras-GTP was in mediating a conformational change in inactive Raf that induced its recruitment to the plasma membrane, as this was only observed in the presence of over-expressed or activated Ras (Traverse *et al.*, 1993; Wartmann and Davis, 1994). This was confirmed in studies that targeted C-Raf to the plasma membrane in the absence of activated Ras, by fusing the carboxy terminal of C-Raf to the membrane localisation signal of K-Ras (Raf-CAAX) (Leevers *et al.*, 1994; Stokoe *et al.*, 1994). It was shown that addition of oncogenic Ras or dominant negative Ras had no effect on this constitutively active Raf-CAAX. In addition, further activation of Raf-CAAX occurred by stimulating with epidermal growth factor (Leevers *et al.*, 1993). This showed that Ras plays a role in recruiting C-Raf to the plasma membrane but further mechanisms may be required for the full activation of C-Raf.

It has also been shown that Ras also recruits A-Raf and B-Raf to the plasma membrane. Cells were micro-injected with expression vectors for A-Raf or B-Raf constructs in the presence or absence of expression vectors for oncogenic Ras. When expressed alone, the Raf proteins were found to be located in the cytoplasm, but upon co-expression with oncogenic Ras, both A-Raf and B-Raf were found to be translocated to the plasma membrane (Marais *et al.*, 1997).

### **1.3.6 Interaction of Raf with other Ras family members**

The Ras super-family of proteins includes at least 21 members. Studies have shown that some of the other members of the Ras family can also interact with the Raf proteins. TC21 binds to C-Raf in a GTP-dependent manner (Movilla *et al.*, 1999). Oncogenic TC21 can interact with C-Raf and B-Raf, but not A-Raf, and this results in the recruitment of the two Raf isoforms to the plasma membrane (Rosario *et al.*, 1999). It was observed that Raf was required for TC21-mediated transformation via the ERK pathway (Rosario *et al.*, 1999). The interaction of TC21 with C-Raf has also been observed more recently via co-expression studies (Rodriguez-Viciano *et al.*, 2004). These findings showed C-Raf was the only isoform to be activated upon co-transfection. This study also looked at the ability of other Ras family proteins to activate the Raf protein kinases, and downstream effectors. C-Raf was also found to be activated by R-Ras3 and Rit. R-Ras3 also stimulated A-Raf, but no additional Ras family members were able to activate B-Raf (Rodriguez-Viciano *et al.*, 2004). Conflicted results have been proposed for the role of the Ras family member Rap1A in its interaction with the Raf proteins. Rap1A can bind to C-Raf but cannot activate it; instead it has been shown to suppress its Ras-dependant activation (Cook *et al.*, 1993). It is thought this may be due to Rap1A recruiting C-Raf to membrane domains that do not allow its full activation (Carey *et al.*, 2003). However, B-Raf is activated by Rap1A (Ohtsuka *et al.*, 1996). Furthermore, B-Raf activation induced by cyclic AMP and nerve growth factor in PC12 was reported to be mediated by Rap1A and not Ras (Vossler *et al.*, 1997; York *et al.*, 1998) and B-Raf is required for Rap1A mediated differentiation of megakaryocytes (Garcia *et al.*, 2001). The difference in activation is thought to be in the strength of the interaction of Rap1A with the CRD of C-Raf (Okada *et al.*, 1999). Rap1A binds very strongly to the CRD of C-Raf, but more weakly to B-Raf. It was shown that if the CRD of C-Raf and B-Raf are switched, C-Raf is activated by Rap1A, but B-Raf loses its response to Rap1A (Okada *et al.*, 1999). A Rap1A interaction with *Drosophila* Raf (which of the three mammalian Rafs shares the strongest sequence homology with mammalian B-Raf) has also been observed (Lee *et al.*, 2002), suggesting the interaction with Rap1A may be evolutionarily conserved.

### **1.4 Phosphorylation events of C-Raf**

The full activation of C-Raf requires additional events upon the recruitment of C-Raf to the plasma membrane by Ras. The observations that hyperphosphorylation of C-Raf in

response to many signalling events (Morrison *et al.*, 1993) have for some time suggested that phosphorylation plays a role in the activation of C-Raf. Studies have shown a number of key residues require phosphorylation or dephosphorylation to allow C-Raf to be fully activated (Figure 1.5).

#### **1.4.1 Phosphorylation of tyrosine 341**

Tyrosine residue 341, which lies within the kinase domain of C-Raf (Figure 1.5), is phosphorylated during the activation of C-Raf. It was initially shown using a baculovirus expression system that tyrosine residues 340 and 341 were major phosphorylation sites in insect cells (Fabian *et al.*, 1993). Furthermore, mutations of these sites to phenylalanines (RafFF) resulted in a C-Raf protein that could not be activated by tyrosine kinases. Over-expression studies in NIH3T3 cells, again expressing RafFF, indicated that phosphorylation of tyrosine residues 340 and 341 is required in mammalian cells (Marais *et al.*, 1995). Phosphorylation of the tyrosines could be mediated by the membrane associated protein tyrosine kinase Rous sarcoma virus (v-Src) *in vitro*. This correlated with data stating C-Raf was required for the transformation of cells by v-Src (Qureshi *et al.*, 1993). Indeed findings demonstrated a synergistic relationship between oncogenic Ras, v-Src and C-Raf, as expression of the three proteins led to increased activity of C-Raf *in vitro* (Williams *et al.*, 1992; Fabian *et al.*, 1993; Dent and Sturgill., 1994; Marais *et al.*, 1995). However, it is still unknown if Src is the activator of the tyrosines residues *in vivo*. It was later observed that phosphorylation of Tyr341 was crucial for the activation of C-Raf but phosphorylation of Tyr340 was not essential (Mason *et al.*, 1999). Substitution of either Tyr340 or Tyr341 with alanine was performed, followed by expression of these mutant forms of C-Raf in COS cells. A reduction in kinase activity was observed for Y341A mutants but not for Y340A mutants. These findings were confirmed using phosphospecific antibodies to show Ser338 and Tyr341 were phosphorylated upon activation of C-Raf via oncogenic Ras and Src, but Tyr340 was not (Mason *et al.*, 1999).

In A-Raf the corresponding tyrosine residue at 340 and 341 are conserved (residues 301 and 302). Like C-Raf, A-Raf is activated by both oncogenic Ras and oncogenic Src, and together they lead to a synergistic stronger activation of A-Raf (Marais *et al.*, 1997). This activation requires the phosphorylation of tyrosine 302, as mutating this site to phenylalanine (along with tyrosine 301) did not lead to activation by oncogenic Src. In B-

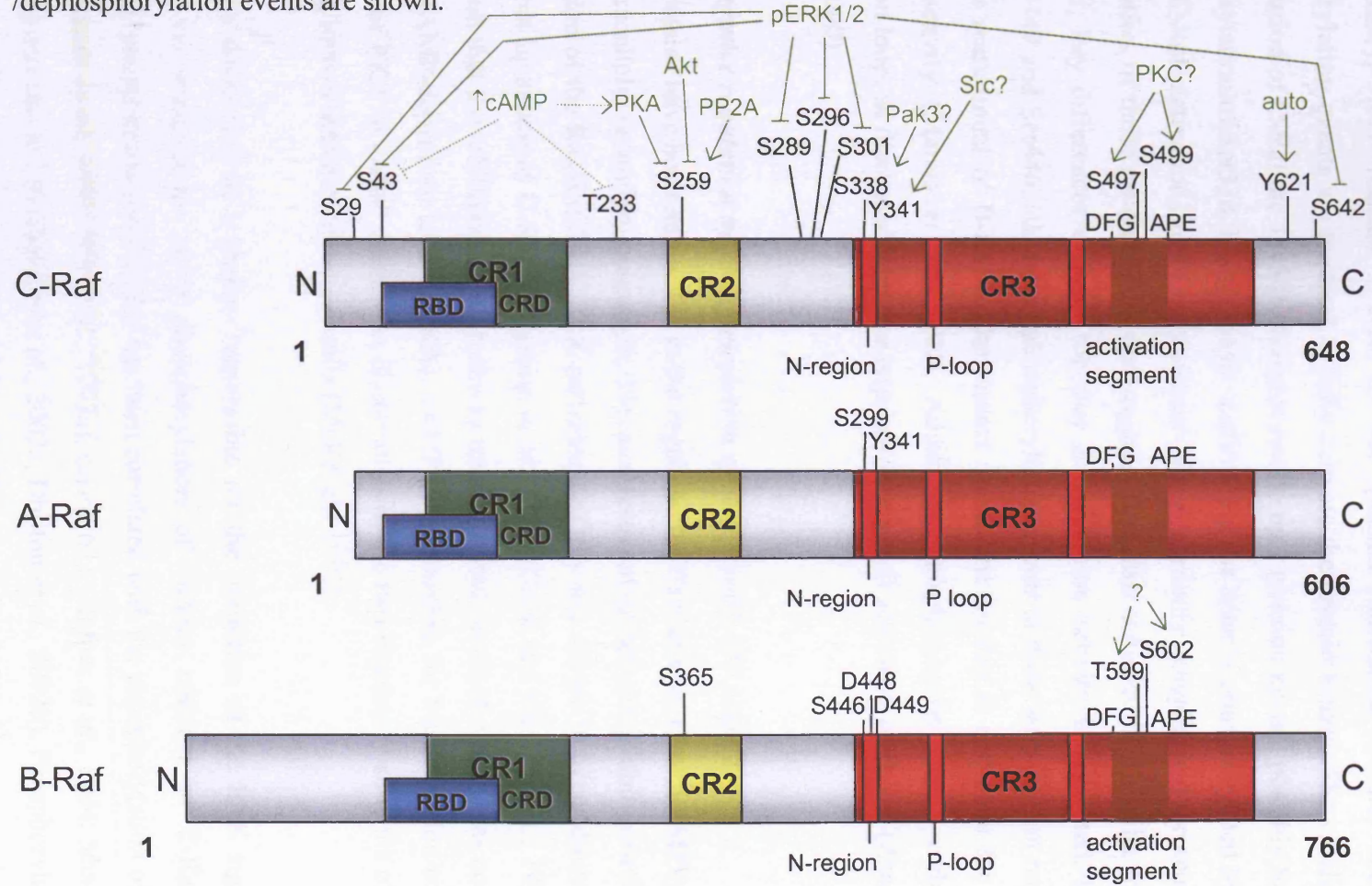
Raf the homologous sites to tyrosine 340 and 341 are aspartic acid residues 448 and 449. Due to the negative charge of these amino acids it is thought they may mimic the phosphorylated tyrosines of C-Raf and A-Raf. This leads to an increased basal activity of B-Raf when compared to C-Raf and A-Raf. Thus B-Raf requires Ras for translocation to the plasma membrane, but does not require phosphorylation by tyrosine kinases, such as Src for its activity (Marais *et al.*, 1997). As mentioned earlier, within B-Raf, Asp448 has been shown to help stabilise the small lobe of the protein kinase (Wan *et al.*, 2004). It is therefore likely that the phosphorylation of Tyr340/341 of C-Raf, and Tyr301/302 of A-Raf, are required during the activation of the protein to aid this stabilisation.

#### ***1.4.2 Phosphorylation of Serine 338***

Serine 338 is another residue essential for C-Raf activation. Like Tyr341, it is located in the N-region, within the kinase domain of the protein kinase (Figure 1.5). It has been shown that mutating this residue has a detrimental effect on C-Raf activity (Diaz *et al.*, 1997; Barnard *et al.*, 1998; Mason *et al.*, 1999). The protein suggested to be responsible for the phosphorylation of Ser338 is p21-activated kinase 3 (Pak3) (King *et al.*, 1998). Pak3 phosphorylation of C-Raf on Ser338 *in vitro* and *in vivo* was observed and further observations suggested both Pak3 and Ras were required for signal transduction via C-Raf. Pak3 is activated by binding to Cdc42 and Rac (Manser *et al.*, 1994), which are themselves phosphorylated and activated by PI3-K (Rodriguez-Viciano *et al.*, 1994). PI3-K is also an effector of Ras-GTP, therefore implying that Ras indirectly can activate C-Raf by activating Pak3 (Sun *et al.*, 2000). However, observations have been made to challenge the role of Pak3 in C-Raf activation. Chiloeches *et al.* (2001) found PI3-K inhibitors were unable to prevent serine 338 phosphorylation, and that activated mutants of Pak3 were able to induce serine 338 phosphorylation but not C-Raf activation. Both these findings suggest that, although Pak3 is able to phosphorylate Ser338, it may not play a role in the activation of C-Raf.

In A-Raf, the corresponding residue to Ser338 is Ser299. The role of this serine in the activation of A-Raf has not been investigated. The homologous site in B-Raf is also a serine, located at position 446. Unlike C-Raf Ser446 is constitutively phosphorylated. The constitutive phosphorylation of Ser446, together with the location of aspartic acid residues at 448 and 449, contribute to the higher basal level activity of B-Raf. This basal activity is

**Figure 1.5** Domain structures of the three Raf protein kinases indicating key residues thought to be important in the activation of B-Raf, C-Raf and A-Raf. The potential kinases/phosphatases responsible for the phosphorylation /dephosphorylation events are shown.



10-20-fold higher than that for C-Raf and A-Raf in unstimulated cells as measured by immunoprecipitation (IP) kinase assays (Marais *et al.*, 1997).

In summary, Ras recruits C-Raf to the plasma membrane where additional phosphorylation events are required to fully activate the protein kinase. The crucial sites for activation of C-Raf are Tyr341 phosphorylation by a tyrosine kinase, possibly Src, and phosphorylation of Ser338. It is yet to be confirmed if the latter is phosphorylated by Pak3 during C-Raf activation, or if this occurs via a currently unidentified protein. The conservation of these residues in A-Raf suggests it is also activated in a similar manner. However, key differences exist in the way B-Raf kinase activity is regulated. Due to Asp448/449 and Ser446, additional phosphorylation events at these sites are not required; therefore recruitment of B-Raf to the plasma membrane by Ras is sufficient for B-Raf kinase activity (Marais *et al.*, 1997). Additional phosphorylation events within the activation loop, as discussed later, are required for the full activation of B-Raf (Zhang and Guan, 2000).

#### ***1.4.3 Negative regulation by phosphorylation of residues 43, 259 and 621***

Other proteins have been implicated in the regulation of Raf activity. Cyclic AMP (cAMP) is an intracellular secondary messenger. Elevated levels of cAMP can inhibit growth factor stimulation of the Ras/Raf/MEK/ERK pathway, and this was shown to occur downstream of Ras but upstream of C-Raf (Burgering *et al.*, 1993; Cook and McCormick., 1993). It was found that the inhibition of the pathway upon elevated levels of cAMP was occurring via the cAMP-dependent kinase (PKA). cAMP is responsible for the activation of PKA. Binding of PKA to cAMP causes the dissociation of the two regulatory subunits of PKA, releasing its two active catalytic subunits (McKnight 1991).

PKA was discovered as a protein responsible for the inhibition of the ERK signalling cascade via observations upon phosphorylation of various residues of C-Raf. The inhibitory phosphorylation of C-Raf has been correlated with the phosphorylation of serine 43 (Morrison *et al.*, 1993; Wu *et al.*, 1993a), serine 621 (Hafner *et al.*, 1994; Mischak *et al.*, 1996) and serine 259 (Dhillon *et al.*, 2002a; Dhillon *et al.*, 2002b). Phosphorylation of Ser43 lowered the affinity of C-Raf for Ras-GTP (Wu *et al.*, 1993a). However, subsequent studies showed upon mutating Ser43, cAMP did not alter the inhibition of C-Raf activity

(Sidovar *et al.*, 2000; Dhillon *et al.*, 2002a), thus indicating this was not a crucial site for negative regulation by PKA.

The role of Ser621 as an inhibitory site was suggested due to its phosphorylation leading to inhibition of catalytic activity (Mischak *et al.*, 1996). However, these studies were carried out using only the isolated kinase domain of C-Raf, so the role of Ser621 in full length C-Raf is less clear. Mutations of Ser621 are incompatible with the kinase function of C-Raf (Morrison *et al.*, 1993; Mischak *et al.*, 1996) so have further hindered the study of this residue. However, it has since been discovered that Ser621 is a site of autophosphorylation during the activation of full length C-Raf (Thorson *et al.*, 1998), indicating that its phosphorylation may not play a role in the inhibition of C-Raf.

It appears that Ser259 may be the major target for inhibitory phosphorylation of full length C-Raf by PKA. Mutation of this site led to C-Raf being largely resistant to PKA inhibition (Dhillon *et al.*, 2002a). Furthermore, mutating Ser259 resulted in elevated levels of C-Raf kinase activity by enhanced binding to Ras (Dhillon *et al.*, 2002b). The dephosphorylation of Ser259 is suggested as an important event in C-Raf activation, allowing release of the repression of C-Raf.

Recent findings have also indicated elevated cAMP can cause C-Raf inhibition by phosphorylation of C-Raf on Ser43 or Ser259, as previously reported, but also upon phosphorylation of Ser233 (Dumaz *et al.*, 2002 and 2003). Elevated levels of cAMP blocked NIH 3T3 cell growth by independent phosphorylation of C-Raf on Ser43, Ser233 and Ser259, leading to C-Raf inhibition via Ras-dependent and Ras-independent mechanisms. Furthermore, mutating the three serine residues to alanine, in the presence of elevated cAMP, rescued ERK activity but did not rescue DNA synthesis. This indicates cAMP targets other pathways, as well as the C-Raf pathway, in the suppression of NIH 3T3 cell growth (Dumaz *et al.*, 2002). In CCL39 cells it has been shown cAMP targets cyclin D1 expression, but over-expression of cyclin D1 was only able to partially restore growth in these cells (Dumaz *et al.*, 2002).

The relationship between B-Raf and cAMP appear to differ to that of C-Raf and cAMP. Whereas elevated levels of cAMP led to an inhibition of C-Raf activity, increased cAMP levels have been shown to lead to B-Raf induced elevated ERK activity in various cell

lines (Vossler *et al.*, 1997). cAMP activates a small G-protein, Rap1 via cAMP dependent phosphorylation by PKA (Altschuler and Lapetina., 1993). Several studies have indicated a relationship between Rap1 and B-Raf. Rap-1 was shown to activate ERKs in PC12 cells despite C-Raf being inhibited. This required the activity of B-Raf and was independent of Ras (Vossler *et al.*, 1997). Rap-1 was observed to directly activate B-Raf *in vitro* (Ohtsuka *et al.*, 1996; Vossler *et al.*, 1997) and a Rap-1/B-Raf complex formation has been observed upon PC12 cell stimulation with cAMP and NGF (Vossler *et al.*, 1997; York *et al.*, 1998). Therefore elevated cAMP levels lead to increased B-Raf activity via Rap1, which in turn promotes increased ERK activity. Studies to investigate the role of A-Raf in relation to PKA, cAMP or Rap-1 have not been reported.

#### ***1.4.4 C-Raf regulation by feedback phosphorylation of numerous serine residues***

A recent study identified six sites of phosphorylation that may play a key role in the negative regulation of C-Raf (Dougherty *et al.*, 2005). NIH3T3 cells were stimulated with various growth factors and the C-Raf kinase activity measured by IP kinase assays. Activity peaked after 5 min of PDGF treatment and returned close to basal levels by 15 mins. An electrophoretic mobility shift of C-Raf due to increased phosphorylation was observed 15 mins after mitogenic stimulation and persisted for several hours (Dougherty *et al.*, 2005). The hyper-phosphorylation of C-Raf appeared to coincide with its inactivation. Subsequent analysis identified Ser29, Ser43, S289, S296, S301 and S642 as the sites of phosphorylation. Furthermore, mutation of these sites led to loss of the hyper-phosphorylation, pro-longed membrane localisation and sustained mitogen-induced C-Raf kinase activity (Dougherty *et al.*, 2005). S43 has previously been identified as a site of negative phosphorylation (Morrison *et al.*, 1993; Wu *et al.*, 1993a), but no reports have suggested the other five serines as inhibitory sites in C-Raf regulation. Hyper-phosphorylation of these sites was shown to occur via ERK and this desensitized C-Raf to prevent any additional activation events. This therefore indicated regulation of C-Raf via feedback phosphorylation. It was further observed that PP2A and Pin1 interact with the desensitized C-Raf to return it to its resting and activation-competent state (Dougherty *et al.*, 2005).

A study has indicated B-Raf is also subject to an ERK-mediated feedback mechanism. Using chicken DT40 B cells it was observed that upon B-cell antigen receptor signalling,

during which B-Raf is known to activate ERK (Brummer *et al.*, 2002), B-Raf became hyper-phosphorylated. This was shown to occur on a C-terminal SPKTP sequence of B-Raf by ERK2 (Brummer *et al.*, 2003).

#### **1.4.5 Other potential phosphorylation sites of C-Raf**

Two other sites have been implicated in C-Raf activation. Ser497 and Ser499 can be directly phosphorylated by protein kinase C (PKC) $\alpha$ , a member of the PKC family of proteins. PKC proteins can be activated by tyrosine kinase linked or seven transmembrane receptors via diacylglycerol (Liscovitch, 1992), or by tumour-promoting phorbol esters such as 12-O-tetradecanoyl-phorbol-13-acetate (TPA) (Arcoleo and Weinstein, 1985). Phosphorylation of Ser497 and Ser499 was shown to lead to activation of C-Raf *in vitro* and *in vivo* (Kolch *et al.*, 1993; Carroll and May, 1994). Ser499 was required for the transformation of NIH3T3 cells via a synergistic cooperation of C-Raf and PKC $\alpha$ . Mutating Ser499 impeded C-Raf activation by PKC $\alpha$ , but had no effect on stimulation via Ras or Src. However, later studies observed that the loss of Ser499 and Ser497 did not have any effect on C-Raf stimulation by PKC $\alpha$  or Ras (Barnard *et al.*, 1998; Schonwasser *et al.*, 1998; Chong *et al.*, 2001). It has been suggested that Ras-GTP/Raf complexes are required for C-Raf activation by PKC (Marais *et al.*, 1998). Mutating C-Raf to prevent it associating with Ras blocked PKC activation of C-Raf. Furthermore, dominant negative Ras did not have an effect on C-Raf activation by PKC, suggesting although Ras is required for C-Raf activation by PKC, the mechanism is likely to be distinct from that involving the downstream activation of C-Raf via receptor tyrosine kinases (Marais *et al.*, 1998).

#### **1.4.6 B-Raf specific phosphorylation sites**

The phosphorylation of residues Thr599 and Ser602 of B-Raf are additional phosphorylation sites required for full activation of B-Raf (Zhang and Guan, 2000). Mutation of these sites to alanine abolishes B-Raf activity by oncogenic Ras and replacing them with acidic residues leads to constitutively active B-Raf (Zhang and Guan, 2000). The kinase responsible for the phosphorylation of these sites is yet to be identified. As discussed earlier, Thr599 is important in the hydrophobic interactions between the P-loop and the activation segments of B-Raf. Its phosphorylation is thought to aid the adoption of the DFG motif into its active conformation (Wan *et al.*, 2004). In C-Raf and A-Raf, these

sites are conserved and also require phosphorylation for activation. The equivalent residues in C-Raf are Thr491 and Ser494. Phosphorylation of these sites aid activation, but alone is not sufficient for the full activation of C-Raf (Chong *et al.*, 2001).

The equivalent residue of B-Raf to the negatively phosphorylated Ser259 of C-Raf is Ser365. It is thought that Ser365 negatively regulates B-Raf activity. The serum and glucocorticoid-inducible kinase (SGK) phosphorylates Ser365 and strongly inhibits B-Raf kinase activity (Zhang *et al.*, 2001). Mutating this residue to alanine does not allow SGK induced inhibition of B-Raf.

#### ***1.4.7 Autoregulation of the Raf protein kinases***

In *Xenopus* oocytes it has been shown that the amino terminus of C-Raf contains an autoinhibitory domain that can block the function of the catalytic domain (Cutler *et al.*, 1997). More recently, using HEK 293 cells it was shown that an autoinhibitory domain also exists in mammalian cells. This domain was found to be located at the N-terminus of C-Raf and consists of at least the first 247 amino acids of C-Raf, encompassing the RBD and a portion of the CRD, but not CR2 (Tran *et al.*, 2003). Furthermore it was shown that this regulatory domain functioned by interacting with the catalytic domain of C-Raf and thus prevented activation of ERK2. Phosphorylations of Ser338 and Tyr340/341 were shown to relieve the autoinhibitory effect by reducing the affinity of the amino terminus for the phosphorylated catalytic domain. Thr491 and Ser494, two sites within the activation loop of C-Raf, that have been shown to require phosphorylation during the activation of the protein, were observed as not being involved in relieving the autoinhibition.

Studies have also found a functional N-terminal autoinhibitory domain in B-Raf (Tran *et al.*, 2005). Similar to C-Raf, the N-terminal domain of B-Raf was found to inhibit the catalytic domain of B-Raf in HEK 293 cells. The autoinhibitory domain was found to contain at least residues 100 to 345 of B-Raf. This region includes both the RBD and CRD of B-Raf. The first 100 amino acids were found not to be required for this autoinhibitory regulation. The regulation of this autoinhibition by other residues within the protein was found to be distinct to that observed for C-Raf. Ser446, the equivalent residue to Ser338 of C-Raf, was found not be as important in relieving the autoinhibitory effect for B-Raf.

However, both Ras and PAK1 were shown to slightly increase the phosphorylated levels of Ser446 and it was shown that constitutively phosphorylated Ser446 primes the protein for activation, as upon its mutation, the affinity of the autoinhibitory domain for the catalytic domain increases. However, unlike observations for C-Raf, residues of the activation loop were found to be important in relieving the autoinhibition of B-Raf. Acidic substitutions of Thr599 and Ser602 were seen to block the autoinhibition by affecting the manner in which the two domains interacted. This was also the case upon introduction of V600E B-Raf (Tran *et al.*, 2005). It was also shown that the regulatory domain of C-Raf was able to interact with the catalytic domain of B-Raf, albeit with lower affinity, suggesting cross-regulation may exist between the proteins.

## 1.5 Chaperones

There is growing evidence that the Raf proteins are part of multi-protein complexes. They have been observed to bind to themselves (Luo *et al.*, 1996), bind to the other Raf isoforms (Weber *et al.*, 2001; Wan *et al.*, 2004) and to other members of the Ras/Raf/MEK/ERK pathway, as well as numerous scaffold proteins (Kolch *et al.*, 2000). It is thought the Raf proteins form part of a large signalling complex to aid their activation. Many chaperones are thought to be involved in the activation of the Raf protein kinases. They include; 14-3-3 proteins, heat-shock protein of 90KDa (Hsp90), p50 (Cdc37), suppressor of Ras-8 (Sur-8), Raf kinase inhibitor protein (RKIP) and kinase suppressor of Ras (KSR). The roles each of these are thought to play is described in more detail below.

### 1.5.1 14-3-3

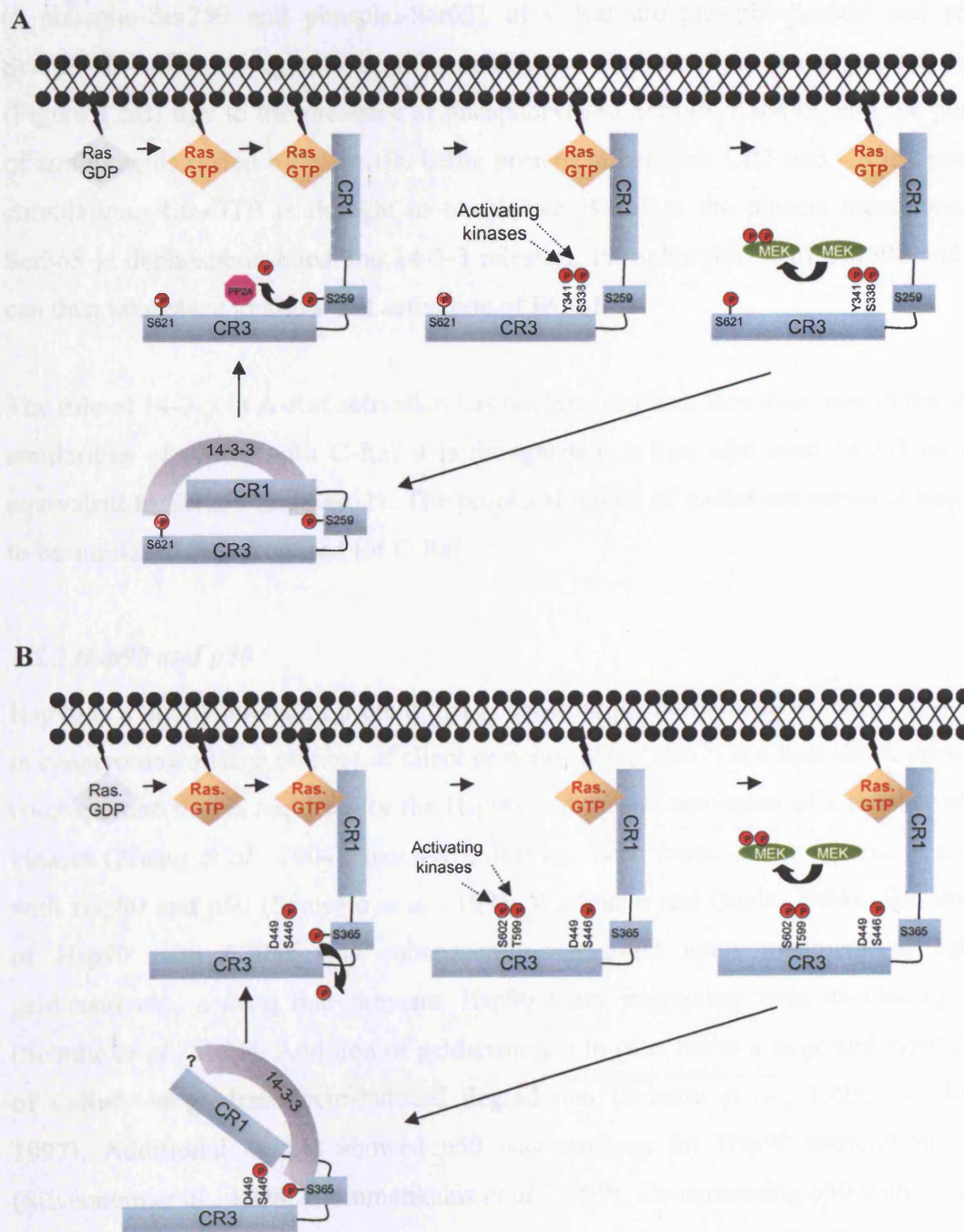
The 14-3-3 family of adaptor-scaffold proteins are highly conserved acidic proteins that can bind to a large number of client proteins (Muslin and Xing, 2000). In some cases phosphorylation of the client protein is required for binding, but in other cases binding is phosphorylation independent (Petosa *et al.*, 1998). It is thought that a major role of 14-3-3 proteins is to bind and sequester client proteins into inappropriate subcellular compartments and thereby preventing their activity (Muslin and Xing, 2000). 14-3-3 has been shown to bind to C-Raf and some suggest its binding is essential for C-Raf activity (Fantl *et al.*, 1994; Freed *et al.*, 1994; Irie *et al.*, 1994; Li *et al.*, 1995; Thorson *et al.*, 1998; Yip-Schneider *et al.*, 2000). However, others have concluded 14-3-3 is not essential for C-Raf activity (Fu *et al.*, 1994; Michaud *et al.*, 1995; Suen *et al.*, 1995). This controversy

arises from the fact that there appears to be two 14-3-3 binding sites on C-Raf that may play opposing roles. 14-3-3 binds to Ser259 in the CR2 region and Ser621 in the CR3 region of C-Raf (Morrison *et al.*, 1993; Morrison, 1995). As mentioned earlier, phosphorylation of Ser259 is thought to suppress C-Raf activity, as mutating this residue to alanine leads to a constitutively active form of C-Raf (Morrison *et al.*, 1993; Clark *et al.*, 1997). Also, Akt and PKA can suppress C-Raf activity by directly phosphorylating Ser259 (Zimmermann and Moelling, 1999; Dhillon *et al.*, 2002b), and it has been shown that protein phosphatase 1 (PP1) and 2A (PP2A) mediate dephosphorylation of Ser259, allowing growth factor stimulated C-Raf activation (Abraham *et al.*, 2000; Jaumot and Hancock, 2001; Kubicek *et al.*, 2002). As mutations of Ser621 inactivate the protein (Morrison *et al.*, 1993), it is difficult to fully understand the role 14-3-3 binding to the CR3 plays. It has been suggested that displacement of 14-3-3 from CR3, together with the dephosphorylation of Ser621, are required for C-Raf activity (Roy *et al.*, 1998; Mischak *et al.*, 1996). However, others state that 14-3-3 binding to, rather than the displacement from, CR3 is required for C-Raf activation. Reduced catalytic activity of C-Raf was observed upon addition of phosphopeptides that displaced 14-3-3 from the catalytic domain of C-Raf (Yip-Schneider *et al.*, 2000). Furthermore, binding of 14-3-3 to CR3 has been shown to protect Ser621 from dephosphorylation, maintaining C-Raf activity (Thorson *et al.*, 1998). Overall, the full mechanism for the role of 14-3-3 in C-Raf activation is yet to be attained.

B-Raf was first shown to interact with 14-3-3 in bovine brain, where it was isolated in a complex with 14-3-3 proteins (Yamamori *et al.*, 1995). It was subsequently shown that the binding involves separate interactions with the N- and C-terminals of B-Raf. Serine 729 in the catalytic domain, equivalent to Ser621 of C-Raf, was suggested as part of a consensus 14-3-3 interaction motif (Papin *et al.*, 1996).

Using current knowledge, Kolch *et al.* (2000) have produced a model proposing the mechanism of C-Raf activation, including the role that 14-3-3 may play (Figure 1.6A). In unstimulated cells, 14-3-3 is bound to C-Raf at phospho-Ser259 and phospho-Ser621 (Morrison *et al.*, 1993; Morrison, 1995) to maintain it in an inactive state. Activation of Ras leads to it binding to C-Raf, and C-Raf being translocated to the plasma membrane (Leever *et al.*, 1993; Stokoe *et al.*, 1993). Here, PP2A removes the phosphate group from Ser259 and 14-3-3 binding is lost (Abraham *et al.*, 2000). This enables activating tyrosine

**Figure 1.6** Models to show the proposed mechanisms of activation of (A) C-Raf and (B) B-Raf. Both proteins reside in the cytoplasm in an inactive state bound to 14-3-3. Recruitment to the plasma membrane by Ras-GTP allows phosphorylation/dephosphorylation events to occur which allows dissociation from 14-3-3 and results in a fully activated Raf protein kinase. Various chaperones, other than 14-3-3, are also thought to be involved in this process, but are not shown on the diagram. (See Section 1.5).



and serine kinases to phosphorylate Tyr341 and Ser338 respectively, for full C-Raf activation.

The model for the activation of B-Raf is thought to be similar, but has a number of variations (Mercer and Pritchard 2003). B-Raf has been shown to interact with 14-3-3 proteins *in vitro* (Papin *et al.*, 1996). It is postulated that B-Raf resides in the cytoplasm bound to 14-3-3. Although the binding sites have not been determined the conserved sites to phospho-Ser259 and phospho-Ser621 of C-Raf are phospho-Ser365 and phospho-Ser729. B-Raf is thought to be in a more open conformation in comparison to C-Raf (Figure 1.6B) due to the presence of phosphorylated Ser446, Asp449, and the possibility of amino acids coded by exon 10a being present in between CR1 and CR3. Upon ligand stimulation, Ras-GTP is thought to translocate B-Raf to the plasma membrane, where Ser365 is dephosphorylated and 14-3-3 released. Phosphorylation of Thr599 and Ser602 can then take place to allow full activation of B-Raf.

The role of 14-3-3 in A-Raf activation has not been studied. However, due to the structural similarities of A-Raf with C-Raf it is thought that it may also bind 14-3-3 on residues equivalent to Ser259 and Ser621. The proposed model of A-Raf activation is also thought to be similar to that proposed for C-Raf.

### **1.5.2 Hsp90 and p50**

Hsp90 is a highly abundant protein that is essential for normal cell function. It is involved in chaperoning a large number of client proteins. p50 (Cdc37) is a heat shock protein and a co-chaperone that is required for the Hsp90 folding and activation of a number of protein kinases (Zhang *et al.*, 2004). Inactive C-Raf has been found in the cytosol in a complex with Hsp90 and p50 (Stancato *et al.*, 1993; Wartmann and Davis, 1994). The association of Hsp90 with C-Raf was subsequently suggested upon treatment of cells with geldanamycin, a drug that prevents Hsp90 from interacting with its binding partners (Schulte *et al.*, 1995). Addition of geldanamycin to cells led to a large and rapid depletion of C-Raf via geldanamycin-induced degradation (Schulte *et al.*, 1995; Schulte *et al.*, 1997). Additional studies showed p50 was required for Hsp90 association of C-Raf (Silverstein *et al.*, 1998; Grammatikakis *et al.*, 1999). Co-expressing p50 with C-Raf led to enhanced Ras and Src induced activity of C-Raf in insect cells. Furthermore, over-

expression of mutant p50, which prevents recruitment of Hsp90 to C-Raf, inhibited C-Raf activation by growth factors (Grammatikakis *et al.*, 1999). It was therefore suggested that formation of a ternary C-Raf/p50/Hsp90 complex is crucial for C-Raf activity. No studies have reported the role of Hsp90 and p50 in the activation of A-Raf. B-Raf has been shown to complex with Hsp90 upon NGF treatment of PC12 cells (Jaiswal *et al.*, 1996), but the involvement of p50 in this association is not known.

### **1.5.3 Sur-8**

Suppressor of Ras-8 (Sur-8) is a non-enzymatic accessory protein identified in *Caenorhabditis elegans*. Sur-8 has been observed to positively regulate Ras-mediated signalling. It was suggested Sur-8 acts downstream or at the level of Ras and may function as part of a Ras/Raf complex (Sieburth *et al.*, 1998). It was subsequently shown that Sur-8 complexed with Ras and Raf, and led to enhanced ERK activity in the presence of C-Raf (Li *et al.*, 2000). The biochemical mechanism of Sur-8 in the activation of C-Raf remains unclear. It is also unknown whether Sur-8 plays a role in A-Raf and B-Raf activation.

### **1.5.4 KSR**

The role of the kinase suppressor of Ras (KSR) in Ras signalling is as a scaffold protein (Muller *et al.*, 2001; Roy *et al.*, 2002). Upon growth factor stimulation KSR promoted MEK phosphorylation by Raf, in a Ras dependent manner. Furthermore, the activity of KSR was shown to be dependent on its ability to independently bind Raf and MEK, suggesting it is involved in co-ordinating a C-Raf/MEK complex (Roy *et al.*, 2002). Studies using RNA interference have confirmed KSR is required for Ras-mediated MAP kinase activation (Anselmo *et al.*, 2002; Ohmachi *et al.*, 2002). A number of proteins involved in the mechanisms of C-Raf activation may play a part in the ability of KSR to facilitate the formation of a C-Raf/MEK complex. 14-3-3 has been shown to bind to KSR (Cacace *et al.*, 1999) and sequester it in the cytoplasm (Muller *et al.*, 2001). More recently it has been discovered that PP2A dephosphorylates KSR as well as C-Raf, and this is required for KSR-mediated ERK activation (Ory *et al.*, 2003).

KSR was identified as a putative kinase protein based on sequence homology to Raf. However, the majority of studies have suggested KSR acts as a scaffold protein and do not report a functional role for the kinase domain. Furthermore, two predicted kinase dead

mutants of KSR were able to complement *ksr-1* loss-of-function alleles in *C. elegans* and reported kinase independent functions in mice (Stewart *et al.*, 1999).

### **1.5.5 RKIP**

Raf Kinase Inhibitory Protein (RKIP, also known as PEBP) is a ubiquitously expressed, evolutionary conserved protein. It has been shown that RKIP can interact and inhibit the activity of a number of kinases including C-Raf (Yeung *et al.*, 1999). RKIP was reported to be an interacting partner of C-Raf, and a negative regulator of the MAPK cascade (Yeung *et al.*, 1999). RKIP was found to be a selective inhibitor of the activation of MEK by C-Raf (Yeung *et al.*, 1999). It was thought that RKIP was involved in competitive interference leading to the dissociation of a C-Raf/MEK complex (Yeung *et al.*, 2000). PKC phosphorylation of RKIP was seen to overcome the inhibition caused by RKIP on MAP kinase signalling, by releasing RKIP from C-Raf (Corbit *et al.*, 2003). Recently a new mechanism has been suggested in which RKIP regulates MAPK signalling. RKIP was shown to bind to subdomains I and II of C-Raf, a region that contains Ser338 and Tyr341 (Yeung *et al.*, 2000). It was shown that RKIP expression inhibited the phosphorylation of Ser338 by Pak and the phosphorylation of Try341 by Src. Moreover, mutating Ser338 and Try341 led to resistance to RKIP inhibition (Trakul *et al.*, 2005).

B-Raf also interacts with RKIP. RKIP has been shown to inhibit B-Raf induced cell signalling in COS-1 and PC12 cells (Park *et al.*, 2005). Another study recently showed that RKIP associates with B-Raf in 293T cells and that this binding is more robust than with C-Raf (Trakul *et al.*, 2005). However, RKIP depletion in both rat hippocampal H19-7 cells and human 293T cells had no effect on EGF-stimulated B-Raf activity (Trakul *et al.*, 2005). Taken together, the data suggests that the role of RKIP in suppressing B-Raf-mediated MAP kinase activity is likely to be cell specific.

## **1.6. Downstream of the Raf protein kinases**

### **1.6.1 MEKs and ERKs**

Early links were made between Ras and ERK upon the findings that oncogenic Ras leads to the activation of ERK1/2 (Leever and Marshall, 1992; Wood *et al.*, 1992), and growth factor stimulation was unable to activate ERK in the presence of a dominant negative form of Ras (de Vries-Smits *et al.*, 1992; Thomas *et al.*, 1992; Wood *et al.*, 1992). C-Raf was

shown to be the protein downstream of Ras that activates ERK (Dent *et al.*, 1992; Howe *et al.*, 1992). Both, v-Raf transformed NIH 3T3 cells and COS cells transfected with C-Raf, were able to activate ERK2. Dominant negative mutants of C-Raf were found to block Ras signalling to ERKs by binding to the Ras effector domain (Kolch *et al.*, 1996). Stimulation of Raf transfected cells with TPA or EGF led to ERK2 activation independent of Ras (Howe *et al.*, 1992). Raf protein kinases do not directly activate ERK. MAPK/ERK kinases (MEKs) are responsible for the phosphorylation and activation of ERK (Gomez and Cohen, 1991; Crews *et al.*, 1992; Nakielny *et al.*, 1992; Seger *et al.*, 1992; Matsuda *et al.*, 1992).

*Mek* cDNAs of two differing forms have been cloned from mouse, rat, human and *Xenopus* (Seger *et al.*, 1992, Wu *et al.*, 1993b, Zheng and Guan, 1993). These give rise to two forms of the protein, namely MEK1 and MEK2. These are dual specificity threonine and tyrosine protein kinases. MEKs are the major and only widely accepted downstream effectors of the Raf protein kinases. All three members of the Raf family can phosphorylate and activate MEK1 and MEK2 *in vitro* (Dent *et al.*, 1992; Howe *et al.*, 1992; Kyriakis *et al.*, 1992; Catling *et al.*, 1994; Pritchard *et al.*, 1995; Reuter *et al.*, 1995). MEK1 is activated by the phosphorylation of Ser218 and Ser222, located in the activation loop of the kinase (Alessi *et al.*, 1994; Zheng and Guan., 1994; Yan and Templeton., 1994). MEK1/2 contain a proline-rich sequence in their kinase region. The role of this sequence is thought to be for the recognition and activation of the MEKs by Raf proteins (Catling *et al.*, 1995). It is thought this sequence may be important for MEK activation by Raf protein kinases, as no other MKKs have been found to contain this sequence.

Other proteins have been shown to activate MEK, but to a lesser degree than the Raf protein kinases. These include MEKK-1 (Lange-Carter *et al.*, 1993), Mos (Pham *et al.*, 1995) and Tpl-2 (Salmeron *et al.*, 1996). Although the Raf protein kinases are the predominant MEK activators, the ability of each Raf isoform to activate MEK also varies. B-Raf is by far the strongest activator of MEK in many cell types. This has been concluded for a number of cell types including fibroblasts, neuronal tissue and lymphocytes (Hüser *et al.*, 2001; Catling *et al.*, 1994; Reuter *et al.*, 1995; Jaiswal *et al.*, 1994; Eychene *et al.*, 1995; Jaiswal *et al.*, 1996; Kao *et al.*, 2001). C-Raf activates MEK to a lesser extent than B-Raf, but to a greater extent than A-Raf, which shows very little activity towards MEK (Pritchard *et al.*, 1995; Marais *et al.*, 1997, Papin *et al.*, 1998; Hüser

*et al.*, 2001). The differing abilities of each Raf isoform in activating MEK suggests they may play different roles in cell signalling.

In mammals there are two forms of ERK proteins; ERK1 and ERK2. The ERKs are phosphorylated by MEK1/2 on threonine and tyrosine residues within the sequence -Thr-Glu-Tyr-. The exact phosphorylation sites were mapped to residues Thr183 and Tyr185 (Payne *et al.*, 1991). ERK proteins are serine/threonine protein kinases that can activate a wide range of substrates. They are located both in the cytoplasm and the nucleus, so provide a physical link between these two regions of the cell. Upon mitogenic stimulation ERK has been observed to translocate from the cytoplasm to the nucleus (Chen *et al.*, 1992; Sanghera *et al.*, 1992). ERK1/2 provide a link from the outside of the cell to the nucleus.

### **1.6.2 Other Raf protein binding partners**

The Raf protein kinases have been shown to interact with other proteins besides MEK1 and MEK2. A-Raf interacts with the  $\beta$  regulatory subunit of casein kinase 2 (CK2) (Boldyreff and Issinger, 1997) and been shown to interact with two proteins that may be involved in the mitochondrial transport of A-Raf, namely hTOM and hTIM (Yuryev *et al.*, 2000). C-Raf has been shown to have MEK-independent roles in apoptosis (Hüser *et al.*, 2001; Mikula *et al.*, 2001) that may involve binding to other proteins. This is discussed in more detail later in this chapter. A large number of Raf-associating proteins have been described in the literature. Some of which are phosphorylated by Raf in *in vitro* kinase assays. However, none have yet been proven to be true physiological substrates of Raf. (A summary of Raf-associating proteins are reported in the review by Kolch, 2000.)

### **1.6.3 Downstream of ERKs**

ERK1/2 have a wide substrate specificity and the identification of new substrates is still underway. ERK1/2 are proline-directed protein kinases and have been shown to have specificity for substrates containing the sequence ser-(Thr)-Pro ((S/T)P) with a *trans* prolyl bond adjacent to the reactive serine residue (Weiwad *et al.*, 2000). It is thought ERK1/2 may be involved in a feedback mechanism, as two of their targets are their upstream activators C-Raf and MEK (Anderson *et al.*, 1991; Lee *et al.*, 1992; Matsuda *et al.*, 1993). ERK has been observed to hyperphosphorylate specific sites and desensitize C-Raf,

preventing any additional activation events, and indicating regulation of C-Raf via feedback phosphorylation. It was further shown that PP2A and Pin1 interact with the desensitized C-Raf to return it to its resting and activation-competent state (Dougherty *et al.*, 2005). PP2A dephosphorylates p(S/T)P sites in the *trans* form and this would agree with the role of ERK in its phosphorylation of *trans* (S/T)P sites. Pin1 isomerase binds to p(S/T)P sites and can convert them between *trans* and *cis* forms. It is thought some of the hyperphosphorylated sites of C-Raf may switch to a *cis* formation after ERK phosphorylation, therefore requiring Pin1 activity before dephosphorylation by PP2A can occur (Dougherty *et al.*, 2005).

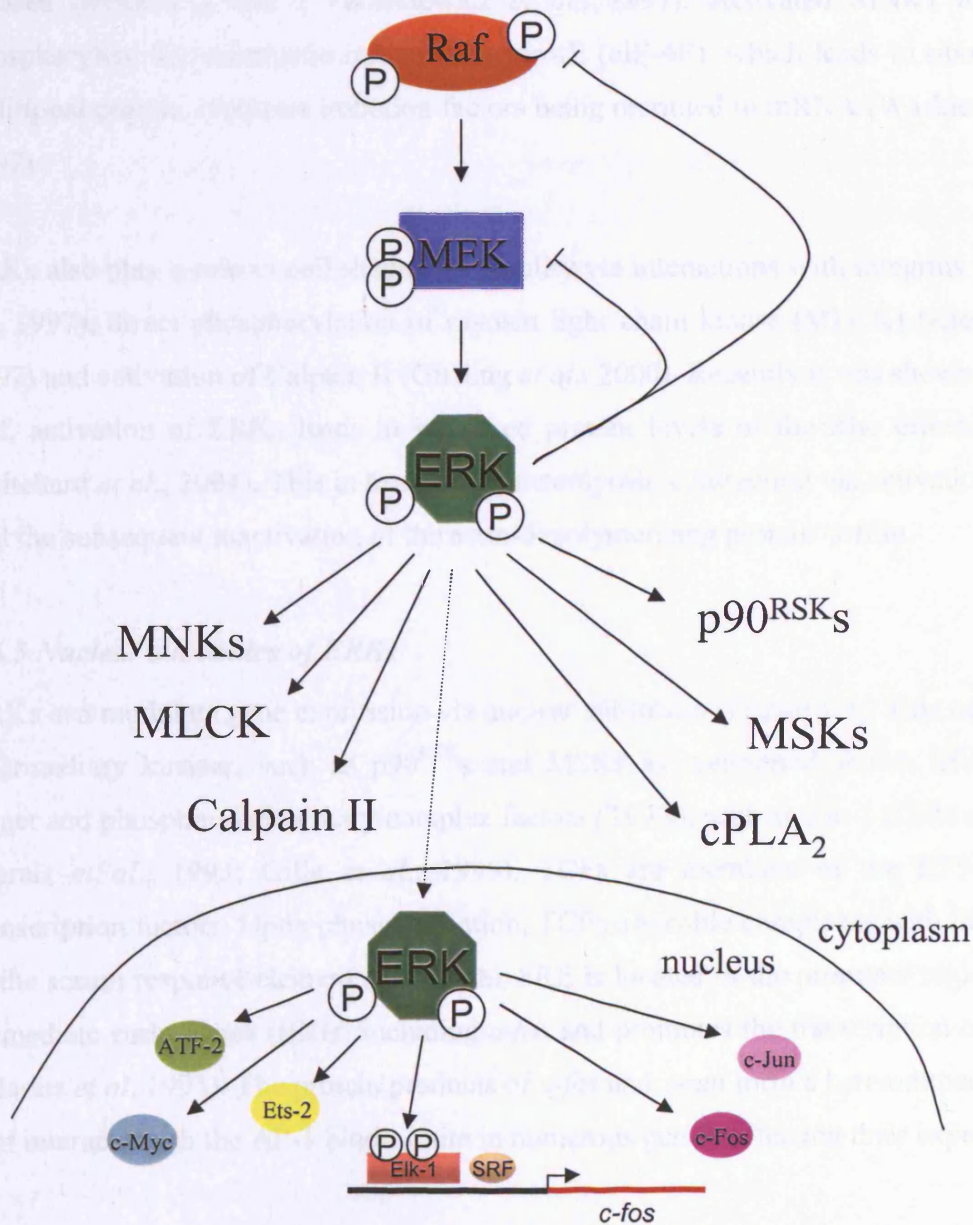
#### 1.6.4 Cytoplasmic substrates of ERKs

Downstream substrates of the ERKs include membrane and cytoplasmic substrates (Figure 1.7) including the EGF receptor (Northwood *et al.*, 1991; Takishima *et al.*, 1991) and cPLA<sub>2</sub> (Lin *et al.*, 1993).

ERK1/2 target protein kinases such as the p90 ribosomal S6 kinases (p90<sup>RSK</sup>s) (Sturgill *et al.*, 1988). There are four human RSK isoforms, all of which are activated by ERK1/2. Inactive p90<sup>RSK</sup>s reside in the cytoplasm. Like ERKs, upon activation they can either remain in the cytoplasm or translocate to the nucleus. Once activated, downstream targets phosphorylated by p90<sup>RSK</sup>s include proteins involved in transcriptional activation, such as the c-AMP-response element binding protein (CREB) (Xing *et al.*, 1996; Pende *et al.*, 1997; Xing *et al.*, 1998), c-Fos (Chen *et al.*, 1993; Chen *et al.*, 1996), and the serum response factor (SRF) (Rivera *et al.*, 1993). As well as their role in transcriptional regulation, p90<sup>RSK</sup>s may play a part in cell cycle control. A role for p90<sup>RSK</sup>s in promoting cell cycle progression via the possible phosphorylation of the cyclin-dependent kinase inhibitor p27<sup>KIP1</sup> has been reported (Fujita *et al.*, 2003). p90<sup>RSK</sup>s are also involved in cell survival, as discussed later in this chapter.

Another subfamily of proteins that are ERK substrates are the mitogen- and stress activated kinases (MSKs). There are two members of this subfamily, MSK1 and MSK2. These proteins share a high sequence homology with the p90<sup>RSK</sup>s, but unlike the p90<sup>RSK</sup>s, are known to be activated by stress stimuli as well as mitogens. MSKs are involved in transcriptional regulation by mediating activation of CREB and ATF-1 (Deak *et al.*, 1998;

**Figure 1.7** Substrates of the ERK1/2 protein kinases. ERK1/2 target both cytoplasmic and nuclear substrates.



Wiggin *et al.*, 2002; Lee *et al.*, 2003a) and the transcriptional regulation of *nurr77* (Darragh *et al.*, 2005). MSKs are also involved in nucleosomal responses by the phosphorylation of histone H3 (Soloaga *et al.*, 2003).

Another set of ERK1/2 substrates are the serine/threonine kinases; MAP kinase interacting kinases (MNKs) 1 and 2 (Waskiewicz *et al.*, 1997). Activated MNK1 and MNK2 phosphorylate the eukaryotic initiation factor 4E (eIF-4E), which leads to ribosomes and additional protein synthesis initiation factors being recruited to mRNA (Waskiewicz *et al.*, 1997).

ERKs also play a role in cell shape and motility via interactions with integrins (Hughes *et al.*, 1997), direct phosphorylation of myosin light chain kinase (MLCK) (Klemke *et al.*, 1997) and activation of Calpain II (Glading *et al.*, 2000). Recently it was shown that via B-Raf, activation of ERKs leads to increased protein levels of the Rho effector ROCKII (Pritchard *et al.*, 2004). This in turn affects actomyosin contraction via activation of LIMK and the subsequent inactivation of the actin-depolymerising protein cofilin.

### **1.6.5 Nuclear substrates of ERKs**

ERKs can modulate gene expression via nuclear substrates (Figure 1.7). This can occur via intermediary kinases, such as p90<sup>RSK</sup>s and MSKs as mentioned above. ERKs directly target and phosphorylate ternary complex factors (TCFs), such as Elk-1 (Gille *et al.*, 1992; Marais *et al.*, 1993; Gille *et al.*, 1995). TCFs are members of the ETS family of transcription factors. Upon phosphorylation, TCFs assemble complexes with SRF proteins at the serum response element (SRE). The SRE is located in the promoter region of many immediate early genes (IEGs) including *c-fos* and promotes the transcription of the genes (Marais *et al.*, 1993). The protein products of *c-fos* and *c-jun* form a heterodimeric complex that interacts with the AP-1 binding site in numerous genes, affecting their expression.

ERKs have been observed to directly phosphorylate a number of IEG products. These include members of the AP-1 family of transcription factors, such as c-Jun (Pulverer *et al.*, 1991; Smeal *et al.*, 1991), c-Fos (Chen *et al.*, 1993; Chen *et al.*, 1996) as well as ATF-2 (Abdel-Hafiz *et al.*, 1992). Other transcription factors phosphorylated by the ERKs include

c-Myc (Alvarez *et al.*, 1991; Gupta *et al.*, 1993), and the TNF Ets-2 (McCarthy *et al.*, 1997).

Recently a mechanism has been discovered that allows cells to interpret differences in ERK activity. This has been shown to occur via c-Fos (Murphy *et al.*, 2002). It appears the phosphorylation of c-Fos by ERK is dependent on the duration of ERK activity. Transient ERK activity was observed upon treatment of fibroblasts with EGF, but sustained ERK activity was seen upon stimulation with PDGF. The latter stimulation promoted cell proliferation (Murphy *et al.*, 2002). It was discovered that upon transient ERK activity c-Fos was present in the nucleus but not phosphorylated, leading to it being unstable and therefore degraded. However, sustained ERK activity led to the phosphorylation of c-Fos, this in turn exposed a DEF domain on c-Fos, which promoted further phosphorylation by ERK, resulting in a stabilised form of c-Fos. This stabilised form of c-Fos was found to take part in mechanisms to promote cell proliferation (Murphy *et al.*, 2002), as described in Section 1.7. It is thought ERK activity may influence other IEGs in this way, as putative DEF domains have been located in c-Myc, as well as the AP-1 proteins Fra-1, Fra-2, JunB and JunD (Murphy *et al.*, 2002).

### 1.7 Proliferation

The cell cycle is made up of four phases; G1, S, G2 and M. When no growth factor stimulation is supplied to a cell it remains in a resting state known as G0. Progression from the resting state into the cell cycle leads to entry into G1. This transition is stimulated by growth factors, and these are also required to ensure subsequent continuation through G1 and into the S phase. S phase is where DNA duplication takes place and is followed by G2. Transition through G2 leads to the M phase where chromosome segregation and cytokinesis occur. There are many check points during the cell cycle to try to ensure inappropriate proliferation does not take place. The control of the cell cycle relies on a series of kinase activities that promote transition through each phase. Cyclin-dependent kinases (cdks) are key regulatory proteins important in these transitions. Cdks rely on protein binding partners for their activity, namely cyclins.

The cyclins involved early on in the G1 to S phase transition are cyclins D1, D2 and D3. The cdk binding partners of the D type cyclins are cdk4 and cdk6. Cyclin D-cdk4/6

complexes were found to be essential for entry into the G1 phase (Sherr, 1994). Cyclin E, which associates with cdk2, regulates the G1 to S phase transition towards the end of G1 (Ohtsubo *et al.*, 1995). Cyclin D is synthesised as long as mitogenic stimulation persists. Upon stimulation, during early to mid G1, D-type cyclins and their associated cdks phosphorylate the retinoblastoma protein (Rb) (Kato *et al.*, 1993). Phosphorylated Rb (pRb) is disrupted from the complex it forms with E2F transcription factors. Upon release E2F transcription factors can positively regulate the transcription of genes whose products are required for the latter part of G1, including cyclin E (Buchkovich *et al.*, 1989; Kato *et al.*, 1993; Brehm *et al.*, 1998). Cyclin E-cdk2 complexes are partly responsible for maintaining pRb in a hyperphosphorylated state for the remainder of the cell cycle. Hyperphosphorylated pRb is unable to bind to its complex partners, enabling them to promote expression of genes required for S phase such as cyclin A and cdc25.

Cdk activity can be counteracted by cell cycle inhibitory proteins known as Cdk inhibitors (CKIs). CKIs bind to cdks alone or to cdk-cyclin complexes in order to regulate cdk activity. There are two distinct families of CKIs; the cyclin-dependent kinase-interacting protein/kinase-interacting protein (Cip/Kip) family and the inhibitor of cyclin-dependent kinase 4 (INK4) family (Sherr and Roberts, 1995). The INK4 family includes p15 (INK4b), p16 (INK4a), p18 (INK4c) and p19 (INK4d). These inhibitory proteins specifically inactivate cdk4 and cdk6. They form stable complexes with the cdks before cyclin-binding can take place, thus preventing binding with the D-type cyclins (Carnero and Hannon, 1998). The Cip/Kip family includes p21 (Waf1, Cip1), p27 (Cip2, Kip1) and p57 (Kip2). These CKIs can inactivate the cyclin E-cdk complexes as well as the cyclin D-cdk complexes (Polyak *et al.*, 1994; Harper *et al.*, 1995; Lee *et al.*, 1995b). However p21<sup>CIP1</sup> has also been shown to promote the cell cycle by attaching to cyclin D-cdk4 complexes (LaBaer *et al.*, 1997), and p27<sup>KIP</sup> has been shown to play a role in tumourigenesis and may also promote proliferation under some circumstances (Nho and Sheaff *et al.*, 2003). Therefore these proteins may be involved in cell proliferation as well as inhibition.

Entry from G0 and progression through G1 requires mitogenic stimuli and it has long been thought that the sustained expression of D-type cyclins via mitogenic stimuli is required for progression from G1 to S phase (Sherr and Roberts, 1999). However, recent findings from the generation of mice lacking all three cyclin D genes question this view (Kozar *et*

*al.*, 2004). Cyclin D-null mice survived to mid-gestation and only showed abnormalities at E13.5. Many of the cyclin D-null MEFs generated were able to resume proliferation upon serum stimulation after a brief period of quiescence, and this was thought to be due to cyclin E-cdk2 complexes being able to compensate for the lack of activity of cyclin D-cdk4/6 complexes (Kozar *et al.*, 2004). These findings suggest D-type cyclins are non-essential for somatic cell cycles. A role for cyclin D was suggested for the exit from quiescence, as not all cells were able to re-enter the cell cycle and severe re-entry defects were observed upon stimulation with low serum concentrations. Similar conclusions were also drawn upon the production of cyclin E-null mice (Geng *et al.*, 2003). Production of null mice for the cdk4 and cdk6 protein kinases has also questioned their essential requirement during the cell cycle, as cdk2 was shown to compensate in their absence (Reviewed in Sherr and Roberts, 2004).

### **1.7.1 The Raf/MEK/ERK cascade and proliferation**

The Raf/MEK/ERK pathway couples signals from cell surface receptors to transcription factors, including many involved in cellular proliferation. ERKs have been shown to play a role in the regulation of the G1 to S phase of the cell cycle. Upon activation ERKs translocate to the nucleus where they can phosphorylate transcription factors including members of the c-Fos (c-Fos, FosB, Fra-1 and Fra-2) and c-Jun (c-Jun, Jun-B and Jun-D) families of proteins (Whitmarsh and Davis, 1996; Balmano and Cook, 1999; Cook *et al.*, 1999; Shaulian and Karin, 2002). Members of these families form heterodimeric AP-1 complexes that are able to bind to AP-1 binding sites found in the promoter region of many genes, including cyclin D1 (Angel and Karin, 1991; Albanese *et al.*, 1995). This promotes the expression of cyclin D1, leading to the phosphorylation and derepression of the Rb protein by the cyclin D/cdk4/6 complexes, resulting in the release of the E2F transcription factors. This in turn allows expression of various genes required to progress through the G1 to S phase of the cell cycle.

ERKs are also shown to play a role in cellular proliferation by phosphorylating the transcription factor c-Myc (Alvarez *et al.*, 1991; Gupta *et al.*, 1993), which has been suggested to target cdk4 (Hermeking *et al.*, 2000). ERKs also phosphorylate p90<sup>RSK</sup>s. p90<sup>RSK</sup>s in turn can regulate the SRE (Rivera *et al.*, 1993), CREB (Xing *et al.*, 1996; Pende *et al.*, 1997; Xing *et al.*, 1998) and c-Fos (Chen *et al.*, 1993; Chen *et al.*, 1996). p90<sup>RSK</sup>s

have also been linked to the phosphorylation of the CKI, p27<sup>KIP1</sup>. This phosphorylation allows 14-3-3 to bind to p27<sup>KIP1</sup>, leading to its cytoplasmic localisation (Fujita *et al.*, 2003). p27<sup>KIP1</sup> is also targeted by c-Myc, whereas p21<sup>CIP1</sup> is a transcriptional target of both Ets-1 and c-Myc (Beier *et al.*, 1999; Gartel *et al.*, 2001). Cyclin E is transcriptionally activated by CREB, AP-1 and c-Myc (Jansen-Durr *et al.*, 1993; Perez-Roger *et al.*, 1997).

### **1.7.2 Raf protein kinases and proliferation**

Expression of activated Raf proteins has been associated with increased cell proliferation in many cell types including hematopoietic cells (Muszynski *et al.*, 1995), murine NIH 3T3 fibroblasts (Kerkhoff and Rapp, 1997; Kerkhoff *et al.*, 1998) and A10 smooth muscle cells (Cioffi *et al.*, 1997). However, overexpression of activated Raf proteins have also been shown to lead to cell cycle arrest in some cell lines including rat Schwann cells, human promyelocytic leukaemia cells (Lloyd *et al.*, 1997) and small cell lung cancer cells (Ravi *et al.*, 1998). The conflicting results observed are thought to depend on the Raf isoform being expressed and its level of activity.

Studies involving conditionally-active  $\Delta$ Raf:ER proteins have been used to investigate the role Raf proteins play in cell proliferation. Constructs were produced by fusing the CR3 domain of each Raf isoform with the human hormone-binding domain of the estrogen receptor (hbER) to give  $\Delta$ C-Raf:ER,  $\Delta$ B-Raf:ER and  $\Delta$ A-Raf:ER (Samuels *et al.*, 1993; Pritchard *et al.*, 1995). Raf is activated in cells expressing these constructs by the addition of estradiol. Adding estradiol to quiescent NIH 3T3 cells expressing either  $\Delta$ C-Raf:ER or  $\Delta$ B-Raf:ER did not promote cell cycle progression and was shown to inhibit mitogenic responses of the cells to subsequent additions of EGF and PDGF. In contrast, estradiol addition to  $\Delta$ A-Raf:ER expressing NIH 3T3 allowed quiescent cells to enter S phase, and no inhibition to mitogenic responses of the cells upon subsequent growth factor stimulation was observed (Pritchard *et al.*, 1995). The differences observed in the ability to promote cell proliferation by the three isoforms of Raf was thought to be due to the differences observed in their abilities to activate MEK.  $\Delta$ B-Raf:ER was found to phosphorylate and activate MEK with the greatest efficiency, followed by  $\Delta$ C-Raf:ER, with  $\Delta$ A-Raf:ER activating MEK the least efficiently (Pritchard *et al.*, 1995).

Further studies utilising the conditionally-active  $\Delta$ Raf:ER constructs were subsequently performed. It was observed that all three activated  $\Delta$ Raf:ER proteins were able to strongly induce cyclin D1 expression, and that this induction correlated with the differing abilities of each Raf isoform to activate MEK/ERK. Cyclin E was also induced by all three activated  $\Delta$ Raf:ER proteins but this did not correlate with MEK activation (Woods *et al.*, 1997). Investigating CKIs showed that all three activated  $\Delta$ Raf:ER proteins were able to repress p27<sup>KIP1</sup> expression, but differences were observed in the regulation of p21<sup>CIP1</sup>. Both  $\Delta$ C-Raf:ER and  $\Delta$ B-Raf:ER strongly induced the expression of p21<sup>CIP1</sup>, whereas  $\Delta$ A-Raf:ER did not. This provided an explanation as to why both  $\Delta$ C-Raf:ER and  $\Delta$ B-Raf:ER activation led to G1 cell cycle arrest, but activation of  $\Delta$ A-Raf:ER allowed entry into the cell cycle (Woods *et al.*, 1997). Furthermore, it was shown that the activation of the various  $\Delta$ Raf:ER proteins could be manipulated by altering the concentration of estradiol used for stimulation. It was concluded that low levels of Raf activity led to activation of both cyclin D1-cdk4 and cyclin E1-cdk2 complexes, leading to NIH 3T3 cell proliferation, whereas high levels of Raf activity associated with high MAPK activity caused cell cycle arrest and correlated with p21<sup>CIP1</sup> induction and inhibition of cyclin-cdk activity.

A study looking into the relationship of cAMP, C-Raf, ERK activity and cell cycle re-entry utilised the conditionally-active  $\Delta$ C-Raf:ER construct mentioned earlier (Samuels *et al.*, 1993; Pritchard *et al.*, 1995). Three cell lines, namely CC139, NIH 3T3 and Rat-1 cells, expressing the  $\Delta$ C-Raf:ER construct were analysed.  $\Delta$ C-Raf:ER chimeras contain the kinase domain of C-Raf only and thus lack the three serine residues (Ser43, Ser233 and Ser259) thought to be involved in cAMP mediated inhibition of C-Raf. All three cell lines were found to be resistant to inhibition of C-Raf induced ERK1/2 activity by cAMP, suggesting the importance of the N terminal in C-Raf inhibition via elevated cAMP levels (Balmanno *et al.*, 2003). Furthermore, although  $\Delta$ C-Raf:ER signalling to various AP-1 proteins was found to be insensitive to cAMP,  $\Delta$ C-Raf:ER stimulated DNA synthesis was still inhibited by cAMP. Therefore, since cAMP did not inhibit ERK activity downstream of C-Raf in these cell lines, but blocked cell cycle re-entry downstream of ERK1/2, it suggested cAMP plays a role in the regulation of other targets of S-phase. Assessment of various proteins involved in S-phase indicated cAMP was able to inhibit cdk2 activation via  $\Delta$ C-Raf:ER. This was postulated to occur via blockage of cdc25A and cyclin A and possibly by preventing p27<sup>KIP</sup> degradation (Balmanno *et al.*, 2003). This study again

indicates cAMP regulates downstream targets, as well as proteins of the Raf/MEK/ERK pathway.

A direct link between the Raf and Akt signalling pathway during cell cycle re-entry has also been reported (Gille *et al.*, 1999). Recent work has investigated the mechanisms that may be involved and has shown both pathways can co-operate to promote cell proliferation (Mirza *et al.*, 2004). Using NIH 3T3 cells containing conditionally active forms of Raf and Akt, it was observed co-activation of Raf and Akt led to co-operation in the induction of cyclin D1 and in the repression of p27<sup>KIP1</sup> expression. Furthermore it was found that Akt was able to promote the removal of Raf-induced p21<sup>CIP</sup> suppression of cdk2 complexes, leading to sustained cyclin E/cdk2 activity (Mirza *et al.*, 2004).

A direct link between Rb and C-Raf has also been suggested. Rb was shown to physically interact with C-Raf both *in vitro* and *in vivo* in human fibroblasts. Moreover, this interaction required mitogenic stimulation, was only present in proliferating cells and is thought to aid proliferation by inhibiting Rb activity, thus reversing the Rb-mediated suppression of E2F transcription factors (Wang *et al.*, 1998a). Furthermore, it was observed that the inactivation of Rb by C-Raf is independent of the Ras/Raf/MEK/ERK cascade and cdks (Dasgupta *et al.*, 2004). Using a peptide to disrupt the Rb/C-Raf interaction, a reduction in tumour growth was observed in nude mice (Dasgupta *et al.*, 2004). These data suggests an important role for C-Raf in cell proliferation that is independent of its MEK kinase activity.

## 1.8 Apoptosis

Apoptosis or programmed cell death is a mode of cell death used by multicellular organisms to maintain cellular homeostasis. Loss of control of the apoptotic programme contributes to the development of many diseases including cancer, AIDS, neuro-degenerative diseases, stroke and heart failure. The morphological definition of apoptosis includes cell shrinkage, chromatin compaction, plasma-membrane blebbing and collapse of the cell into small intact fragments (apoptotic bodies) that are removed by phagocytes (Savill and Fadok, 2000).

Apoptosis can be induced by a variety of stimuli including activation of death receptors, UV or  $\gamma$ -irradiation, growth factor withdrawal and chemotherapeutic drugs. Detailed studies of apoptosis were first carried out in *Caenorhabditis elegans*, in which a number of genes involved in apoptosis, including members of the *ced* family, have been characterised (Hengartner *et al.*, 1994). In mammals, genes shown to have similarities to the *ced* genes include the caspase gene family. This gene family encodes for cysteine-dependent aspartic acid-directed proteases that have been found to be central regulators in the process of apoptosis. Caspases consist of an N terminal pro-domain, followed by large and small subunits. They are synthesised as relatively inactive zymogens and conversion into an active enzyme requires a minimum of two cleavages, both occurring at specific aspartic acid cleavage sites (Cohen, 1997).

The caspases can be divided into two sub-groups; initiator (upstream) caspases, such as caspases 8, 9 and 10, and effector (downstream) caspases including caspases 3, 6 and 7. Initiator caspases tend to have large pro-domains and initiate the apoptotic response by activating the effector caspases. The latter consist of shorter pro-domains and are thought to be involved in the majority of substrate proteolysis that occurs during apoptosis (Earnshaw *et al.*, 1999). Over 50 direct or indirect substrates of the caspases have been proposed. Caspases cleave key structural and regulatory proteins including a large range of cytoskeletal and nuclear proteins, as well as some involved in signalling pathways (reviewed in Earnshaw *et al.*, 1999). Two pathways through which the activation of pro-caspases are triggered have been identified. These are the death receptor-mediated apoptosis pathway and the mitochondria-mediated apoptosis pathway.

### ***1.8.1 Death receptor-mediated apoptosis pathway***

The death receptor-mediated apoptosis pathway is activated by death receptors. (Schmitz *et al.*, 2000; Figure 1.8) These receptors are members of a subgroup of the type 1 TNF/NFG receptor superfamily. They contain an intracellular death domain required for the transduction of the apoptotic signal. Members of the superfamily include TNF-R1, CD95, TRAIL-R1, TRAIL-R2 and DR6. Each death receptor is activated through its own natural ligand. These ligands have co-evolved as the TNF family. The process via which death receptors mediate apoptosis is most well studied for CD95. Upon binding of CD95 ligand, the CD95 receptor is triggered to undergo trimerization. This facilitates the binding

of the adaptor molecule FADD (Fas-associated death domain)/Mort1 via interactions in the C-termini of both polypeptides. Pro-caspase 8 is also recruited, leading to oligomerisation of CD95 and the formation of the death-inducing signalling complex (DISC). Pro-caspase 8 is subsequently auto-proteolytically cleaved at the DISC and initiates the activation of the effector caspase 3 (Schmitz *et al.*, 2000). Another death receptor TNF-R1, binds the adapter molecule TRADD (TNFR-associated death domain) upon ligand activation. However, TNF-R1 does not initiate apoptosis via a membrane bound DISC, but via a secondary intracellular signalling complex involving FADD and caspase 8 (Micheau & Tschopp, 2003).

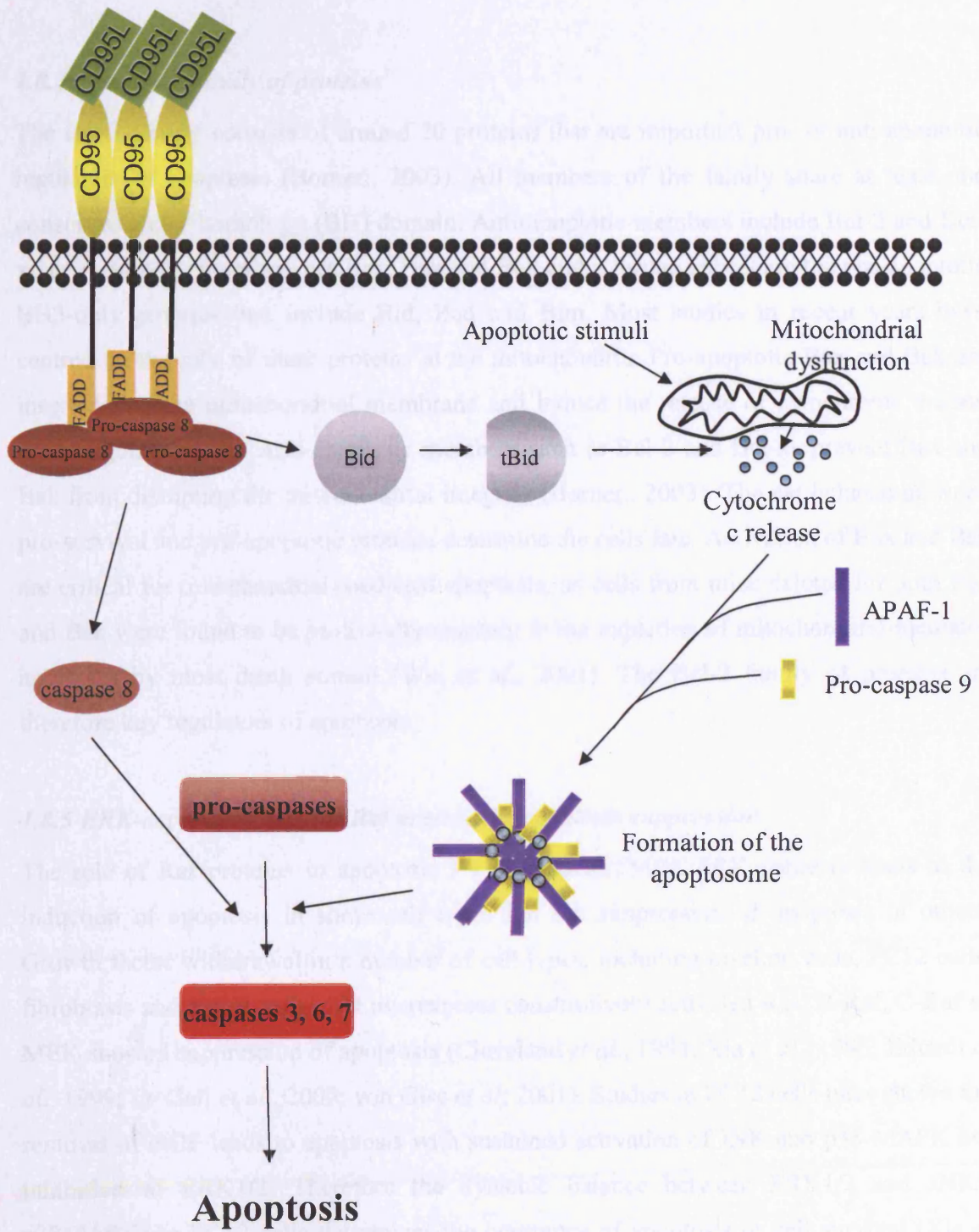
### ***1.8.2 Mitochondria-mediated apoptosis pathway***

Some stimuli including stress signals trigger apoptosis without the involvement of death receptors (Figure 1.8). Activation of initiator caspases can lead to the release of the electron transport protein cytochrome *c* into the cytosol (Yang *et al.*, 1997; Kluck *et al.*, 1997; Liu *et al.*, 1996). The release of cytochrome *c* is tightly regulated by members of the Bcl-2 family of proteins. Released cytochrome *c* binds to the co-factor apoptotic protease activating factor-1 (Apaf-1), in the presence of dATP/ATP, and promotes the assembly of the apoptosome. This large multimeric complex is formed by the oligomerisation of Apaf-1, and leads to the recruitment and activation of procaspase 9 into the complex (Zou *et al.*, 1999; Acehan *et al.*, 2002). This results in the auto-processing and cleavage of the effector pro-caspases 3 and 7 by the activated caspase 9.

### ***1.8.3 Linkage of the death receptor & mitochondria mediated apoptosis pathways***

The two apoptotic pathways are linked via caspase 8 as shown in Figure 1.8. Caspase 8 can lead to apoptosis via the death receptor mediated pathway. However, it is also involved in the induction of mitochondrial damage via Bid. Bid, a death agonist and member of the Bcl-2 family, has been shown to be cleaved, and thus activated by caspase 8, in response to death receptor signals (Li *et al.*, 1998). Truncated Bid (tBid) translocates to the mitochondria where it can induce oligomerization of Bax and/or Bak (Korsmeyer *et al.*, 2000). Cytochrome *c* is then released from the mitochondria. The precise mechanism via which this occurs still remains unclear. It has been suggested that tBid itself may induce the release, however tBid may also be indirectly involved and the release may be induced by Bax, Bak or another protein.

**Figure 1.8** Death receptor (CD95) and mitochondrial mediated apoptosis pathways. The two pathways are linked via caspase 8-mediated truncation of Bid.



The precise role of cytochrome *c* release in Fas mediated apoptosis still remains unclear. Although studies have shown the involvement of cytochrome *c* in CD95 ligand mediated apoptosis in hepatocytes (Yin *et al.*, 1999), this has been shown not to be the case in other cell lines, such as lymphoid cells and embryonic fibroblasts (Gross *et al.*, 1999).

#### ***1.8.4 The Bcl-2 family of proteins***

The Bcl-2 family consists of around 20 proteins that are important pro- or anti-apoptotic regulators of apoptosis (Borner., 2003). All members of the family share at least one conserved Bcl-2 homology (BH) domain. Anti-apoptotic members include Bcl-2 and Bcl-x<sub>L</sub>, pro-apoptotic members are Bax, Bak and Bok and a further subset are the pro-apoptotic BH3-only proteins that include Bid, Bad and Bim. Most studies in recent years have centred on the role of these proteins at the mitochondria. Pro-apoptotic Bax and Bak are inserted into the mitochondrial membrane and induce the release of cytochrome *c* upon their oligomerisation. Anti-apoptotic members such as Bcl-2 and Bcl-x<sub>L</sub> prevent Bax and Bak from disrupting the mitochondrial integrity (Borner., 2003). The net balance between pro-survival and pro-apoptotic proteins determine the cells fate. Activation of Bax and Bak are critical for mitochondrial-mediated apoptosis, as cells from mice deleted for both Bax and Bak were found to be profoundly resistant to the induction of mitochondrial-mediated apoptosis by most death stimuli (Wei *et al.*, 2001). The Bcl-2 family of proteins are therefore key regulators of apoptosis.

#### ***1.8.5 ERK-dependent role for Raf proteins in apoptosis suppression***

The role of Raf proteins in apoptosis via the Ras/Raf/MEK/ERK pathway leads to the induction of apoptosis in some cell types but the suppression of apoptosis in others. Growth factor withdrawal in a number of cell types, including myeloid cells, PC12 cells, fibroblasts and pro-B cells, that overexpress constitutively activated Ras, B-Raf, C-Raf or MEK showed suppression of apoptosis (Cleveland *et al.*, 1994; Xia *et al.*, 1995; Erhardt *et al.*, 1999; Le Gall *et al.*, 2000; von Gise *et al.*; 2001). Studies in PC12 cells have shown the removal of NGF leads to apoptosis with sustained activation of JNK and p38-MAPK but inhibition of ERK1/2. Therefore the dynamic balance between ERK1/2 and JNK/-p38MAPKs in PC12 cells determines the occurrence of apoptosis or cell survival (Xia *et al.*, 1995).

As well as activating the Raf/MEK/ERK pathway, Ras is the activator of the PI3-K/Akt pathway. This pathway is important for its role in cell survival. Ras interlinking the two pathways may have an effect on whether the Raf/MEK/ERK pathway has pro- or anti-apoptotic effects. In fibroblasts Ras utilises the PI3-K/Akt pathway in the suppression of c-Myc induced apoptosis (Kauffmann-Zeh *et al.*, 1997). However, in this system, serum withdrawal promoted apoptosis via the Raf/MEK/ERK pathway, and this was rescued by activated PI3-K. It has also been observed in myeloid cells that PI3-K/Akt is required for constitutively active C-Raf or MEK1 suppression of apoptosis (von Gise *et al.*; 2001). Therefore it is likely that Ras determines the suppression or induction of apoptosis via these two pathways.

B-Raf has been directly linked with suppressing apoptosis via the activation of MEK/ERK (Erhardt *et al.*, 1999). Fibroblasts over-expressing B-Raf, subjected to growth factor deprivation, were resistant to apoptosis and this resistance was lost when a specific MEK inhibitor was used. Furthermore, the over-expression of B-Raf within these cells resulted in increased ERK activity, but no alterations in the PI3-K/Akt pathway. The anti-apoptotic effects of B-Raf were shown to be downstream of the release of cytochrome c from the mitochondria (Erhardt *et al.*, 1999). ERKs have been shown to regulate a number of proteins involved in apoptosis. This includes both nuclear and cytoplasmic targets as described below.

### **1.8.6 Bim**

Bim, a BH3-only protein member of the Bcl-2 family promotes apoptosis (O'Connor *et al.*, 1998). There are currently ten known Bim variants, all thought to be obtained by alternative splicing (O'Connor *et al.*, 1998; Miyashita *et al.*, 2001; Marani *et al.*, 2002). Two of these variants, Bim<sub>EL</sub> and Bim<sub>L</sub> have been linked to the Ras/Raf/MEK/ERK pathway. Bim<sub>EL</sub> and Bim<sub>L</sub> can bind to Bcl-2 or Bcl-x<sub>L</sub>, which in turn leads to the release of pro-apoptotic Bax and Bak, thus promoting apoptosis. ERK1/2 can repress Bim expression independently of the JNK and PI3-K pathways (Weston *et al.*, 2003). Serum withdrawal induced apoptosis in CC139 fibroblasts caused a rapid *de novo* accumulation of Bim<sub>EL</sub> and this expression was reduced upon activation of the ERK1/2 pathway. The ERK1/2 pathway also promotes phosphorylation of Bim<sub>EL</sub> and this targets Bim<sub>EL</sub> for degradation via the proteasome (Ley *et al.*, 2003). ERK1/2 has subsequently been observed to directly

phosphorylate Bim<sub>EL</sub> at serine 65, and there are two other Bim<sub>EL</sub> sites that undergo phosphorylation by ERK1/2 (Ley *et al.*, 2004). The Ras/Raf/MEK/ERK pathway may also play a role in inhibiting Bim<sub>EL</sub> and Bim<sub>L</sub> in detachment-induced apoptosis (Marani *et al.*, 2004). Therefore ERKs play a role in preventing apoptosis via the phosphorylation and subsequent degradation of Bim variants.

### 1.8.7 p90<sup>RSK</sup>

ERKs phosphorylate and activate p90<sup>RSK</sup> proteins (Sturgill *et al.*, 1988). These proteins are a family of serine/threonine kinases consisting of four mammalian isoforms. Activated p90<sup>RSK</sup> has both cytoplasmic and nuclear substrates. In the nucleus p90<sup>RSK</sup> is shown to phosphorylate CREB (Xing *et al.*, 1996; Pende *et al.*, 1997; Xing *et al.*, 1998), c-Fos (Chen *et al.*, 1993; Chen *et al.*, 1996), and the SRF (Rivera *et al.*, 1993). It may also play a direct role in promoting the cell cycle via p27<sup>KIP1</sup> (Fujita *et al.*, 2003). The p90<sup>RSK</sup> proteins are also involved in promoting cell survival via direct phosphorylation and inactivation of the Bcl-2 pro-apoptotic protein Bad. p90<sup>RSK</sup> phosphorylates Bad at Ser112, and this stimulates binding of Bad to 14-3-3, sequestering Bad, thus preventing Bad-mediated cell death (Tan *et al.*, 1999). The Ras/Raf/MEK/ERK signalling cascade was observed to induce Bad phosphorylation by p90<sup>RSK</sup> in a growth factor dependent manner in neuronal cells (Bonni *et al.*, 1999).

### 1.8.8 Caspase 9

A direct link between the role of ERK in cell survival and caspase 9 has been found. An *in vitro* study using cytosolic HeLa cell extracts discovered that caspase 9 activity was suppressed by okadaic acid, and this could be overcome via treatment with the MEK inhibitors PD98059 and UO126 (Allan *et al.*, 2003). Further analysis showed addition of okadaic acid was leading to induced activity of ERK1/2, and suppression of this activity corresponded to the induction of caspase 9 in various cell types. It was discovered that pro-caspase 9 is phosphorylated *in vitro* on Thr125 by ERK2 upon growth factor stimulation, and that ERK1/2 co-precipitated with the phosphorylated form of pro-caspase 9. Furthermore, phosphorylation of Thr125 prevented caspase 9 processing and caspase 3 activation, even when apoptosome formation was induced (Allan *et al.*, 2003). These data strongly suggest a role for ERK in the suppression of apoptosis via phosphorylation of caspase 9.

### **1.8.9 ERK-independent roles for Raf proteins in apoptosis suppression**

Studies have indicated roles for C-Raf in suppressing apoptosis that are independent of its role in the Ras/Raf/MEK/ERK pathway. Two independent studies analysing apoptosis in *C-raf*<sup>-/-</sup> mice show an increased susceptibility to apoptosis that is independent of C-Raf MEK kinase activity (Hüser *et al.*, 2001; Mikula *et al.*, 2001). Both studies showed increased susceptibility to apoptosis in *C-raf*<sup>-/-</sup> fibroblasts upon treatment with various stimuli, including CD95 ligand, etoposide, growth factor withdrawal and actinomycin D, but no increase was observed for TNF- $\alpha$ -mediated apoptosis. However, MEK and ERK activation were found to be normal in these cells. In skeletal myoblasts it was shown that high signalling levels of C-Raf can suppress apoptosis in this cell line and use of a MEK inhibitor does not block this suppression (DeChant *et al.*, 2002), again indicating a role of C-Raf in MEK kinase-independent cell survival.

### **1.8.10 Bcl-2 family members**

A number of pathways have been suggested to account for the MEK kinase-independent role of C-Raf in the suppression of apoptosis (Figure 1.9). C-Raf has been shown to interact with the anti-apoptotic Bcl-2 protein via co-immunoprecipitation experiments (Wang *et al.*, 1994). This led to synergistic apoptosis suppression upon withdrawal of Interleukin-3 (IL-3) in IL-3-dependent hemopoietic cells, but results indicated this was not due to C-Raf directly phosphorylating Bcl-2. Observations were made that C-Raf can bind to the BH4 domain of Bcl-2 and target C-Raf to the mitochondria (Wang *et al.*, 1996a). However, it has subsequently been stated that this may have only occurred due to the over-expression of Bcl-2 in these cells (Rapp *et al.*, 2004) It was also observed that a mitochondrial targeted form of the kinase domain of C-Raf suppresses apoptosis to the same extent as C-Raf and Bcl-2 combined, suggesting they may not be directly involved in suppressing apoptosis (Wang *et al.*, 1996a). An independent study to those described above observed Bcl-2 does not require C-Raf kinase activity for its role in cell survival (Olivier *et al.*, 1997). C-Raf and Bcl-2 have also been shown to act independently in suppressing apoptosis (Zhong *et al.*, 2001). Therefore it is unclear as to if C-Raf and Bcl-2 act directly together in suppressing apoptosis and if they play a role together at the mitochondria.

Bad, the pro-apoptotic member of the Bcl-2 family, in its non-phosphorylated form, binds to the anti-apoptotic Bcl-x<sub>L</sub> protein. This sequesters Bcl-x<sub>L</sub>, preventing it from suppressing apoptosis at the mitochondria, thus allowing the release of cytochrome *c*. Bad can be phosphorylated on serines 112 and 136 (Datta *et al.*, 1997; Bonni *et al.*, 1999), which leads to the binding of 14-3-3 proteins. This causes cytoplasmic relocalisation of Bad, thus leaving Bcl-x<sub>L</sub> free in its role to suppress apoptosis (Zha *et al.*, 1996). A mitochondrial targeted kinase domain of C-Raf was shown to phosphorylate Bad (Wang *et al.*, 1996b), but no further role for C-Raf in suppressing apoptosis by sequestering Bad has been reported.

### **1.8.11 Bag-1**

Bag-1 is a multifunctional protein that was originally discovered as a binding partner of Bcl-2 (Takayama *et al.*, 1995). More recent findings have indicated Bag-1 interacts with the Hsc70 and Hsp70 heat shock proteins (Takayama & Reed., 2001) and may play a role in regulating cell growth and survival (Townsend *et al.*, 2005). Bag-1 binds to and activates C-Raf (Wang *et al.*, 1996b). Recent data have suggested that Bag-1 plays a role in the suppression of apoptosis by C-Raf in tumour cells (Götz *et al.*, 2004). When a lung cancer mouse model expressing constitutively active C-Raf was crossed to Bag-1 heterozygote mice, tumour cells showed increased apoptosis. The precise interaction in cell survival between C-Raf, Bag, and the possible involvements of Hsc70, Hsp70, Bcl-2 and Bad, still needs to be addressed.

### **1.8.12 NF- $\kappa$ B**

The nuclear factor  $\kappa$ B (NF $\kappa$ B) family of transcription factors consists of five members (NF $\kappa$ B1 [p105/p50], NF $\kappa$ B-2 [p100/p52], RelA [p65], RelB and RelC) that reside in the cytoplasm in their inactive form. They are retained in the cytoplasm, as dimers, by being bound to specific inhibitors known as I $\kappa$ Bs (Mercurio *et al.*, 1993). Stimuli, such as TNF $\alpha$ , IL-1 and viral DNA lead to phosphorylation of the I $\kappa$ B proteins on serine residues of the NH<sub>2</sub> terminal domain (Traenckner *et al.*, 1995). The I $\kappa$ B-kinase complex, (IKK) is the complex responsible for phosphorylating the I $\kappa$ Bs (Zandi *et al.*, 1998). This leads to polyubiquitination and degradation of the I $\kappa$ B proteins by the proteasome pathway, allowing the freed NF $\kappa$ B dimers to translocate to the nucleus (Chen *et al.*, 1995;

Traenckner *et al.*, 1995). At the nucleus NF $\kappa$ B proteins are involved in the activation of gene transcription of many genes including those associated with the inflammatory response, development and cell survival (Beg and Baltimore, 1996; Van Antwerp *et al.*, 1996). More recently, a second pathway involving NF $\kappa$ B proteins has been discovered. The role of this alternative pathway is thought to be in the development and maintenance of secondary lymphoid organs (Bonizzi and Karin, 2004).

The role of NF $\kappa$ B in the suppression of apoptosis is via the induction of a number of genes. NF $\kappa$ B induces; growth and DNA damage 45 $\beta$  (Gadd45 $\beta$ ) which is involved in DNA damage and cell cycle repair (Da Smaele *et al.*, 2001); Bcl-x<sub>L</sub> (Chen *et al.*, 2000); Bcl-2 in some cell types (Heckman *et al.*, 2002) and inhibitor of apoptosis (IAP) proteins 1 and 2 (Chu *et al.*, 1997; Wang *et al.*, 1998b). The IAPs are a family of proteins that suppress apoptosis by directly inhibiting caspases (Deveraux and Reed, 1999). NF $\kappa$ B is also responsible for upregulating the caspase 8 inhibitor C-FLIP, which leads to resistance to death induced apoptosis (Micheau *et al.*, 2001).

C-Raf has been shown to increase the transcriptional activity of NF $\kappa$ B independently of its role in the Ras/Raf/MEK/ERK pathway (Norris and Baldwin., 1999). Findings have revealed C-Raf is involved in the dissociation of the NF $\kappa$ B- I $\kappa$ B complex (Li and Sedivy, 1993), although the involvement of C-Raf may be indirect. C-Raf associates with casein kinase II, and this in turn can interact with I $\kappa$ B and leads to its dissociation from NF $\kappa$ B (Janosch *et al.*, 1996). Evidence also exists to suggest C-Raf indirectly activates NF $\kappa$ B via the membrane shuttle kinase MEKK1 (Baumann *et al.*, 2000). Co-transfecting C-Raf with a dominant negative form of MEKK1 strongly reduced NF $\kappa$ B dependent reporter gene activity, and led to a synergistic activation of the reporter construct in the presence of MEKK1 and C-Raf. However, no direct links between NF $\kappa$ B and C-Raf in apoptosis have been found. This is further supported by the observation that NF $\kappa$ B activity is not altered in *C-raf*<sup>-/-</sup> macrophages that show increase susceptibility to apoptosis (Jesenberger *et al.*, 2001).

It is still unclear whether MEK independent suppression of apoptosis by C-Raf occurs at the mitochondria, or indeed if C-Raf activation must occur at the mitochondria. As stated earlier, mitochondrial targeted C-Raf as been observed to protect mammalian

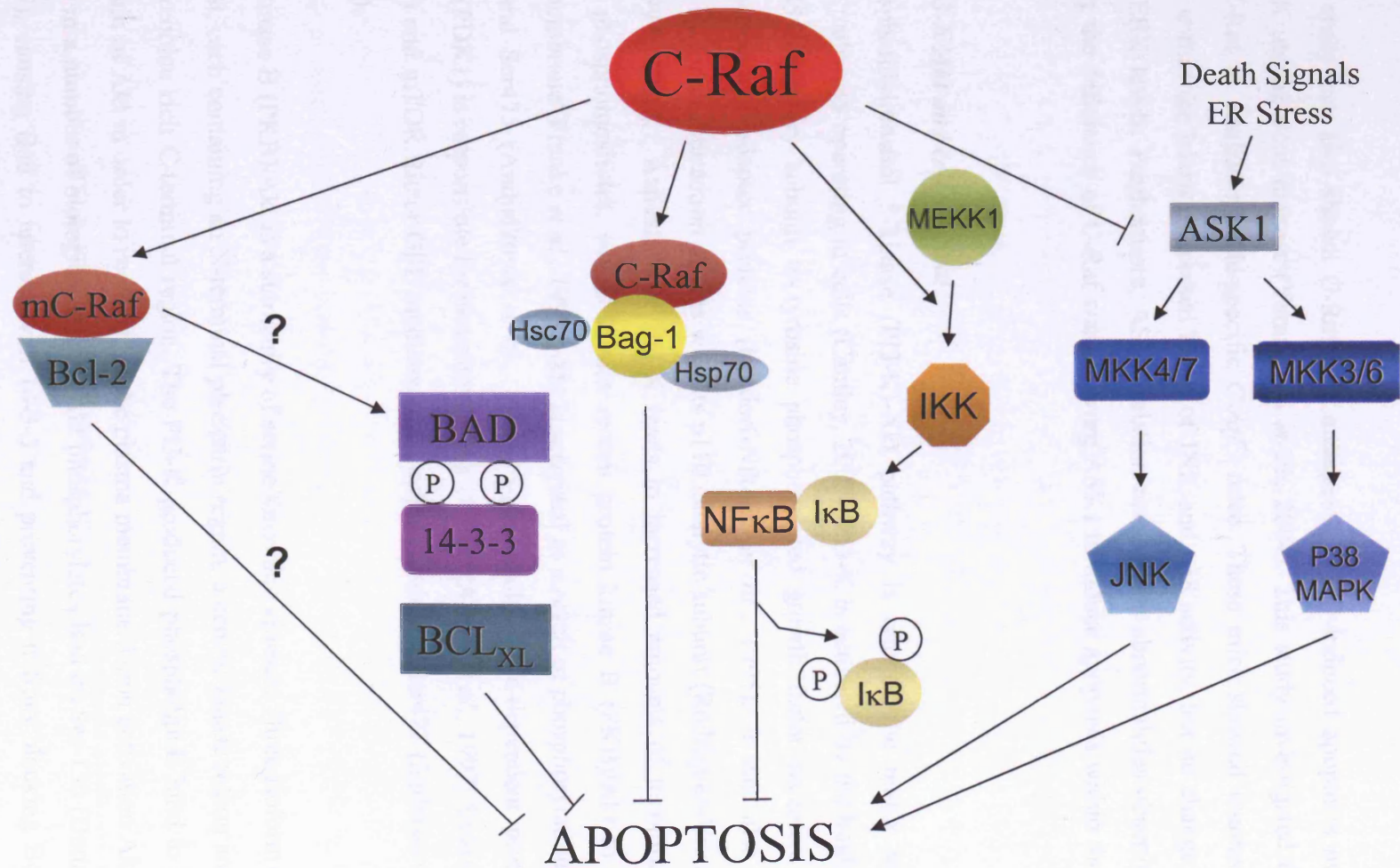
hemopoietic 32D cells from apoptosis by preventing cytochrome *c* release (Wang *et al.*, 1996a). It was also shown that expression of mitochondrial C-Raf led to increased cell survival in 32D cells (Peruzzi *et al.*, 1999). Furthermore, mitochondrial C-Raf has been found to protect cells via Bcl-2 or Bad independent pathways (Zhong *et al.*, 2001). C-Raf has been observed to interact with the voltage dependent anion channel (VDAC) (Le Mellay *et al.*, 2002). This channel is a mitochondrial pore involved in the exchange of metabolites. The kinase domain of C-Raf was found to directly interact with VDAC and was thought to affect metabolite flow in and out of the mitochondria. The role this may play in apoptosis has not been investigated. However, in *C-raf*<sup>-/-</sup> macrophages that showed increase susceptibility to apoptosis, assessment of alteration of mitochondrial function showed no significant cytochrome *c* release in these cells, and suggested apoptosis was not occurring due to mitochondrial fragility (Jesenberger *et al.*, 2001). Therefore, although C-Raf has been observed to interact with various proteins at the mitochondria, the roles these interactions may or may not play in suppressing apoptosis are yet to be fully resolved.

### **1.8.13 ASK1**

Apoptosis signal-regulating kinase 1 (ASK1) is a ubiquitously expressed MKKK. It activates the stress induced MKK4/MKK7-JNK and MKK3/MKK6-p38-MAPK signalling cascades (Ichijo *et al.*, 1997). As described earlier, these signalling cascades are MAPK cascades, involving a three tiered structure, as described for the Ras/Raf/MEK/ERK pathway (Figure 1.1). The over-expression of wild-type or activated alleles of ASK1 activates JNK and p38-MAPK and induces apoptosis in various cells through mitochondria-dependent caspase activation (Ichijo *et al.*, 1997; Hatai *et al.*, 2000). ASK1-deficient cells are resistant to H<sub>2</sub>O<sub>2</sub>- and TNF- induced apoptosis (Tobiume *et al.*, 2001), thus suggesting ASK1 plays a crucial role in stress-induced apoptosis.

C-Raf has been shown to interact with ASK1 *in vitro* and *in vivo* (Chen *et al.*, 2001). Over-expression of C-Raf leads to decreased apoptosis in ASK1 expressing HeLa cells, suggesting C-Raf plays a role in antagonising ASK1 activity. Using MEK antagonists, it was shown that this role does not require the MEK-ERK pathway. Furthermore, kinase inactive forms of C-Raf were able to inhibit ASK1 induced apoptosis (Chen *et al.*, 2001). Therefore these results show that the inhibition of ASK-1-induced apoptosis by

**Figure 1.9** Potential mechanisms via which C-Raf may be involved in MEK/ERK independent suppression of apoptosis.



interaction with C-Raf does not require C-Raf kinase activity, nor is it dependent on the ability of C-Raf to activate ERKs.

A recent study has also shown C-Raf may antagonise ASK1-induced apoptosis in a MEK-ERK independent manner (Yamaguchi *et al.*, 2004). This study investigated the role of C-Raf in cardiac muscle-specific *C-raf*<sup>-/-</sup> mice. These mice showed increased apoptosis within the hearts, increased levels of JNK and p38 activity, but no change in MEK or ERK levels. Furthermore, ASK1 ablation rescued the abnormalities observed, suggesting the deficiency of C-Raf was allowing ASK1 to induce apoptosis within these cells.

#### **1.8.14 PI3-K/Akt and cell survival**

The phosphatidylinositol 3-kinase (PI3-K)-Akt pathway is one of the major anti-apoptotic pathways operating in cells (Cantley, 2002). PI3-K is activated by the binding of its p85 regulatory subunit to tyrosine phosphorylated growth factor receptors or receptor-associated adaptor proteins (Rordorf-Nikolic *et al.*, 1995). It can also be activated by direct interaction of Ras with its p110 catalytic subunit (Rodriguez-Viciana *et al.*, 1994; 1996). Activation of PI3-K leads to increased amounts of membrane-localised phosphoinositides, which in turn recruit protein kinase B (PKB)/Akt to the plasma membrane (Franke *et al.*, 1997). Akt is activated as a result of phosphorylation on Thr308 and Ser473 (Andjelkovic *et al.*, 1999). 3-phosphoinositide-dependent protein kinase 1 (PDK1) is responsible for phosphorylating Thr308 (Alessi *et al.*, 1997; Stokoe *et al.*, 1997) and mTOR:Rictor:GβL mediates the phosphorylation at Ser473 (Sarbasov *et al.*, 2005).

Protein kinase B (PKB)/Akt is a subfamily of serine/threonine kinases. Three isoform ( $\alpha$ ,  $\beta$ ,  $\gamma$ ) exist, each containing an N-terminal pleckstrin region, a central kinase region and a serine/threonine rich C-terminal region. The PI3-K produced phospholipids bind to the PH domain of Akt in order to recruit it to the plasma membrane. Upon activation Akt is involved in a number of biological effects. Akt phosphorylates Bad on Ser-136 (Datta *et al.*, 1997), causing Bad to interact with 14-3-3 and preventing it from blocking Bcl-2 protective functions. Akt is also linked to the phosphorylation of other proteins involved

in apoptosis, including Mdm2 (Mayo *et al.*, 2001; Gottlieb *et al.*, 2002), and CREB (Du *et al.*, 1998).

Cross-talk between the PI3-K/Akt pathway and the Ras/Raf/MEK/ERK pathway has been demonstrated. Akt was shown to directly phosphorylate C-Raf on Ser259 in human embryonic kidney (HEK293) cells (Zimmermann and Moelling, 1999). This led to a decrease in C-Raf activity by allowing association of C-Raf with 14-3-3 and thus maintaining C-Raf in an inactive conformation. Akt was also observed to phosphorylate and terminate C-Raf kinase activity in PDGF-stimulated vascular smooth muscle cells (Reusch *et al.*, 2001). In a similar fashion to C-Raf, Akt has been shown to phosphorylate and inhibit B-Raf. B-Raf is phosphorylated on three sites by Akt, including Ser365, the equivalent residue to Ser259 of C-Raf (Guan *et al.*, 2000). More recently it was suggested that the cellular response due to the cross-talk between the PI3-K/Akt pathway and the Ras/Raf/MEK/ERK pathway is dependent on the type of ligand, its concentration and the time course of the interactions (Moelling *et al.*, 2002). High levels of insulin-like growth factor (IGF-1) strongly and rapidly induced Akt activity, allowing inhibition of C-Raf in human breast cancer cells. However, low dose induction by IGF-1 did not lead to C-Raf inhibition by Akt. Furthermore, PMA stimulation of the cells led to delayed Akt activity and no cross-talk with C-Raf, leading to growth arrest. Therefore Akt can negatively regulate the Raf kinases in some cellular circumstances.

### 1.9 Cellular Transformation

Although *raf* genes were initially identified as oncogenes in retroviruses that led to tumours in mice and chickens (Rapp *et al.*, 1983; Sutcliffe *et al.*, 1984), until recent years there were no known direct links between the alteration in expression or activity of *RAF* genes and incidences of human cancer. It was originally thought that any cancers involving the *RAF* protein kinases were via their role in the Ras/Raf/MEK/ERK pathway, as mutations of the *RAS* gene are observed in a large percentage of human cancers (Bos, 1989) and constitutively active forms of MEK and Raf have also been shown to be important in Ras-mediated transformations (Kolch *et al.*, 1991; Cowley *et al.*, 1994). A number of solid tumour cancers including those of the colon, pancreas and lung, containing activated *RAS* alleles, were shown to express constitutively phosphorylated ERK (Hoshino *et al.*, 1999). Constitutively active C-RAF has also been observed in some

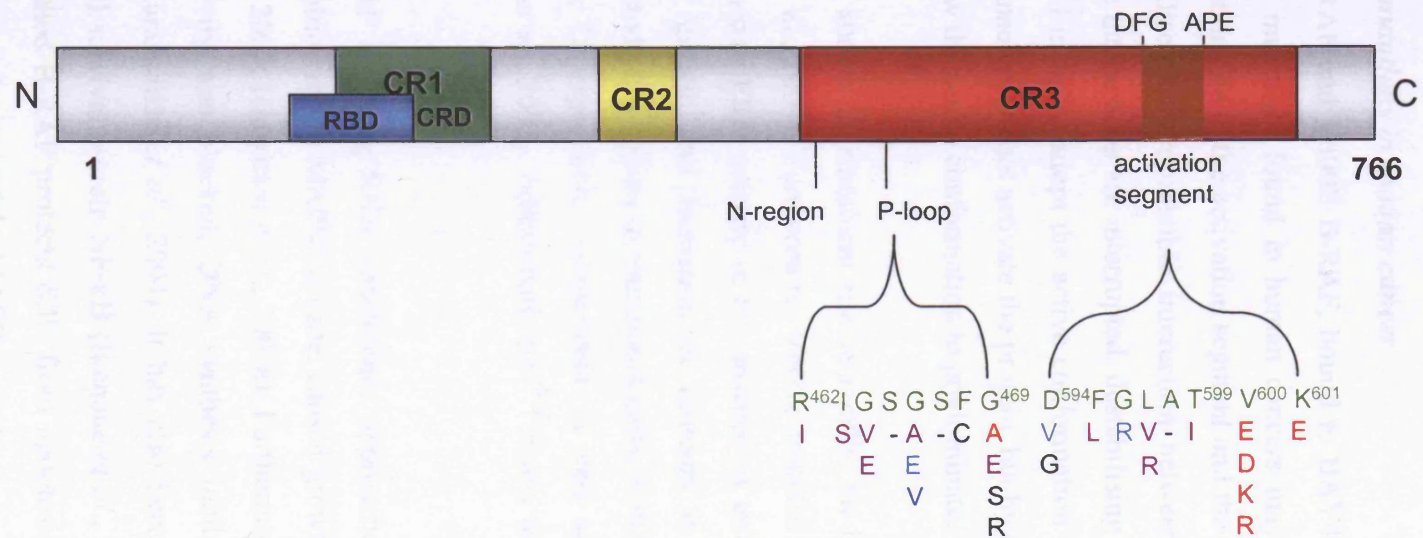
cancer samples with activated *RAS* alleles (Berger *et al.*, 1997). Many studies have made attempts to discover single point mutations in *C-RAF*, without success. The availability of high throughput sequencing in recent years has allowed the discovery of a direct link between mutations of the *B-RAF* gene and human cancers.

### ***1.9.1 Mutations of B-RAF in human cancers***

Davies *et al* (2002) screened 923 cancer samples and reported *B-RAF* somatic mis-sense mutations in 66 % of human malignant melanomas and 15 % of colorectal cancers. Mutations were found at a lower frequency in gliomas, lung cancers, sarcomas, ovarian carcinomas, breast cancers and liver cancers. No mutations were detected for *C-RAF*. Over 40 different mis-sense *B-RAF* mutations, involving 24 different codons were identified. The majority of these are very rare and only occurred in 0.1-2 % of all samples studied. However, one particular mutation involving a thymidine to adenosine transversion at nucleotide 1799 of the activation segment, converting valine 600 to glutamate, occurs much more frequently (Figure 1.10) (Davies *et al.*, 2002). This mutation has since been observed in over 90 % of melanomas and thyroid cancers and is highly represented in colorectal cancer (Cohen *et al.*, 2003; Fukushima *et al.*, 2003; Kimura *et al.*, 2003; Kumar *et al.*, 2003; Yuen *et al.*, 2002; Davies *et al.*, 2002). However, it was rarely observed in non-small cell lung carcinomas (Brose *et al.*, 2002) and not seen in breast cancers (Gast *et al.*, 2005). Other *B-RAF* mutations of the activation loop observed in cancer cell lines include V600D, L597R, G596R and F595L (Figure 1.10). Mutations were also seen in the glycine-rich loop (Figure 1.2) affecting residues G464, G466 and G469 (Figure 1.10). A further number of mutations were observed outside of the activation segment and G-loop (Davies *et al.*, 2002). V600E *B-RAF* mutations in NIH3T3 cells and murine melanocytes were found to stimulate constitutive ERK signalling, induce proliferation and transformation, and allow these cells to grow as tumours in nude mice (Davies *et al.*, 2002; Ikenoue *et al.*, 2003, 2004; Houben *et al.*, 2004; Wan *et al.*, 2004; Wellbrock *et al.*, 2004).

Only 1 % of cancer samples containing *B-RAF* mutations have also been shown to simultaneously contain *RAS* mutations, the majority of these being non-V600 (Davies *et al.*, 2002; Rajagopalan *et al.*, 2002; Yuen *et al.*, 2002). However, mutations of *B-RAF* occur in similar types of cancer as those of *RAS*, and in colorectal cancer the genes are both mutated within the same types of premalignant lesions and involve problems in DNA

**Figure 1.10** Structural diagram of B-Raf showing mutations observed in the glycine-rich P-loop and the activation segment upon sequence screening numerous cancer samples. Residues wild type of B-RAF are indicated in green; strong activating mutations shown in red; intermediate in purple; impaired activity mutations in blue and untested mutations in black. Refer to text for full explanation of the activity of the various types of mutations.



mismatch repair (Rajagopalan *et al.*, 2002; Yuen *et al.*, 2002). Thus suggesting B-RAF and RAS act similarly in delivering their tumourigenic effects through similar mechanisms involving the deregulation of ERK activity.

### ***1.9.2 Relating structure to B-RAF mutations in human cancer***

Solving the crystal structure of B-RAF and V600E B-RAF, bound to BAY43-9006, has given insight into how the *B-RAF* mutations found in human cancers may lead to its activation. The majority of the mutations lie in the activation segment and the glycine-rich loop, involving residues that stabilise the hydrophobic interaction between these two regions. Thus, upon mutation, these interactions are interrupted, destabilising the inactive conformation and allowing the DFG motif to adopt the active conformation (Wan *et al.*, 2004). Therefore, the mutations themselves do not activate the protein, but by destabilising the inactive conformation, they allow the active conformation to predominate.

V600E mutated B-RAF has been shown to transform melan-a cells, an immortalised melanocyte cell line (Wellbrock *et al.*, 2004). Furthermore, V600E mutated B-RAF was shown to stimulate constitutively active ERK activity in the absence of growth stimuli, leading to anchorage-independent growth and formation of tumours in nude mice (Wellbrock *et al.*, 2004). Another study has shown in melanoma cells, V600 mutated B-RAF leads to constitutive cyclin D expression, independent of cell adhesion, but dependent on ERK activity (Bhatt *et al.*, 2005). Additionally p27<sup>KIP</sup> levels were observed to be down-regulated in these cells.

Depletion of V600 mutated B-RAF by using RNA interference approaches in human tumour cells lines showed the inhibition of the MAPK cascade, caused growth arrest, and promoted apoptosis (Calipel *et al.*, 2003; Hingorani *et al.*, 2003a). Furthermore, using the inhibitor BAY43-9006, ERK activity was blocked, DNA synthesis inhibited and an increase in apoptosis observed (Karasarides *et al.*, 2004). It has also been shown that V600E B-RAF can activate the cell survival protein NF- $\kappa$ B (Ikenoue *et al.*, 2003, 2004). These findings suggest V600 mutated B-RAF protects cells from apoptosis, as well as being involved in cell proliferation via induction of the MAPK cascade.

Studying 22 of the various mutants of *B-RAF* found in human cancers showed they can be divided into three groups depending on their basal *in vitro* B-RAF kinase activity; high activity mutants, intermediate activity mutants and impaired activity mutants (Wan *et al.*, 2004). High activity mutants exceeded wild-type B-RAF activity between 100- and 700-fold. V600E is a member of this group, with a 460-fold increase over B-RAF wild-type kinase activity. Intermediate activity mutants showed a 1- to 10-fold increase over wild-type activity and impaired activity mutants were less active than wild-type B-RAF. High and intermediate activity mutants were able to stimulate ERK phosphorylation *in vitro* and the ERK activity levels were similar to those observed for oncogenic RAS. However, despite the increase in levels of B-RAF activity observed, the high and intermediate activity mutants only raised ERK activity 2- to 4.6- fold. This is likely to be due to the ability of hyperactivation of ERK to induce cell cycle arrest or senescence, which would not be favoured in a tumour cell line. Impaired activity mutants had basal B-RAF levels that were reduced to between 30 % and 80 % of wild-type B-RAF. However, despite having impaired *in vitro* kinase activity, three out of four of the impaired activity mutants were able to activate ERK when ectopically expressed in COS cells, although to lower levels than the other groups of mutants. The stimulation of MEK by B-RAF impaired activity mutants was found to occur due to induction by endogenous C-RAF (Wan *et al.*, 2004). Previous studies had shown C-RAF and B-RAF form complexes in mammalian cells (Weber *et al.*, 2001). It was observed that endogenously expressed wild-type B-RAF, and the various mutants of B-RAF, formed a complex with endogenous C-RAF. It was confirmed that C-RAF was activated in the B-RAF impaired activity mutants using C-RAF immunoprecipitation kinase assays, in which C-RAF activation was strongly induced. This was supported by depletion of C-RAF using an RNA interference approach leading to suppression of ERK activity in B-RAF impaired activity mutants only (Wan *et al.*, 2004).

One of the impaired mutants, D594V B-RAF, was unable to activate ERK in COS cells. This mutant also did not phosphorylate MEK *in vitro*, or activate C-RAF or NF- $\kappa$ B in cells (Ikenoue *et al.*, 2003; Wan *et al.*, 2004). D594 is an important catalytic residue conserved in all kinases. It is part of the conserved DFG motif at the start of the activation segment and is involved in binding an ATP chelating metal (Hanks and Hunter, 1995; Johnson *et al.*, 1998). The incidence of mutations at this site in cancer samples analysed is low,

however, other mutations at this site have been observed. The D594V mutation has also been observed in colon cancer (Yuen *et al.*, 2002). A D594E mutation has been detected in an invasive melanoma sample (Thomas *et al.*, 2004). D594G mutations have been observed in samples of primary melanoma (Deichmann *et al.*, 2004), melanocytic nevus (Kumar *et al.*, 2004), stomach cancer (Lee *et al.*, 2003b), non Hodgkins lymphoma (Lee *et al.*, 2003c), and colon cancer (Yuen *et al.*, 2002; Wang *et al.*, 2003; Fransen *et al.*, 2004). A D594K mutation was observed in two colon cancer samples (Oliveira *et al.*, 2003). Similar mutations at this site are not observed for C-RAF or A-RAF, suggesting although it is rare, this is unlikely to be a random event. A number of these mutants have been observed in coincidence with RAS mutations (Yuen *et al.*, 2002; Houben *et al.*, 2004). It may be that these mutants convey a dominant-negative effect on RAS to prevent a high level of ERK activity. Alternatively, D594 mutants may be involved in cancer via a yet undiscovered mechanism.

### ***1.9.3 The role of V600 mutated B-RAF in human cancer***

The precise events that lead to mutations in the *B-RAF* gene still remain unclear. As V600E is the major mutation in melanomas, suggestions of UV exposure causing this mutation were considered. However, the A to T mutation of V600E is distinct from the C to T and CC to TT pyrimidine dimer mutations common to UV-induced DNA damage (Daya-Grosjean *et al.*, 1995). Furthermore, this would not account for V600E mutations of colorectal, thyroid and ovarian cancers. It is likely that the DNA surrounding this codon, plus the biology or environment of the cell contribute to the high frequency of the V600E mutation, although a possible role of UV exposure cannot be discounted (Gray-Schopfer *et al.*, 2005).

Although B-Raf was shown to act as an oncogene in some cell lines, as indicated by its ability upon mutation of V600 to transform NIH3T3 cells and murine melanocytes (Davies *et al.*, 2002; Ikenoue *et al.*, 2003, 2004; Houben *et al.*, 2004; Wan *et al.*, 2004; Wellbrock *et al.*, 2004), for other cell lines this is not the case. V600E mutations have been detected in naevi (Pollock *et al.*, 2003). These are the first lesions associated with melanoma development that may remain dormant for many years. V600E mutations have also been detected in premalignant colon polyps and early Duke's stage of colorectal cancer. Therefore, although B-RAF mutations appear to be an early event in tumourigenesis, the

mutation alone is not sufficient to induce cancer in humans (Rajagopalan *et al.*, 2002; Yuen *et al.*, 2002). It is likely that mutations in other genes are also required to induce tumour development.

A candidate gene that may be also be mutated in the presence of *B-RAF* mutations is *INK4a*. This gene encodes for the cyclin-dependent kinase inhibitor p16. p16<sup>INK4a</sup> mutations are observed in a high proportion of melanoma cell lines (Ruas *et al.*, 1998; Rizos *et al.*, 1999), and loss of this protein leads to susceptibility to malignant melanomas in mice (Krimpenfort *et al.*, 2001; Sharpless *et al.*, 2001). Another gene that has been found to be mutated in melanomas is *CDK4* (Zuo *et al.*, 1996; Rizos *et al.*, 1999), this may also play a role in the development of metastatic melanoma involving *B-RAF* mutations. Both *INK4a* and *CDK4* are involved in the cell cycle and it is thought tumour development involving *B-RAF* mutations may occur via changes to the cell cycle. Indeed, a number of cell cycle proteins have shown increased expression levels in melanomas, including cyclin D1 (Ewanowich *et al.*, 2001), and cyclin E (Georgieva *et al.*, 2001). As B-RAF can influence cell cycle progression via ERK activation leading to induction of cyclins D and E, it may be via this pathway that B-RAF plays its role in the development of melanomas. There is a very complex relationship observed between ERK activity and the cell cycle. If the ERK signal is too strong it can cause cells to stop cycling and lead to differentiation or senescence (Sewing *et al.*, 1997; Woods *et al.*, 1997; Kerkhoff *et al.*, 1998). This may be why increased expression levels of the CKI, p21<sup>CIP1</sup> have been reported in melanomas (Trotter *et al.*, 1997).

## 1.10 Manipulating the mouse genome

### 1.10.1 Embryonic stem cells

Embryonic stem (ES) cells are stem cells derived from the undifferentiated inner mass cells of a blastocyst, an early stage embryo consisting of 50-150 cells (E3.5). They are pluripotent, meaning they are able to grow into any of the cell types in the body. ES cells were first successfully cultured in 1981 (Evans and Kaufman, 1981; Martin, 1981). ES cells can be cultured by growing them on a feeder layer consisting of mitotically inactivated MEFs. These feeder cells assist in the attachment of the ES cells and provide nutrients necessary in helping to maintain the pluripotent capacity of the ES cells. Growth

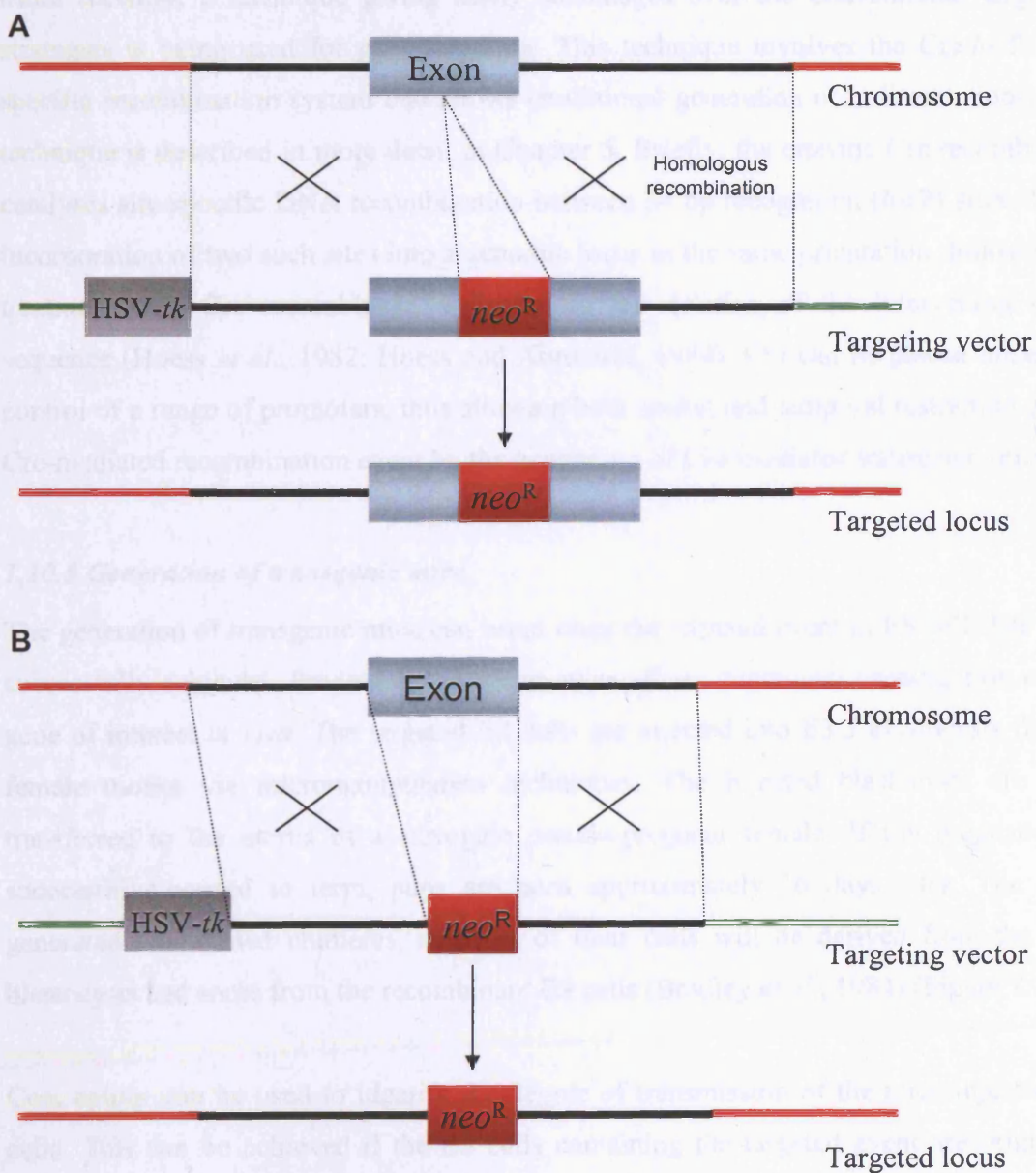
medium must be supplemented with the regulatory factor such as leukemia inhibitory factor (LIF), to suppress the differentiation of the cultured ES cells (Smith *et al.*, 1988).

ES cells can be manipulated in culture to allow the incorporation of exogenous DNA. A common method used to introduce DNA to ES cells is electroporation. This technique involves the application of a high voltage electrical pulse to a suspension of the ES cells and DNA. This allows the DNA to enter the ES cells (Reiss *et al.*, 1986). The first germline transmission of exogenous DNA introduced to ES cells occurred using retroviral vectors (Robertson *et al.*, 1986).

### **1.10.2 Gene targeting in ES cells**

Homologous recombination applied to gene targeting allows the introduction of exogenous homologous sequences to the chromosome of interest. This occurs by identical sequences of DNA recombining. For this to take place a targeting vector is first engineered. The targeting vector is usually designed to include homologous DNA sequences and a positive selectable marker. Homologous DNA sequences are normally between 5-7 kb in length. As the homologous recombination between the endogenous DNA sequences and the exogenous DNA sequences of the targeting vector is fairly inefficient, selectable markers are used. A positive selectable marker is incorporated to allow selection of the ES cells that have stably integrated the targeting vector. An example of a commonly used positive selectable marker is the neomycin resistance gene (*neo*<sup>R</sup>) whose gene products confer resistance to the antibiotic geneticin (G418). A positive selectable marker can be designed to be incorporated into the gene of interest in such a way that it can itself lead to a mutation, by disrupting a coding region of gene or replacing a specific region (Figure 1.11). Negative selectable markers, such as the herpes simplex virus thymidine kinase gene (HSV-*tk*), are sometimes used to aid recovery of the homologous recombination event. In this case, the negative selectable marker is incorporated in the targeting vector outside of the targeting event (Figure 1.11). Thus, it will only be present in the final targeted vector if non-homologous recombination events have occurred. A drug called gancyclovir will kill any cell containing the *tk* gene and thus only cells containing the targeted event will survive if gancyclovir selection is applied.

**Figure 1.11** Homologous recombination to create null alleles via gene targeting, using a positive selectable marker (*neo<sup>R</sup>*) and a negative marker (*HSV-tk*). (A) Homologous recombination leads to the positive selectable marker disrupting the coding exon (B) Homologous recombination in which the positive selectable marker replaces the coding exon. The negative selectable marker (*HSV-tk*) is not expressed in the final targeted locus as it lies outside of the homologous sequence of the targeting vector. Homologous sequences in the vector and locus are shown in black; sequences of the chromosome not homologous to the vector sequence are shown in red and bacterial plasmid sequences not homologous to the chromosome sequence are shown in green.



Upon homologous recombination, the aim of using the targeting vector is to mutate the specific chromosomal locus of interest. A number of different types of mutations can be incorporated using this method including null mutations, point mutations, deletions of specific functional domains, chromosomal translocations and gain-of-function mutations. Gene targeting of ES cells was first reported in 1987. Homologous recombination was used to inactivate the endogenous hypoxanthine phosphoribosyl transferase (*hprt*) gene by incorporation of the *neo*<sup>R</sup> gene into an exon of the *hprt* gene (Thomas and Capecchi, 1987).

More recently, a technique giving many advantages over the conventional targeting strategies is being used for gene targeting. This technique involves the Cre/*loxP* site-specific recombination system that allows conditional generation of null mutations. The technique is described in more detail in Chapter 5. Briefly, the enzyme Cre recombinase catalyses site-specific DNA recombination between 34 bp recognition (*loxP*) sites. Thus, incorporation of two such sites into a genomic locus in the same orientation, followed by treatment with Cre recombinase, will lead to the deletion of the intervening DNA sequence (Hoess *et al.*, 1982; Hoess and Abremski, 1984). Cre can be placed under the control of a range of promoters, thus allowing both spatial and temporal restriction of the Cre-mediated recombination event by the generation of Cre-mediated transgenic mice.

### ***1.10.3 Generation of transgenic mice***

The generation of transgenic mice can occur once the targeted event in ES cells has been successfully achieved. Producing transgenic mice allows functional investigation of the gene of interest *in vivo*. The targeted ES cells are injected into E3.5 blastocysts from a female mouse via micromanipulation techniques. The injected blastocysts are then transferred to the uterus of a surrogate pseudo-pregnant female. If the pregnancy is successfully carried to term, pups are born approximately 16 days later. The pups generated are termed chimeras, as some of their cells will be derived from the host blastocysts and some from the recombinant ES cells (Bradley *et al.*, 1984) (Figure 1.12).

Coat colour can be used to identify the degree of transmission of the microinjected ES cells. This can be achieved if the ES cells containing the targeted event are originally obtained from a mouse of a specific fur colour (e.g. white). The ES cells are then

transferred to blastocysts of an alternative fur colour (e.g. black), The pups produced will therefore be black if no recombinant ES cells have been transmitted, or brown if transmission of the ES cells has taken place.

Germline transmission signifies that the recombinant ES cells have contributed to the germline of the chimera. This can be assessed via mating of the chimeras to wild-type C57BL6 mice. Most ES cells used are originally derived from male embryos. As male ES cells are used, it is less likely that the female chimeras will transmit the ES cell targeted event through the germline. Mating of a chimeric male with an C57BL6 female will generate pups whose coat colour can again be used to inform whether germline transmission has been successful (Figures 1.12 and 1.13). Subsequent screening for the original mutation introduced to the ES cells is carried out for any animals thought to carry the recombinant ES cells. All animals positive for the mutation are heterozygotes, in that every cell of the animal will contain the mutation on one chromosome. These mice can be used to set up a breeding colony.

### **1.11 Ras/Raf/MEK/ERK knockouts/knockins in mice**

Gene targeting has been used to produce mice that have individual genes knocked out or knockin mutations. A number of different studies have assessed various proteins involved in the Ras/Raf/MEK/ERK signalling cascade. Using knockouts to investigate genes provides complementary information to RNAi studies and over-expression studies.

#### ***1.11.1 Ras knockout and knockin mice***

Knockout and knockin studies have investigated the role in development of the three *ras* genes, namely *N-ras*, *H-ras* and *K-ras*, that encode for the four Ras proteins. Studies investigating mice homozygous for the *N-ras* null mutation (*N-ras*<sup>-/-</sup>) showed no major phenotype. Development, growth and fertility of these mice were indistinguishable from their wild-type littermates, suggesting N-Ras is non-essential for mouse development (Umanoff *et al.*, 1995) Mice generated expressing a *H-ras* null mutation (*H-ras*<sup>-/-</sup>) were also found to show no distinguishable differences in development, growth and fertility in comparison to their wild-type littermates (Ise *et al.*, 2000). Therefore H-Ras is also shown to not be essential for embryogenesis. Investigation of mice homozygous for the *K-ras* null mutation (*K-ras*<sup>-/-</sup>) on an inbred background strain were found to die between

**Figure 1.12** Generation of transgenic mice from ES cells. **(A)** Targeted albino coat colour ES cells are microinjected into a black coat colour E3.5 blastocyst. **(B)** Blastocysts are transferred to surrogate female. **(C)** Chimeric pups are produced harbouring cells from both the original injected ES cells and the host blastocyst. **(D)** Chimeras are mated with wild-type C57BL6 mice. **(E)** F1 progeny are produced. Successful germline transmission can be assessed from coat colour. Agouti coloured offspring will have transmitted the targeted ES cells, whereas black coloured mice originate from the host blastocyst.

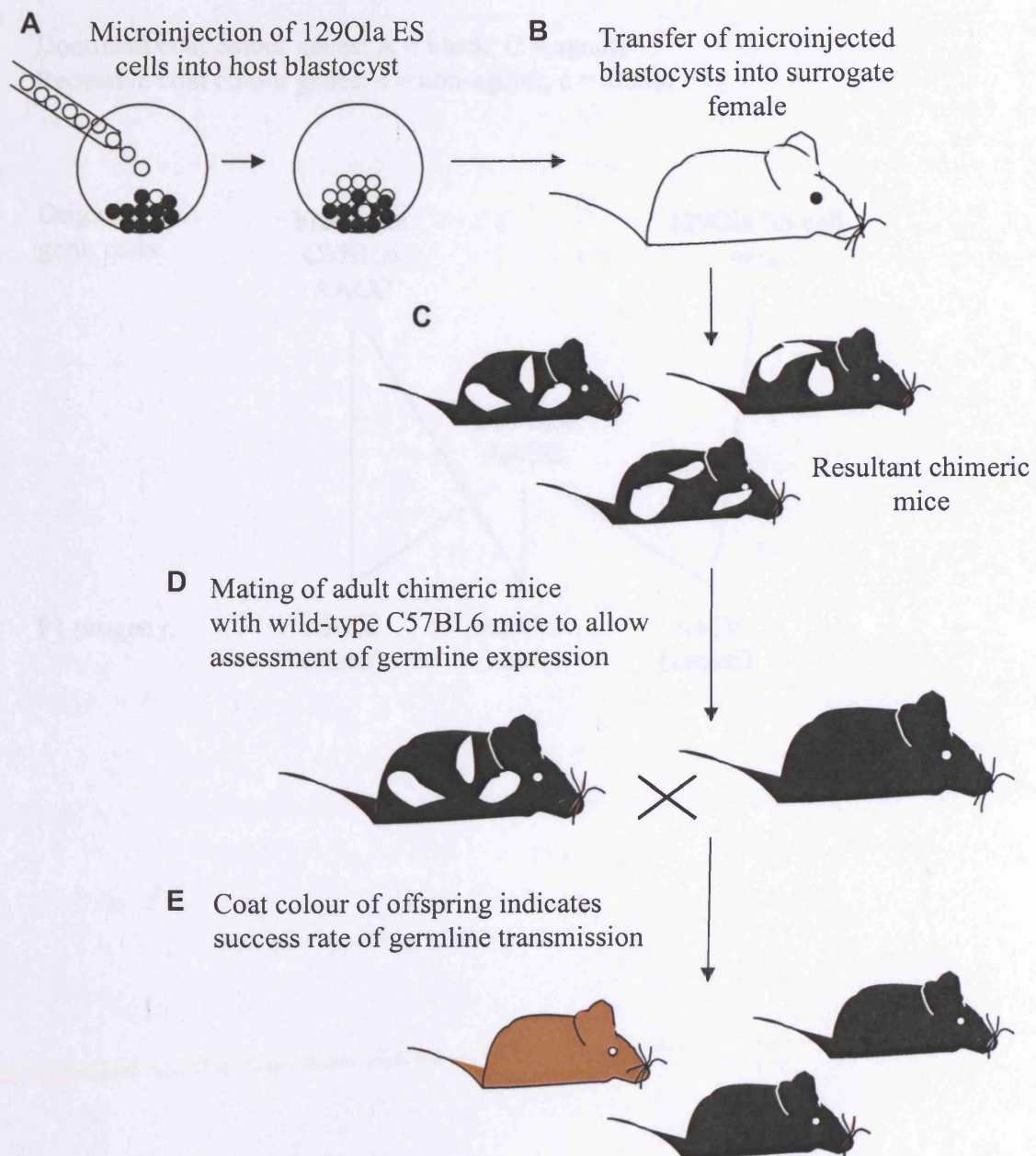
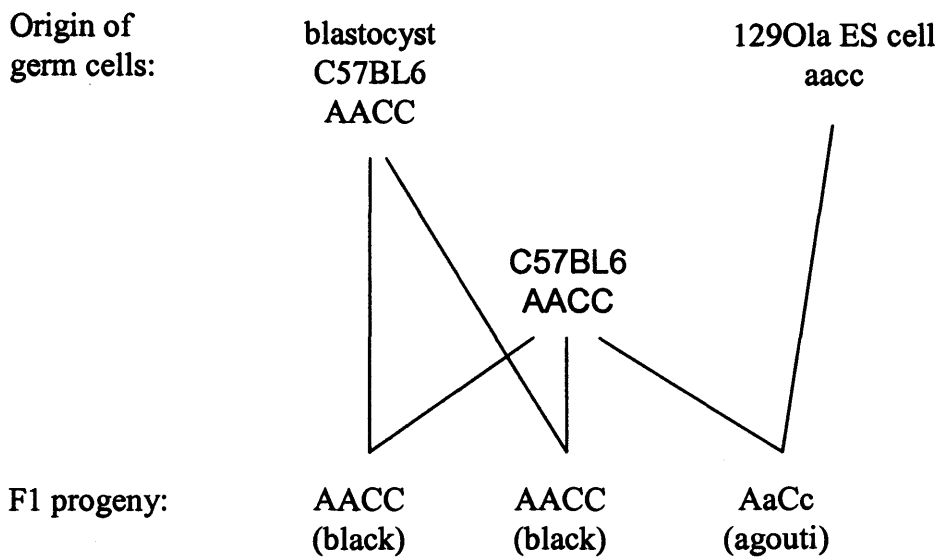


**Figure 1.13** Assessment of germline transmission of ES cells via coat colour of resulting F1 progeny from matings of chimeric mice with wild-type C57BL6 mice. Agouti mice in the F1 progeny indicates the germ cells originated from the microinjected 129Ola ES cells, black coat coloured mice obtained germ cells from the host blastocyst.

Coat colour genes:

Dominant coat colour genes: A = black; C = agouti

Recessive coat colour genes: a = non-agouti; c = albino



E12 and E14. These mice were characterised as having foetal liver defects and anaemia, thus indicating that K-Ras is vital for embryogenesis (Johnson *et al.*, 1997). Double mutations of both *N-ras* and *H-ras* (*N-ras*<sup>-/-</sup> *H-ras*<sup>-/-</sup>) have confirmed the non-essential roles of these genes in embryogenesis. No major phenotype was observed in these double knockout mice indicating K-Ras is essential and sufficient for normal mouse development (Estenban *et al.*, 2001).

By investigating *N-ras*<sup>-/-</sup> *K-ras*<sup>+/-</sup> embryos, functional overlap of the three *ras* genes has been suggested. The expression of only one functional *K-ras* allele resulted in embryonic lethality between E10 and E12. Furthermore, *K-ras*<sup>-/-</sup> *N-ras*<sup>+/-</sup> embryos exhibited a more severe phenotype than observed for *K-ras*<sup>-/-</sup> embryos (Johnson *et al.*, 1997). A more recent study has shown replacing K-Ras with H-Ras, by modifying the *K-ras* gene to encode for H-Ras, allows normal embryonic development, thus indicating K-Ras and H-Ras have overlapping roles (Potenza *et al.*, 2005). Adult mice generated from this study had cardiovascular problems, suggesting that although H-Ras appears to be able to replace the role of K-Ras in embryogenesis, it can not substitute all functions of K-Ras.

A Ras knockin mutation of *K-ras*<sup>G12D</sup> has been used to produce mice expressing oncogenic Ras. Activation of endogenous *K-ras*<sup>G12D</sup> expression was shown to lead to epithelial neoplasms in the lungs (Jackson *et al.*, 2001) and pancreas (Hingorani *et al.*, 2003b). Using a conditional system, the widespread expression of *K-ras*<sup>G12D</sup> was shown to lead to embryonic lethality, whereas spatially controlled expression in the lungs and gastro-intestinal tract induced epithelial hyperplasia *in vivo* (Tuveson *et al.*, 2004). Analysis of *K-ras*<sup>G12D</sup> expressing MEFs showed these cells had enhanced proliferative properties, lacked contact inhibition and were immortal, despite no further genetic abnormalities. Furthermore, Ras effector pathways did not show elevated levels of phosphorylated ERK1/2 and phosphorylated pAkt (Tuveson *et al.*, 2004).

### **1.11.2 Raf knockout and knockin mice**

Knockout studies have been performed for all three *raf* genes. Homozygous *A-raf* null mutation mice (*A-raf*<sup>-/-</sup>) produced on the C57BL6 and 129Ola genetic backgrounds survive to adulthood and are fertile. These mice were slightly small than their wild-type littermates and also displayed neurological abnormalities and a feeding ataxia (Pritchard

*et al.*, 1996). A-Raf is therefore non-essential for mouse embryogenesis, but is required for certain aspects of neurological development. Homozygous *B-raf* null mutation embryos (*B-raf*<sup>-/-</sup>) produced on the C57BL6 genetic background died *in utero* between 10.5 and 12.5 days. Examination of the phenotype of the *B-raf*<sup>-/-</sup> embryos showed vascular abnormalities and increased endothelial apoptosis (Wojnowski *et al.*, 1997). B-Raf is therefore essential for embryogenesis and plays a role in cellular survival. The first study to obtain homozygous *C-raf* null mutation mice (*C-raf*<sup>-/-</sup>) produced embryos in which an aberrant 62 KDa C-Raf protein was expressed, and this was found to have residual kinase activity. However, even with the expression of this truncated C-Raf protein, the embryos generated died *in utero*, with the time-point depending on the genetic background. Furthermore, growth retardation and abnormalities of the skin and lungs were observed. Mouse embryonic fibroblasts derived from these embryos showed reduced cell proliferation rates in comparison to their wild-type littermates (Wojnowski *et al.*, 1998). The generation of completely null *C-raf*<sup>-/-</sup> mice has since been achieved. *C-raf*<sup>-/-</sup> embryos produced on a mixed 129Ola/C57BL6 genetic background died *in utero* around E9.5. These embryos showed defects in vascularization and placenta development as well as increased apoptosis of many tissues, although cell proliferation was not affected. *C-raf*<sup>-/-</sup> mice produced on a mixed 129Ola/MF-1 genetic background survived to a few days after birth. These mice were smaller than their wild-type litter mates and displayed disorganised placenta and were anaemic (Hüser *et al.*, 2001). ERK activity was no different in *C-raf*<sup>-/-</sup> MEFs derived from these embryos compared to MEFs derived from wild-type littermates. However, the *C-raf*<sup>-/-</sup> MEFs showed increased susceptibility to programmed cell death (PCD) upon treatment with various apoptotic agents (Hüser *et al.*, 2001).

*C-raf*<sup>-/-</sup> embryos were also produced in an independent study to that described above. These embryos, produced on the 129/Sv genetic background and a mixed 129Ola/C57BL6 genetic background died during mid-gestation and were smaller than their wild-type litter mates. As with the study described above, abnormalities were observed in the placenta. The *C-raf*<sup>-/-</sup> embryos were anaemic and increased apoptosis of foetal liver cells were also observed (Mikula *et al.*, 2001). MEFs derived from the *C-raf*<sup>-/-</sup> embryos showed normal ERK activation, and were susceptible to increased apoptosis upon treatment with various apoptotic agents when compared to MEFs derived from their wild-type littermates (Mikula *et al.*, 2001). Overall the findings described indicate C-Raf

is essential for mouse development and plays an important role in the prevention of apoptosis that is independent of MEK/ERK. Further analysis to investigate the anaemic phenotype of the *C-raf*<sup>-/-</sup> embryos showed C-Raf plays a role in erythropoiesis (Kolbus *et al.*, 2002).

A double knockout mutant of both A-Raf and C-Raf has also been described. This showed *A-raf*<sup>-/-</sup> *C-raf*<sup>-/-</sup> embryos have a more severe phenotype than either single null mutation. Embryos died at around E10.5 on the MF-1 genetic background and were extremely small. MEFs generated from the *A-raf*<sup>-/-</sup> *C-raf*<sup>-/-</sup> embryos showed reduced transient levels of ERK associated with a delay in entering the S-phase of the cell cycle (Mercer *et al.*, 2005). Therefore A-Raf and C-Raf work together in a MEK kinase-dependent manner to influence cell proliferation.

C-Raf mice have also previously been generated containing a knockin mutation of Tyr340/341 of the catalytic segment. These residues were mutated to phenylalanine, generating *C-raf*<sup>FF/FF</sup> mice (Hüser *et al.*, 2001). These mice showed no *in vitro* activity towards MEK, yet developed normally and survived to adulthood. They also showed normal ERK activation, and unlike *C-raf*<sup>-/-</sup> embryos, no increased susceptibility to apoptosis was observed upon treatment with various apoptotic agents. These findings indicated that the role of C-Raf in suppressing apoptosis was independent of its MEK kinase activity.

### **1.11.3 MEK knockout mice**

Disruption of the *mek1* gene led to the production of *mek1*<sup>-/-</sup> embryos. These embryos died at E10.5 of embryogenesis and showed reduced vascularization of the placenta. This was due to decreased vascular epithelial cells of the labyrinthine region. This was explained by the decreased migration of *mek1*<sup>-/-</sup> MEFs compared to wild-type cells, suggesting vascular epithelial cells were unable to invade the labyrinthine region of the placenta. MEK2 and ERK levels were normal in the *mek1*<sup>-/-</sup> MEFs (Giroux *et al.*, 1999). MEK1 may therefore be required for promoting vascularization of the labyrinthine region of the placenta and play a role in cell migration.

#### 1.11.4 ERK knockout mice

Homozygous *erk1* null mutation mice (*erk1*<sup>-/-</sup>) survive to adulthood, are fertile and of normal size. However, these mice showed a defect in thymocyte maturation, displaying half the number of expected mature thymocytes. A reduced level of proliferation was observed in these *erk1*<sup>-/-</sup> thymocytes (Pages *et al.*, 1999). ERK1 is therefore non-essential for mouse embryogenesis, but is required for thymocyte development. More recent studies of these *erk1*<sup>-/-</sup> mice suggested a role for ERK1 in adipocyte differentiation (Bost *et al.*, 2005). ERK2, however does appear to be essential for mouse embryogenesis (Saba-El-Leil *et al.*, 2003). Disruption of the *erk2* gene, to produce *erk2* null mice showed embryos were not produced beyond E8.5. ERK1 was not able to compensate for the lack of ERK2. Further analysis of the embryos indicated a specific requirement for ERK2 in normal trophoblast development.

#### 1.12 Aims

The aims of this thesis were to further contribute to the characterisation of the C-Raf and B-Raf protein kinases by:

- The characterisation of the apoptotic phenotype of *C-raf*<sup>-/-</sup> MEFs.
- The characterisation of *B-raf*<sup>-/-</sup> MEFs with regard to growth, proliferation and apoptosis.
- The generation of conditional *B-raf* kinase-inactive mice via the use of Cre/*loxP* technology.
- Generation and analysis of *B-raf* kinase-inactive MEFs with respect to growth, proliferation and apoptosis.

## 2. MATERIALS AND METHODS

### 2.1. Molecular Biology

Unless otherwise stated, all chemicals were obtained from Sigma and all restriction endonucleases from New England Biolabs.

#### 2.1.1 Plasmids

The plasmids used were:

pPGK-puro (Figure 2.1A)

pCre-PAC (Figure 2.1B)

pEFm.6, pEFm.6-C-RAF, pEFm.6-kinase inactive C-RAF, pEFm.6-MEK inactive C-RAF, and pEFm.6-RAS binding mutant C-RAF (gifts from R. Marais, The Institute of Cancer Research, London; Marais *et al.*, 1995)



### **2.1.2 Ethanol Precipitation**

To the DNA sample, 2 x volume of 100 % [v/v] ethanol and 1/10<sup>th</sup> x volume of 3 M NaOAc were added. The mixture was placed at -20° C for 2-16 hours. The solution was centrifuged at 13,000 rpm at 4° C for 10 min. The supernatant was discarded and the pellet washed in 500 µl of 70 % [v/v] ethanol. The tube was centrifuged at 13,000 rpm for 5 min and the supernatant discarded. The pellet was air dried and resuspended in sterile H<sub>2</sub>O.

### **2.1.3 Agarose gel electrophoresis**

Pure agarose (Seakem, Flowgen) was melted in 1 x TAE (40 mM Tris base, 1 mM EDTA pH 8.0), to obtain a 0.8-2 % [w/v] agarose solution. Gels were electrophoresed in 1 x TAE. 6 x loading dye (15 % [w/v] Ficoll 400, 0.5 % [w/v] orange G) was added to the samples and the samples loaded into the wells of the gel. 5 µl of a 1 Kb Plus DNA ladder (Life Technologies) was loaded besides the samples, to verify the size of the DNA bands produced. Gels were electrophoresed at 80 V and stained in 0.5 µg/µl ethidium bromide. DNA bands were visualised using a Bio-Rad gel documentation system.

### **2.1.4 Production of competent DH5α**

A single colony was picked from a streaked agar plate and inoculated into 5 ml of SOB media (2 % [w/v] bactotryptone (Oxoid), 0.5 % [w/v] bacto yeast extract (Oxoid), 10 mM NaCl, 2.5 mM KCl, 10 mM MgCl<sub>2</sub>, 10 mM MgSO<sub>4</sub>), and placed at 37° C in a 225 rpm shaking incubator overnight. The following morning 0.45 ml of the overnight starter culture was sub-cultured into 45 ml of warm SOB. The culture was grown up at 37° C in a 225 rpm shaking incubator overnight, until an OD<sub>600</sub> of 0.3-0.5 was obtained. The culture was centrifuged at 4000 rpm at 4° C for 5 min. The supernatant was discarded and the cells gently resuspended in 40 ml of ice-cold transformation buffer 1 (10 mM MES [2-(N-Morpholino) ethanesulphonic acid] pH 6.3, 45 mM MnCl<sub>2</sub>, 10 mM CaCl<sub>2</sub>, 100 mM KCl, 3 mM HCC [(NH<sub>3</sub>)<sub>6</sub>CoCl<sub>3</sub>] and placed on ice for 5 min. The suspension was centrifuged at 3000 rpm at 4° C for 8 min. The supernatant was discarded and the cells resuspended in 4 ml of ice-cold transformation buffer 2 (10 mM MES [2-(N-Morpholino) propanesulphonic acid] pH 6.5, 45 mM CaCl<sub>2</sub>, 10 mM RbCl, 15 % [v/v] glycerol). The competent cells were aliquoted and flash frozen in a dry ice/IMS bath and stored at -80°C. The transforming competency of the DH5α was confirmed using a known amount of plasmid DNA.

### ***2.1.5 Transformation of competent DH5 $\alpha$***

50  $\mu$ l of bacteria was thawed on ice and transferred to a polypropylene tube. 5  $\mu$ l of ligation mix was added and the tube incubated on ice for 30 min. The tube was heat shocked at 42° C for 45 s and placed on ice for 2 min. 1 ml Luria Bertani (LB) medium (1 % [w/v] bactotryptone, 0.5 % [w/v] bacto yeast extract, 17 mM NaCl) was added to the tube and placed at 37° C in a 225 rpm shaking incubator for 1 hour. The contents of the tube were transferred into a 1.5 ml eppendorf and centrifuged at 10,000 rpm for 1 min. The majority of the supernatant was removed, leaving 100  $\mu$ l behind, in which the pellet was resuspended. The transformation reaction was spread onto a LB agar plate (1.5 % [w/v] agar bacteriological (Oxoid), 1 % [w/v] bactotryptone, 0.5 % [w/v] bacto yeast extract, 17 mM NaCl) containing 100  $\mu$ g/ml ampicillin, the plate inverted and incubated at 37° C overnight.

### ***2.1.6 Minipreparation of plasmid DNA from bacteria***

A colony was picked from an LB agar plate and inoculated into 5 ml of LB media. The culture was placed at 37° C in a 225 rpm shaking incubator overnight. 1 ml of the bacterial culture produced was centrifuged at 13,000 rpm for 1 min. The supernatant was discarded and the pellet resuspended in 100  $\mu$ l of resuspension buffer (50 mM Tris-HCl pH 8.0, 10 mM EDTA, 100  $\mu$ g/ml RNase A). 200  $\mu$ l of lysis buffer (0.2 M NaOH, 1 % [w/v] SDS) was added and the tube inverted several times. 150  $\mu$ l of neutralisation buffer (5 M KOAc, pH 5.5) was added, the tube mixed and centrifuged at 13,000 rpm for 5 min. The supernatant was retained and the DNA precipitated by the addition of 400  $\mu$ l isopropanol and centrifuging at 13,000 rpm for 5 min. The supernatant was discarded and the pellet washed in 70 % [v/v] ethanol. The tube was centrifuged at 13,000 rpm for 1 min and the supernatant discarded. The pellet was air dried and resuspended in 50  $\mu$ l TE (10 mM Tris pH 8.0, 1 mM EDTA pH 8.0) containing 50  $\mu$ g/ml RNase.

### ***2.1.7 Midipreparation of plasmid DNA from bacteria***

100  $\mu$ l of bacterial culture was taken from a 5 ml starter culture and inoculated into a sterile flask containing 50 ml of LB media and 50  $\mu$ g/ml ampicillin. The flask was placed at 37° C in a 225 rpm shaking incubator overnight. The following morning the bacteria

were harvested and the plasmid DNA extracted using a plasmid midi kit (Qiagen). The method used was as described in the manufacturer's manual.

#### ***2.1.8 Caesium chloride preparation of plasmid DNA from bacteria***

4 ml of bacterial culture was taken from a 5 ml starter culture and inoculated into a sterile flask containing 500 ml of LB media and 50 µg/ml ampicillin. The flask was placed at 37° C in a 225 rpm shaking incubator overnight. The following morning the bacteria were harvested by centrifuging at 6000 rpm at 4° C for 10 min. (Sorvall RC-SB refrigerated, super speed centrifuge, Du Pont Instruments). The pellet was resuspended in 10 ml resuspension buffer. 20 ml of lysis buffer was added and the tube incubated on ice for 5 min. 15 ml of cold neutralisation buffer was added and the tube incubated on ice for a further 5 min. The tube was centrifuged at 9000 rpm at 4° C for 15 min and the supernatant discarded. The pellet was air dried and resuspended in 5.5 ml of TE containing 550 µl of 5 mg/ml ethidium bromide and 6 g CsCl. The tube was centrifuged at 4000 rpm at 4° C for 5 min. The resulting clear solution was syringed into two quick seal ultra centrifuge tubes (Beckman). The tubes were heat sealed and centrifuged at 100,000 rpm at 20° C for 16 hours. The lower plasmid band produced was retained and the DNA extracted by 10 x washes with an equal volume of water-saturated isobutanol. To precipitate the DNA, 2 x volume of H<sub>2</sub>O plus 2 x volume of 100 % [v/v] ethanol were added. The tube was centrifuged at 11,000 rpm for 15 min and the supernatant discarded. The pellet was washed in 70 % [v/v] ethanol. The tube was centrifuged at 11,000 rpm for 5 min and the supernatant discarded. The pellet was air dried and resuspended in 550 µl TE.

#### ***2.1.9 Restriction digest of plasmid DNA***

For plasmids, the appropriate enzyme was added to the plasmid DNA with 1 x the appropriate buffer (supplied by the manufacturer). The digest reactions were incubated at 37° C for 2 hours.

#### ***2.1.10 Removal of 5' phosphate groups from linearised DNA***

0.5 units/µg DNA of calf intestinal alkaline phosphatase was added to the digest reaction and incubated at 37° C for 1 hour. 5 mM EDTA was added to the reaction and incubated at 75° C for 10 min.

### ***2.1.11 Purification of gel fragments***

The DNA band was excised from the gel with a sharp sterile scalpel. The DNA was purified from the gel fragment using a QIAquick gel extraction kit (Qiagen). The method used was as described in the manufacturer's manual.

### ***2.1.12 Ligation of DNA fragments***

The appropriate volume of linearised vector (10-50 ng) and the appropriate volume of insert (100-200 ng) were added to 2.5 µl of 10 x T4 ligase buffer and 1 unit of T4 DNA ligase, in a total volume of 25 µl. The reaction was incubated at 16° C for 16 hours.

### ***2.1.13 Primer synthesis and DNA sequencing***

Primer synthesis was carried out by the Protein and Nucleic Acid Chemistry Laboratory (PNAACL), University of Leicester, or by Invitrogen. All DNA sequencing was performed by PNAACL.

### ***2.1.14 Lysis of cells to extract genomic DNA***

Media was removed from cells and the cells washed in an appropriate volume of PBS (136 mM NaCl, 8 mM Na<sub>2</sub>HPO<sub>4</sub>, 2.7 mM KCl, 1.5 mM KH<sub>2</sub>PO<sub>4</sub>). The required volume of DNA lysis buffer (50 mM Tris pH 7.6, 1 mM EDTA, 100 mM NaCl, 0.2 % [w/v] SDS) containing 100 µg/ml of freshly added proteinase K, was added to the cells, and the cells placed at 37° C for 20 hours. The lysate produced was transferred to an eppendorf. Two volumes of 100 % [v/v] ethanol were added to the tubes. The tubes were centrifuged at 13,000 rpm at 4° C for 10 min. The supernatant was removed and the DNA washed in 70 % [v/v] ethanol. The supernatant was aspirated and the DNA dried and resuspended in an appropriate volume of TE.

### ***2.1.15 Lysis of cells to extract RNA***

Media was removed from a confluent 6 cm dish and the cells washed in an appropriate volume of PBS (136 mM NaCl, 8 mM Na<sub>2</sub>HPO<sub>4</sub>, 2.7 mM KCl, 1.5 mM KH<sub>2</sub>PO<sub>4</sub>). Total RNA was obtained using an RNeasy mini kit (Qiagen). The method used was as described in the manufacturer's manual.

### ***2.1.16 Synthesis of cDNA from total RNA***

First-strand cDNA, for subsequent PCR amplification, was synthesised from 2 µg of total RNA using an ImProm-II Reverse Transcription System kit (Promega). The method used was as described in the manufacturer's instructions.

### ***2.1.17 Lysis of mouse tail samples***

3 mm of mouse tail was provided in an eppendorf for genotyping. Tail samples were lysed by placing in 200 µl of tail lysis buffer (50 mM Tris HCl pH 8.0, 100 mM EDTA, 1 % [w/v] SDS) containing 100 µg/ml of freshly added proteinase K. Samples were placed at 65° C for approximately 20 hours, until all of the tail samples had been lysed. The tubes were then placed at 95° C for 10 min to heat inactivate the proteinase K.

### ***2.1.18 Lysis of mouse tail samples for long range Polymerase Chain Reaction (PCR)***

3 mm of mouse tail was provided in an eppendorf for genotyping. Tail samples were lysed using a Genelute Mammalian Genomic DNA kit (Sigma). The method used was as described in the manufacturer's manual.

### ***2.1.19 Polymerase Chain Reaction***

Each PuReTaq™ Ready-to-go™ PCR bead (Amersham) was rehydrated with H<sub>2</sub>O and the appropriate primers to give a final primer concentration of 1 pmol/µl in a total volume of 25 µl. 1 µl of DNA sample was added to 9 µl of the rehydrated bead/primer mix. The reaction was overlaid with mineral oil and placed in a Genius PCR machine (Techne). Alternatively, Reddymix PCR Master Mix (Abgene) was used instead of PCR beads. Primers were added to the Reddymix to give a final primer concentration of 1 pmol/µl in a total volume of 25 µl. 1 µl of DNA sample was added to 10 µl of the Reddymix/primer mix. The reaction was overlaid with mineral oil and placed in a Genius PCR machine. The PCR conditions used are indicated below:

Initial denaturation of DNA at 94° C followed by 35 cycles for 3 steps:

Step 1. 94° C for 30 s

Step 2. X° C for 30 s (Table 2.1)

Step 3. 72° C for 1 min per Kb of product

### 2.1.20 B-raf long range PCR

To the appropriate amount of DNA, 10 µl of PCR reaction mix was added. The mix was made up of 1 x AJB buffer (11.1 x stock; 2 M Tris-HCl pH 8.8, 1 M (NH<sub>4</sub>)<sub>2</sub>SO<sub>4</sub>, 1 M MgCl<sub>2</sub>, 100 % [v/v] 2-mercaptoethanol, 10 mM EDTA pH 8.0, 100 mM dATP, 100 mM dCTP, 100 mM dGTP, 100 mM dTTP, 10 mg/ml BSA), 2 % [v/v] DMSO, 2.5 units/µl Expand Long Template PCR DNA polymerase mix (Roche) and 1 pmol/µl final concentration of Ocp147 and Ocp153. The following PCR conditions were used:

Step 1. 92 °C for 2 min.

Step 2. 92 °C for 10 s, 60 °C for 30 s, 68 °C for 20 s for 10 cycles

Step 3. 92 °C for 10 s, 60 °C for 30 s, 68 °C for 20 s + X s (where X = + 20 s per cycle) for 20 cycles

Step 4. 72 °C for 10 min.

**Table 2.1** PCR primers and annealing temperatures

Primer name	Sequence 5' to 3'	Annealing temperature
Ocp66	CGT GCA ATC CAT CTT GTT CA	60° C
Ocp69	AGG GGA TCG GCA ATA AAA AG	60° C
Ocp 75	AGT GCC AGC GGG GCT GCT AAA	68° C
Ocp 84	GTT CTC AAG AAC CTG ATG GAC A	60° C
Ocp 85	CTA GAG CCT GTT TTG CAC GTT C	60° C
Ocp106	GCT TAC ATT TGC TTC TGA CA	60° C
Ocp107	GTGATACTT GTG GGC CAG G	60° C
Ocp112	GCC TAT GAA GAG TAC ACT AGC AAG CTA GAT GCC C	68° C
Ocp114	TAT GGT GGG ACG AGG ATA C	60° C
Ocp115	CTC TTC ATG GCT TTT GGT CAG	60° C
Ocp121	ACC TGA AAT CTT CAA AAT GCT T	60° C
Ocp122	TGA AGA ATG TGA CCA ACT GAG A	60° C
Ocp125	GCC CAG GCT CTT TAT GAG AA	60° C
Ocp128	TAG GTT TCT GTG GTG ACT TGG GGT TGT TCC GTG A	68° C
Ocp129	CTG CAG GTC GAC ACT AGT TTA GG	60° C
Ocp132	ATG TCT GTA CAC TAC TAA TTA TG	60° C
Ocp137	GCT TGG CTG GAC GTA AAC TC	60° C
Ocp142	ATT CCA ACA CAC TAT TGT TGC T	60° C
Ocp143	AGT CAA TCA TCC ACA GAG ACC T	60° C
Ocp147	GCG TGA AGA ACG AGA TCA GC	68° C
OCP153	CTT CCC AAG TTG CTC TCC AC	68° C

### **2.1.21 Southern blot analysis**

DNA samples were electrophoresed at 20 V through a 0.8 % agarose gel overnight. The gel was soaked in 0.25 M HCl for 15 min. Sponges were placed in a deep trough and a piece of gel blotting paper (Schleicher & Schuell) cut to the size of the gel, placed onto the sponges. 0.4 M NaOH buffer was added to the trough until the sponges and blotting paper were fully soaked and the buffer had reached a height equal to half the height of the sponges. The gel was inverted and placed on top of the blotting paper, ensuring no air bubbles were present. A zeta-probe GTgenomic tested blotting filter (Bio-Rad), cut to the size of the gel, was placed onto the gel and any air bubbles removed. Three pieces of 3 mm blotting paper, each cut to the size of the gel and immersed in water, were placed on top of the gel, again ensuring no air bubbles were present between each layer. Paper towels were placed on top of the blotting paper, to a height of 15 cm, followed by a 100 g weight. The structure was left in place for a minimum of 15 hours, with the buffer topped up, and wet paper towels replaced, as and when necessary. The filter was then orientated and immersed in 2 x SSC (dilution of 20 x stock; 3 M NaCl, 0.3 M Na<sub>3</sub>C<sub>6</sub>H<sub>8</sub>O<sub>7</sub> pH 7) for 1 min. The filter was baked at 80° C for 30 min.

### **2.1.22 Probe radio-labelling and hybridisation**

The baked filter was placed into a tube containing 15 ml Church buffer (0.5 M NaH<sub>3</sub>PO<sub>4</sub> pH 7.2, 7 % [w/v] SDS, 0.5 M EDTA, pH 8.0). The filter was pre-hybridised by placing in a revolving oven at 65°C for 1 hour. Meanwhile, the appropriate volume of H<sub>2</sub>O was added to 50 ng of probe DNA, to give a final volume of 45 µl. The DNA was denatured by placing at 95° C for 5 min, and immediately placed on ice for 2 min. The DNA solution was transferred to a reaction bead mix (Ready-To-Go DNA labelling beads, Amersham Biosciences). 5 µl of [ $\alpha$ -<sup>32</sup>P] dCTP nucleotide (Amersham Bioscience) was added to the reaction. The reaction was incubated at 37° C for 30 min to allow labelling of the DNA. To remove unincorporated nucleotides, the reaction mix was added to the resin of a ProbeQuant G-50 Micro column (Amersham Bioscience). The column was centrifuged at 3000 rpm for 2 min and the purified sample boiled at 95°C for 10 min. The hybridisation reaction was commenced by addition of the purified sample to the tube containing the pre-hybridised filter and Church buffer. The hybridisation reaction was carried out for 16 hours.

## 2.2. Cell culture

All reagents were obtained from Invitrogen Life Technologies unless otherwise stated.

### *2.2.1 Production of primary mouse embryonic fibroblasts (MEFs) from E12.5 mouse embryos*

Embryos at E12.5 were dissected from a mouse uterus and transferred into a petri dish stored on ice. Each embryo was then processed in turn. The embryo was washed in an appropriate volume of ice-cold PBS. The tail was removed and placed in an eppendorf to be lysed for genotyping. The head and liver were removed and discarded. The remaining tissue was sliced up using a sterile scalpel and placed in a tube containing 5 ml ice-cold PBS. The PBS was aspirated and the mashed tissue washed with an additional 5 ml of PBS. 2 ml of 0.05 % [v/v] trypsin was added to the tube and incubated at 4° C for 3-6 hours. The tube was then incubated at 37° C for 20 min and the trypsin aspirated. The mashed tissue pellet was resuspended in 5 ml of MEF growth media (Dulbecco's Modified Eagles Medium with 4500 mg/l D-glucose, supplemented with 10 % [v/v] foetal calf serum (SeraQ), 100 units/ml penicillin, 100 µg/ml streptomycin, 20 mM L-glutamate) and transferred to a 10 cm cell culture dish, containing 5 ml of growth media. The dish was incubated at 37° C and 10 % CO<sub>2</sub> in a humidified atmosphere, and the media changed regularly.

### *2.2.2 Maintenance of MEFs*

Primary MEFs, cultured at 37° C, or MEFs containing the Simian Virus 40 large T antigen (tsSV40T), cultured at 33° C, were replenished from liquid nitrogen. The cell suspension was thawed at 37 °C and added to a tube containing 4 ml of MEF growth media. The resulting cell suspension was centrifuged at 1250 rpm for 5 min. The supernatant was discarded and the cell pellet resuspended in 5 ml of growth media. The cell suspension was transferred to a 10 cm cell culture dish, in a total volume of 10 ml growth media. The cells were incubated at 37 °C or 33° C and 10 % CO<sub>2</sub> in a humidified atmosphere. The media was changed every two days, until the cells were confluent. The cells were then passaged. The media was aspirated from the dish, 5 ml of PBS added and aspirated. 0.05 % [v/v] of trypsin was added and the dish incubated at 37° C or 33° C for 5 min. 5 ml of media was added to the dish and the cell suspension pipetted gently up and down, to obtain

a single-cell suspension. The cell suspension was divided 1 in 3 between three 10 cm dishes. 8 ml of growth media was added to each dish and the cells incubated as stated above. The cells were continually passaged and maintained until they reached a high passage number, at which point they were discarded.

### ***2.2.3 Freezing down stocks of cell lines***

The media was aspirated from a 10 cm dish containing fully confluent cells. 5 ml of PBS was added to the dish and removed. 1 ml of 0.05 % [v/v] trypsin was added and the dish incubated at 37° C, or 33° C for tsSV40T containing cells, for 5 min. 5 ml of media was added to the dish and the resulting cell suspension centrifuged at 1250 rpm for 5 min. The supernatant was discarded and the cell pellet resuspended in 3 ml of freezing media (45 % [v/v] growth media, 45 % [v/v] foetal calf serum, 10 % [v/v] DMSO). The cell suspension was transferred to 3 cryovials and stored at -80° C overnight. The cryovials were then transferred to a liquid nitrogen cell storage tank.

### ***2.2.4 Transfection of tsSV40T transfected MEFs with lipofectamine™***

Cells were seeded in 10 cm cell culture dishes at  $6 \times 10^5$  cells per dish in 10 ml growth media. The cells were incubated at 33° C and 10 % CO<sub>2</sub> in a humidified atmosphere. The following morning Lipofectamine™ reagent (Invitrogen) was used for the transfections. The protocol used was as described by the manufacturers manual. For each 10 cm plate, 8 µg of plasmid DNA, 0.8 µg of pGK-puro plasmid (Figure 2.1A) DNA and 36 µl of Lipofectamine™ were used. The Lipofectamine™ and DNA were mixed and incubated at room temperature for 45 min. Optimem serum-free medium was then added to the mixture, and the mixture added to the cells drop-wise. The cells were incubated for 5 hours. MEF growth media containing 20 % [v/v] serum was added to the cells and the cells incubated overnight. The following morning the media on the cells was changed and the cells incubated for 24 hours. The cells were placed on 10 µg/ml puromycin (Sigma) selection until cell clones formed.

### ***2.2.5 Selection of resistant MEF clones***

The 10 cm plate containing the MEF clones was washed twice with 10 ml PBS. 20 ml of PBS was added to the plate. Each clone was picked in 20 µl of PBS and transferred to a

well of a 96 well plate containing 20  $\mu$ l of 0.1 % [v/v] trypsin, The 96 well plate was placed at 37 °C for 5 min. Meanwhile, a 48 well plate was prepared with 0.5 ml of MEF growth media/well. 100  $\mu$ l of media was removed from each 48 well and mixed with the contents of a well of the 96 well plate. The resulting cell suspension was transferred back into the 48 well. Once all clones had been picked and transferred to the 48 well plate, the plate was incubated at 37° C, or 33° C for tsSV40T containing cells, and 10 % CO<sub>2</sub> in a humidified atmosphere. The media was changed daily until the cells reached confluency.

### ***2.2.6 Transfection of MEFs via Nucleofector™ technology***

Cells were seeded in 15 cm culture dish at  $4 \times 10^6$  cells per dish in 25 ml growth media, 24 hours prior to the transfection being performed. The following morning  $1 \times 10^6$  cells and 10  $\mu$ g plasmid DNA were used per transfection. The protocol used was as described in the manufacturer's manual. The Nucleofector™ programme used was T20 with Nucleofector™ Solution 6457. The transfected cells were seeded onto a 10 cm plate or divided between two 6 cm plate, and placed at 37°C and 10 % CO<sub>2</sub> in a humidified atmosphere. For tsSV40T containing cells, the cells were placed at 33° C and 10 % CO<sub>2</sub> in a humidified atmosphere for 6 hours.

### ***2.2.7 Mitomycin C treatment of primary MEFs***

MEFs were derived from embryos at E14, as described previously. At 80 % confluency, 2  $\mu$ g/ml of mitomycin C was added to the culture medium for 3 hours. The mitomycin C containing media was discarded and the MEFs washed 3 times with PBS. The MEFs were trypsinised and frozen down at  $1.5 \times 10^6$  cells in freezing vials, as previously described.

### ***2.2.8 Maintenance of embryonic stem (ES) cells***

The E14.1a ES cell line was previously derived from the 129Ola mouse strain. For maintenance: The surface of a 10 cm plate was coated with sterile 0.1 % [w/v] gelatine for 5 min.  $1 \times 10^6$  mitomycin C treated MEFs were thawed and seeded onto the plate in MEF growth media. After 24 hours, a cryovial of ES cells was thawed. The cell suspension was thawed at 37° C and added to a tube containing 5 ml of ES cell growth media. (Dulbecco's Modified Eagles Medium with L-glutamine and 4500 mg/l D-glucose, supplemented with 15 % [v/v] foetal embryonic stem cell qualified foetal bovine serum [Labtech

International], 100 units/ml penicillin, 100 µg/ml streptomycin, 20 mM L-glutamate, 1 mM non-essential amino acids, 10 mM sodium pyruvate, 115 µM β-mercaptoethanol, 1 ml recombinant leukaemia inhibitory factor (LIF) (S. Munson, University of Leicester)]. The cell suspension was centrifuged at 1250 rpm for 5 min. The supernatant was discarded and the cells resuspended in 5 ml of ES cell growth media. The cell suspension was transferred to the 10 cm cell culture dish containing mitomycin C treated MEFs, in a total volume of 10 ml ES cell growth media. The cells were incubated at 37° C and 10 % CO<sub>2</sub> in a humidified atmosphere. The media was changed daily until the cells reached 70 % confluency. The cells were then passaged. The media was aspirated from the dish, 5 ml of PBS added and aspirated. 0.05 % [v/v] of trypsin was added and the dish incubated at 37° C for 5 min. 5ml of ES cell media was added to the dish and the cell suspension pipetted gently up and down, to obtain a single-cell suspension. The cell suspension was divided 1 in 3 between three 10 cm dishes, that 24 hours previously had been coated in 0.1 % [w/v] gelatin and seeded with mitomycin C treated MEFs. 8 ml of ES cell growth media was added to each dish and the cells incubated as stated above. The cells were continually passaged and maintained until they reached a high passage number, at which point they were discarded.

### ***2.2.9 Electroporation of ES cells***

ES cells were passaged 48 hours before the electroporation. The cells were fed with fresh ES cell growth media 5 hours prior to the electroporation. The cells were washed with PBS and trypsinised by the addition of 0.05 % [v/v] trypsin.  $5 \times 10^8$  cells were harvested, washed with PBS and resuspended in a volume of 1.6 ml PBS. 60 µg of purified, linearised DNA was added to the cell suspension. The suspension was divided between two electroporation cuvettes (Bio-Rad). The cuvettes were placed in a Gene pulser equipped with a capacitance extender (Bio-Rad) and electroporated at 0.25 V and 500 µFD. The cuvettes were left at room temperature for 5 min and the cells from each cuvette subsequently plated onto 1 x 10 cm culture dish containing mitomycin C treated MEFs. The cells were incubated at 37° C and 10 % CO<sub>2</sub> in a humidified atmosphere for 24 hours. The cells were then placed in ES growth media containing 250 µg/ml geneticin for 7 days until clones had formed.

### ***2.2.10 Selection of resistant ES cell clones***

Twenty four hours prior to picking of clones, a 48 well plate was gelatinised and seeded with mitomycin C treated MEFs. The following day the 10 cm plate containing the ES cell clones was washed twice with 10 ml PBS. 20 ml of PBS was added to the plate. Each clone was picked in 20  $\mu$ l of PBS and transferred to a well of a 96 well plate containing 20  $\mu$ l of 0.1 % [v/v] trypsin. The plate was placed at 37° C for 5 min. Meanwhile the media was removed from the mytomycin C treated MEFs and replaced with 0.5 ml ES growth media. 100  $\mu$ l of media was removed from each 48 well and mixed with the contents of a well of the 96 well plate. The resulting cell suspension was transferred back into the 48 well. Once all clones had been picked and transferred to the 48 well plate, the plate was incubated at 37° C, and 10 % CO<sub>2</sub> in a humidified atmosphere. The media was changed daily until the cells reached confluency.

### ***2.2.11 Freezing down and seeding for DNA analysis of ES cell/MEF clones***

Confluent 48 well clones were trypsinised in 50  $\mu$ l of 0.05 [v/v] trypsin. 100  $\mu$ l of the appropriate growth media was added to the well. 100  $\mu$ l of the resulting cell suspension was added to the well of a 96 well plate containing 2 x freezing media (40 % [v/v] growth media, 40 % [v/v] growth serum, 20 % [v/v] DMSO). 30 to 40 clones were transferred per 96 well plate. The plate was frozen at -80° C. The remaining 50  $\mu$ l of cell suspension was transferred to the well of a 12 well plate (pre-coated in 0.1 % [w/v] gelatin for ES clones) to grow for DNA analysis.

### ***2.2.12 Generation of transgenic mice***

ES cells were seeded as previously described. The cells were grown until 70 % confluency. The cells were trypsinised as previously described and 5 ml of growth media added. The resulting cell suspension was centrifuged at 1250 rpm for 5 min. The cell pellet was resuspended in 500  $\mu$ l injection media (Dulbecco's Modified Eagles medium with 4500 mg/l D-glucose, supplemented with 10 % [v/v] foetal embryonic stem cell qualified foetal bovine serum [Labtech International], 100 units/ml penicillin, 100  $\mu$ g/ml streptomycin, 20 mM L-glutamate, 10 mM sodium pyruvate). The cells were injected into donor blastocytes and implanted into a donor mother by Ms J Brown and Mr A. Oakden at the Division of Biomedical Services, The University of Leicester.

### **2.2.13 Cre transfection of ES cells**

ES cells were seeded in 2 x 10 cm plates, previously gelatinised (0.1 % [w/v] gelatin) and seeded with  $1 \times 10^6$  mitomycin C treated MEFs, until 70 % confluency.  $5 \times 10^6$  ES cells were harvested, centrifuged at 1250 rpm for 5 min, and resuspended in 800  $\mu$ l of PBS. 30  $\mu$ g of pCre-PAC plasmid (Figure 2.1B) was added to the cell suspension. The suspension was transferred to an electroporation cuvette (Bio-Rad) and left at room temperature for 5 min. The cuvette was placed in a Gene pulser equipped with a capacitance extender (Bio-Rad) and electroporated at 260 V and 960  $\mu$ FD. The cells were left at room temperature for 5 min and plated onto a 10 cm culture dish containing mitomycin C treated MEFs. The cells were incubated at 37° C and 10 % CO<sub>2</sub> in a humidified atmosphere for 24 hours. The ES cells were then placed on selection by the addition of 2  $\mu$ g/ml puromycin for 36 hours. The cells were harvested and re-plated at  $1 \times 10^3$  cells onto a 10 cm culture dish containing mitomycin C treated MEFs. The cells were grown in ES growth media until clones had formed.

## **2.3. MEF analysis**

### **2.3.1 Annexin V FITC staining of cells**

Cells were seeded at  $1.5 \times 10^5$  in a volume of 3 ml growth media, in 6 cm cell culture dishes. Two dishes were seeded for each cell type. The cells were incubated at 37° C, or 33° C for tsSV40T transformed cells, and 10 % CO<sub>2</sub> in a humidified atmosphere for 24 hours. The media was replaced with fresh growth media and the cells placed at 37° C, or at the restrictive temperature of 39° C for tsSV40T containing cells, and 10 % CO<sub>2</sub> in a humidified atmosphere for 24 hours. To one dish for each cell type, the media was replaced with fresh media. The second dish was stimulated by the addition of 50 ng/ml anti-CD95 antibody (BD Pharmingen) and 0.5  $\mu$ M cycloheximide in 3 ml of growth media, or placed in serum-free media. The cells were incubated at 37° C or 39° C for 20 hours. The media was removed from each dish and collected into a tube. Each dish was washed with PBS, which was also added to the corresponding collection tube. 1 ml of 0.025 % [v/v] trypsin was added to each dish and the dishes incubated at 37° C for 20 min. 1 ml of growth media was added to each plate to neutralise the trypsin. The subsequent cell suspension was added to the corresponding collection tube. The tubes were centrifuged at 1500 rpm for 5 min. The supernatant was discarded and the resulting pellet

resuspended in 1 ml of growth media. The tubes were placed at 37° C for 5 min. 0.5 ml was removed from each tube and either discarded or kept for protein analysis. The remaining 0.5 ml was centrifuged at 1500 rpm for 5 min. The supernatant was discarded and each pellet resuspended in 1 x Annexin binding buffer (Bender Medsystems) containing 3 µl Annexin V-FITC (Bender Medsystems) and transferred to FACScan tubes. The tubes were incubated at room temperature for 10 min. 1 µg/ml propidium iodide (Bender Medsystems) was added to each tube and the tubes incubated on ice. The apoptotic phenotype of the cells were analysed by fluorescence activated cell sorting (FACS) (Becton Dickinson). The results were analysed by plotting graphs of propidium iodide staining versus Annexin V FITC staining. Cells that were either Annexin V positive, or both Annexin V and propidium iodide positive, were counted as apoptotic.

### ***2.3.2 Cell growth curves***

MEFs were seeded at  $1 \times 10^4$  per well of a 24 well plate in 1 ml of MEF growth media. For the next eight consecutive days, three wells were washed with PBS and trypsinised by the addition of 0.05 % [v/v] trypsin. The cells in each well were counted using a haemocytometer, and the values recorded. The media was changed four days after seeding.

### ***2.3.3 DNA staining***

MEFs were seeded at  $5 \times 10^4$  cells in a 6 cm culture dish in 3 ml MEF growth media. The following day the cells were washed with PBS and trypsinised by the addition of 0.05 % [v/v] trypsin. 4 ml of growth media was added to the cells and the cell suspension centrifuged at 1250 rpm for 5 min. The cell pellet was resuspended in 100 µl cold PBS and 1 ml of 70 % [v/v] ethanol added. The resulting cell solution was placed on ice for 30 min. The fixed cells were centrifuged at 4° C and 1250 rpm for 5 min and the cell pellet resuspended in 1 ml PBS containing 10 µg/ml propidium iodide and 100 µg/ml RNase. The cell suspension was left at room temperature for 1 hour and analysed by FACS.

### ***2.3.4 Immunofluorescence of cells***

Cells were plated at  $6 \times 10^4$  cells/ml on coverslips, previously coated in 10 µg/ml fibronectin, and cultivated until 80 % confluent. The cells were fixed with 2 % [v/v]

paraformaldehyde in PBS for 20 min, followed by permeabilisation by the addition of 0.2 % [v/v] Triton X-100 for 5 min. The cells were treated with 1 % [w/v] BSA/PBS blocking solution for 16 h, followed by incubation with 250 ng/ml primary antibody for 1 h. After 3 washes with 0.02 % [w/v] BSA/PBS, the cells were incubated with 200 µg/ml secondary antibody for 1 h, followed by a further 3 washes with 0.02 % [w/v] BSA/PBS. The cells were incubated with 33 nM Texas Red-X phalloidin (Molecular Probes) for 20 min to allow staining of F-actin, followed by 3 washes with 0.02 % [w/v] BSA/PBS. To observe staining of the mitochondria, Mitotracker (Molecular Probes) was used in place of Texas Red-X phalloidin. Cells were incubated with 25 nM Mitotracker Red CMXRos for 30 min. Cells were mounted on slides and viewed using a Nikon Eclipse TE300 microscope.

### ***2.3.5 5-Bromo-2'-deoxy-uridine (BrdU) cell analysis***

Cells were seeded at  $1 \times 10^4$  in 2 ml growth media on coverslips in an 8 well plate until 60 % confluent. The media was removed, cells washed with PBS and incubated in serum-free growth media for 8 hours. BrdU analysis was then commenced using a BrdU labelling and detection kit I (Roche). 1 x BrdU labelling reagent was added to the cells in 2 ml of growth media for the required time length. The immunofluorescence method used was as described in the manufacturer's manual.

## **2.4. Protein analysis**

### ***2.4.1 Production of cell lysates cells for protein analysis***

Growth media was removed from 6 cm dishes containing fully confluent cells. Cells were stimulated or left untreated as required. To serum stimulate cells; the cells were initially placed in media containing 0.5 % serum for 24 hours. Cells were then stimulated by addition of growth media containing 10 % serum, for the desired length of time. The cells were then lysed in one of two ways. Either, the media was removed, cells washed with PBS and lysed directly in 100 µl 1x laemmli loading buffer (62.5 mM Tris 6.8, 2 % [w/v] SDS, 5 % [v/v] β-mercaptoethanol, 10 % [v/v] glycerol, 0.04 % [w/v] pyronin Y), or if proteins involved in cell death pathways were to be subsequently detected, whole cell lysates were produced by scraping cells directly from the plate, and transferring the cell suspension obtained to a tube. The tube was centrifuged at 4° C and 1000 rpm for 3 min. The pellet was washed with ice-cold PBS and lysed in 150 µl lysis sample buffer (62.5

mM Tris HCl pH 6.8, 15 % [v/v] glycerol, 2 % [w/v] SDS, 5 % [v/v]  $\beta$ -mercaptoethanol, 0.5 mg/ml bromophenol blue). The lysates were sonicated for 15 s, boiled at 95° C and stored at -20° C.

#### **2.4.2 Stimulation of cells and production of clear cell lysates for protein analysis**

Growth media was removed from 6 cm dishes containing fully confluent cells, and replaced with 1 ml serum-free medium. The plate was incubated at 37° C and 10 % CO<sub>2</sub> in a humidified atmosphere for 20 min. The appropriate concentrations of stimuli were then added to the wells, as shown by the following table.

**Table 2.2** Concentrations of various stimuli used for cell analysis

Stimulus	Final concentration
Serum	10 % (v/v)
PMA	40 $\mu$ M
PDGF	50 ng/ml
EGF	10 ng/ml

1 ml of 2 x final concentration of stimulus was added to the media in the wells. The cells were then incubated for the appropriate amount of time. The media was removed from the wells and the plates immediately placed on ice. 1 ml of ice-cold PBS was added to each well and aspirated. The cells were lysed by the addition of 1 ml of ice-cold versene (Life Technologies) and transferred to eppendorfs. The cells were pelleted by centrifuging at 3000 rpm at 4° C for 2 min. The pellet obtained was washed with ice-cold PBS and centrifuged at 3000 rpm at 4° C for 2 min. The resulting pellet was lysed in 50  $\mu$ l of GLB (1 % [v/v] Triton X-100, 20 mM Tris pH 8.0, 137 mM NaCl, 15 % [v/v] glycerol, 5 mM EDTA) with added protease and phosphatase inhibitors (10 mM  $\beta$ -G<sup>p</sup> pH 7.5 HCl, 1 mM AEBSF, 2 mM benzamidine, 0.5 mM Na<sub>3</sub>VO<sub>4</sub>, 0.5 mM DTT, 10  $\mu$ g/ml leupeptin, 10  $\mu$ g/ml aprotinin). The tubes were placed on ice for 15 min and then centrifuged at 13000 rpm at 4° C for 10 min. The supernatant was transferred to a fresh eppendorf. 5  $\mu$ l was removed from samples requiring protein determination. The tubes were then snap frozen in liquid N<sub>2</sub> and stored at -80° C. Clear lysates for Western blot analysis were combined with 1 x laemmli loading buffer, boiled for 5 min and stored at -20° C.

### ***2.4.3 Stimulation of cells and production of clear cell lysates for protein analysis***

Growth media was removed from 10 cm dishes containing fully confluent cells and replaced with serum-free medium. The plate was incubated at 37° C and 10 % CO<sub>2</sub> in a humidified atmosphere for 48 hours. Cells were then left untreated or treated with 25 ng/ml EGF for 5 min. The media was removed from the plates and the plates immediately placed on ice. 1 ml of ice-cold PBS was added to each well and aspirated. The cells were lysed by the addition of 100 µl of lysis buffer (20 mM Tris pH 8.0, 1 % Triton X-100, 2 mM EDTA, 1 mM NaVO<sub>4</sub>, 50 mM NaF, 5 mM 2-glycerolphosphate, 0.1 % 2-mercaptoethanol, 1 mM AEBSF) and transferred to eppendorfs. The lysates were snap frozen and plated at -80° C for 24 hours.

### ***2.4.4 Bicinchoninic acid (BCA) protein analysis***

1-5 µl of each clear protein lysate sample was added to a well of a 96 clear-view plate. BSA and/or H<sub>2</sub>O was added to empty wells of the plate, to give a BSA concentration range of 0-20 µg/µl. 200 µl of a mixture of BCA™ protein reagents A and B (50:1) (Pierce) was added to each well. The plate was incubated at 37°C for 30 min. The OD<sub>630</sub> was measured using an EL 340 microplate reader (Bio-TEK™ Instruments). The protein concentration of each sample was calculated by comparison to the BSA standard curve generated.

### ***2.4.5 Immunoprecipitation assay***

1 mg of cell lysate was placed in 500 µl of lysis buffer (20 mM Tris pH 8.0, 1 % Triton X-100 [v/v], 2 mM EDTA, 1 mM NaVO<sub>4</sub>, 50 mM NaF, 5 mM 2-glycerolphosphate, 0.1 % 2-mercaptoethanol [v/v], 1 mM AEBSF) and incubated with 1 µg monoclonal mouse anti-caspase 9 antibody (Chemicon) at 4° C for 1 hour. 40 µl of washed protein A sepharose beads (Sigma) were then added and incubated at 4° C for 1 hour. Immunoprecipitates were washed 3 x in lysis buffer before boiling in 1 x laemmli loading buffer.

### ***2.4.6 Sodium dodecyl sulfate polyacrylamide gel electrophoresis (SDS-PAGE)***

SDS-PAGE gels were cast using a Mini-PROTEAN 3 cell (Bio-Rad). Separation and stacking gel solutions were made up as shown in Table 2.3. The TEMED was added immediately prior to gel pouring. The gel cassette was placed in a gel running tank containing 1 x SDS PAGE running buffer (25 mM Tris, 1.92 mM glycine 0.1 % [w/v]

SDS). Protein samples were added to the wells of the gel. The samples were electrophoresed alongside a high, low or pre-stained molecular weight SDS PAGE protein marker. The gel was run at 150 V until the dye front had reached the bottom of the plates.

**Table 2.3** Recipes for SDS PAGE separation and stacking gels.

Per gel	8 % separation gel	10 % separation gel	15% separation gel	4 % stacking gel
Water	1.75 ml	3.0 ml	0.9 ml	1.8 ml
1.5 M Tris-HCl (pH 8.8)	0.95 ml	1.4 ml	1.0 ml	-
0.5 M Tris-HCl (pH 6.8)	-	-	-	0.8 ml
30 % Protogel	1 ml	1.9 ml	1.9 ml	0.4 ml
10 % SDS	37.5 $\mu$ l	56 $\mu$ l	38 $\mu$ l	30 $\mu$ l
10 % APS	37.5 $\mu$ l	56 $\mu$ l	38 $\mu$ l	30 $\mu$ l

#### 2.4.7 Western blot analysis

The gel was soaked in gel transfer solution (25 mM Tris, 1.92 mM Glycine, 0.01 % [w/v] SDS) for 20 min. Two pieces of gel blotting paper (Schleicher & Schuell) were cut to the size of the gel. The transfer was then assembled on a Trans-Blot<sup>®</sup> SD semi-dry transfer cell (Bio-Rad). One piece of the filter paper was moistened in membrane transfer solution (25 mM Tris, 1.92 mM Glycine, 0.01 % [w/v] SDS, 20 % [v/v] methanol) and placed on the transfer cell. A piece of 0.45  $\mu$ m Protran BA85 cellulose nitrate membrane (Schleicher & Schuell) or 0.45  $\mu$ m PVDF transfer membrane (Amersham Biosciences), cut to the size of the gel, was moistened in membrane transfer solution or 100 % [v/v] methanol respectively, and overlaid on the filter paper. The gel was carefully placed on top of the membrane, ensuring no air bubbles were created. The second piece of filter paper was moistened in gel transfer solution and placed on top of the gel. The transfer cell was run for 1.5 hours at 1 mA/cm<sup>2</sup> of gel. The membrane was washed for 3 x 5 min with Tris-buffered saline (10 mM Tris-HCl pH 7.6, 150 mM NaCl) containing 0.05% [v/v] Tween 20 (TBS/Tween). The membrane was blocked in 5 % [w/v] Marvel (made up using TBS/Tween) for 1 hour at room temperature. The membrane was washed three times for 5 min per wash with TBS/Tween and incubated in the primary antibody (diluted with TBS/Tween) (Table 2.4a/b), overnight at 4° C. The following morning the membrane was washed three times for 5 min per wash with TBS/Tween and the secondary antibody

(conjugated to horseradish peroxidase and diluted 1 in 3500 with TBS/Tween) added for 1 hour at room temperature. The membrane was washed three times for 5 min per wash with TBS/Tween. The enhanced chemiluminescence detection system (Pierce) was used to visualise the protein of interest. Equal ratios of the two solutions were mixed, and 2 ml of the resulting mixture evenly distributed over the membrane for 3 min. Excess liquid was removed and the membrane exposure to photographic film (Fuji) at room temperature, for various time lengths.

**Table 2.4a** Antibodies used for Western blot analysis

Primary antibody	Protein size detected (KDa)	Dilution	Source and secondary antibody	Company
B-Raf	95	1:1000	mouse monoclonal	Santa Cruz Biotechnology, Inc
C-Raf	74	1:1000	mouse monoclonal	BD Transduction laboratories
A-Raf	68	1:1000	rabbit polyclonal	Santa Cruz Biotechnology, Inc
SV40 large T antigen	85	1:5000	mouse monoclonal	BD Pharmingen
phospho-MEK	45	1:1000	rabbit polyclonal	Cell Signaling Technology
phospho-ERK1/2	44/42	1:1000	mouse monoclonal	Cell Signaling Technology
ERK 1	44/42	1:1000	rabbit polyclonal	Santa Cruz Biotechnology, Inc
phospho-p38 MAPK	38	1:1000	mouse monoclonal	Cell Signaling Technology
p38 MAPK	38	1:1000	mouse monoclonal	Santa Cruz Biotechnology, Inc
phospho-Akt (Ser473)	60	1:1000	rabbit polyclonal	Cell Signaling Technology
p21	21	1:1000	mouse monoclonal	Cell Signaling Technology
p27	27	1:1000	rabbit polyclonal	Santa Cruz Biotechnology, Inc
Cyclin D1	36	1:1000	mouse monoclonal	Cell Signaling Technology
cdk 4	30	1:1000	mouse monoclonal	Cell Signaling Technology
cdk 6	36	1:1000	mouse monoclonal	Cell Signaling Technology
cyclin E	53	1:1000	rabbit polyclonal	Cell Signaling Technology
cdk2	36	1:1000	rabbit polyclonal	Cell Signaling Technology

**Table 2.4b** Antibodies used for Western blot analysis

Primary antibody	Protein size detected (KDa)	Dilution	Source and secondary antibody	Company
<i>c-fos</i>	62	1:1000	rabbit polyclonal	Santa Cruz Biotechnology, Inc
actin	45	1:2000	1:2000	Sigma-Aldrich
vinculin	116	1:2000	1:2000	Gift from Dr. V. Koteliansky, CNRS, Paris
cleaved caspase 3	18	1:1000	rabbit polyclonal	Trevigen
caspase 9	49	1:1000	sheep polyclonal	Gift from Dr. P. Clarke, University of Dundee
phospho-Thr125-caspase 9	49	1:1000	rabbit polyclonal	Gift from Dr. P. Clarke, University of Dundee
Bim	23 (BimEL) 16 (BimL)	1:1000	rabbit polyclonal	Chemicon
phospho-p90RSK (Thr 573)	90	1:1000	rabbit polyclonal	Cell Signaling Technology

### 2.5. Statistical analysis

Statistical data in results chapters 3-6 were derived using the student's t-Test in Microsoft Excel. For analysis, two data sets were compared via a paired t-test and using the two-tailed distribution setting. The *P* values generated indicate the significance of the data, with a value of  $P \leq 0.05$  indicating significant data.

### 3. CHARACTERISATION OF THE ROLE OF C-Raf IN CELL SURVIVAL USING *C-raf*<sup>-/-</sup> MOUSE EMBRYONIC FIBROBLASTS

#### 3.1 Introduction

##### 3.1.1 Investigation of the role of C-Raf in apoptosis

The most studied and characterised role for C-Raf is its involvement in the Ras/Raf/MEK/ERK pathway. Ras interacts with Raf upon mitogenic stimuli and is required to translocate Raf to the plasma membrane (Leevers *et al.*, 1993; Stokoe *et al.*, 1993). At the plasma membrane Raf proteins are known to be involved in a number of phosphorylation and dephosphorylation events that can lead to their full activation (Marais *et al.*, 1997; Mason *et al.*, 1999; Zhang and Guan, 2000; Morrison *et al.*, 1993; Wu *et al.*, 1993a). Upon activation, Raf proteins activate MEK1/2 (Dent *et al.*, 1992; Howe *et al.*, 1992; Kyriakis *et al.*, 1992) which in turn activate ERK1/2 (Payne *et al.*, 1991). ERK1/2 are involved in the activation of numerous cytoplasmic and nuclear substrates.

Although the Raf protein kinases are the predominant MEK activators, the ability of each Raf isoform to activate MEK also varies. B-Raf is by far the strongest activator of MEK. This has been concluded for a number of cell types including fibroblasts, neuronal tissue and lymphocytes (Hüser *et al.*, 2001; Catling *et al.*, 1994; Reuter *et al.*, 1995; Jaiswal *et al.*, 1994; Eychene *et al.*, 1995; Jaiswal *et al.*, 1996; Kao *et al.*, 2001). C-Raf activates MEK to a lesser extent than B-Raf, but to a greater extent than A-Raf, which shows very little activity towards MEK (Pritchard *et al.*, 1995; Marais *et al.*, 1997, Papin *et al.*, 1998; Hüser *et al.*, 2001). The differing abilities of each Raf isoform in activating MEK suggests they may play different roles in signalling through the MEK/ERK pathway.

Studies have indicated a role for C-Raf in suppressing apoptosis that is independent of its role in the Ras/Raf/MEK/ERK pathway. Two independent studies analysing apoptosis in *C-raf*<sup>-/-</sup> mice showed an increased susceptibility to apoptosis that was independent of C-Raf MEK kinase activity. The increased apoptosis was observed in response to Fas stimulation but not in response to TNF stimulation (Hüser *et al.*, 2001; Mikula *et al.*, 2001).

*C-raf*<sup>-/-</sup> mice produced on a mixed 129Ola/MF-1 genetic background survived to a few days after birth. These mice were smaller than their wild-type litter mates and displayed disorganised placenta and were anaemic (Hüser *et al.*, 2001). ERK activity was no different in *C-raf*<sup>-/-</sup> MEFs derived from these embryos compared to MEFs derived from wild-type littermates. However, the *C-raf*<sup>-/-</sup> MEFs did show increased susceptibility to programmed cell death (PCD) upon treatment with various apoptotic agents (Hüser *et al.*, 2001).

In a second study, embryos produced on the 129/Sv genetic background, and a mixed 129Ola/C57BL6 genetic background, died during mid-gestation and were smaller than their wild-type littermates. As with the study described above, abnormalities were observed in the placenta. Increased apoptosis of foetal liver cells were also observed (Mikula *et al.*, 2001). MEFs derived from the *C-raf*<sup>-/-</sup> embryos showed normal MEK and ERK activation, and were susceptible to increased apoptosis upon treatment with various apoptotic agents when compared to MEFs derived from their wild-type littermates (Mikula *et al.*, 2001).

Overall the findings described indicate C-Raf is essential for mouse development and plays an important role in the prevention of apoptosis. This role is affected by the strain, as a greater degree of apoptosis was observed for MEFs produced from the 129Ola/C57BL6 genetic background than the 129Ola/MF-1 genetic background (Hüser *et al.*, 2001). A further study showed increase susceptibility to apoptosis in *C-raf*<sup>-/-</sup> macrophages (Jesenberger *et al.*, 2001).

Homozygous mice were also generated with Tyr340/341 mutated to phenylalanine, namely *C-raf*<sup>FF/FF</sup> mice (Hüser *et al.*, 2001). These mice showed no detectable *in vitro* activity towards MEK, yet developed normally and survived to adulthood. They also showed normal ERK activation, and unlike the *C-raf*<sup>-/-</sup> embryos, no increased susceptibility to apoptosis was observed upon treatment with various apoptotic agents. These findings indicated that the role of C-Raf in suppressing apoptosis is most likely independent of its MEK kinase activity.

It has also been shown in skeletal myoblasts that high signalling levels of C-Raf can suppress apoptosis in this cell line and use of a MEK inhibitor did not block this

suppression (DeChant *et al.*, 2002). Again, this indicates a role of C-Raf in MEK kinase independent cell survival.

A number of pathways have been suggested to account for the MEK kinase independent role of C-Raf in the suppression of apoptosis (Figure 1.9). C-Raf has been shown to interact with the anti-apoptotic Bcl-2 protein via co-immunoprecipitation experiments (Wang *et al.*, 1994). This leads to synergistic apoptosis suppression upon withdrawal of Interleukin-3 (IL-3) in IL-3-dependent hemopoietic cells, but results indicated this was not due to C-Raf directly phosphorylating Bcl-2. Observations were made that C-Raf can bind to the BH4 domain of Bcl-2 and target C-Raf to the mitochondria (Wang *et al.*, 1996a). However, it has subsequently been stated that this may have only occurred due to the over-expression of Bcl-2 in these cells (Rapp *et al.*, 2004). It was also observed that a mitochondrial targeted form of the kinase domain of C-Raf suppresses apoptosis to the same extent as C-Raf and Bcl-2 combined, suggesting they may not be directly involved in suppressing apoptosis (Wang *et al.*, 1996a). An independent study to those described above observed Bcl-2 does not require C-Raf kinase activity for its role in cell survival (Olivier *et al.*, 1997). C-Raf and Bcl-2 have also been shown to act independently in suppressing apoptosis (Zhong *et al.*, 2001). Therefore it is unclear as to if C-Raf and Bcl-2 act directly together in suppressing apoptosis and if they play a role together at the mitochondria.

Bad, the pro-apoptotic member of the Bcl-2 family, in its non-phosphorylated form, binds to the anti-apoptotic Bcl-x<sub>L</sub> protein. This sequesters Bcl-x<sub>L</sub>, preventing it from suppressing apoptosis at the mitochondria, thus allowing the release of cytochrome c. Bad can be phosphorylated leading to the binding of 14-3-3 proteins. This causes cytoplasmic relocation of Bad, thus leaving Bcl-x<sub>L</sub> free in its role to suppress apoptosis (Zha *et al.*, 1996). A mitochondrial targeted kinase domain of C-Raf was shown to phosphorylate Bad (Wang *et al.*, 1996b), but no further role for C-Raf in suppressing apoptosis by sequestering Bad has been reported.

Bag-1 is a multifunctional protein that interacts with the Hsc70 and Hsp70 heat shock proteins (Takayama & Reed, 2001) and may play a role in regulating cell growth and survival (Townsend *et al.*, 2005). Bag-1 binds to and activates C-Raf (Wang *et al.*, 1996b). Recent data have suggested that Bag-1 plays a role in the suppression of apoptosis by C-

Raf in tumour cells (Götz *et al.*, 2004). When a lung cancer mouse model expressing constitutively active C-Raf was crossed to Bag-1 heterozygote mice, tumour cells showed increased apoptosis. The precise interaction in cell survival between C-Raf, Bag, and the possible involvements of Hsc70, Hsp70, Bcl-2 and Bad, still need to be addressed.

The NF $\kappa$ B family of transcription factors are retained in the cytoplasm, as dimers, by being bound to specific inhibitors known as I $\kappa$ Bs (Mercurio *et al.*, 1993). The I $\kappa$ B-kinase complex, (IKK) is responsible for phosphorylating the I $\kappa$ Bs (Zandi *et al.*, 1998). This leads to polyubiquitination and degradation of the I $\kappa$ B proteins by the proteasome pathway, allowing the freed NF $\kappa$ B dimers to translocate to the nucleus (Chen *et al.*, 1995; Traenckner *et al.*, 1995). At the nucleus NF $\kappa$ B proteins are involved in the activation of gene transcription of many genes including those associated with the inflammatory response, development and cell survival (Beg and Baltimore, 1996; Van Antwerp *et al.*, 1996). The role of NF $\kappa$ B in the suppression of apoptosis is via the induction of a number of genes, including the inhibitor of apoptosis proteins (IAP) 1 and 2 (Chu *et al.*, 1997; Wang *et al.*, 1998). The IAPs are a family of proteins that suppress apoptosis by directly inhibiting caspases (Deveraux and Reed, 1999). NF $\kappa$ B is also responsible for upregulating the caspase 8 inhibitor C-FLIP, which leads to resistance to death induced apoptosis (Micheau *et al.*, 2001).

C-Raf has been shown to increase the transcriptional activity of NF $\kappa$ B independently of its role in the Ras/Raf/MEK/ERK pathway (Norris and Baldwin, 1999). Findings have revealed C-Raf is involved in the dissociation of the NF $\kappa$ B- I $\kappa$ B complex (Li and Sedivy, 1993), although the involvement of C-Raf may be indirect. C-Raf associates with casein kinase II, and this in turn can interact with I $\kappa$ B and leads to its dissociation from NF $\kappa$ B (Janosch *et al.*, 1996). Evidence also exists to suggest C-Raf indirectly activates NF $\kappa$ B via the membrane shuttle kinase MEKK1 (Baumann *et al.*, 2000). Co-transfecting C-Raf with a dominant negative form of MEKK1 strongly reduced NF $\kappa$ B dependent reporter gene activity, and led to a synergistic activation of the reporter construct in the presence of MEKK1 and C-Raf. No direct links between NF $\kappa$ B and C-Raf in apoptosis have been found. This is further supported by the observation that NF $\kappa$ B activity is not altered in C-*raf*<sup>-/-</sup> macrophages that show increase susceptibility to apoptosis (Jesenberger *et al.*, 2001).

Apoptosis signal-regulating kinase 1 (ASK1) is a ubiquitously expressed MKKK. It activates the stress induced MKK4/MKK7-JNK and MKK3/MKK6-p38-MAPK signalling cascades (Ichijo *et al.*, 1997). The over-expression of wild-type or activated alleles of ASK1 activates JNK and p38 and induces apoptosis in various cells through mitochondria-dependent caspase activation (Ichijo *et al.*, 1997; Hatai *et al.*, 2000). ASK1-deficient cells are resistant to H<sub>2</sub>O<sub>2</sub>- and TNF- induced apoptosis (Tobiume *et al.*, 2001), thus suggesting ASK1 plays a crucial role in stress-induced apoptosis.

C-Raf has been shown to interact with ASK1 *in vitro* and *in vivo* (Chen *et al.*, 2001). Over-expression of C-Raf leads to decreased apoptosis in ASK1 expressing HeLa cells, suggesting C-Raf plays a role in antagonising ASK1 activity. Using MEK antagonists, it was shown that this role does not require the MEK-ERK pathway. Furthermore, kinase inactive forms of C-Raf were able to inhibit ASK1 induced apoptosis (Chen *et al.*, 2001). Therefore these results show that the inhibition of ASK-1-induced apoptosis by interaction with C-Raf does not require C-Raf kinase activity, nor is it dependent on the ability of C-Raf to activate ERKs.

A recent study has also shown C-Raf may antagonise ASK1-induced apoptosis in a MEK-ERK independent manner (Yamaguchi *et al.*, 2004). This study investigated the role of C-Raf in cardiac muscle-specific *C-raf*<sup>-/-</sup> mice. These mice showed increased apoptosis within the hearts, increased levels of JNK and p38 activity, but no change in MEK or ERK levels. Furthermore, ASK1 ablation rescued the abnormalities observed, suggesting the deficiency of C-Raf was allowing ASK1 to induce apoptosis within these cells.

It is still unclear whether MEK independent suppression of apoptosis by C-Raf occurs at the mitochondria, or indeed if C-Raf activation must occur at the mitochondria. As stated earlier, mitochondrial targeted C-Raf has been observed to protect mammalian hemopoietic 32D cells from apoptosis by preventing cytochrome *c* release (Wang *et al.*, 1996a). It was also shown that expression of mitochondrial C-Raf led to increased cell survival in 32D cells (Perruzi *et al.*, 1999). Furthermore, mitochondrial C-Raf has been found to protect cells via Bcl-2 or Bad independent pathways (Zhong *et al.*, 2001). C-Raf has been observed to interact with the voltage dependent anion channel (VDAC) (Le Mellay *et al.*, 2002). This channel is a mitochondrial pore involved in the exchange of

metabolites. The kinase domain of C-Raf was found to directly interact with VDAC and was thought to affect metabolite flow in and out of the mitochondria. The role this may play in apoptosis has not been investigated. However, in *C-raf*<sup>-/-</sup> macrophages that showed increase susceptibility to apoptosis, assessment of alteration of mitochondrial function showed no significant cytochrome *c* release in these cells, and suggested apoptosis was not occurring due to mitochondrial fragility (Jesenberger *et al.*, 2001). Therefore, although C-Raf has been observed to interact with various proteins at the mitochondria, the roles these interactions may or may not play in suppressing apoptosis are yet to be fully resolved.

### 3.2 Aims

As the role of C-Raf in apoptosis is yet to be fully understood, the aims of this chapter were to characterise the mechanistic role C-Raf may play in CD95-mediated apoptosis. This was achieved by assessing the sensitivity to  $\alpha$ -CD95 antibody-induced-apoptosis of *C-raf*<sup>-/-</sup> immortalised MEFs upon transfection with expression vectors containing various human *C-RAF* cDNAs. The ability of full length C-RAF, a kinase inactive version of C-RAF, a MEK kinase inactive form of C-RAF, a Ras binding mutant of C-RAF or a Ras version of C-RAF that was targeted to the mitochondria, to rescue  $\alpha$ -CD95 antibody-induced-apoptosis was assessed in comparison to MEFs transfected with an empty backbone vector.

### 3.3 Results

#### 3.3.1 *Reproduction of the apoptotic phenotype of tsSV40T transformed C-raf*<sup>+/+</sup> *and C-raf*<sup>-/-</sup> *MEFs*

As reported earlier, analysis of *C-raf*<sup>-/-</sup> MEFs derived on a 129Ola/MF-1 background showed an increased susceptibility to  $\alpha$ -CD95 antibody induced apoptosis when compared to *C-raf*<sup>+/+</sup> MEFs (Huser *et al.*, 2001). To allow further characterisation of these cells, these findings needed to be reproduced. As the main aim of this chapter was to analyse the cells upon transfection, and due to the difficulties in transfecting primary cells, studies were carried out using *C-raf*<sup>+/+</sup> and *C-raf*<sup>-/-</sup> immortalised MEFs. *C-raf*<sup>+/+</sup> (line 34-3) and *C-raf*<sup>-/-</sup> (line 34-2) MEFs were previously immortalised using a temperature sensitive version

of the simian virus 40 (SV40) viral gene encoding the large T antigen (Jat and Sharp, 1989). The large T antigen allows interaction with various cellular gene products, including the tumour suppressor proteins p53 and pRB family members, giving the cells their ability to grow indefinitely. Immortalisation can give rise to altered characteristics of the cells when compared to their primary counterparts. Therefore to account for this, the temperature sensitive version of the T antigen was used. Placing the immortalised cells at the permissive temperature of 33° C allowed the expression of the SV40T antigen. However, on transferring to the restrictive temperature of 39° C, the SV40T antigen was degraded. The plasmid used to create the immortalised cells was pZIPSVtsA58. This plasmid contains the thermolabile large T antigen encoded by the SV40 early region mutant tsA58, the Moloney murine Leukaemia virus (M-MuLV) transcriptional unit derived from an integrated M-MuLV provirus, pBR322 sequences required for the propagation of the vector DNA in *E.Coli*, and the *neo*<sup>R</sup> gene (Jat and Sharp, 1989).

Initial studies of the immortalised MEFs to confirm the ability of the tsSV40T antigen to be degraded upon placing at 39° C were performed. Cells were seeded at  $1.5 \times 10^6$  in 2 x 6 cm dishes and placed at 33° C. After 24 hours one plate was transferred to 39°C and the second plate remained at 33°C. Following a further 24 hours incubation, protein lysates were prepared from the MEFs, followed by SDS-PAGE and western blot analysis. Blots were incubated with an  $\alpha$ -large T antigen antibody. An  $\alpha$ -ERK1 antibody was used as a protein loading control. The results showed the levels of SV40T antigen decreased upon transfer from 33° C to 39° C, although it was not fully degraded (Figure 3.1A). This agreed with previous findings (K. Mercer – unpublished results).

The expression of C-Raf in the tsSV40T transformed cells was also confirmed. Cells were seeded at  $1.5 \times 10^6$  in a 6 cm dish. Protein lysates were produced for each cell line. The lysates were evaluated by SDS-PAGE followed by Western blotting analysis. The blots produced were incubated with an  $\alpha$ -C-Raf antibody. An  $\alpha$ -actin antibody was used as a protein loading control. The results confirmed the expression of C-Raf for the tsSV40T transformed *C-raf*<sup>+/+</sup> cells and the absence of C-Raf for the tsSV40T transformed *C-raf*<sup>-/-</sup> MEFs (Figure 3.1B).

In order to reproduce the previous findings with regards to the C-Raf apoptotic phenotype, tsSV40T transformed MEFs were seeded at a density of  $1.5 \times 10^5$  in 6 cm dishes. The

following day the growth media was changed and the cells transferred from 33° C to 39° C for 24 hours. Apoptosis was induced by the addition of 50 ng/ml  $\alpha$ -CD95 antibody plus 0.5  $\mu$ M cycloheximide for 20 hours. Both suspended and attached cells were harvested, annexin V FITC and propidium iodide (PI) added and flow cytometric analysis performed. During apoptosis, changes in the plasma membrane structure occur, including the surface exposure of phosphatidyl-serine groups. Annexin V can bind to these exposed phosphatidyl serine groups and therefore is an indicator of apoptosis. When bound to FITC, Annexin V can be analysed by fluorescent activated cell sorting (FACS). Addition of PI allows detection of necrotic cells, as PI is a membrane impermeable DNA stain and cannot enter apoptotic cells. Plotting annexin V FITC versus PI allows the separation of apoptotic cells from necrotic cells and therefore allows the analysis of apoptotic cells only. A typical cytogram is shown in Figure 3.2. Analysis of the results obtained showed a significant increase in apoptosis upon  $\alpha$ -CD95 antibody treatment of tsSV40T transformed *C-raf*<sup>-/-</sup> MEFs compared to tsSV40T transformed *C-raf*<sup>+/+</sup> MEFs (Figure 3.3A). The graph represents pooled data from 12 experiments. Upon treatment, 39 %  $\pm$  4 of *C-raf*<sup>-/-</sup> MEFs compared to 30 %  $\pm$  4 of *C-raf*<sup>+/+</sup> MEFs underwent apoptosis (n=12, *P*=0.0008). Unstimulated MEFs for both cell lines gave similar apoptosis values, averaging 15 %  $\pm$  2 (n=12; *P*=0.588).

Apoptosis was also confirmed by detecting the levels of active caspase 3 upon  $\alpha$ -CD95 antibody stimulation of the cells. *C-raf*<sup>+/-</sup> and *C-raf*<sup>-/-</sup> primary cells were seeded at 1.5 x 10<sup>6</sup> in a 6 cm dish. The following day cells were either left untreated or stimulated with 50 ng/ml  $\alpha$ -CD95 antibody plus 0.5  $\mu$ M cycloheximide for 20 hours. Both suspended and attached cells were lysed and protein lysates produced for each cell line. The lysates were evaluated by SDS-PAGE followed by Western blotting analysis. The blots produced were incubated with an  $\alpha$ -active caspase 3 antibody. An  $\alpha$ -actin antibody was used as a protein loading control (Figure 3.3B). A significant increase in cleaved caspase 3 was observed for *C-raf*<sup>-/-</sup> primary cells upon  $\alpha$ -CD95 antibody stimulation, when compared to the small increase seen for *C-raf*<sup>+/-</sup> primary cells.

To confirm apoptosis and not necrosis was occurring in the cells, Hoechst 33256 staining was performed. This allows nuclear staining of all cells, but leads to much brighter staining of condensed apoptotic nuclei. In unstimulated cells no apoptosis was observed

**Figure 3.1** Analysis of tsSV40T MEFs. **(A)** Western blot analysis to detect levels of large T antigen in *C-raf*<sup>+/+</sup> and *C-raf*<sup>-/-</sup> tsSV40T MEFs after incubating at 33° C or 39° C for 48 hours. ERK1 was used as a control for protein loading **(B)** Western blot analysis to detect C-Raf (upper panel) and actin as a control for protein loading (lower panel) in *C-raf*<sup>+/+</sup> and *C-raf*<sup>-/-</sup> tsSV40T MEFs.

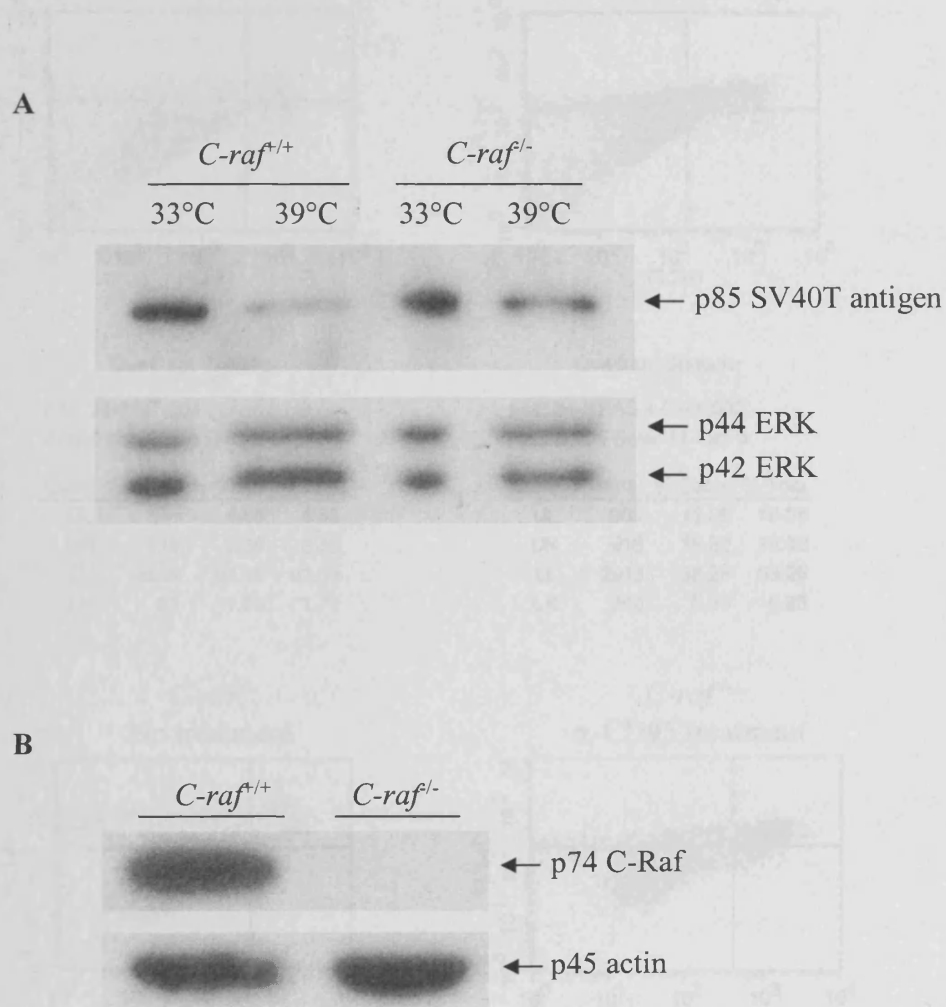
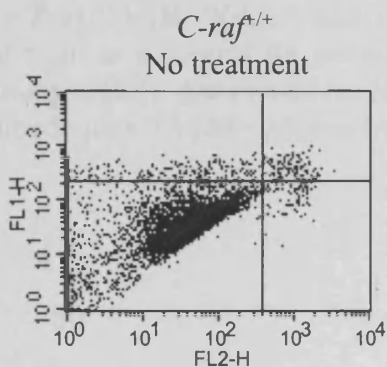


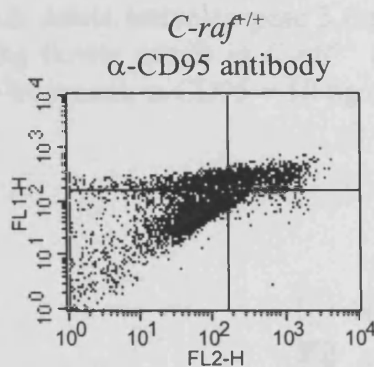
**Figure 3.2** Representative FACS Scan cytogram. Propidium iodide (X axis) was plotted against annexin V FITC (Y axis). Quadrant statistical analysis was performed. The percentage of apoptosis was calculated by addition of percentages in the upper left (UL) and upper right (UR) corners of the quadrant statistics produced.



Quadrant Statistics:

File: 34-3 NT.001  
Acquisition Date: 17-Oct-0

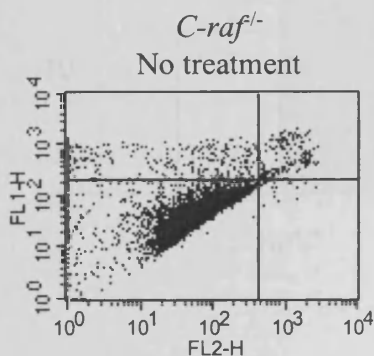
Quad	Events	% Gatec	% Tota
UL	234	4.68	4.68
UR	119	2.38	2.38
LL	4559	91.18	91.18
LR	88	1.76	1.76



Quadrant Statistics:

File: 34-3 FAS + CHX.002  
Acquisition Date: 17-Oct-0

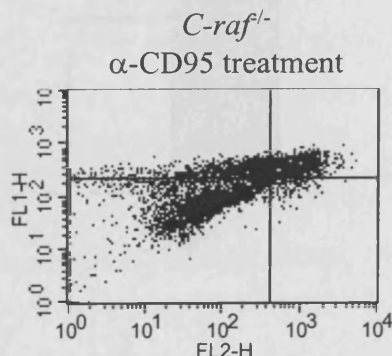
Quad	Events	% Gatec	% Tota
UL	903	18.06	18.06
UR	916	18.32	18.32
LL	2913	58.26	58.26
LR	268	5.36	5.36



Quadrant Statistics:

File: 34-2 NT.003  
Acquisition Date: 17-Oct-0

Quad	Events	% Gatec	% Tota
UL	354	7.08	7.08
UR	194	3.88	3.88
LL	4429	88.58	88.58
LR	23	0.46	0.46

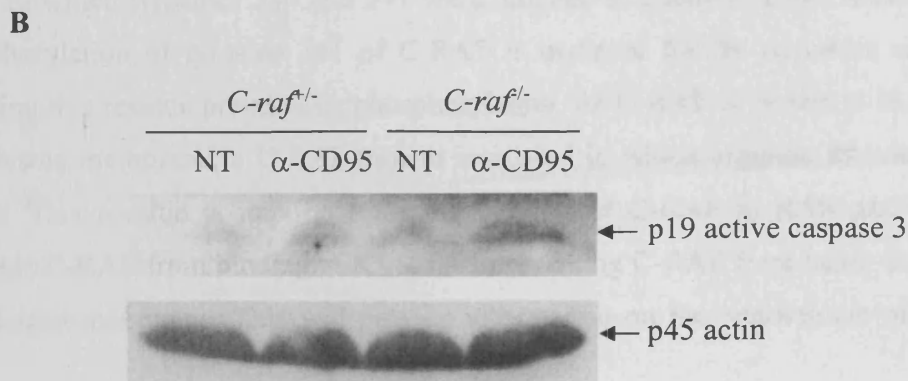
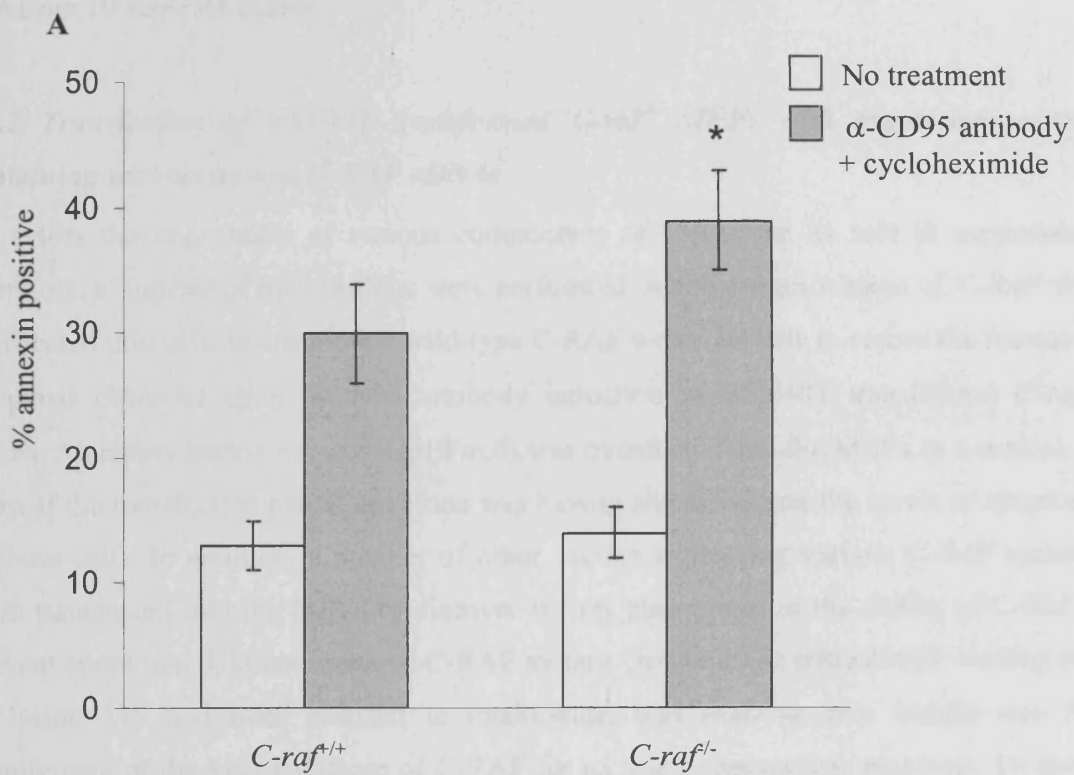


Quadrant Statistics:

File: 34-2 FAS + CHX.004  
Acquisition Date: 17-Oct-0

Quad	Events	% Gatec	% Tota
UL	1303	26.06	26.06
UR	875	17.50	17.50
LL	2703	54.06	54.06
LR	119	2.38	2.38

**Figure 3.3** Apoptotic analysis of C-Raf MEFs. **(A)** Percentage of annexin V positive stained cells, calculated from annexin V FITC staining followed by flow cytometric analysis. *C-raf*<sup>+/+</sup> and *C-raf*<sup>-/-</sup> tsSV40T immortalised MEFs were left untreated or apoptosis induced by addition of 50 ng/ml  $\alpha$ -CD95 antibody plus 0.5  $\mu$ M cycloheximide. The data represents mean $\pm$ SEM (n=12). *P* values were generated for *C-raf*<sup>-/-</sup> MEFs via paired t-Tests against *C-raf*<sup>+/+</sup> MEFs. (\* = *P* $\leq$ 0.05). **(B)** Western blot analysis to detect active caspase 3 (upper panel) and actin as a control for protein loading (lower panel) in *C-raf*<sup>+/+</sup> and *C-raf*<sup>-/-</sup> primary MEFs. Abbreviations; NT = no treatment;  $\alpha$ -CD95 = 50 ng/ml  $\alpha$ -CD95 antibody plus 0.5  $\mu$ M cycloheximide.

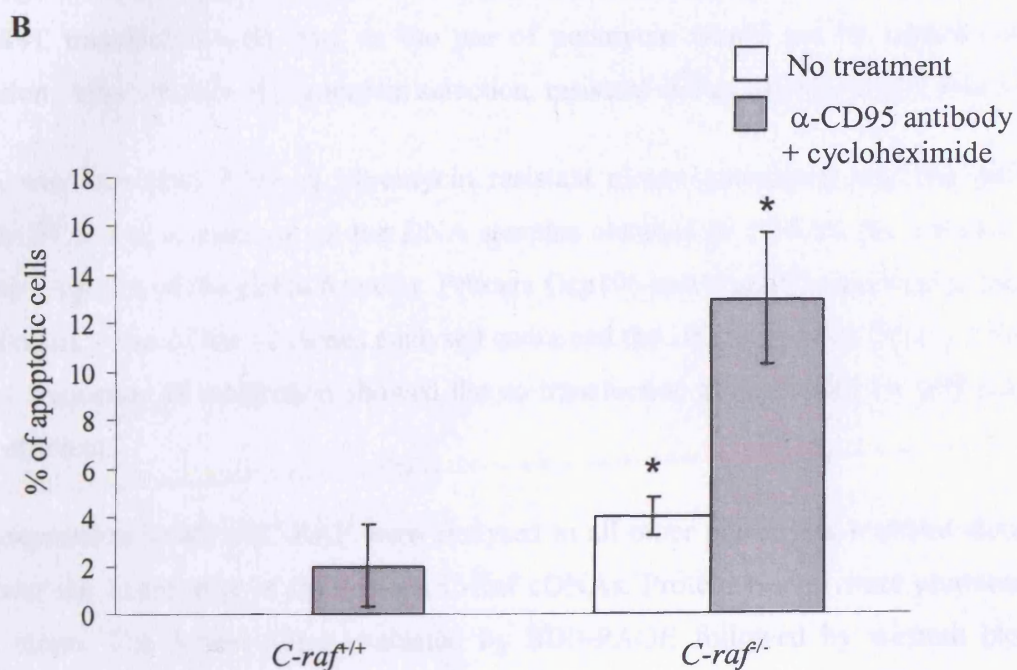
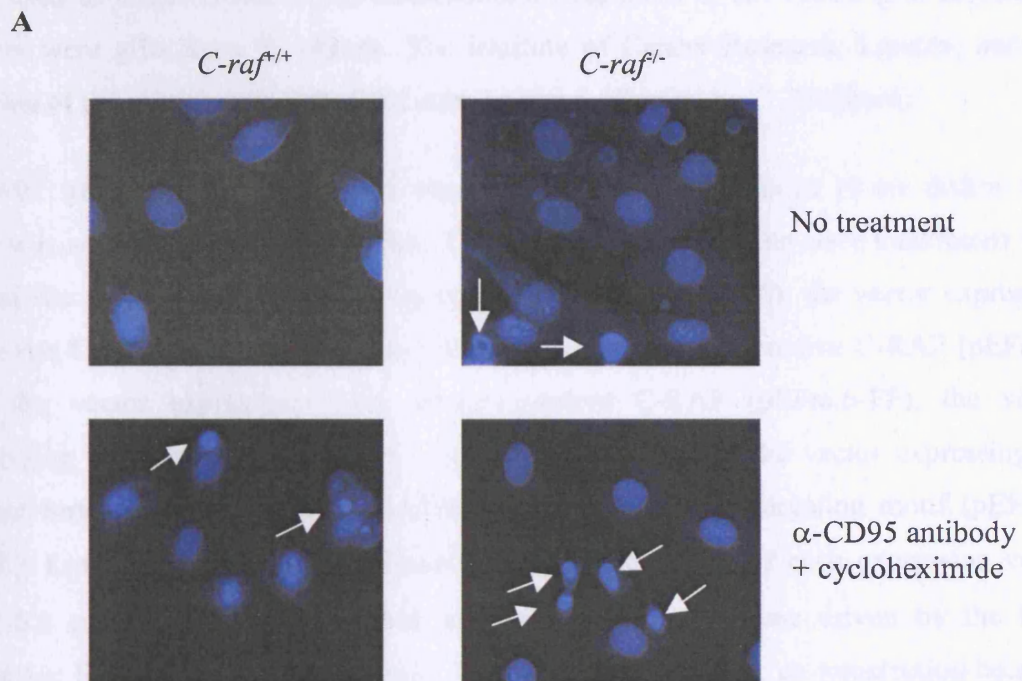


for *C-raf*<sup>+/+</sup> cells, but a few apoptotic cells were seen for *C-raf*<sup>-/-</sup> MEFs. (Figure 3.4A), suggesting a slight increase in apoptosis in unstimulated *C-raf*<sup>-/-</sup> MEFs. Upon  $\alpha$ -CD95 antibody plus cycloheximide treatment a greater number of brightly stained nuclei were observed for the *C-raf*<sup>-/-</sup> MEFs, confirming an increased level of apoptosis in these cells (Figure 3.4A). Numerical analysis of the Hoechst 33256 staining showed a significant increase in the level of apoptosis upon  $\alpha$ -CD95 antibody plus cycloheximide treatment for the *C-raf*<sup>-/-</sup> MEFs. 2 %  $\pm$  1 of unstimulated *C-raf*<sup>-/-</sup> cells were apoptotic compared with 0 % of *C-raf*<sup>+/+</sup> MEFs ( $P=0.07$ ; Figure 3.4B). This increased to 13 %  $\pm$  3 for stimulated *C-raf*<sup>-/-</sup> MEFs compared to 4 %  $\pm$  2 for *C-raf*<sup>+/+</sup> treated cells ( $P=0.015$ ). Values indicate pooled data from 10 separate counts.

### **3.3.2 Transfection of tsSV40T transformed *C-raf*<sup>-/-</sup> MEFs with expression vectors containing various human C-RAF cDNAs**

To assess the importance of various components of C-Raf for its role in suppressing apoptosis, a number of transfections were performed. A full-length version of *C-RAF* was transfected into cells to ensure that wild-type C-RAF would be able to rescue the increased apoptosis observed upon  $\alpha$ -CD95 antibody induction of tsSV40T transformed *C-raf*<sup>-/-</sup> MEFs. An empty backbone vector (pEFm.6) was transfected into the MEFs as a control, to show if the transfection procedure alone was having any effects on the levels of apoptosis in these cells. In addition, a number of other vectors expressing various *C-RAF* mutants were transfected into the MEFs to discover if they play a role in the ability of C-Raf to prevent apoptosis. A kinase inactive C-RAF mutant, in which the critical ATP binding site of lysine 375 had been mutated to methionine, was used to gain insight into the requirement of the kinase domain of C-RAF for its role in preventing apoptosis. To show if the activation of MEKs plays a part in cell survival, a MEK kinase inactive form of C-RAF, in which tyrosines 340 and 341 were mutated to phenylalanines, was utilised. The phosphorylation of tyrosine 341 of C-RAF is essential for its activation and therefore mutating this residue prevents its phosphorylation. As C-RAF is known to bind to RAS at the plasma membrane, a C-RAF mutant was used in which arginine 89 was mutated to lysine. This residue is important for the binding of C-RAF to RAS and its mutation prevents C-RAF from binding to RAS, thus preventing C-RAF from being translocated to the plasma membrane. This will provide information on the requirement of RAS in the

**Figure 3.4** Apoptotic analysis of tsSV40T immortalised MEFs. (A) Hoechst 33258 staining of *C-raf*<sup>+/+</sup> and *C-raf*<sup>-/-</sup> MEFs following treatment with 50 ng/ml  $\alpha$ -CD95 antibody plus 0.5  $\mu$ M cycloheximide or no treatment. Arrows indicate apoptotic nuclei. (B) Analysis of Hoechst 33258 staining carried out in (A). 300 cells were scored for the presence of apoptotic nuclei and the percentage of apoptotic cells calculated. The data represents mean $\pm$ -SEM (n=10). *P* values were generated for *C-raf*<sup>-/-</sup> MEFs via paired t-Tests against *C-raf*<sup>+/+</sup> MEFs. (\* = *P*≤0.05).



prevention of CD95-mediated apoptosis by C-RAF. As previously stated, reports have shown that cell survival involving C-Raf may take place at the mitochondria. To evaluate this, the R89L mutant of C-RAF was again used. However, a mitochondrial targeting motif was added to target the C-RAF construct to the mitochondria. The mitochondrial targeting motif used consisted of residues 1-30 of the transmembrane domain of the yeast outer mitochondrial membrane protein MAS70p (Hase et al., 1984), which has previously been used to target C-Raf to the mitochondria (Salomoni et al., 1998). (All expression vectors were gifts from R. Marais, The Institute of Cancer Research, London, and the addition of the mitochondrial targeted domain was performed by C. Pritchard).

tsSV40T transformed *C-raf*<sup>-/-</sup> MEFs were seeded at  $6 \times 10^5$  cells in 10 cm dishes. One plate was seeded for each transfection. The following day the cells were transfected with one of the various vectors; the empty backbone vector (pEFm.6), the vector expressing wild-type C-RAF (pEFm.6-WT), the vector expressing kinase inactive C-RAF (pEFm.6-KI), the vector expressing MEK kinase inactive C-RAF (pEFm.6-FF), the vector expressing the Ras mutant form of C-RAF (pEFm.6-89L) or the vector expressing the mutant form of C-RAF with the addition of a mitochondrial targeting motif (pEFm.6-m89L). Lipofectamine reagent was used to co-transfect 8  $\mu$ g of each expression vector with 0.8  $\mu$ g pPGK-puro (a plasmid harbouring the *puro*<sup>R</sup> gene driven by the PGK promoter; Figure 2.1). The pPGK-puro plasmid was required for co-transfection because, although the expression vectors all contained a *neo*<sup>R</sup> gene, this was also present in the tsSV40T transformed cell line, so the use of neomycin would not be suitable during selection. After 10 days of puromycin selection, resistant clones were picked (Table 3.1).

DNA was harvested from all puromycin resistant clones transfected with the pEFm.6 vector. PCR was carried out on the DNA samples obtained to evaluate the presence of a 200 bp fragment of the pEFm.6 vector. Primers Ocp106 and Ocp107 were used to amplify the product. 3 out of the 12 clones analysed contained the 200 bp product (Figure 3.5A). A 1 in 4 frequency of integration showed the co-transfection method used for pEFm.6 was very efficient.

The expression levels of C-RAF were analysed in all other puromycin resistant clones to discover the expression of the various C-Raf cDNAs. Protein lysates were produced for each clone. The lysates were evaluated by SDS-PAGE followed by western blotting

analysis. The blots produced were incubated with an  $\alpha$ -C-Raf antibody. An  $\alpha$ -actin antibody was used as a protein loading control. 4 out of 22 clones (#111, #113, #115 and #271; Figure 3.5B) transfected with the pEFm.6-WT vector were positive for C-Raf, 4 of the 24 clones (#37, #38, #146 and #148; Figure 3.5B) analysed for the pEFm.6-KI vector were C-Raf positive, 3 clones (#17, #18 and #19; Figure 3.5B) from the 24 evaluated were positive for the pEFm.6-FF vector, transfection of the pEFm.6-89L vector produced 6 positive clones from the 22 tested (#108, #179 and #180; Figure 3.5B, and not shown #258, #271b and #272), and 6 out of 12 clones (#136, #137 and #185; Figure 3.5B, and not shown #115b, #260 and #277) were positive for the pEFm.6-m89L vector. The frequency of integration varied from 1 in 8 for pEFm.6-FF up to 1 in 2 for pEFm.6-m89L.

**Table 3.1** Summary of puromycin resistant clones obtained upon transfection of tsSV40T transformed *C-raf*<sup>-/-</sup> MEFs with various human *C-RAF* cDNAs. Puromycin resistant clones were analysed by PCR for pEFm.6, and via western blot analysis to detect C-RAF expression levels for all other clones.

Expression construct	Total number of puromycin resistant clones picked	Clone numbers positive for pEFm. PCR or C-Raf expression
pEFm.6	12	35, 36, 208
pEFm.6-WT	22	111, 113, 115, 271
pEFm.6-KI	24	37, 38, 146, 148
pEFm.6-FF	24	17, 18, 19
pEFm.6-89L	22	108, 179, 180, 258, 271b, 272
pEFm.6-m89L	12	115b, 136, 137, 185, 260, 277

To ensure the mitochondrial motif added to C-RAF pEFm.6-m89L was fully functional, immunofluorescence studies were carried out on the pEFm.6-m89L MEFs. The MEFs were plated at  $6 \times 10^4$  cells on coverslips that had been previously coated in  $10 \mu\text{g/ml}$  fibronectin. Cells were fixed, permeabilised and blocking solution added. MEFs were subsequently incubation with  $250 \text{ ng/ml}$   $\alpha$ -C-Raf antibody, followed by incubation with  $200 \mu\text{g/ml}$  FITC- $\alpha$ -mouse secondary antibody. To stain the mitochondria of the cells, subsequent staining with  $25 \text{ nM}$  Mitotracker Red CMXRos was carried out. The coverslips were mounted and the cells viewed using a fluorescence microscope. Figure 3.6 shows a

**Figure 3.5** Screening of transfected *C-raf*<sup>-/-</sup> immortalised MEFs. **(A)** Detection of positive clones transfected with the pEFm.6 vector by PCR using primers Ocp106 and Ocp107. Amplification of a 200 bp product was observed for three out of the twelve clones tested. Abbreviations: M = 1 Kb DNA ladder; -ve = negative control; +ve = positive control; numbers correspond to clone numbers. **(B)** Western blot analysis to detect C-RAF (upper panel) and actin (lower panel) in *C-raf*<sup>-/-</sup> tsSV40T MEFs transfected with various human *C-RAF* cDNAs. Abbreviations; pEFm.6 = empty backbone vector, WT = wild-type C-RAF-, KI = kinase inactive mutant of C-RAF, FF = MEK inactive mutant of C-RAF, 89L = Ras binding mutant of C-RAF and m89L = Ras binding mutant of C-RAF with an additional mitochondrial targeting motif.

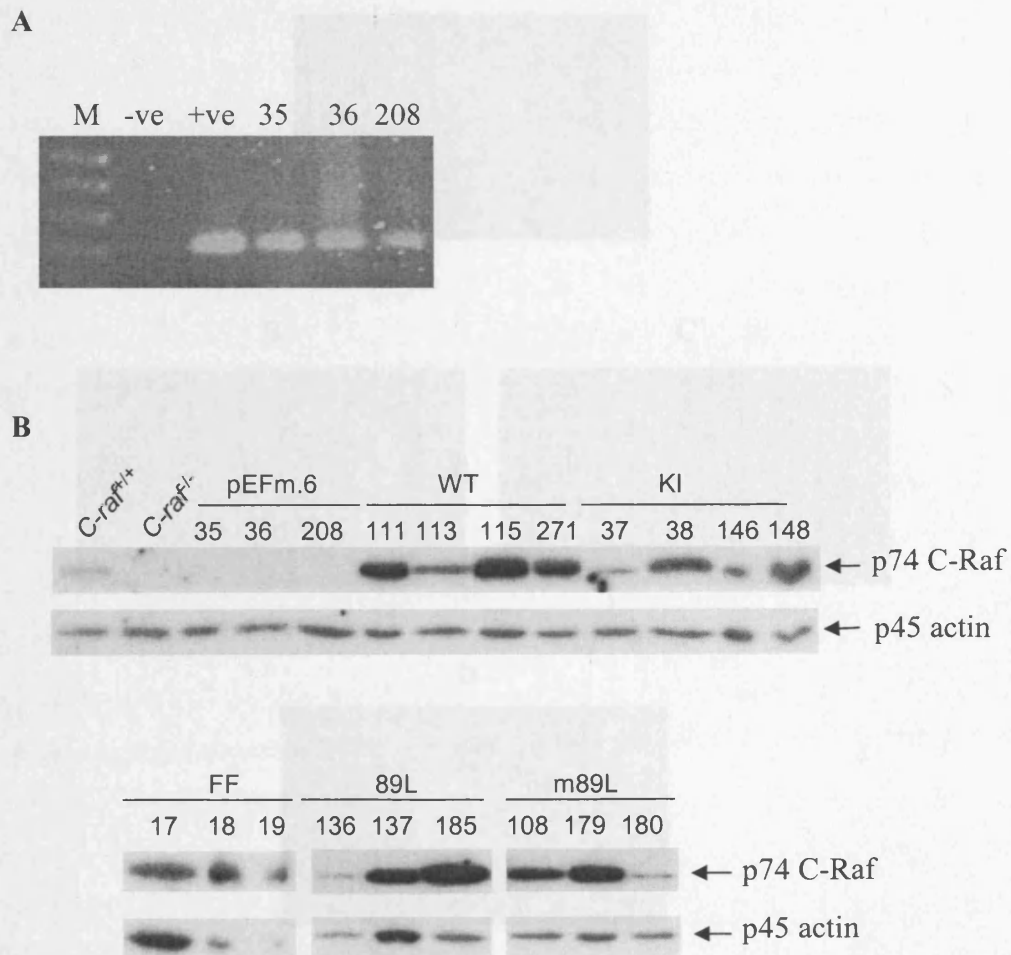
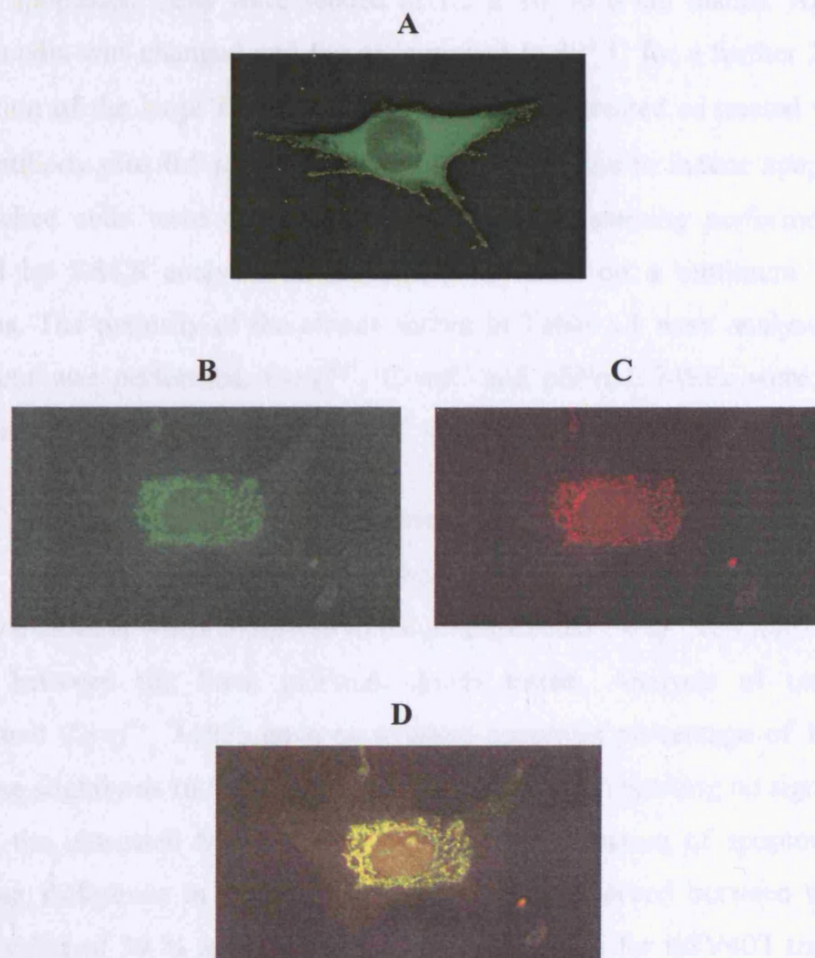


**Figure 3.6** Immunofluorescence analysis of tsSV40T transformed *C-raf*<sup>+/+</sup> MEFs, and tsSV40T transformed *C-raf*<sup>-/-</sup> MEFs transfected with a RAS binding mutant of C-RAF with an additional mitochondrial targeting motif (pEFm.6-m89L). (A) *C-raf*<sup>+/+</sup> MEFs were incubated with  $\alpha$ -C-Raf antibody. (B) pEFm.6-m89L MEFs were incubated with (B)  $\alpha$ -C-Raf antibody, and (C) Mitotracker red CMXRos. (D) shows a merged image of (B) and (C). The cells shown are representative cells from all cells examined.



typical *C-raf*<sup>+/+</sup> cell stained with C-Raf (3.6A), a pEFm.6-m89L cell stained with C-Raf (3.6B) and with Mitotracker Red CMXRos (3.6C). The merged image (3.6D) shows that C-Raf is targeted to the mitochondria and therefore these cells could be used to analyse the mitochondrial role of C-Raf in suppressing CD95-mediated apoptosis.

### **3.3.3 Characterisation of the apoptotic phenotype of tsSV40T transformed *C-raf*<sup>-/-</sup> MEFs transfected with various human *C-RAF* cDNAs.**

To discover if the expression of the various *C-RAF* constructs rescues the apoptotic phenotype of *C-raf*<sup>-/-</sup> MEFs, the majority of the stable clones produced were induced to undergo apoptosis. Cells were seeded at  $1.5 \times 10^5$  in 6 cm dishes. After 24 hours the growth media was changed and the cells moved to 39° C for a further 24 hours to allow degradation of the large T antigen. Cells were left untreated or treated with 50 ng/ml  $\alpha$ -CD95 antibody plus 0.5  $\mu$ M cycloheximide for 20 hours to induce apoptosis. Suspended and attached cells were collected, annexin V FITC staining performed and PI added, followed by FACS analysis. Each clone was tested on a minimum of three separate occasions. The majority of the clones shown in Table 3.1 were analysed. Each time the experiment was performed, *C-raf*<sup>+/+</sup>, *C-raf*<sup>-/-</sup> and pEFm.6 MEFs were also analysed as assay controls.

tsSV40T transformed *C-raf*<sup>-/-</sup> MEFs containing the pEFm.6 vector showed a slight increase in the levels of apoptosis in both untreated cells and in response to  $\alpha$ -CD95 antibody treatment when compared to the untransfected *C-raf*<sup>-/-</sup> cell line. The values varied slightly between the three pEFm.6 clones tested. Analysis of untreated tsSV40T transformed *C-raf*<sup>-/-</sup> MEFs gave an average apoptosis percentage of 14 %  $\pm$  2 and this value rose slightly to 16 %  $\pm$  1 for the pEFm.6 clones, suggesting no significant difference between the untreated MEFs ( $P=0.43$ ). However, induction of apoptosis led to a more significant difference in the increase of apoptosis observed between the cell lines. An average value of 39 %  $\pm$  4 (n=12) underwent apoptosis for tsSV40T transformed *C-raf*<sup>-/-</sup> MEFs and this value increased to an average value of 46 %  $\pm$  3 ( $P=0.0003$ ) when the values for the three pEFm.6 clones analysed were pooled (Figure 3.7). Individually,  $\alpha$ -CD95 antibody treatment induced 44 %  $\pm$  4 apoptosis for #35 pEFm.6 (n= 8;  $P=0.07$ ), 55 %  $\pm$  5 for #36 pEFm.6 (n= 11  $P=0.00004$ ) and 39 %  $\pm$  4 for #208 pEFm.6 (n=6  $P=0.03$ ) (Figure 3.7). These data indicate that manipulation of tsSV40T transformed *C-raf*<sup>-/-</sup> MEFs, by transfection of the cells, led to an increased level of apoptosis upon  $\alpha$ -CD95 antibody

induction. The pEFm.6 MEFs therefore served as a control for comparison to the tsSV40T transformed *C-raf*<sup>-/-</sup> MEFs transfected with the various *C-RAF* cDNAs, rather than using the non-transfected tsSV40T transformed *C-raf*<sup>-/-</sup> MEFs. pEFm.6 MEFs were therefore used as the control in statistical analysis of all subsequent apoptosis assays (Figures 3.7-3.13).

tsSV40T transformed *C-Raf*<sup>-/-</sup> MEFs expressing wild-type C-Raf did show a decrease in  $\alpha$ -CD95 antibody induced apoptosis when compared to the pEFm.6 control cells. The reduction varied slightly between clones and this variation corresponded with the expression levels of C-Raf for three of the clones (Figures 3.5B and 3.8). #115 pEFm.6-WT showed the greatest reduction in the level of apoptosis observed and this corresponded with the highest level of C-Raf expression of this clone when compared to the other three clones analysed. Upon induction, apoptosis levels observed were 33 %  $\pm$  5 for #111 pEFm.6-WT (n=8;  $P=0.0001$ ), 35 %  $\pm$  4 for #113 pEFm.6-WT (n=8;  $P=0.03$ ), 30 %  $\pm$  4 for #115 pEFm.6-WT (n=9;  $P=0.0004$ ) and 35 %  $\pm$  4 for #271 pEFm.6-WT (n=7;  $P=0.2$ ) (Figure 3.8). The level of apoptosis observed for #271 pEFm.6-WT was slightly higher than expected when compared to the level of C-Raf expression for the cell line. Overall, when pooled, the data gave an average apoptosis value of 33 %  $\pm$  2 ( $P=0.003$ ) for pEFm.6-WT MEFs (Figure 3.12). This value was significantly lower than the 46 %  $\pm$  2.6 observed for pEFm.6 cells and also lower than the 39 %  $\pm$  4 average percentage apoptosis seen for non-transfected tsSV40T transformed *C-raf*<sup>-/-</sup> MEFs upon induction with  $\alpha$ -CD95 antibody. The levels of apoptosis were not completely reduced to the 30 %  $\pm$  4 observed for tsSV40T transformed *C-raf*<sup>+/+</sup> MEFs. However, the reduction of apoptosis to levels below those observed for both, pEFm.6 control cells and the non-transfected tsSV40T transformed *C-raf*<sup>-/-</sup> MEFs, shows that expression of C-Raf in the pEFm.6-WT MEFs was able to rescue the apoptotic phenotype caused by the absence of C-Raf. It therefore confirmed the method was valid for rescuing the C-Raf apoptosis suppressing phenotype.

Expression of kinase inactive C-Raf in the tsSV40T transformed *C-raf*<sup>-/-</sup> MEFs showed a reduction in the percentage of apoptosis observed upon  $\alpha$ -CD95 antibody treatment compared to that observed for the pEFm.6 control cells. Some variation was observed between the four pEFm.6-KI clones analysed. The clonal variation again corresponded to the varying expression levels of C-Raf. The lowest level of C-Raf was expressed for #37

**Figure 3.7** Apoptotic analysis of *C-raf*<sup>-/-</sup> tsSV40T immortalised MEFs transfected with an empty backbone vector, pEFm.6. MEFs were induced to undergo apoptosis by treating with 50 ng/ml  $\alpha$ -CD95 antibody plus 0.5  $\mu$ M cycloheximide or left untreated. Apoptosis was evaluated using annexin V FITC staining followed by flow cytometric analysis. Graph of pooled data for *C-raf*<sup>+/+</sup> MEFs, pooled data for *C-raf*<sup>-/-</sup> MEFs (n=12) and three *C-raf*<sup>-/-</sup> clones transfected with pEFm.6. The data represents mean $\pm$ SEM (n=8 for #35 pEFm.6; n=11 for #36 pEFm.6; n=6 for #208 pEFm.6). *P* values were generated for treated cells using paired t-Tests against *C-raf*<sup>+/+</sup> MEFs. (\* = *P* $\leq$ 0.05).

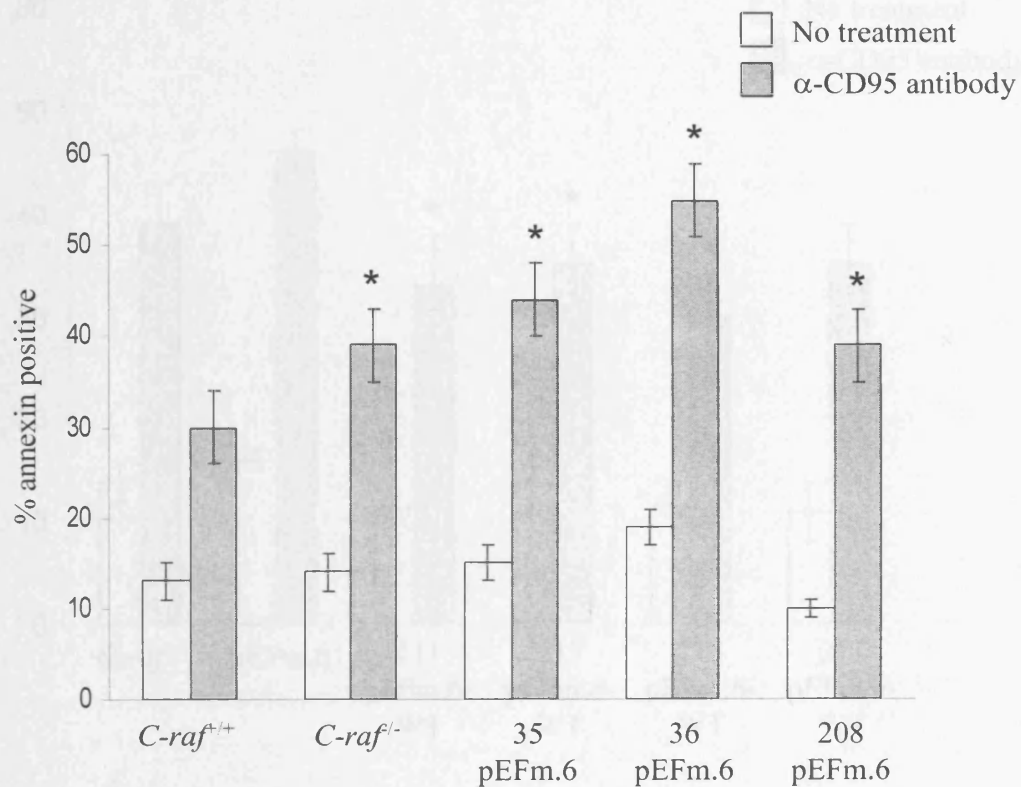


**Figure 3.8** Apoptotic analysis of *C-raf*<sup>-/-</sup> tsSV40T immortalised MEFs expressing wild-type (WT) C-RAF, and induced to undergo apoptosis by treating with 50 ng/ml  $\alpha$ -CD95 antibody plus 0.5  $\mu$ M cycloheximide or left untreated. Apoptosis was evaluated using annexin V FITC staining followed by flow cytometric analysis. Graph of pooled data for *C-raf*<sup>-/-</sup> MEFs, pooled data for pEFm.6 MEFs and four *C-raf*<sup>-/-</sup> clones expressing wild type C-RAF. The data represents mean $\pm$ SEM (n=8 for #111 pEFm.6-WT; n=8 for #113 pEFm.6-WT; n=9 for #115 pEFm.6-WT; n=7 for #271 pEFm.6-WT). *P* values were generated for pEFm.6-WT treated cells using paired t-Tests against pEFm.6 MEFs. (\* = *P*≤0.05).

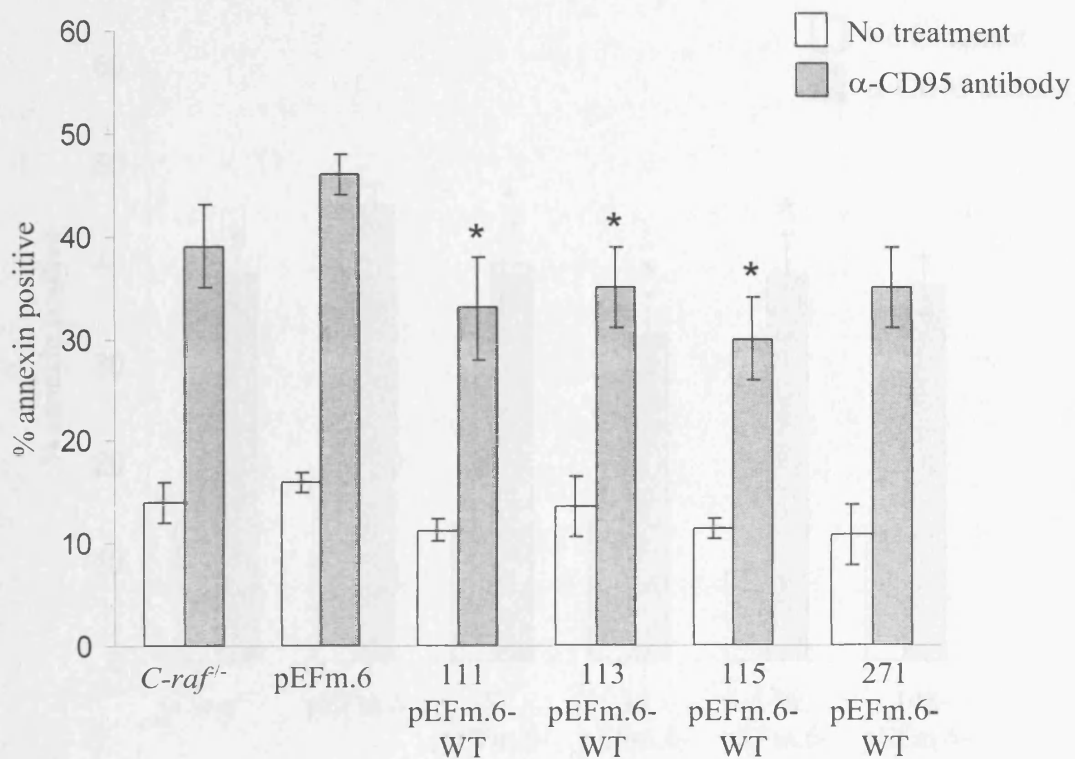
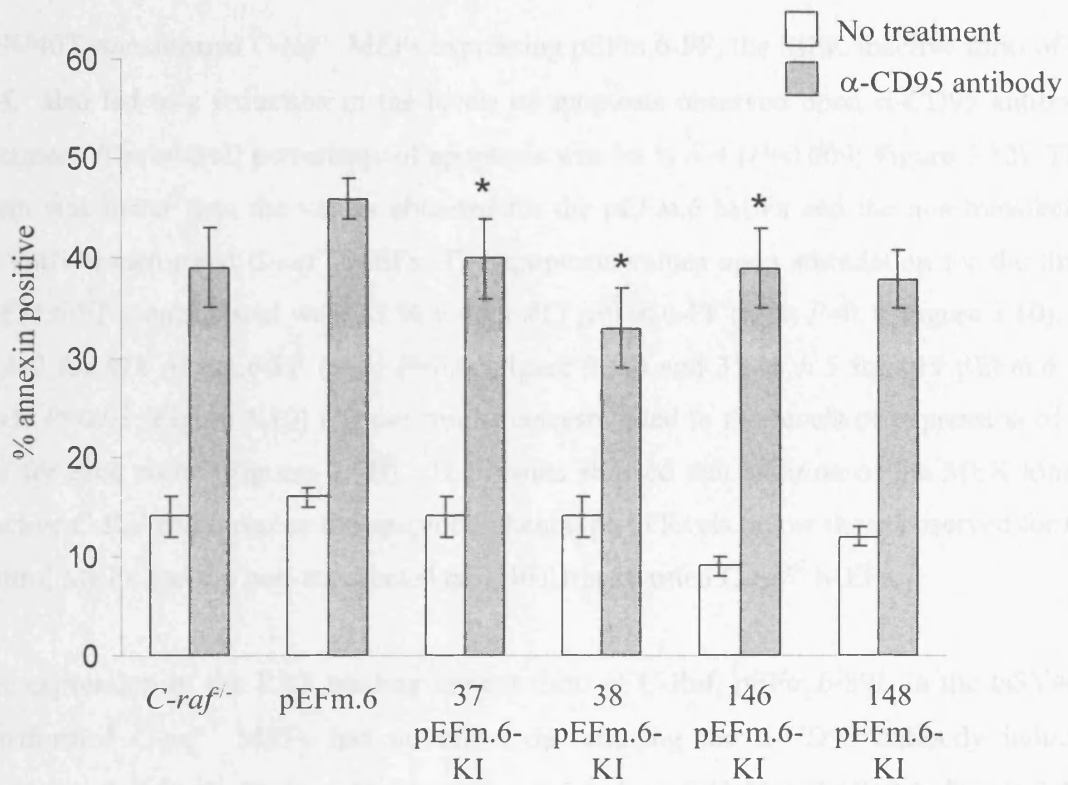


**Figure 3.9** Apoptotic analysis of *C-raf*<sup>-/-</sup> tsSV40T immortalised MEFs expressing kinase inactive (KI) human C-RAF. Cells were left untreated or treated with 50 ng/ml  $\alpha$ -CD95 antibody plus 0.5  $\mu$ M cycloheximide to induce apoptosis. Evaluation of apoptosis was carried out using annexin V FITC staining followed by flow cytometric analysis. Graph of pooled data for *C-raf*<sup>-/-</sup> MEFs, pooled data for pEFm.6 MEFs and four *C-raf*<sup>-/-</sup> clones expressing a kinase inactive mutant of C-RAF. The data represents mean $\pm$ SEM (n=9 for #37 pEFm.6-KI; n=9 for #38 pEFm.6-KI; n=5 for #146 pEFm.6-KI; n=4 for #148 pEFm.6-KI). *P* values were generated for treated cells using paired t-Tests against pEFm.6 MEFs. (\* = *P*≤0.05).



pEFm.6-KI and this showed the smallest decrease in apoptosis at  $40 \% \pm 4$  ( $n=9$ ;  $P=0.05$ ; Figures 3.5B and 3.9). The greatest reduction in apoptosis was observed for #38 pEFm.6-KI at  $36 \% \pm 4$  ( $n=9$ ;  $P=0.02$ ) and this was also the pEFm.6-KI clone expressing the highest protein levels of C-Raf (Figures 3.5B and 3.9). The levels of induced apoptosis observed for the other clones tested were  $39 \% \pm 4$  for #146 pEFm.6-KI ( $n=5$ ;  $P=0.001$ ) and  $38 \% \pm 3$  for #148 pEFm.6-KI ( $n=4$ ;  $P=0.4$ ) (Figure 3.9). The overall pooled apoptosis value for the tsSV40T transformed *C-raf*<sup>-/-</sup> MEFs expressing a kinase inactive form of C-Raf was  $38 \% \pm 4$  ( $p=0.003$ ; Figure 3.12). This is significantly lower than that observed for pEFm.6 and just below the  $39 \% \pm 4$  average percentage apoptosis observed for non-transfected tsSV40T transformed *C-raf*<sup>-/-</sup> MEFs.

tsSV40T transformed *C-raf*<sup>-/-</sup> MEFs expressing pEFm.6-FF, the MEK inactive form of C-Raf, also led to a reduction in the levels of apoptosis observed upon  $\alpha$ -CD95 antibody treatment. The overall percentage of apoptosis was  $36 \% \pm 4$  ( $P=0.009$ ; Figure 3.12). This again was lower than the values obtained for the pEFm.6 MEFs and the non-transfected tsSV40T transformed *C-raf*<sup>-/-</sup> MEFs. The apoptosis values upon stimulation for the three pEFM.6-FF clones tested were  $37 \% \pm 4$  for #17 pEFm.6-FF ( $n=4$ ;  $P=0.1$ ; Figure 3.10),  $36 \% \pm 9$  for #18 pEFm.6-FF ( $n=3$ ;  $P=0.6$ ; Figure 3.10) and  $35 \% \pm 5$  for #19 pEFm.6-FF ( $n=5$ ;  $P=0.01$ ; Figure 3.10). These results corresponded to the levels of expression of C-Raf for each clone (Figures 3.5B). The results showed that addition of the MEK kinase inactive C-Raf could rescue the apoptotic phenotype to levels below those observed for the control MEFs and the non-transfected tsSV40T transformed *C-raf*<sup>-/-</sup> MEFs.

The expression of the RAS binding mutant form of C-Raf, pEFm.6-89L in the tsSV40T transformed *C-raf*<sup>-/-</sup> MEFs had no effect on reducing the  $\alpha$ -CD95 antibody induced apoptotic phenotype. Upon analysis, an average value of  $43 \% \pm 2$  ( $P=0.4$ ; Figure 3.12) was observed. This was higher than the  $39 \% \pm 4$  observed for tsSV40T transformed *C-raf*<sup>-/-</sup> MEFs and slightly lower than the value for pEFM.6 MEFs of  $46 \% \pm 2.6$ , but of no significant difference ( $P=0.4$ ). The results for the individual clones were  $48 \% \pm 4$  for #136 pEFm.6-89L ( $n=2$ ;  $P=0.2$ ; Figure 3.11A),  $36 \% \pm 7$  for #137 pEFm.6-89L ( $n=3$ ;  $P=0.2$ ; Figure 3.11A) and  $45 \% \pm 1$  for #185 pEFm.6-89L ( $n=3$ ;  $P=0.9$ ; Figure 3.11A). The data showed there was no significant alteration in the  $\alpha$ -CD95 antibody induced apoptosis value upon addition of the Ras mutant form of C-Raf.

**Figure 3.10** Apoptotic analysis of *C-raf*<sup>-/-</sup> tsSV40T immortalised MEFs expressing MEK kinase inactive (FF) human C-RAF. MEFs were induced to undergo apoptosis by treating with 50 ng/ml  $\alpha$ -CD95 antibody plus 0.5  $\mu$ M cycloheximide or left untreated. Apoptosis was evaluated using annexin V FITC staining followed by flow cytometric analysis. Graph of pooled data for *C-raf*<sup>-/-</sup> MEFs, pooled data for pEFm.6 MEFs and three *C-raf*<sup>-/-</sup> clones expressing a MEK kinase inactive mutant of C-RAF. The data represents mean $\pm$ -SEM (n=4 for #17 pEFm.6-FF; n=3 for #18 pEFm.6-FF; n=5 for #19 pEFm.6-FF). *P* values were generated for treated cells using paired t-Tests against pEFm.6 MEFs. (\* = *P*≤0.05).

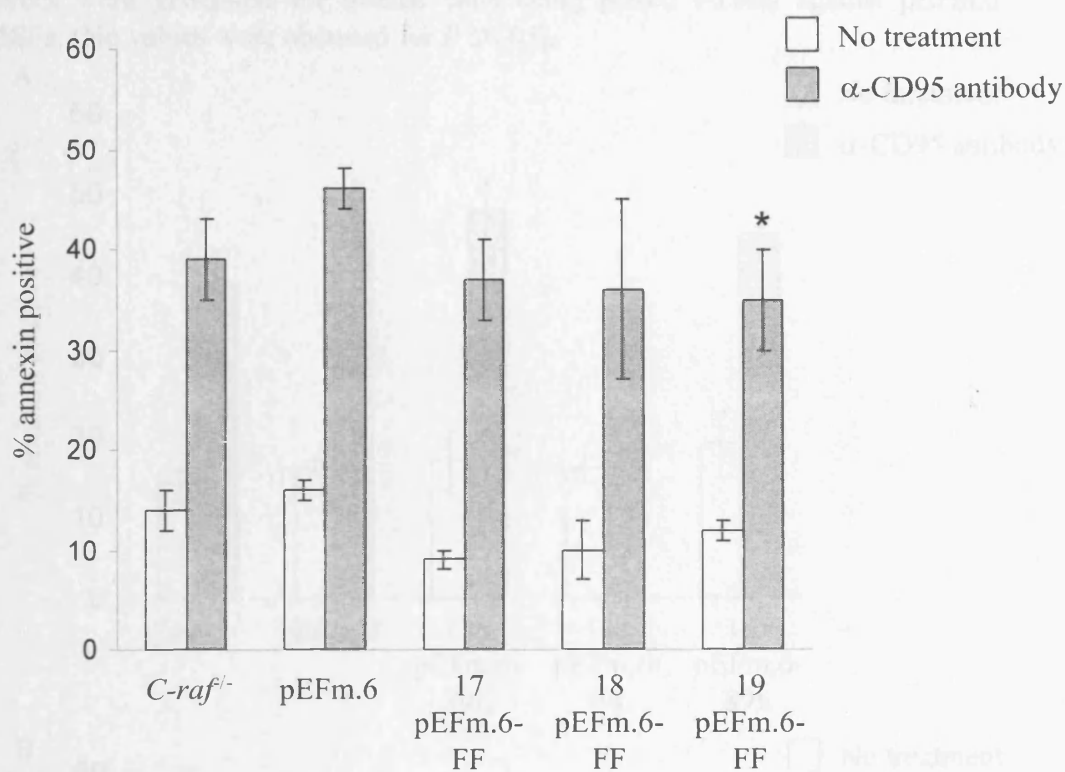


**Figure 3.11** Apoptotic analysis of *C-raf*<sup>-/-</sup> tsSV40T immortalised MEFs expressing mutant forms of human C-RAF. MEFs were induced to undergo apoptosis by treating with 50 ng/ml  $\alpha$ -CD95 antibody plus 0.5  $\mu$ M cycloheximide or left untreated. Apoptosis was evaluated using annexin V FITC staining followed by flow cytometric analysis. **(A)** Graph of pooled data for *C-raf*<sup>-/-</sup> MEFs, pooled data for pEFm.6 MEFs and three *C-raf*<sup>-/-</sup> clones expressing a Ras binding mutant (89L) of *C-RAF*. **(B)** Graph of pooled data for *C-raf*<sup>-/-</sup> MEFs, pooled data for pEFm.6 MEFs and three *C-raf*<sup>-/-</sup> clones expressing a Ras binding mutant (89L) of *C-RAF* with the addition of a mitochondrial targeting motif (m89L). The data represents mean $\pm$ SEM (For (A), n=2 for #136 pEFm.6-89L; n=3 for #137 pEFm.6-89L; n=3 for #185 pEFm.6-FF. For (B) n=3 for #108 pEFm.6-m89L; n=3 for #179 pEFm.6-m89L; n=3 for #180 pEFm.6-FF. ). *P* values were generated for treated cells using paired t-Tests against pEFm.6 MEFs. (No values were obtained for *P*  $\leq$  0.05).

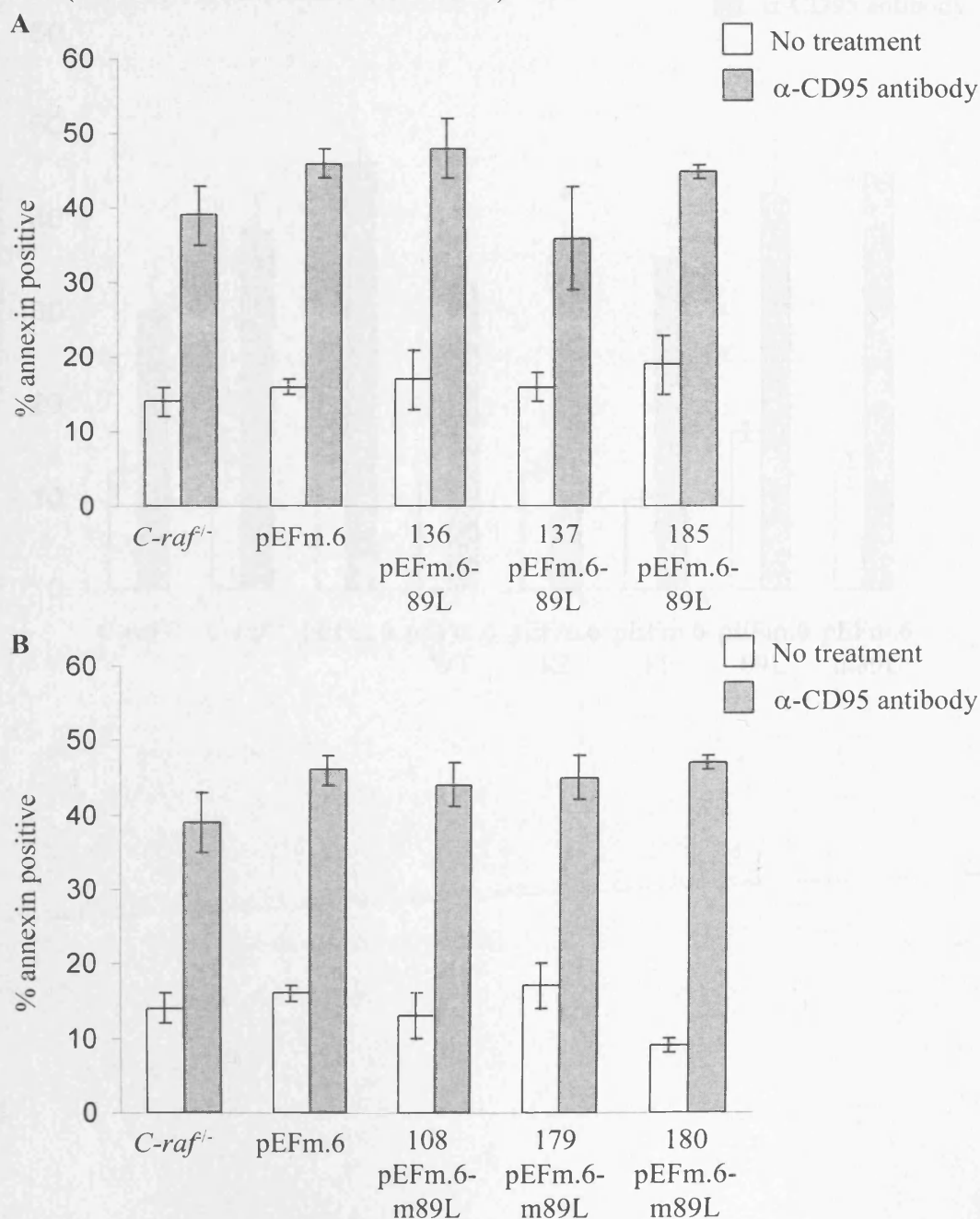
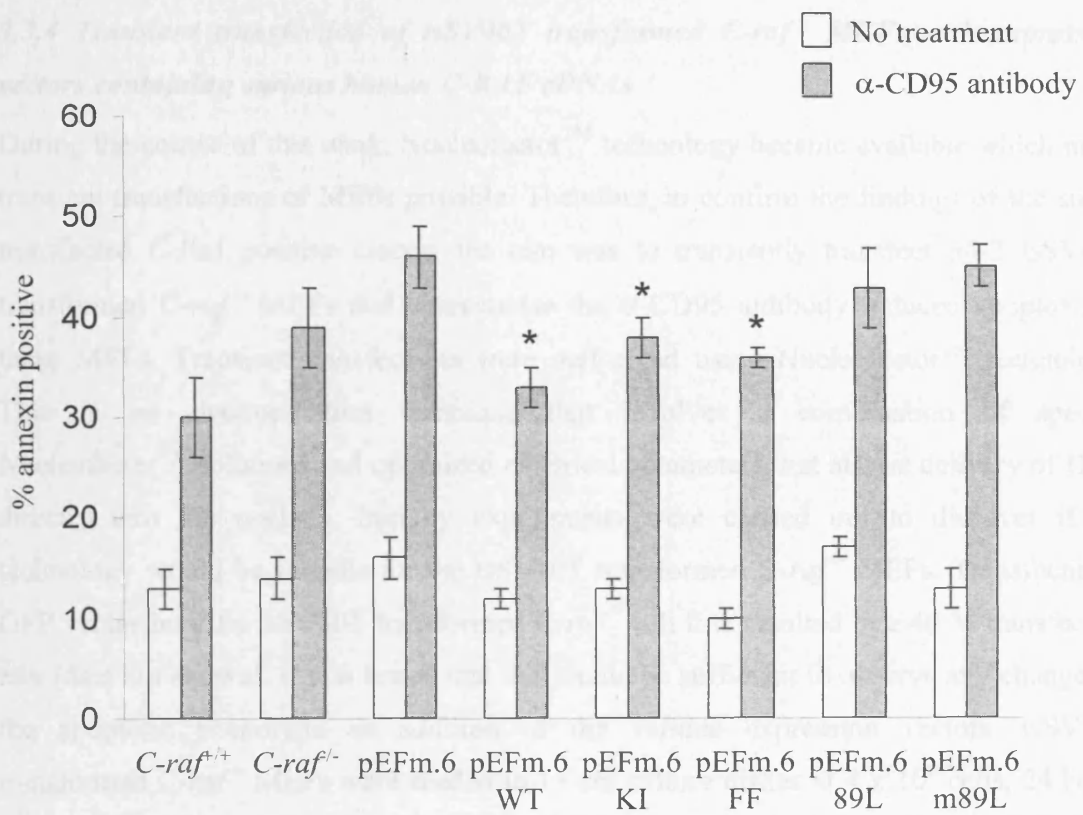


**Figure 3.12** Pooled data from the apoptotic analysis of *C-raf*<sup>-/-</sup> tsSV40T immortalised MEFs expressing mutant forms of human C-RAF. MEFs were induced to undergo apoptosis by treating with 50 ng/ml  $\alpha$ -CD95 antibody plus 0.5  $\mu$ M cycloheximide or left untreated. Apoptosis was evaluated using annexin V FITC staining followed by flow cytometric analysis. The data represents pooled data. Standard error bars are shown. *P* values were generated for treated cells using paired t-Tests against pEFm.6 MEFs. (\* = *P* ≤ 0.05). Abbreviations; pEFm.6 = empty backbone vector, WT = wild-type C-RAF, KI = kinase inactive mutant of C-RAF, FF = MEK inactive mutant of C-RAF, 89L = Ras binding mutant of C-RAF and m89L = Ras binding mutant of C-RAF with an additional mitochondrial targeting motif.



The introduction of the pEFm.6-m89L plasmid also did not lead to a decrease in the levels of apoptosis observed upon  $\alpha$ -CD95 antibody treatment. The percentage of apoptosis for each of the three clones tested were  $44 \% \pm 3$  for #108 pEFm.6-m89L ( $n=3$   $P=0.4$ ; Figure 3.11B),  $45 \% \pm 3$  for #179 pEFm.6-m89L ( $n=3$   $P=0.7$ ; Figure 3.11B) and  $47 \% \pm 1$  for #180 pEFm.6-m89L ( $n=3$   $P=0.4$ ; Figure 3.11B). The average value upon  $\alpha$ -CD95 antibody induced apoptosis for pEFm.6-m89L was  $45 \% \pm 2$  ( $P=1.0$ ; Figure 3.12). This value was higher than that observed for non-transfected tsSV40T transformed *C-raf*<sup>-/-</sup> MEFs and similar to the levels obtained for pEFm.6 MEFs.

### ***3.3.4 Transient transfection of tsSV40T transformed C-raf<sup>-/-</sup> MEFs with expression vectors containing various human C-RAF cDNAs***

During the course of this work, Nucleofector™ technology became available which made transient transfections of MEFs possible. Therefore, to confirm the findings of the stably transfected C-Raf positive clones, the aim was to transiently transfect tsSV40T transformed *C-raf*<sup>-/-</sup> MEFs and characterise the  $\alpha$ -CD95 antibody induced apoptosis of these MEFs. Transient transfections were performed using Nucleofector™ technology. This is an electroporation technique that involves a combination of specific Nucleofector™ solutions and optimized electrical parameters that allows delivery of DNA directly into the nucleus. Initially experiments were carried out to discover if the technology would be suitable for the tsSV40T transformed *C-raf*<sup>-/-</sup> MEFs. Transfecting a GFP vector into the tsSV40T transformed *C-raf*<sup>-/-</sup> cell line resulted in a 40 % transfection rate (data not shown). It was hoped that this would be sufficient to observe any changes in the apoptotic phenotype on addition of the various expression vectors. tsSV40T transformed *C-raf*<sup>-/-</sup> MEFs were seeded in 15 cm culture dishes at  $4 \times 10^6$  cells, 24 hours prior to the transfection occurring. The following day,  $1 \times 10^6$  of the MEFs were used for the Nucleofection, along with 10  $\mu$ g DNA, per transfection. The vectors used for the transfections were; the empty backbone vector pEFm.6, the pEFm.6-WT vector expressing wild-type C-RAF and the pEFm.6-KI vector expressing kinase inactive *C-RAF*.

Protein lysates were produced from all transiently transfected MEFs to analyse expression levels of C-RAF. The lysates were evaluated by SDS-PAGE followed by western blotting analysis. The blots produced were incubated with an  $\alpha$ -C-Raf antibody. An  $\alpha$ -ERK1

antibody was used as a protein loading control. The expression of C-RAF in all transfections can be observed in Figure 3.13A.

### ***3.3.5 Characterisation of the apoptotic phenotype of C-raf<sup>-/-</sup> immortalised MEFs transiently transfected with various human C-RAF cDNAs upon $\alpha$ -CD95 antibody induction***

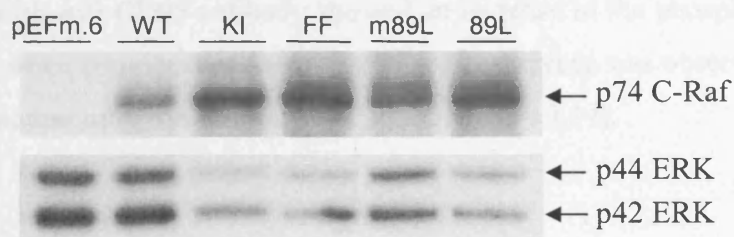
To discover if the transiently expressed clones would reproduce the apoptotic phenotypes observed for the stably transfected clones, they were induced to undergo apoptosis. Immediately after transfecting, the cells were split between 2 x 6 cm plates and incubated at 33° C for 6 hours. The growth media was changed and the cells transferred to 39°C for 24 hours. Cells were induced to undergo apoptosis by the addition of 50 ng/ml  $\alpha$ -CD95 antibody plus 0.5  $\mu$ M cycloheximide for 20 hours. Suspended and attached cells were collected, annexin V FITC staining performed and PI added, followed by FACS analysis.

Addition of the pEFm.6 expression vector led to an increase in apoptosis. A mean value of 50 %  $\pm$  8 apoptosis was observed, compared with the 39 %  $\pm$  4 seen previously in non-transfected tsSV40T transformed C-raf<sup>-/-</sup> cells (Figure 3.13B). This agrees with results observed for the stably transfected pEFm.6 expressing clones, showing that the manipulation of the cells, by addition of the empty backbone vector, gives rise to an increase in the levels of  $\alpha$ -CD95 antibody induced apoptosis. The pEFm.6 transient MEFs were therefore used as a control for the transiently produced MEFs expressing the wild-type and kinase inactive mutant form of C-RAF cDNAs.

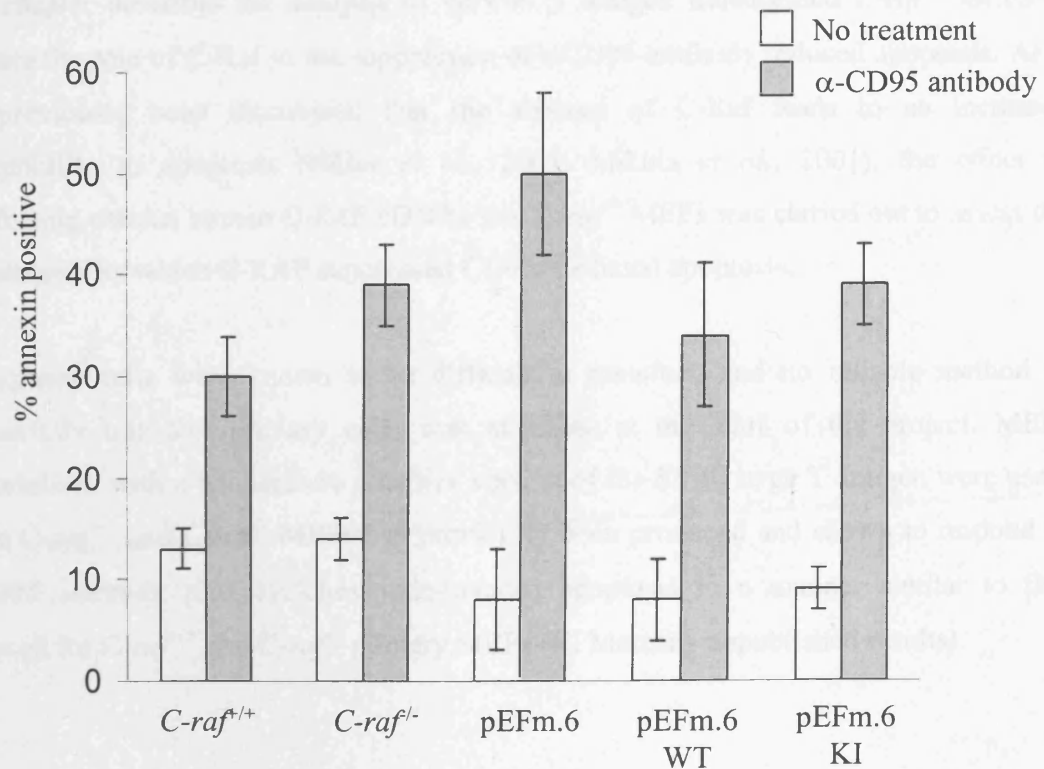
On addition of the pEFm.6-WT plasmid there was a decrease in apoptosis to 34 %  $\pm$  7 (n=3; P=0.3; Figure 3.13B) when compared to the 50 %  $\pm$  8 observed for pEFm.6 transfected alone. Transient expression of the kinase inactive mutant of C-RAF gave 39 %  $\pm$  4 (n=3, P=0.3; Figure 3.13B) apoptosis upon stimulation with  $\alpha$ -CD95 antibody. This was a noticeable reduction when compared to expression of pEFm.6, and suggested that the kinase inactive form of C-RAF was able to rescue the apoptotic phenotype, as observed for the stably transfected clones.

**Figure 3.13** Analysis of *C-raf*<sup>-/-</sup> tsSV40T immortalised MEFs transiently expressing mutant forms of human C-RAF. **(A)** Western blot analysis to detect C-Raf (upper panel) and actin (lower panel). **(B)** MEFs were induced to undergo apoptosis by treating with 50 ng/ml  $\alpha$ -CD95 antibody plus 0.5  $\mu$ M cycloheximide or left untreated. Apoptosis was evaluated using annexin V FITC staining followed by flow cytometric analysis. Graph of pooled data for *C-raf*<sup>-/-</sup> MEFs, pooled data for pEFm.6 MEFs and values for various *C-raf*<sup>-/-</sup> MEFs expressing mutant forms of human C-RAF. The data represents mean $\pm$ SEM (n=3 for pEFm.6-WT; n=3 for pEFm.6-KI; n=3 for pEFm.6-FF. *P* values were generated for treated cells using paired t-Tests against pEFm.6 MEFs. Abbreviations; pEFm.6 = empty backbone vector, WT = wild-type C-RAF and KI = kinase inactive mutant of C-RAF. *P* values were generated for treated cells using paired t-Tests against pEFm.6 MEFs. (No values were obtained for *P*  $\leq$ 0.05).

**A**



**B**



### 3.3.6 Analysis of p38-MAPK phosphorylation upon $\alpha$ -CD95 induced apoptosis of C-Raf primary MEFs

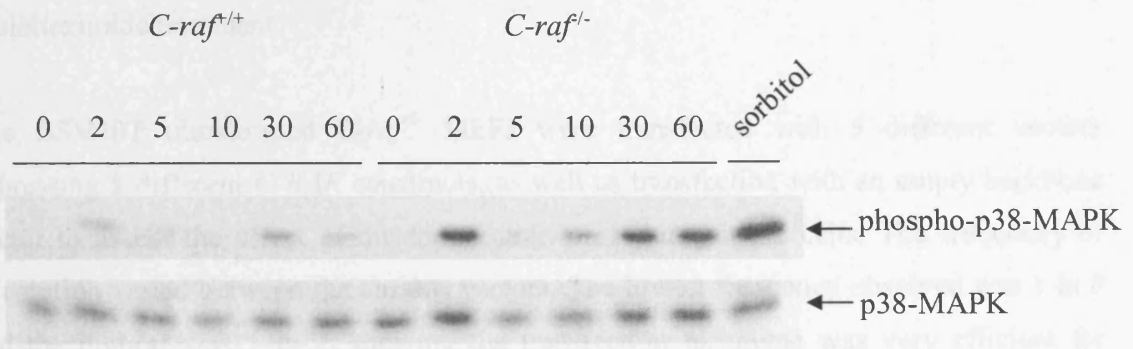
To assess a possible role of C-Raf in the ASK1/p38-MAPK pathway leading to increased susceptibility to  $\alpha$ -CD95 antibody induced apoptosis of *C-raf*<sup>-/-</sup> MEFs, levels of phospho-p38-MAPK were analysed for both *C-raf*<sup>+/+</sup> and *C-raf*<sup>-/-</sup> MEFs. Cells were seeded at  $1.5 \times 10^6$  in 6 cm dishes. 24 hours later cells were placed in serum-free media for 30 minutes. Apoptosis was induced by the addition of 50 ng/ml anti-CD95 antibody and 0.5  $\mu$ M cycloheximide. Cells were lysed at timepoints of 0, 2, 5, 10, 30 and 60 minutes after stimulation. Protein lysates were prepared and SDS-PAGE carried out followed by electro-transfer of the proteins onto nitrocellulose. The blots were incubated with an  $\alpha$ -phospho-p38-MAPK antibody to detect levels of phospho-p38-MAPK. An  $\alpha$ -p38-MAPK antibody was used as a control for protein loading. Analysis of phospho-p38-MAPK levels upon treatment with anti-CD95 antibody showed an increase in the phospho-p38-MAPK levels for *C-raf*<sup>-/-</sup> when compared to *C-raf*<sup>+/+</sup> MEFs. The increase was observed at all time points, except 5 minutes after the stimulus was added (Figure 3.14).

### 3.4 Conclusions

This chapter describes the analysis of tsSV40 T antigen transformed *C-raf*<sup>-/-</sup> MEFs to evaluate the role of C-Raf in the suppression of  $\alpha$ CD95-antibody induced apoptosis. As it had previously been discovered that the absence of C-Raf leads to an increased susceptibility to apoptosis (Hüser *et al.*, 2001; Mikula *et al.*, 2001), the effect of transfecting various human *C-RAF* cDNAs into *C-raf*<sup>-/-</sup> MEFs was carried out to assess the mechanisms by which C-RAF suppressed CD95-mediated apoptosis.

As primary cells were known to be difficult to transfect, and no reliable method to successfully transfect primary cells was available at the start of the project, MEFs immortalised with a temperature sensitive version of the SV40 large T antigen were used. These *C-raf*<sup>+/+</sup> and *C-raf*<sup>-/-</sup> MEFs had previously been produced and shown to respond to  $\alpha$ -CD95 antibody plus cycloheximide-induced apoptosis in a manner similar to that observed for *C-raf*<sup>+/+</sup> and *C-raf*<sup>-/-</sup> primary MEFs (K. Mercer - unpublished results).

**Figure 3.14** Phosphorylation of p38-MAPK for *C-raf*<sup>+/+</sup> and *C-raf*<sup>-/-</sup> primary MEFs over a time course of  $\alpha$ -CD95 antibody induced apoptosis (0 to 60 minutes). Treatment of *C-raf*<sup>+/+</sup> MEFs with 500 mM sorbitol for 30 min was used as a control for phospho-p38-MAPK. Protein lysates were analysed by Western blot analysis followed by detection of phospho-p38-MAPK (upper panel) and total p38-MAPK as a control for protein loading (lower panel).



As stated previously, analysis of the tsSV40T transformed *C-raf*<sup>-/-</sup> MEFs showed that they are susceptible to increased apoptosis in comparison to tsSV40T transformed *C-raf*<sup>+/+</sup> MEFs following  $\alpha$ -CD95 antibody treatment. This chapter confirmed these findings by showing, upon  $\alpha$ -CD95 antibody plus cycloheximide treatment, 39 %  $\pm$  4 of tsSV40T transformed *C-raf*<sup>-/-</sup> MEFs underwent apoptosis compared to 30 %  $\pm$  4 of tsSV40T transformed *C-raf*<sup>+/+</sup> MEFs. The increased apoptosis of the *C-raf*<sup>-/-</sup> MEFs was further confirmed by showing increased levels of cleaved, active caspase 3 in these cells, as well as observing greater amounts of Hoechst 33256 staining upon  $\alpha$ -CD95 antibody plus cycloheximide treatment.

The tsSV40T transformed *C-raf*<sup>-/-</sup> MEFs were transfected with 5 different vectors expressing 5 different *C-RAF* constructs, as well as transfection with an empty backbone vector to assess the affect of the transfection procedure on the cells. The frequency of integration varied between the various vectors. The lowest frequency observed was 1 in 8 and the highest was 1 in 2, showing the transfection technique was very efficient for obtaining clones expressing the various forms of the human *C-RAF* cDNAs. Successful expression of the plasmids was confirmed by detection of the C-Raf protein in these clones.

The three tsSV40T transformed *C-raf*<sup>-/-</sup> MEFs harbouring the backbone vector (pEFm.6) showed an increased susceptibility to apoptosis upon  $\alpha$ -CD95 antibody treatment when compared to non-transfected tsSV40T transformed *C-raf*<sup>-/-</sup> MEFs. This indicated that the manipulation of tsSV40T transformed *C-raf*<sup>-/-</sup> MEFs, by transfection of the cells had led to an increased level of apoptosis upon  $\alpha$ -CD95 antibody induction. This is a phenomenon that is often observed for transfected cells (C. Pritchard and K.Mercer pers.comm). The pEFm.6 MEFs therefore served as a control for comparison to the *C-raf*<sup>-/-</sup> tsSV40T MEFs transfected with the various *C-RAF* cDNAs, rather than comparison with the non-transfected tsSV40T *C-raf*<sup>-/-</sup> MEFs.

Treatment of the four tsSV40T transformed *C-raf*<sup>-/-</sup> MEFs expressing wild-type C-Raf with  $\alpha$ -CD95 antibody rescued the apoptosis phenotype to levels significantly lower than observed for pEFm.6 cells and also lower than those seen for non-transfected tsSV40T transformed *C-raf*<sup>-/-</sup> MEFs upon induction by  $\alpha$ -CD95 antibody. The levels of apoptosis

were not completely reduced to those observed for tsSV40T transformed *C-raf*<sup>+/+</sup> MEFs. This is likely to be due to the variation in the levels of C-Raf expressed in the four clones tested and due to the transfection method leading to an increased susceptibility of the cells to apoptosis. The reduction of apoptosis to levels below those observed for the pEFm.6 control shows that expression of *C-RAF* in the pEFm.6-WT MEFs can rescue the apoptotic phenotype caused by the absence of C-Raf. It therefore confirmed the method was valid for rescuing the C-Raf apoptotic phenotype and showed that the increased apoptosis observed in the tsSV40T transformed *C-raf*<sup>-/-</sup> MEFs was occurring due to the absence of C-Raf only and for no other reason.

Analysis of the three clones expressing pEFm.6-FF, the MEK kinase inactive form of C-Raf, also rescued the levels of apoptosis observed upon  $\alpha$ -CD95 antibody treatment. The overall pooled percentage of apoptosis observed for the three clones was significantly lower than the values obtained for both the pEFm.6 MEFs. The results show that addition of MEK kinase inactive C-Raf can rescue the apoptotic phenotype observed in the absence of C-Raf. The results agreed with the previous findings showing no increased susceptibility to  $\alpha$ -CD95-induced apoptosis occurs in MEK kinase inactive (*C-raf*<sup>FF/FF</sup>) mice (Hüser *et al.*, 2001).

Four tsSV40T transformed *C-raf*<sup>-/-</sup> MEFs expressing kinase inactive C-Raf were obtained and analysed upon treatment with  $\alpha$ -CD95 antibody. All individual clones, as well as the pooled value for all clones, rescued the apoptotic phenotype to levels below those observed for pEFm.6 control cells. The results provide good evidence that the kinase activity of C-Raf is not required for its role in suppressing  $\alpha$ -CD95 antibody-induced apoptosis.

Having determined that the role of C-RAF in suppressing  $\alpha$ -CD95 antibody-induced apoptosis is independent of its kinase activity, as well as its MEK kinase activity, clones expressing a mutant form of C-RAF that was incapable of binding to RAS were analysed. The three clones analysed upon  $\alpha$ -CD95 antibody treatment indicated no significant reduction in apoptosis values when compared to pEFm.6 control cells. This indicates that the role of C-RAF in suppressing  $\alpha$ -CD95 antibody-induced apoptosis is RAS dependent.

and therefore suggests Ras binding to C-Raf is required for its role in suppressing apoptosis.

As previous reports have suggested a possible role of C-Raf in cell survival at the mitochondria, clones expressing C-RAF targeted to the mitochondria were also assessed. The three clones expressing a mitochondrial targeted C-RAF were analysed upon treatment with  $\alpha$ -CD95 antibody. The levels of apoptosis observed were similar to those seen for the pEFm.6 control MEFs. These results indicate that the role of C-RAF in cell survival does not occur at the mitochondria.

During this project, the ability to successfully transiently transfect primary cells became available using the Nucleofector. tsSV40T transformed *C-raf*<sup>-/-</sup> MEFs transiently transfected with either wild-type, or kinase inactive C-RAF were produced, as well as cells containing the backbone vector only. This allowed analysis of a mixed population of cells expressing different levels of C-RAF and therefore eliminated the clonal variation observed for the stable clones, as mentioned above. The results agreed with those observed for the stable clones. Expression of wild-type C-RAF and kinase inactive C-RAF led to apoptosis levels below those observed for pEFm.6 transiently transfected control cells. These data further confirm that the role of C-RAF in cell survival is independent of its kinase activity.

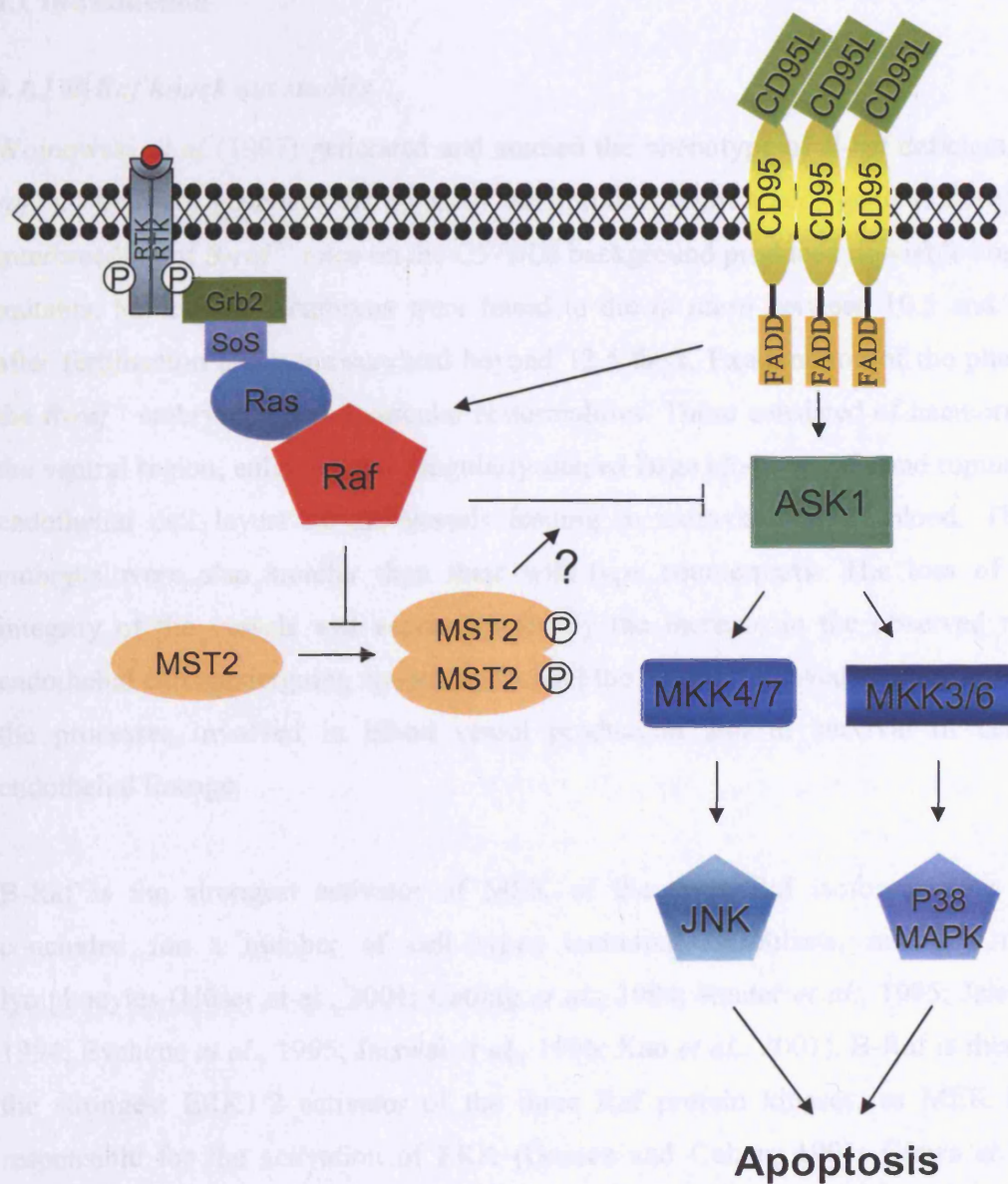
The findings of this chapter agree with previous findings that the regulation of  $\alpha$ -CD95 antibody induced apoptosis by C-Raf is MEK/ERK independent (Hüser *et al.*, 2001), and further shows C-Raf does not require its kinase activity for its role in suppressing apoptosis. These studies also show that Ras binding to C-Raf is important in antagonising the apoptotic effect of  $\alpha$ -CD95 antibody. A kinase independent role of C-Raf in suppressing  $\alpha$ -CD95 induced apoptosis is supported by the findings that kinase inactive forms of C-Raf are able to inhibit ASK1 induced apoptosis (Chen *et al.*, 2001). Furthermore, a mouse recently generated in the laboratory with a homozygous knockin mutation of <sup>K483M</sup>C-Raf, creating a C-Raf inactive kinase, has been observed to survive to adulthood without any characteristics of increased susceptibility to apoptosis (K. Mercer pers.comm). Analysis of kinase inactive C-Raf MEFs generated from these mice have

shown no increased susceptibility to apoptosis upon  $\alpha$ -CD95 antibody treatment (K. Mercer pers.comm).

Of the various mechanisms by which C-Raf has been shown to suppress  $\alpha$ -CD95-antibody induced apoptosis, the best evidence is for the involvement of ASK1. A recent study has shown C-Raf antagonises ASK1-induced apoptosis in a MEK-ERK independent manner (Yamaguchi *et al.*, 2004). This study investigated the role of C-Raf in cardiac muscle-specific *C-raf*<sup>-/-</sup> mice. These mice showed increased apoptosis within the hearts, increased levels of JNK and p38-MAPK activity, but no change in MEK or ERK levels. Furthermore, ASK1 ablation rescued the abnormalities observed, suggesting the deficiency of C-Raf was allowing ASK1 to induce apoptosis within these cells. Results from the present project agree with a role of C-Raf in  $\alpha$ -CD95-antibody induced apoptosis by suppressing ASK1 activity. Indeed, analysis of phospho-p38-MAPK levels upon treatment with  $\alpha$ -CD95 antibody showed a reproducible increase in the activation of phospho-p38-MAPK for *C-raf*<sup>-/-</sup> when compared to *C-raf*<sup>+/+</sup> MEFs (Figure 3.14), providing further evidence for the role of C-Raf in regulating this pathway.

ASK1 is known to induce apoptosis upon treatment with TNF and  $\alpha$ -CD95 antibody. However, previous findings have shown that the role of C-Raf in the suppression of apoptosis is selective against  $\alpha$ -CD95 antibody induced apoptosis but not affected by TNF (Hüser *et al.*, 2001; Mikula *et al.*, 2001). This suggests ASK-1 may not be the direct target for C-Raf, as it would therefore also inhibit TNF induced apoptosis. It is possible that C-Raf may be targeting the mammalian sterile 20-like kinase (MST2). This protein has been shown to bind to C-Raf via part of the Raf CR2 domain that is not conserved in B-Raf (O'Neill *et al.*, 2004). C-Raf was observed to prevent dimerisation and phosphorylation of MST2 independent of C-Raf kinase activity. Furthermore, MST2 was selectively activated by  $\alpha$ -CD95 antibody in *C-raf*<sup>-/-</sup> cells, and depletion of MST2 from the cells led to decreased sensitivity to apoptosis (O'Neill *et al.*, 2004). It therefore appears C-Raf may inhibit MST2 in its kinase independent role of suppressing apoptosis. Figure 3.15 summarises the findings of this chapter and indicates that the role C-Raf may play in ASK or MST2-mediated apoptosis. Whether there is a connection between these two pathways or not is not currently known, and the role of Ras binding to C-Raf in these pathways also remains to be assessed.

**Figure 3.15** Possible mechanism by which C-Raf may be involved in the suppression of Fas induced apoptosis. This role is thought to be independent of C-Raf kinase activity.



## 4. CHARACTERISATION OF GROWTH, PROLIFERATION AND APOPTOSIS IN *B-raf*<sup>-/-</sup> MEFs

### 4.1 Introduction

#### 4.1.1 *B-Raf* knock out studies

Wojnowski *et al* (1997) generated and studied the phenotype of *B-raf* deficient mice (*B-raf*<sup>-/-</sup>). The *B-raf* gene was disrupted by the introduction of a *neo*<sup>R</sup> gene to disrupt exon 3. Interbreeding of *B-raf*<sup>+/-</sup> mice on the C57BL6 background produced no viable homozygous mutants. Most *B-raf*<sup>-/-</sup> embryos were found to die *in utero* between 10.5 and 12.5 days after fertilisation and none survived beyond 12.5 days. Examination of the phenotype of the *B-raf*<sup>-/-</sup> embryos showed vascular abnormalities. These consisted of haemorrhaging in the ventral region, enlarged and irregularly shaped large blood vessels and rupturing of the endothelial cell layers of the vessels leading to extravasation of blood. The mutant embryos were also smaller than their wild-type counterparts. The loss of structural integrity of the vessels was accounted for by the increase in the observed number of endothelial cells undergoing apoptosis. Overall the findings showed B-Raf played a role in the processes involved in blood vessel production and in survival of cells of the endothelial lineage.

B-Raf is the strongest activator of MEK of the three Raf isoforms. This has been concluded for a number of cell types including fibroblasts, neuronal tissue and lymphocytes (Hüser *et al.*, 2001; Catling *et al.*, 1994; Reuter *et al.*, 1995; Jaiswal *et al.*, 1994; Eychene *et al.*, 1995; Jaiswal *et al.*, 1996; Kao *et al.*, 2001). B-Raf is therefore also the strongest ERK1/2 activator of the three Raf protein kinases, as MEK is directly responsible for the activation of ERK (Gomez and Cohen, 1991; Crews *et al.*, 1991; Nakielny *et al.*, 1992; Seger *et al.*, 1992; Matsuda *et al.*, 1992). ERK1/2 have a wide substrate specificity, including both cytoplasmic and nuclear proteins. ERK1/2 activity can affect cell proliferation, cell differentiation, apoptosis, translation, cell shape, cell motility and cell adhesion.

### 4.1.2 Role of B-Raf in proliferation

B-Raf has been shown to play a role in the regulation of the G1 to S phase of the cell cycle via activation of ERKs. Upon activation ERKs translocate to the nucleus where they can phosphorylate transcription factors including members of the c-Fos (c-Fos, FosB, Fra-1 and Fra-2) and c-Jun (c-Jun, Jun-B and Jun-D) families of proteins (Whitmarsh and Davis, 1996; Balmanno and Cook, 1999; Cook *et al.*, 1999; Shaulian and Karin, 2002). Members of these families form heterodimeric AP-1 complexes that are able to bind to AP-1 binding sites found in the promoter region of many genes, including cyclin D1 (Angel and Karin, 1991; Albanese *et al.*, 1995). This promotes the expression of cyclin D1, leading to the phosphorylation and de-repression of the Rb protein by the cyclin D-cdk4/6 complexes, resulting in the release of the E2F transcription factors. This in turn allows expression of various genes required to progress from the G1 to S phase of the cell cycle.

Expression of activated Raf proteins has been associated with increased cell proliferation in many cell types including hematopoietic cells (Muszynski *et al.*, 1995), murine NIH 3T3 fibroblasts (Kerkhoff and Rapp, 1997; Kerkhoff *et al.*, 1998) and A10 smooth muscle cells (Cioffi *et al.*, 1997). However, over-expression of activated Raf proteins have also been shown to lead to cell cycle arrest in some cell lines including rat Schwann cells, human promyelocytic leukaemia cells (Lloyd *et al.*, 1997) and small cell lung cancer cells (Ravi *et al.*, 1998). The conflicting results observed are thought to depend on the Raf isoform being expressed and its level of activity.

Studies involving conditionally-active  $\Delta$ Raf:ER proteins have been used to investigate the role Raf proteins play in cell proliferation. Raf is activated in cells expressing  $\Delta$ Raf:ER constructs by the addition of estradiol. Upon estradiol addition,  $\Delta$ B-Raf:ER cells did not promote cell cycle progression and were shown to inhibit mitogenic responses of the cells to subsequent additions of EGF and PDGF (Pritchard *et al.*, 1995). Another study utilising the conditionally-active  $\Delta$ Raf:ER constructs showed  $\Delta$ Raf:ER proteins were able to strongly induce cyclin D1 expression, and that this induction correlated with the differing abilities of each Raf isoform to activate MEK/ERK, thus  $\Delta$ B-Raf:ER had the greatest activity towards cyclin D1 (Woods *et al.*, 1997).  $\Delta$ B-Raf:ER was also shown to strongly induce p21<sup>CIP1</sup>, an inhibitor of cyclin-cdk activity. It was concluded that B-Raf is involved

in both cell proliferation and cell cycle arrest, with the concentration of stimuli added affecting the outcome (Woods *et al.*, 1997).

#### **4.1.3 Role of B-Raf in the suppression of apoptosis**

B-Raf has been directly linked with suppressing apoptosis via the activation of MEK/ERK (Erhardt *et al.*, 1999). Fibroblasts over-expressing B-Raf, subjected to growth factor deprivation, were resistant to apoptosis and this resistance was lost when a specific MEK inhibitor was used. Furthermore, the over-expression of B-Raf resulted in increased ERK activity, but no alterations in the PI3-K/Akt pathway were observed. The anti-apoptotic effects of B-Raf were also shown to be downstream of the release of cytochrome *c* from the mitochondria (Erhardt *et al.*, 1999).

ERKs have been shown to directly regulate a number of proteins involved in apoptosis. Bim, a BH3-only protein member of the Bcl-2 family promotes apoptosis (O'Connor *et al.*, 1998). There are currently ten known Bim variants, all thought to be obtained by alternative splicing (O'Connor *et al.*, 1998; Miyashita *et al.*, 2001; Marani *et al.*, 2002). Two of these variants, Bim<sub>EL</sub> and Bim<sub>L</sub> have been linked to the Ras/Raf/MEK/ERK pathway. Bim<sub>EL</sub> and Bim<sub>L</sub> can bind to Bcl-2 or Bcl-x<sub>L</sub>, which in turn leads to the release of pro-apoptotic Bax and Bak, thus promoting apoptosis. ERK1/2 can repress Bim expression independently of the JNK and PI3-K pathways (Weston *et al.*, 2003). Serum withdrawal induced apoptosis in CC139 fibroblasts caused a rapid *de novo* accumulation of Bim<sub>EL</sub> and this expression was reduced upon activation of the ERK1/2 pathway. The ERK1/2 pathway promotes phosphorylation of Bim<sub>EL</sub> and this targets Bim<sub>EL</sub> for degradation via the proteasome (Ley *et al.*, 2003). ERK1/2 has subsequently been observed to directly phosphorylate Bim<sub>EL</sub> at serine 65, and there are two other uncharacterised Bim<sub>EL</sub> sites that undergo phosphorylation by ERK1/2 (Ley *et al.*, 2004). The Ras/Raf/MEK/ERK pathway may also play a role in inhibiting Bim<sub>EL</sub> and Bim<sub>L</sub> in detachment-induced apoptosis (Marani *et al.*, 2004). Therefore ERKs play a role in preventing apoptosis via the phosphorylation and subsequent degradation of Bim variants in some cell types.

ERKs phosphorylate and activate p90<sup>RSK</sup> proteins (Sturgill *et al.*, 1988). These proteins are a family of serine/threonine kinases consisting of four mammalian isoforms. Activated p90<sup>RSK</sup> has both cytoplasmic and nuclear substrates. In the nucleus p90<sup>RSK</sup> is shown to

phosphorylate CREB (Xing *et al.*, 1996; Pende *et al.*, 1997; Xing *et al.*, 1998), c-Fos (Chen *et al.*, 1993; Chen *et al.*, 1996), and the SRF (Rivera *et al.*, 1993). It may also play a direct role in promoting the cell cycle via p27<sup>KIP1</sup> (Fujita *et al.*, 2003). The p90<sup>RSK</sup> proteins are also involved in promoting cell survival via direct phosphorylation and inactivation of the Bcl-2 pro-apoptotic protein Bad (Hoppe *et al.*, 1999; Tan *et al.*, 1999). p90<sup>RSK</sup> phosphorylates Bad at Ser112, and this stimulates binding of Bad to 14-3-3, sequestering Bad, thus preventing Bad-mediated cell death (Tan *et al.*, 1999). The Ras/Raf/MEK/ERK signalling cascade was observed to induce Bad phosphorylation by p90<sup>RSK</sup> in a growth factor dependent manner in neuronal cells (Bonni *et al.*, 1999).

A direct link between the role of ERK in cell survival and caspase 9 has been found. An *in vitro* study using cytosolic HeLa cell extracts discovered that caspase 9 activity was suppressed by okadaic acid, and this could be overcome via treatment with the MEK inhibitors PD98059 and UO126 (Allan *et al.*, 2003). Further analysis showed addition of okadaic acid was leading to induced activity of ERK1/2, and suppression of this activity corresponded to the induction of caspase 9 in various cell types. It was discovered that pro-caspase 9 is phosphorylated *in vitro* on Thr125 by ERK2 upon growth factor stimulation, and that ERK1/2 co-precipitated with the phosphorylated form of pro-caspase 9. Furthermore, phosphorylation of Thr125 prevented caspase 9 processing and caspase 3 activation, even when apoptosome formation was induced (Allan *et al.*, 2003). These data strongly suggest a role for ERK in the suppression of apoptosis via phosphorylation of caspase 9.

## 4.2 Aims

As previous reports have suggested the potential involvement of B-Raf in apoptosis and proliferation, the aim of this chapter was to characterise the role of B-Raf with respect to both proliferation and apoptosis using *B-raf*<sup>-/-</sup> MEFs. MEK and ERK phosphorylations were analysed in the *B-raf*<sup>-/-</sup> primary MEFs. The apoptotic phenotype was assessed upon  $\alpha$ -CD95 antibody or serum withdrawal induced apoptosis and further studies carried out to characterise the apoptotic phenotype of the cells upon serum withdrawal. Cell growth and proliferation upon serum stimulation were also analysed.

### 4.3 Results

#### 4.3.1 Derivation of *B-raf*<sup>-/-</sup> primary MEFs

B-Raf deficient embryos have previously been produced and reported by Wojnowski *et al* (1997). A *B-raf*<sup>+/-</sup> mouse generated from mice originating from this study was kindly gifted by L. Wojnowski. This mouse was used to set up a breeding colony on the MF-1 background strain (Figure 4.1A) to obtain further *B-raf*<sup>+/-</sup> mice. Resulting *B-raf*<sup>+/-</sup> males and *B-raf*<sup>+/-</sup> females were time-mated (Figure 4.1B), followed by the isolation of primary MEFs from E12.5 embryos. Each MEF cell line was generated from a single embryo. DNA lysates were produced from each cell line and genotyped by PCR. 3 primers were used in conjunction, to assess the presence of the *B-raf* wild type allele and/or the *B-raf* mutant allele. Ocp75 and Ocp112 gave rise to a 220 bp product corresponding to the wild type allele. Ocp75 and Ocp128 amplified a 330 bp product indicating the presence of the mutant allele (Figure 4.2A). An example of PCR results obtained from one timed-mating is shown in Figure 4.2B. In this case, 3 of the MEF cell lines were identified as *B-raf*<sup>-/-</sup> (#1, #5 and #7), 3 cell lines confirmed as *B-raf*<sup>+/+</sup> (#6, #9 and #11) and the remaining 9 cell lines genotyped as *B-raf*<sup>+/-</sup>, which agreed with the expected Mendelian frequency. A number of timed-matings were carried out on the MF-1 background strain to obtain MEFs suitable for analysis.

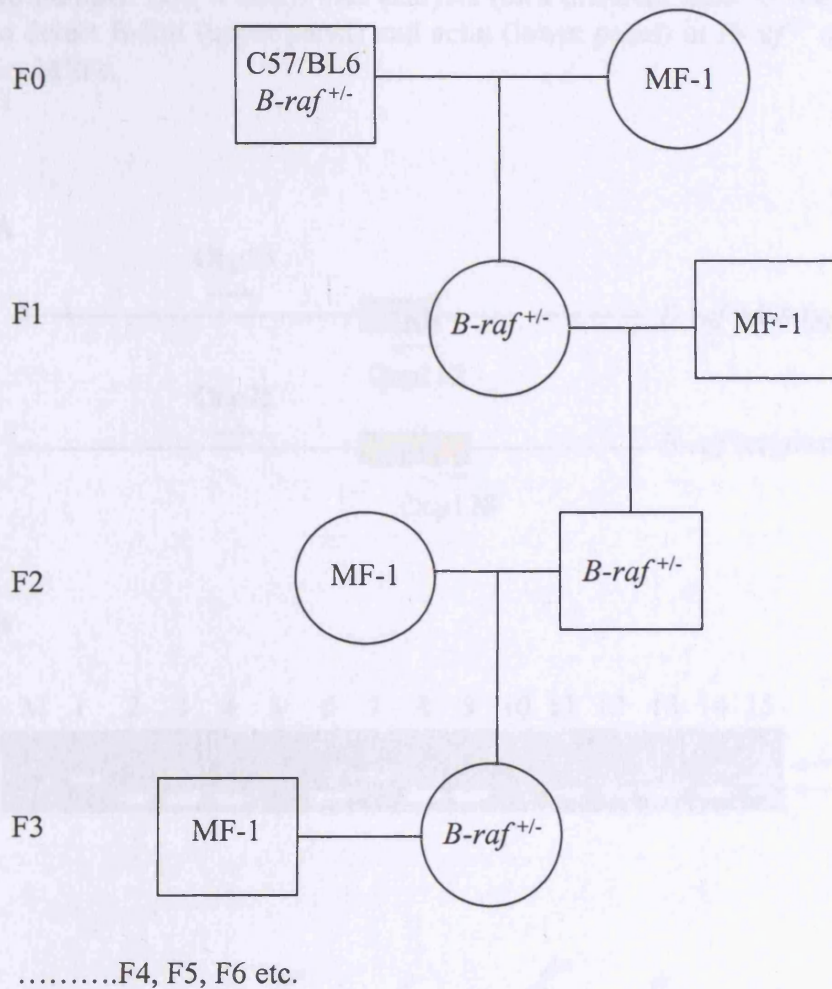
Protein lysates were prepared from the MEFs and used for SDS-PAGE followed by electro-transfer of the proteins onto nitrocellulose. The blots were incubated with an  $\alpha$ -B-Raf antibody and an  $\alpha$ -actin antibody was used as a protein loading control. The results showed that the *B-raf*<sup>-/-</sup> MEFs characterised by PCR did not express the B-Raf protein whereas the *B-raf*<sup>+/+</sup> MEFs did (Figure 4.2C).

#### 4.3.2 Analysis of ERK phosphorylation in *B-raf*<sup>-/-</sup> primary MEFs

To discover if there was any difference in the phosphorylation of ERK1/2 in *B-raf*<sup>-/-</sup> MEFs compared to *B-raf*<sup>+/+</sup> MEFs, the MEFs were treated with different stimuli and the levels of phosphorylated proteins assessed. Cells were seeded at  $1.5 \times 10^6$  cells in 6 cm dishes until confluent. The cells were made quiescent by placing in serum-free medium for 30 minutes, and then stimulated with epidermal growth factor (EGF), phorbol 12-myristate 13-acetate (PMA) or 10 % serum. Cells were lysed at timepoints of 0, 2, 5, 10, 30 and 60 minutes after stimulation. Protein lysates were prepared and used for SDS-PAGE followed by

**Figure 4.1** Breeding strategy for the production of (A) mice expressing the *B-raf* knockout targeting event by backcrossing with mice on the on the MF1 background strain and (B) E12.5 embryos from timed-mating of *B-raf*<sup>+/-</sup> mice generated in (A). Ratios indicate expected frequency based on Mendelian inheritance.

**A**



**B**

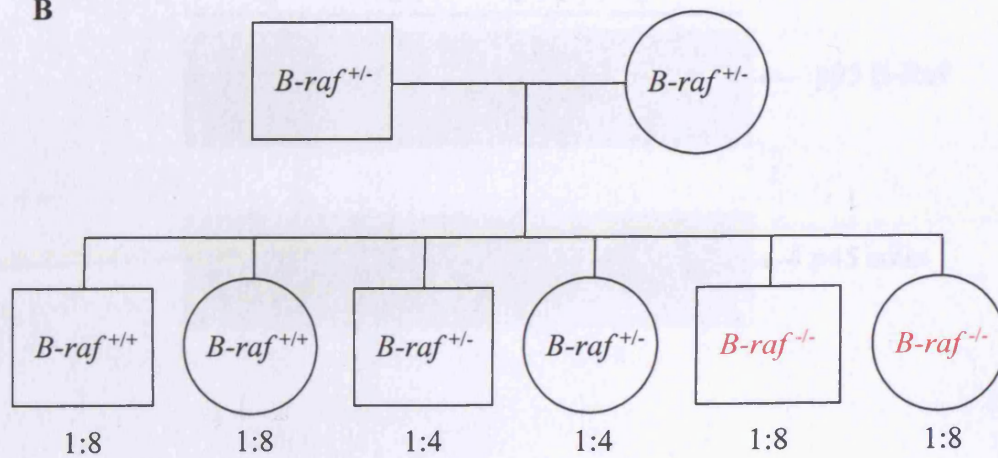
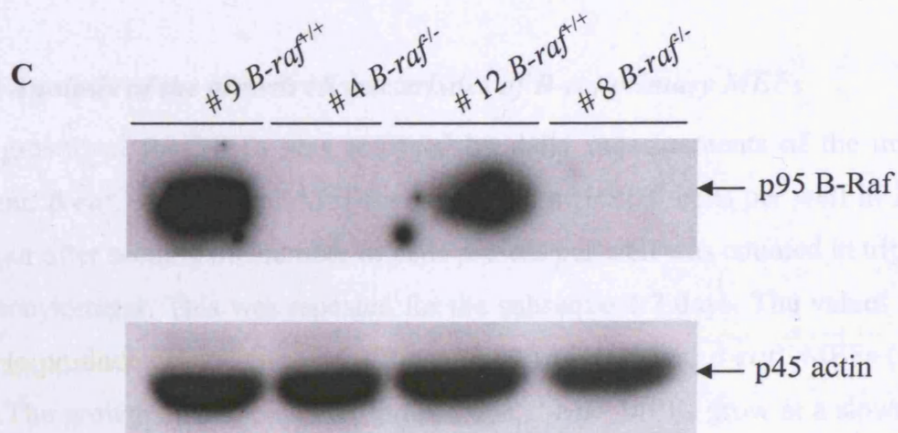
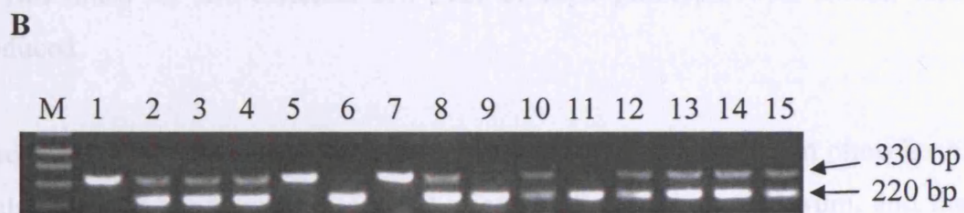
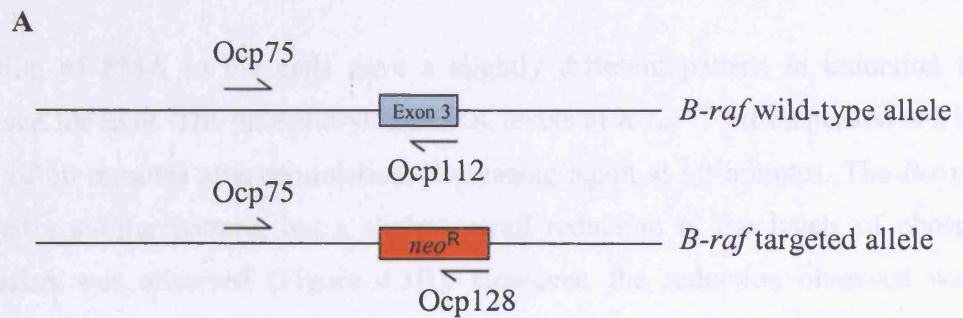


**Figure 4.2** Screening of *B-raf*<sup>f/-</sup> timed-mated litters (A) *B-raf* wild-type and targeted alleles highlighting the positions of primers used in confirming the genotype of embryos generated. (B) PCR of DNA lysates from numerous cell lines generated with primers Ocp75, Ocp112 and Ocp128 amplifying 220 bp and 330 bp products. Abbreviations: M = 1 Kb DNA ladder; numbers correspond to embryo number. (C) Western blot analysis (of a different litter to that shown in (B)) to detect B-Raf (upper panel) and actin (lower panel) in *B-raf*<sup>f/+</sup> and *B-raf*<sup>f/-</sup> primary MEFs.



electro-transfer of the proteins onto nitrocellulose. The blots were incubated with an  $\alpha$ -phospho-ERK antibody to detect the levels of phospho-ERK. An  $\alpha$ -vinculin or  $\alpha$ -actin antibody was used as a control for protein loading. Upon EGF stimulation of *B-raf*<sup>+/+</sup> MEFs the levels of phospho-ERK increased after 2 minutes and peaked at 5 min before decreasing down to basal levels at 60 minutes. *B-raf*<sup>-/-</sup> MEFs showed the same pattern in response to EGF stimulation, however, the levels of phospho-ERK were markedly reduced (Figure 4.3A). This was repeated a minimum of two times for two different cell lines of each genotype, with similar results being obtained.

Addition of PMA to the cells gave a slightly different pattern in induction than that observed for EGF. The phosphorylated ERK levels of *B-raf*<sup>+/+</sup> MEFs peaked at a later time point of 10 minutes after stimulation, decreasing again at 60 minutes. The *B-raf*<sup>-/-</sup> MEFs showed a similar pattern, but a slight overall reduction in the levels of phospho-ERK activation was observed (Figure 4.3B). However, the reduction observed was not as significant as seen for EGF stimulation of the B-Raf MEFs. The findings were repeated at least two times for two different cell lines of each genotype, with similar results being reproduced.

The results upon stimulation with 10 % serum showed an increase in phospho-ERK upon stimulation, peaking between 5 and 10 minutes after addition of serum, and then slowly decreasing. The activation of phospho-ERK was greater for *B-raf*<sup>+/+</sup> MEFs than for *B-raf*<sup>-/-</sup> MEFs (Figure 4.3C).

#### **4.3.3 Analysis of the growth characteristics of *B-raf* primary MEFs**

The growth of the MEFs was analysed by daily measurements of the number of cells present. *B-raf*<sup>+/+</sup> and *B-raf*<sup>-/-</sup> MEFs were seeded at  $1 \times 10^4$  cells per well in 24 well plates. 48 hour after seeding the number of cells present per well was counted in triplicate, using a haemocytometer. This was repeated for the subsequent 7 days. The values obtained were used to produce growth curves for *B-raf*<sup>+/+</sup> (#9 and #12) and *B-raf*<sup>-/-</sup> MEFs (#1, #4, #7 and #10). The growth curves obtained showed that *B-raf*<sup>-/-</sup> MEFs grow at a slower rate than *B-raf*<sup>+/+</sup> MEFs (Figure 4.4). The rate of growth increased steadily between 2 and 6 days after plating and was greatest between 6 and 7 days. This pattern was seen for both *B-raf*<sup>+/+</sup> and

**Figure 4.3** ERK phosphorylation in *B-raf*<sup>+/+</sup> and *B-raf*<sup>-/-</sup> primary MEFs over a time course of stimulation (0 to 60 min) Protein lysates were analysed by Western blot analysis followed by detection of phospho-ERK (upper panels) and vinculin as a control for protein loading (lower panels) (A) Stimulation with 10 ng/ml epidermal growth factor (B) Stimulation with 10 ng/ml phorbol 12-myristate 13-acetate. (C) Stimulation with 10 % serum, with actin as a control for protein loading (lower panel)

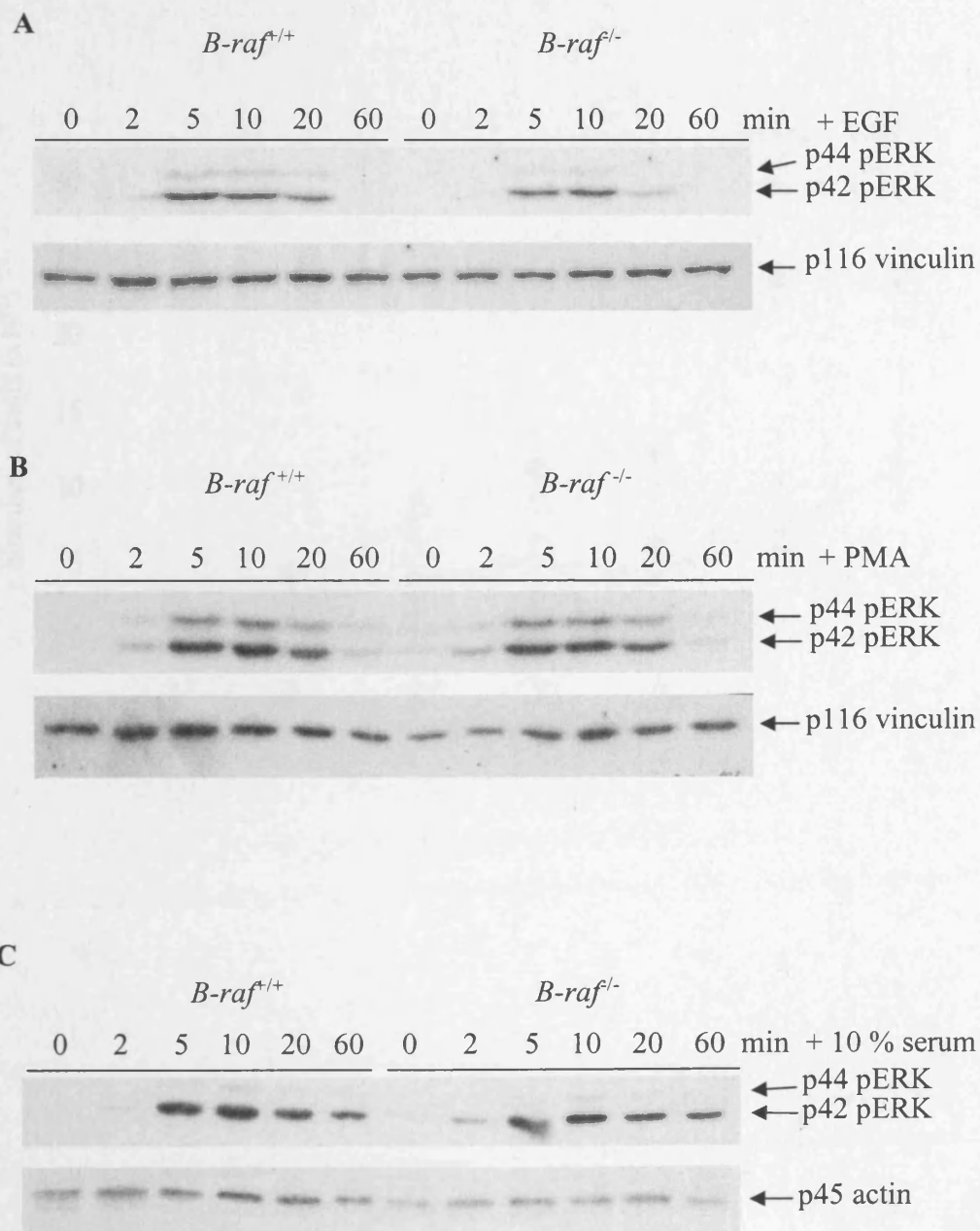
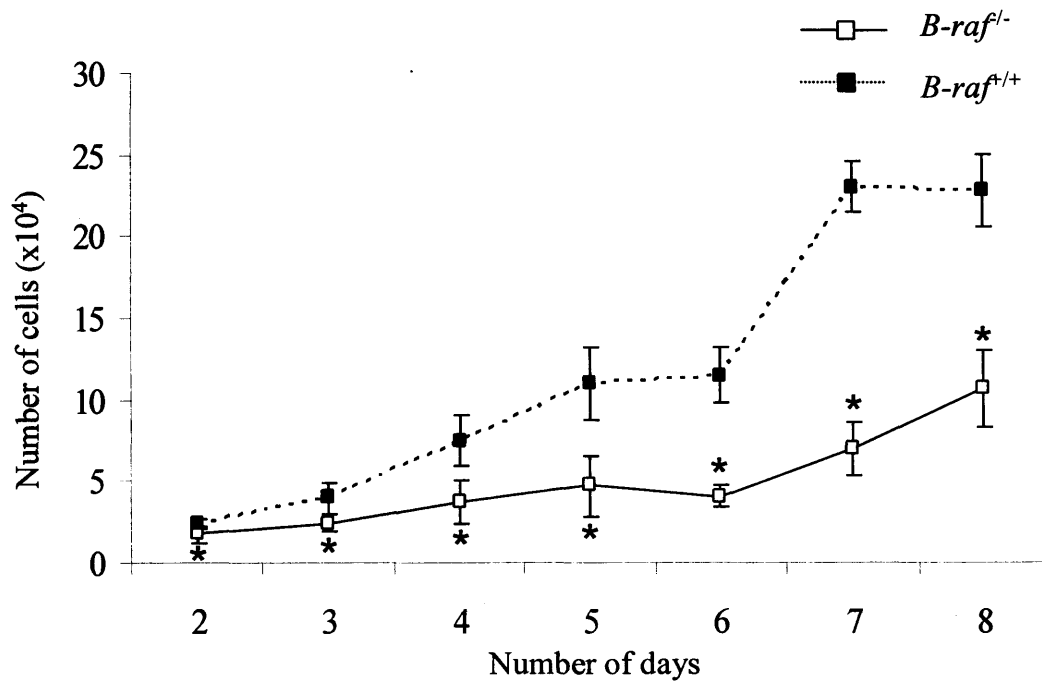


**Figure 4.4** Analysis of the growth characteristics of *B-raf<sup>f/+</sup>* and *B-raf<sup>f/-</sup>* primary MEFs. Cell counts were performed over a period of 8 days and growth profiles produced. Pooled data for *B-raf<sup>f/+</sup>* (closed squares) and *B-raf<sup>f/-</sup>* (opened squares) are indicated. Standard error bars are shown. A *P* value was generated for the overall growth rate of *B-raf<sup>f/-</sup>* MEFs via a paired t-Test against *B-raf<sup>f/+</sup>* MEFs. (\* = *P* ≤ 0.05).



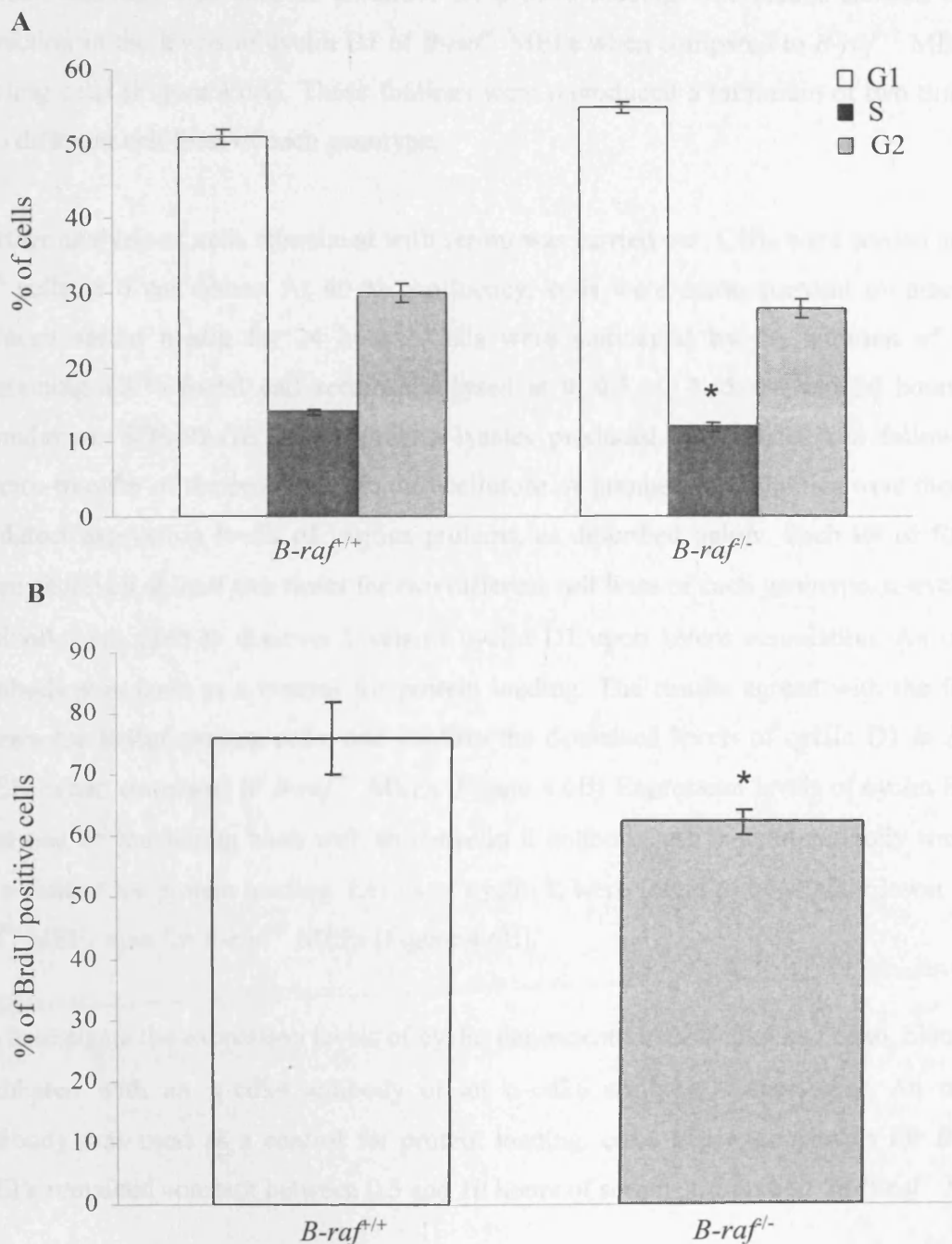
*B-raf*<sup>-/-</sup> MEFs, although the overall growth rate was greater for *B-raf*<sup>+/+</sup> MEFs (n=6;  $P=2 \times 10^{-11}$ ). The data represents pooled data for each genotype from three data sets.

#### 4.3.4 Analysis of proliferation of *B-raf* primary MEFs

To further investigate the slower growth rate of the *B-raf*<sup>-/-</sup> MEFs, DNA staining was carried out to discover the proportion of cells in each phase of the cell cycle. Cells were seeded at  $5 \times 10^4$  in 6 cm dishes. The following day the cells were harvested, fixed and stained with propidium iodide. The cell suspension was analysed by FACS. The results were very similar for both *B-raf*<sup>+/+</sup> and *B-raf*<sup>-/-</sup> MEFs. The proportion of *B-raf*<sup>+/+</sup> cells in G1 was  $51 \% \pm 1$ , compared to  $55 \% \pm 1$  for *B-raf*<sup>-/-</sup> MEFs (n=6;  $P=0.19$ ). Slightly fewer *B-raf*<sup>-/-</sup> MEFs were recorded in S phase,  $12 \% \pm 0.4$  compared to  $14 \% \pm 0.6$  for *B-raf*<sup>-/-</sup> MEFs (n=6;  $P=0.09$ ). The proportion of cells in G2 were also slightly lower for *B-raf*<sup>-/-</sup> MEFs, at  $28 \% \pm 1$  compared to  $30 \% \pm 1$  for *B-raf*<sup>+/+</sup> MEFs (n=6;  $P=0.46$ ; Figure 4.5A). The data showed there was a slight but not highly significant difference in the proportion of cells in each phase of the cell cycle. The data represents two cell lines of each genotype and is pooled for three data sets.

Although there was not a large difference observed in the proportion of cells in each phase, the slightly increased proportion of *B-raf*<sup>-/-</sup> cells in G1 and the slightly decreased number of cells in S phase, led to further proliferation investigations being carried out. To investigate the ability of the MEFs to progress through the cell cycle, DNA synthesis was measured. Cells were plated at  $1 \times 10^4$  on coverslips until 60 % confluent. The cells were made quiescent and stimulated by the addition of 10 % serum in media containing 5-Bromo-2'-deoxy-uridine (BrdU) labelling reagent for 16 hours. The incorporation of the BrdU reagent was measured by the addition of an  $\alpha$ -BrdU antibody followed by the addition of an  $\alpha$ -mouse-Ig-fluorescein conjugated secondary antibody. Cells were analysed using a fluorescent microscope and a minimum of 300 cells were counted per experiment. The cells were noted as fluorescent or non-fluorescent and the percentage of fluorescing BrdU positive cells calculated. The results show a significant difference in the ability of the cell lines to undergo DNA synthesis. Only  $62 \% \pm 2$  of *B-raf*<sup>-/-</sup> MEFs were BrdU positive compared with  $71 \% \pm 7$  of *B-raf*<sup>+/+</sup> MEFs (n=4;  $P=0.03$ ; Figure 4.5B).

**Figure 4.5** Analysis of proliferation in *B-raf*<sup>+/+</sup> and *B-raf*<sup>-/-</sup> primary MEFs. **(A)** DNA staining of MEFs with propidium iodide followed by FACS scan analysis. Graph represents pooled data for *B-raf*<sup>+/+</sup> MEFs compared to *B-raf*<sup>-/-</sup> MEFs, showing the proportion of cells at various stages of the cell cycle. (n=6) Standard error bars are shown. *P* values were generated for *B-raf*<sup>-/-</sup> MEFs via a paired t-Test against *B-raf*<sup>+/+</sup> MEFs for each stage of the cell cycle (\*=*P*≤0.05). **(B)** DNA synthesis analysis via BrdU staining. Cells were stimulated with 10 % serum for 16 hours. Graph represents pooled data for BrdU positive *B-raf*<sup>+/+</sup> MEFs compared to *B-raf*<sup>-/-</sup> MEFs (n=4). A minimum of 300 cells were scored per experiment. Standard error bars are shown. A *P* value was generated for *B-raf*<sup>-/-</sup> MEFs via a paired t-Test against *B-raf*<sup>+/+</sup> MEFs. (\* = *P*≤0.05).



### **4.3.5 Analysis of proteins involved in the G1 to S phase of the cell cycle in *B-raf* primary MEFs**

To investigate what may be leading to the differences in the progression through the cell cycle observed between *B-raf*<sup>-/-</sup> and *B-raf*<sup>+/+</sup> MEFs, some of the proteins known to be regulated via ERK in the G1 to S phase of the cell cycle were analysed. Cells were seeded at  $1.5 \times 10^6$  cells in 6 cm dishes and when confluent, cell lysates produced. The lysates were used for SDS-PAGE, followed by electro-transfer of the proteins onto nitrocellulose. The blots were incubated with an  $\alpha$ -cyclin D1 antibody to detect levels of cyclin D1. An  $\alpha$ -actin antibody was used as a control for protein loading. The results showed a clear reduction in the levels of cyclin D1 of *B-raf*<sup>-/-</sup> MEFs when compared to *B-raf*<sup>+/+</sup> MEFs for cycling cells (Figure 4.6A). These findings were reproduced a minimum of two times for two different cell lines of each genotype.

Further analysis of cells stimulated with serum was carried out. Cells were seeded at  $1.5 \times 10^6$  cells in 6 cm dishes. At 60 % confluency, cells were made quiescent by placing in reduced serum media for 24 hours. Cells were stimulated by the addition of media containing 10 % foetal calf serum and lysed at 0, 0.5, 1, 3, 5, 10 and 20 hours after stimulation. SDS-PAGE of the protein lysates produced was carried out followed by electro-transfer of the proteins onto nitrocellulose. A number of antibodies were then used to detect expression levels of various proteins, as described below. Each set of findings were observed at least two times for two different cell lines of each genotype.  $\alpha$ -cyclin D1 antibody was used to discover levels of cyclin D1 upon serum stimulation. An  $\alpha$ -actin antibody was used as a control for protein loading. The results agreed with the finding shown for B-Raf cycling cells, and confirm the decreased levels of cyclin D1 in *B-raf*<sup>-/-</sup> MEFs when compared to *B-raf*<sup>+/+</sup> MEFs (Figure 4.6B) Expression levels of cyclin E were analysed by incubating blots with an  $\alpha$ -cyclin E antibody. An  $\alpha$ -actin antibody was used as a control for protein loading. Levels of cyclin E were found to be slightly lower for *B-raf*<sup>-/-</sup> MEFs than for *B-raf*<sup>+/+</sup> MEFs (Figure 4.6B).

To investigate the expression levels of cyclin dependent kinases cdk4 and cdk6, blots were incubated with an  $\alpha$ -cdk4 antibody or an  $\alpha$ -cdk6 antibody respectively. An  $\alpha$ -actin antibody was used as a control for protein loading. cdk4 expression levels for *B-raf*<sup>+/+</sup> MEFs remained constant between 0.5 and 10 hours of serum stimulation. In *B-raf*<sup>-/-</sup> MEFs,

the levels decreased slightly upon stimulation and remained fairly constant over the time-course of 10 hours, but were overall markedly reduced (Figure 4.6B). Cdk6 expression levels were greatest at 8 and 10 hours after stimulation for both *B-raf*<sup>+/+</sup> and *B-raf*<sup>-/-</sup> MEFs, but levels were again observed to be lower for *B-raf*<sup>-/-</sup> MEFs (Figure 4.6B).

Investigations into the expression levels of the CDIs, p21<sup>CIP1</sup> and p27<sup>KIP1</sup> were carried out by incubating blots with an  $\alpha$ -p21<sup>CIP1</sup> antibody and an  $\alpha$ -p27<sup>KIP1</sup> antibody respectively. An  $\alpha$ -actin antibody was used as a control for protein loading for p21<sup>CIP1</sup> and  $\alpha$ -ERK1 as a protein loading control for p27<sup>KIP1</sup>. p21<sup>CIP1</sup> levels were markedly increased between 0 and 1 hours of stimulation for *B-raf*<sup>-/-</sup> MEFs when compared to *B-raf*<sup>+/+</sup> MEFs (Figure 4.7A). Analysis of p27<sup>KIP1</sup> levels indicated increased levels 1 hours after stimulation for *B-raf*<sup>-/-</sup> MEFs in comparison to *B-raf*<sup>+/+</sup> MEFs. The levels were higher for *B-raf*<sup>+/+</sup> MEFs between 3 and 20 hours of serum stimulation (Figure 4.7B).

An  $\alpha$ -c-Fos antibody was incubated with blots to discover the expression levels of c-Fos protein being expressed. An  $\alpha$ -actin antibody was used as a control for protein loading. A slight decrease in c-Fos expression levels were observed upon comparison of *B-raf*<sup>-/-</sup> MEFs to *B-raf*<sup>+/+</sup> MEFs (Figure 4.7C).

#### **4.3.6 Analysis of the apoptotic phenotype of *B-raf*<sup>-/-</sup> and *B-raf*<sup>+/+</sup> MEFs upon $\alpha$ -CD95 antibody induction**

To assess apoptosis upon  $\alpha$ -CD95 antibody treatment, MEFs were plated at a density of  $1.5 \times 10^6$  cells onto 6 cm dishes. The cells were fed with growth media 24 hours after plating. Apoptosis was induced 24 hours later by the addition of 50 ng/ml anti-CD95 antibody and 0.5  $\mu$ M cycloheximide for 20 hours. Suspended and attached cells were collected, annexin V FITC staining performed and PI added, followed by FACS analysis. The experiment was performed on four separate occasions. The results showed that there was an increase in apoptosis for *B-raf*<sup>-/-</sup> MEFs (#4 and #8) when compared with *B-raf*<sup>+/+</sup> MEFs (#9 and #12) (Figure 4.8A). Increased apoptosis in *B-raf*<sup>-/-</sup> MEFs was observed for both untreated cells and cells treated with  $\alpha$ -CD95 antibody. Pooling the data for each cell line and each experiment gave an average percentage of apoptosis for the untreated *B-raf*<sup>+/+</sup> MEFs of  $9 \% \pm 1$  and this increased to  $14 \% \pm 1$  ( $n=6$ ;  $P= 0.008$ ) for the untreated *B-*

**Figure 4.6** Cell cycle protein expression levels in *B-raf*<sup>+/+</sup> and *B-raf*<sup>-/-</sup> primary MEFs. **(A)** Protein lysates produced from continuously growing cells were analysed by Western blot analysis followed by detection of cyclin D1 (upper panel), and actin as a control for protein loading (lower panel). **(B)** MEFs were serum induced over a time course of 0 to 20 hours. Protein lysates produced were analysed by Western blot analysis followed by detection of (a) cyclin D1, (b) cyclin E, (c) cdk4, (d) cdk6 and actin as a control for protein loading (lower panel).

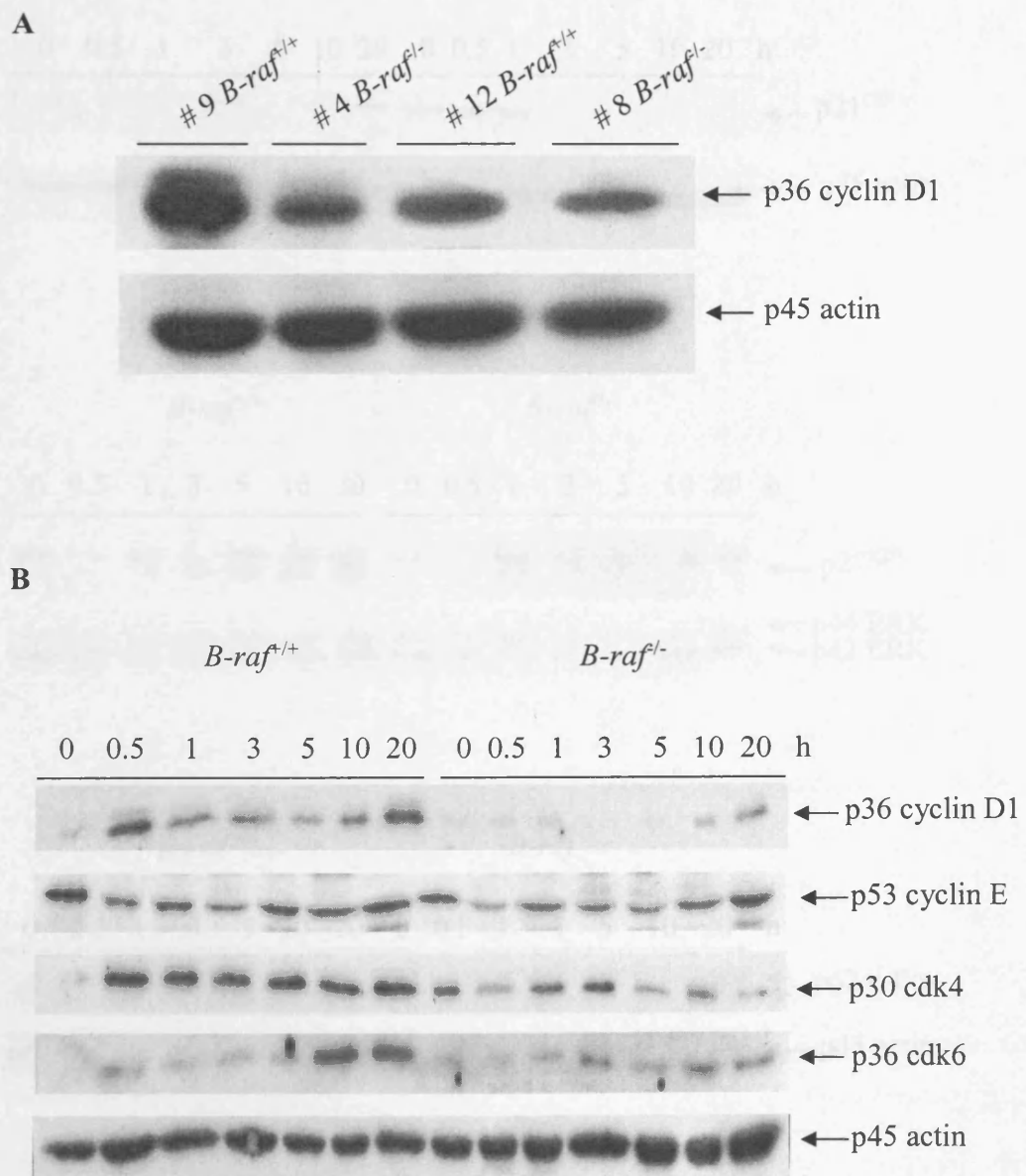


**Figure 4.7** p21<sup>CIP1</sup> and p27<sup>KIP1</sup> protein levels in *B-raf*<sup>+/+</sup> and *B-raf*<sup>-/-</sup> primary MEFs over a time course of serum stimulation (0 to 20 hours). Protein lysates were analysed by Western blot analysis followed by detection of (A) p21<sup>CIP1</sup> (upper panel), and actin as a control for protein loading (lower panel), (B) p27<sup>KIP1</sup> (upper panel) and ERK1 as a control for protein loading (lower panel), (C) c-Fos (upper panel) and actin as a control for protein loading (lower panel).

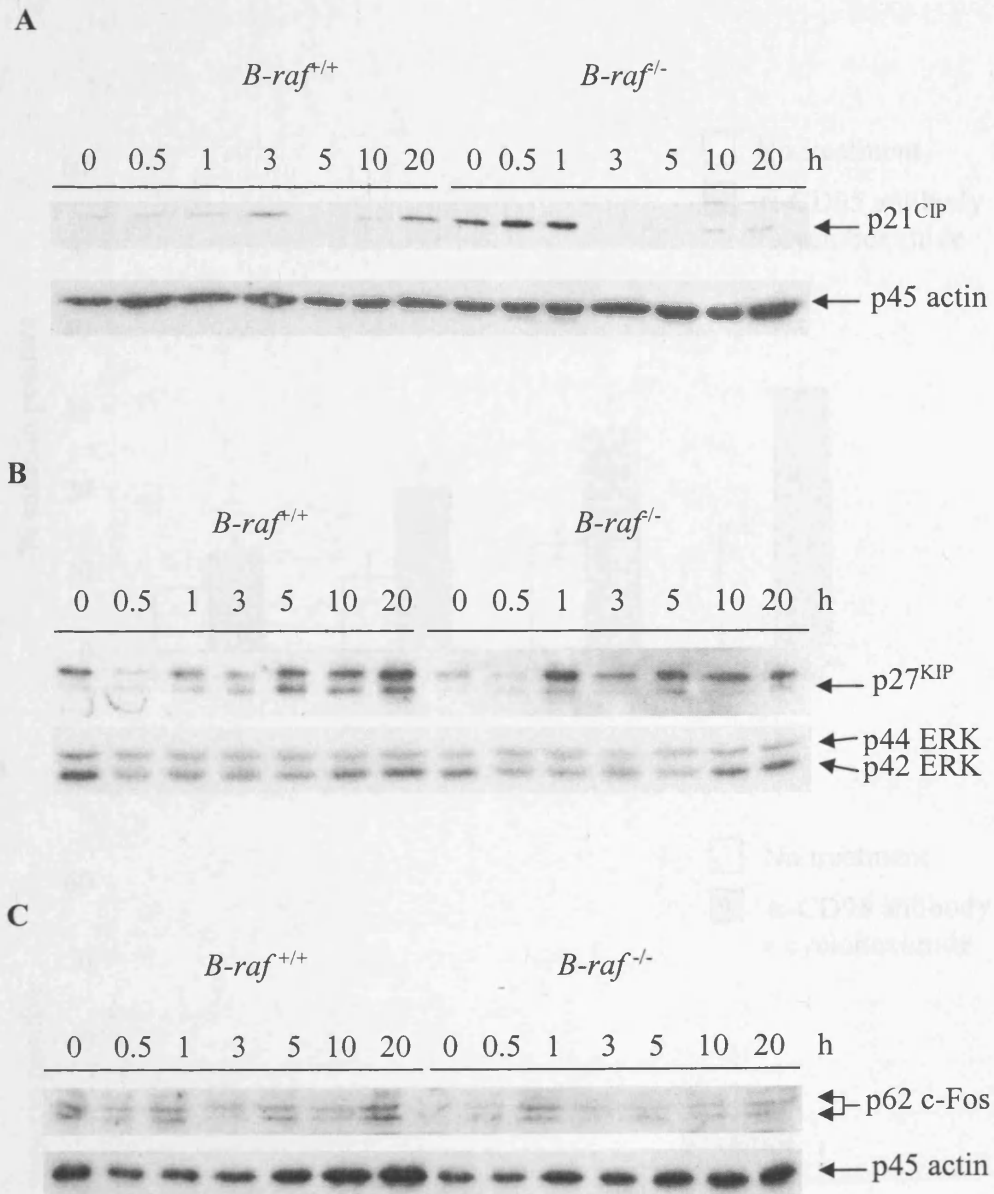
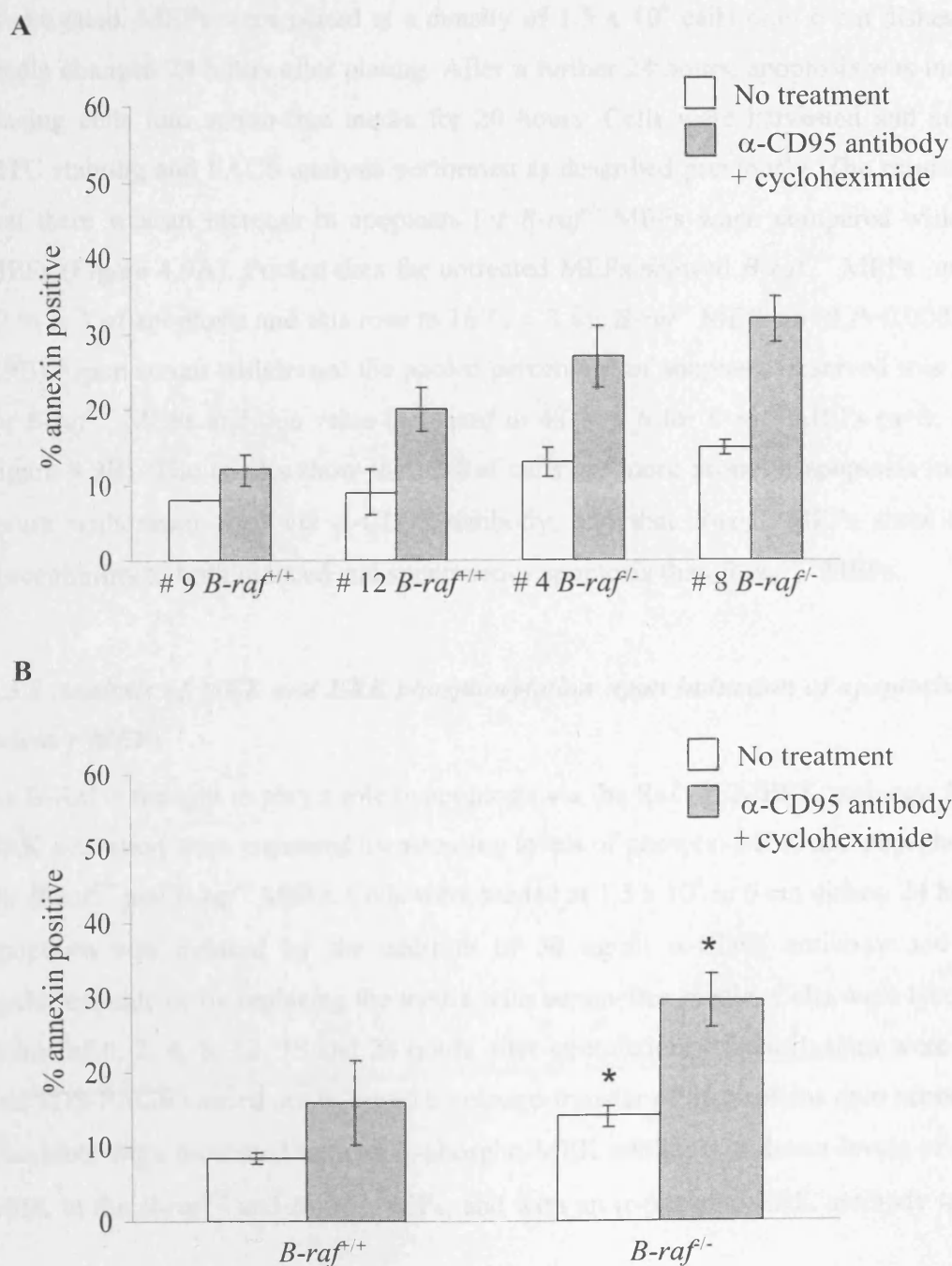


**Figure 4.8** Apoptotic analysis of *B-raf*<sup>+/+</sup> and *B-raf*<sup>-/-</sup> primary MEFs. MEFs were induced to undergo apoptosis by treating with 50 ng/ml  $\alpha$ -CD95 antibody plus 0.5  $\mu$ M cycloheximide or left untreated. Apoptosis was evaluated using annexin V FITC staining followed by flow cytometric analysis. **(A)** Graph showing individual *B-raf*<sup>+/+</sup> and *B-raf*<sup>-/-</sup> cell lines. **(B)** Graph representing pooled data for *B-raf*<sup>+/+</sup> and *B-raf*<sup>-/-</sup> MEFs (n=6). Standard error bars are shown. *P* values were generated for pooled *B-raf*<sup>-/-</sup> MEFs via a paired t-Test against pooled *B-raf*<sup>+/+</sup> MEFs for both treated and untreated cells. (\* = *P*≤0.05).



*raf*<sup>-/-</sup> MEFs. Upon anti-CD95 induction apoptosis levels of 30 % ± 4 were observed for *B-raf*<sup>-/-</sup> MEFs whereas for *B-raf*<sup>+/+</sup> MEFs a value of 16 % ± 6 (n=8; *P*=0.00001) was obtained (Figure 4.8B).

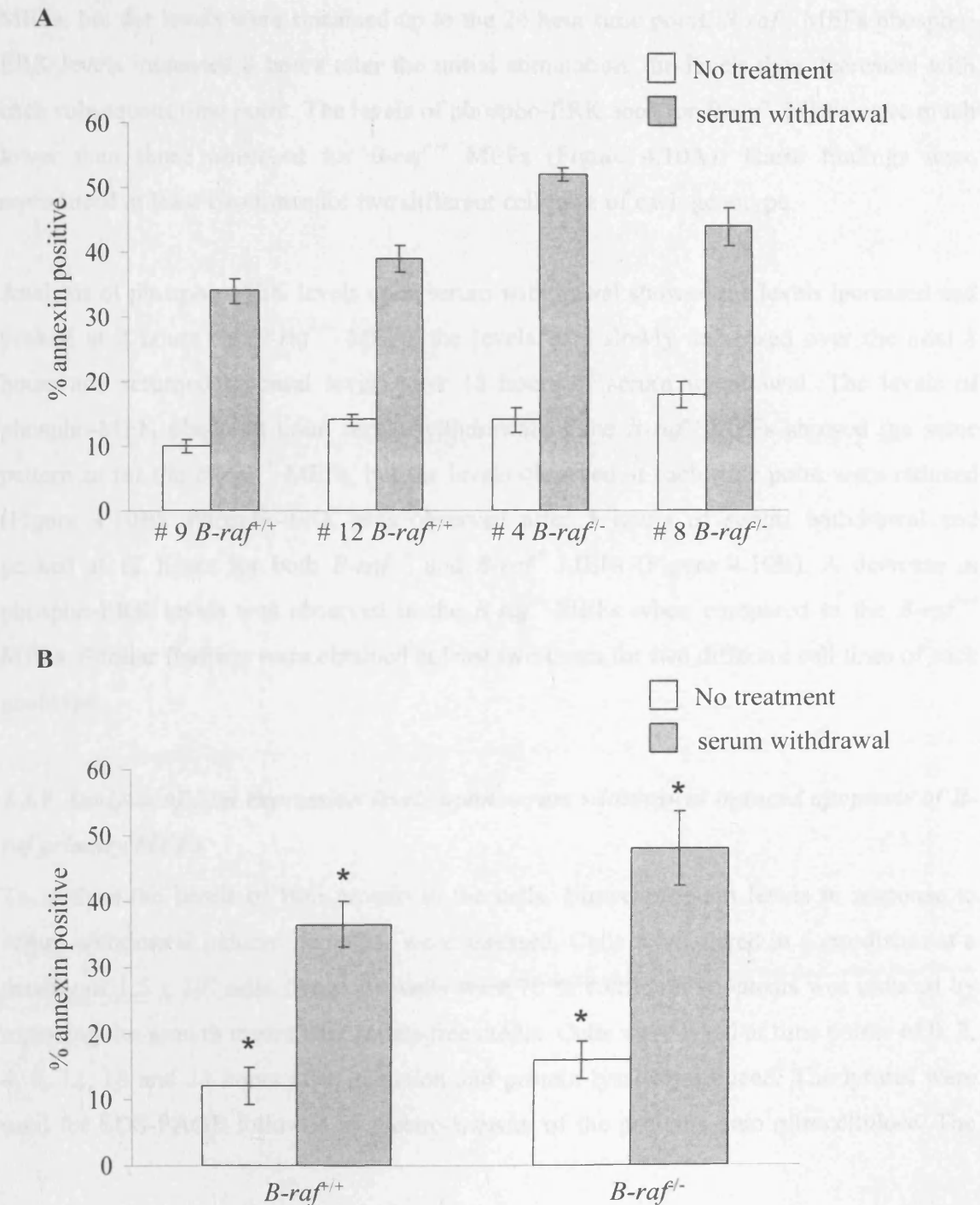
#### **4.3.7 Analysis of the apoptotic phenotype of *B-raf*<sup>-/-</sup> and *B-raf*<sup>+/+</sup> MEFs upon serum withdrawal**

The apoptotic phenotype of the *B-raf*<sup>-/-</sup> MEFs upon serum withdrawal was also investigated. MEFs were plated at a density of 1.5 x 10<sup>6</sup> cells onto 6 cm dishes and the media changed 24 hours after plating. After a further 24 hours, apoptosis was induced by placing cells into serum-free media for 20 hours. Cells were harvested and annexin V FITC staining and FACS analysis performed as described previously. The results showed that there was an increase in apoptosis for *B-raf*<sup>-/-</sup> MEFs when compared with *B-raf*<sup>+/+</sup> MEFs (Figure 4.9A). Pooled data for untreated MEFs showed *B-raf*<sup>+/+</sup> MEFs underwent 12 % ± 3 of apoptosis and this rose to 16 % ± 3 for *B-raf*<sup>-/-</sup> MEFs (n=8 *P*=0.0003; Figure 4.9B). Upon serum withdrawal the pooled percentage of apoptosis observed was 37 % ± 4 for *B-raf*<sup>+/+</sup> MEFs and this value increased to 48 % ± 6 for *B-raf*<sup>-/-</sup> MEFs (n=8; *P*=0.003; Figure 4.9B). The results show that B-Raf cells are more prone to apoptosis induced by serum withdrawal than via α-CD95 antibody, and that *B-raf*<sup>-/-</sup> MEFs show a greater susceptibility to both induced and spontaneous apoptosis than *B-raf*<sup>+/+</sup> MEFs.

#### **4.3.8 Analysis of MEK and ERK phosphorylation upon induction of apoptosis in *B-raf* primary MEFs**

As B-Raf is thought to play a role in apoptosis via the Raf/MEK/ERK pathway, MEK and ERK activation were measured by assessing levels of phospho-MEK and phospho-ERK in the *B-raf*<sup>+/+</sup> and *B-raf*<sup>-/-</sup> MEFs. Cells were seeded at 1.5 x 10<sup>6</sup> in 6 cm dishes. 24 hours later apoptosis was induced by the addition of 50 ng/ml α-CD95 antibody and 0.5 μM cycloheximide or by replacing the media with serum-free media. Cells were lysed at time points of 0, 2, 4, 8, 12, 18 and 24 hours after stimulation. Protein lysates were prepared and SDS-PAGE carried out followed by electro-transfer of the proteins onto nitrocellulose. The blots were incubated with an α-phospho-MEK antibody to detect levels of phospho-MEK in the *B-raf*<sup>+/+</sup> and *B-raf*<sup>-/-</sup> MEFs, and with an α-phospho-ERK antibody to observe

**Figure 4.9** Apoptotic analysis of *B-raf*<sup>f/+</sup> and *B-raf*<sup>f/-</sup> primary MEFs. MEFs were treated by the addition of serum-free media to induce apoptosis or left untreated. Apoptosis was evaluated using annexin V FITC staining followed by flow cytometric analysis. **(A)** Graph showing individual *B-raf*<sup>f/+</sup> and *B-raf*<sup>f/-</sup> cell lines. **(B)** Graph representing pooled data for *B-raf*<sup>f/+</sup> and *B-raf*<sup>f/-</sup> MEFs. (n=8). Standard error bars are shown. *P* values were generated for pooled *B-raf*<sup>f/-</sup> MEFs via a paired t-Test against pooled *B-raf*<sup>f/+</sup> MEFs for both treated and untreated cells. (\* = *P* ≤ 0.05).



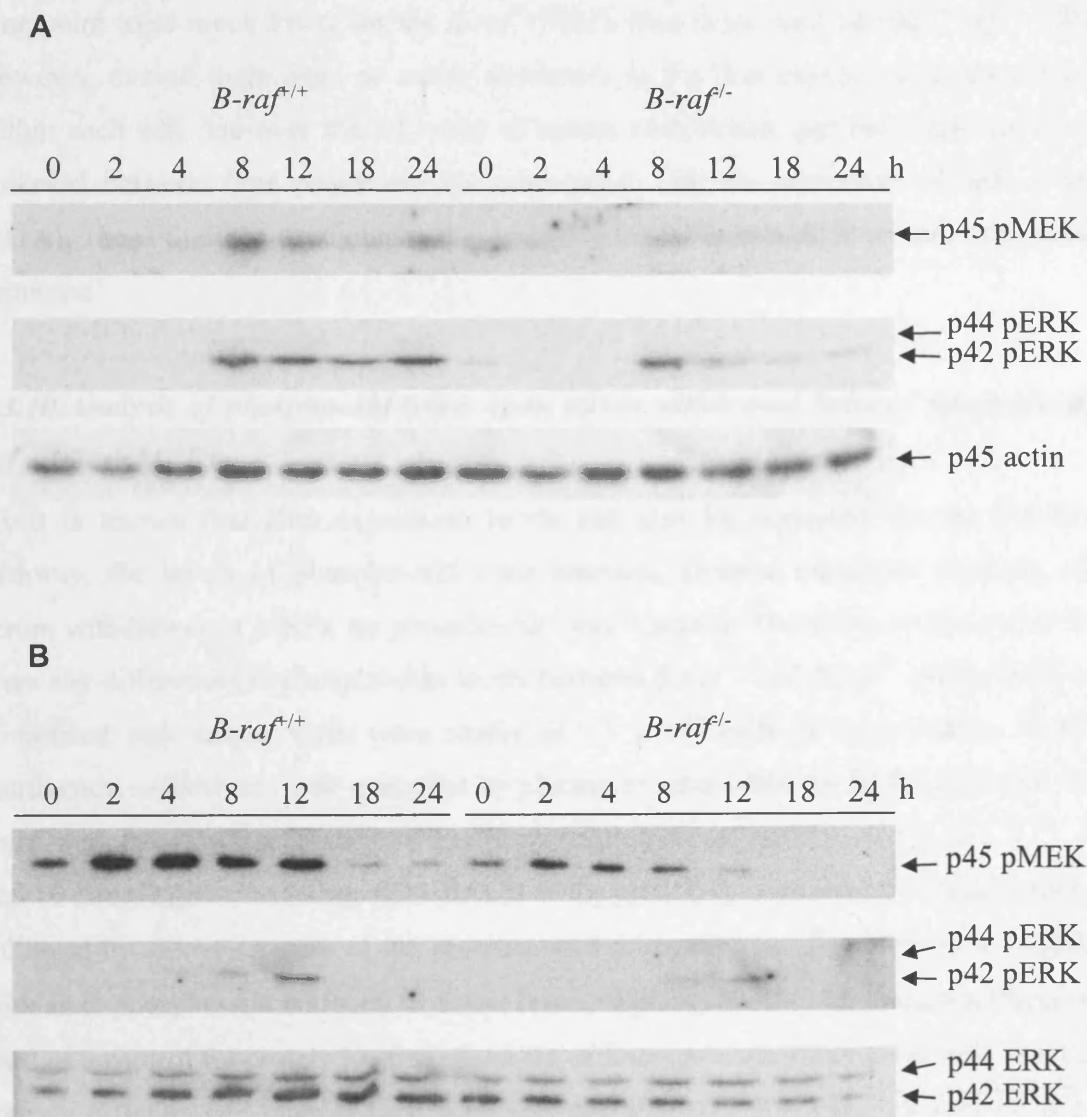
the levels of phospho-ERK. An  $\alpha$ -actin or  $\alpha$ -ERK1 antibody was used as a control for protein loading. Analysis of phospho-MEK levels upon treatment with  $\alpha$ -CD95 antibody showed phosphorylation levels rose after 8 hours of stimulation for *B-raf*<sup>+/+</sup> MEFs and were visible up to 24 hours after the initial treatment. Detection was markedly reduced for the *B-raf*<sup>-/-</sup> MEFs, as phospho-MEK was only barely detectable at the 8 hour time point (Figure 4.10A). The pattern for phospho-ERK was very similar. Levels of phospho-ERK were again initially detected after 8 hours of  $\alpha$ -CD95 antibody treatment for *B-raf*<sup>+/+</sup> MEFs, but the levels were sustained up to the 24 hour time point. *B-raf*<sup>-/-</sup> MEFs phospho-ERK levels increased 8 hours after the initial stimulation, the levels then decreased with each subsequent time point. The levels of phospho-ERK seen for *B-raf*<sup>-/-</sup> MEFs were much lower than those observed for *B-raf*<sup>+/+</sup> MEFs (Figure 4.10A). These findings were reproduced at least two times for two different cell lines of each genotype.

Analysis of phospho-MEK levels upon serum withdrawal showed the levels increased and peaked at 2 hours for *B-raf*<sup>+/+</sup> MEFs, the levels then slowly decreased over the next 8 hours and returned to basal levels after 18 hours of serum withdrawal. The levels of phospho-MEK observed upon serum withdrawal of the *B-raf*<sup>-/-</sup> MEFs showed the same pattern as for the *B-raf*<sup>+/+</sup> MEFs, but the levels observed at each time point were reduced (Figure 4.10B). Phospho-ERK was observed after 8 hours of serum withdrawal and peaked at 12 hours for both *B-raf*<sup>+/+</sup> and *B-raf*<sup>-/-</sup> MEFs (Figure 4.10B). A decrease in phospho-ERK levels was observed in the *B-raf*<sup>-/-</sup> MEFs when compared to the *B-raf*<sup>+/+</sup> MEFs. Similar findings were obtained at least two times for two different cell lines of each genotype.

#### ***4.3.9 Analysis of Bim expression levels upon serum withdrawal induced apoptosis of B-raf primary MEFs***

To analyse the levels of Bim protein in the cells, Bim expression levels in response to serum withdrawal induced apoptosis were assessed. Cells were plated in 6 cm dishes at a density of  $1.5 \times 10^6$  cells. When the cells were 70 % confluent apoptosis was induced by replacing the growth media with serum-free media. Cells were lysed at time points of 0, 2, 4, 8, 12, 18 and 24 hours after induction and protein lysates produced. The lysates were used for SDS-PAGE followed by electro-transfer of the proteins onto nitrocellulose. The

**Figure 4.10** MEK and ERK phosphorylation in *B-raf*<sup>+/+</sup> and *B-raf*<sup>-/-</sup> primary MEFs over a time course of induced apoptosis (0 to 24 hours). (A) Stimulation with 50 ng/ml  $\alpha$ -CD95 antibody plus 0.5  $\mu$ M cycloheximide. Protein lysates were analysed by Western blot analysis followed by detection of phospho-MEK (upper panel), phospho-ERK (middle panel) and actin as a control for protein loading (lower panel). (B) Serum withdrawal. Protein lysates were analysed by Western blot analysis followed by detection of phospho-MEK (upper panel), phospho-ERK (middle panel) and ERK1 as a control for protein loading (lower panel)

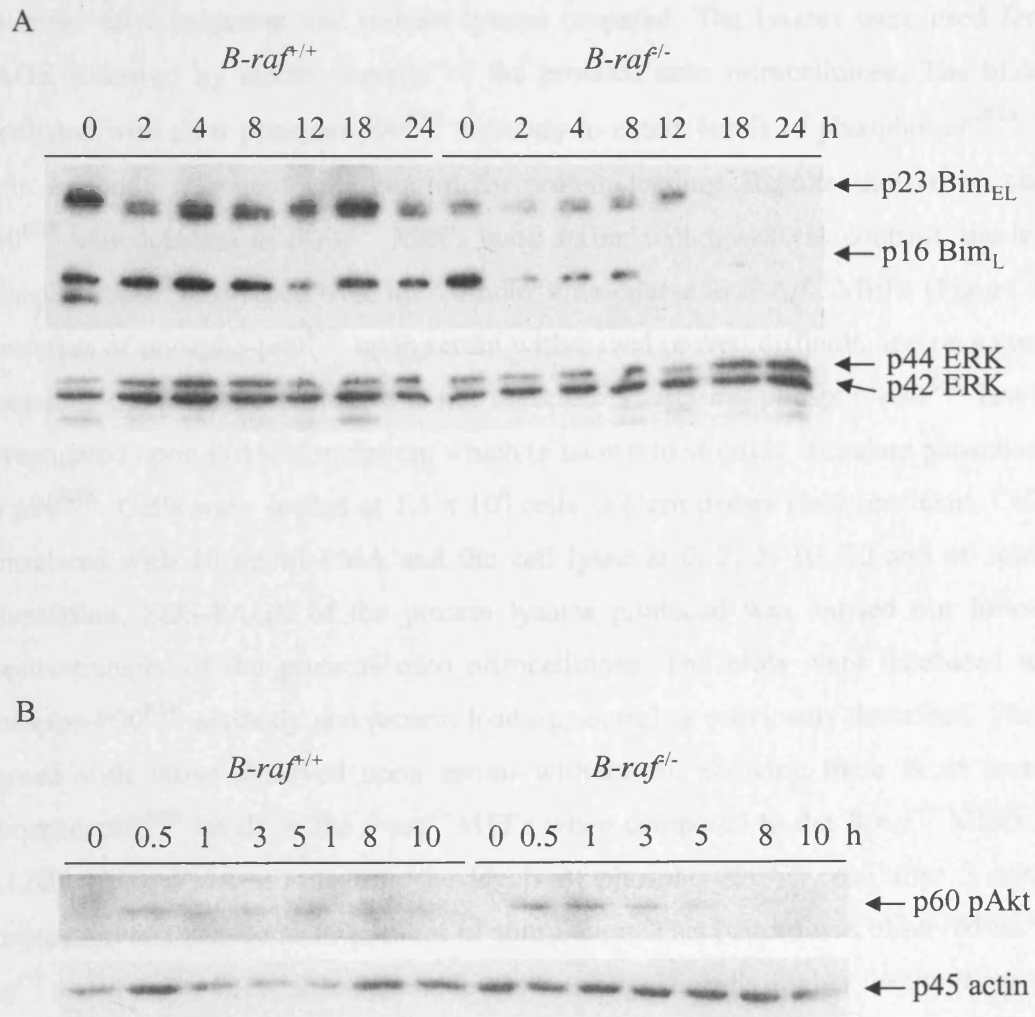


blots were incubated with an  $\alpha$ -Bim antibody that detects two Bim isotypes, Bim<sub>EL</sub> and Bim<sub>L</sub>. An  $\alpha$ -ERK1 antibody was used as a control for protein loading. The results showed that Bim levels altered slightly upon serum withdrawal and peaked at 18 hours after serum withdrawal for *B-raf*<sup>+/+</sup> MEFs (Figure 4.11A). There was a decrease in the expression levels of Bim observed for *B-raf*<sup>-/-</sup> MEFs in comparison to the *B-raf*<sup>+/+</sup> MEFs. The levels decreased upon initial serum withdrawal and then increased slightly between 2 and 12 hours of serum withdrawal induced apoptosis. Very little Bim protein was detected at the 18 or 24 hour time points (Figure 4.11A). The overall expression levels of Bim at each time point were much lower for the *B-raf*<sup>-/-</sup> MEFs than those seen for the *B-raf*<sup>+/+</sup> MEFs. However, overall there were no major alterations in the Bim expression levels observed within each cell line over the 24 hours of serum withdrawal, and the slight differences observed between time points did not correspond with the activation of ERK (Figure 4.11A). These findings were obtained at least two times for two different cell lines of each genotype.

#### ***4.3.10 Analysis of phospho-Akt levels upon serum withdrawal induced apoptosis of B-raf primary MEFs***

As it is known that Bim expression levels can also be regulated via the PI3-K/Akt pathway, the levels of phospho-Akt were assessed. Despite numerous attempts, upon serum withdrawal of MEFs, no phospho-Akt was detected. Therefore, to observe if there were any differences in phospho-Akt levels between *B-raf*<sup>+/+</sup> and *B-raf*<sup>-/-</sup> MEFs, cells were stimulated with serum. Cells were seeded at  $1.5 \times 10^6$  cells in 6 cm dishes. At 60 % confluency, cells were made quiescent by placing in serum-free media for 24 hours. Cells were stimulated by the addition of media containing serum and lysed at 0, 0.5, 1, 3, 5, 8 and 10 hours after stimulating. SDS-PAGE of the protein lysates produced was carried out followed by electro-transfer of the proteins onto nitrocellulose. The blots were incubated with an  $\alpha$ -phospho-Akt antibody to detect levels of phospho-Akt. An  $\alpha$ -actin antibody was used as a control for protein loading. Each set of findings were observed at least two times for two different cell lines of each genotype. phospho-Akt levels were higher for *B-raf*<sup>-/-</sup> MEFs compared to *B-raf*<sup>+/+</sup> MEFs at 0.5 hours after stimulation (Figure 4.11B). However, it was unclear as to if levels were elevated at other time points. Subsequent analysis of phospho-Akt levels upon EGF stimulation also proved inconclusive (data not shown).

**Figure 4.11** Protein expression levels in *B-raf<sup>+/+</sup>* and *B-raf<sup>-/-</sup>* primary MEFs. (A) Apoptosis was induced over a time course of serum withdrawal (0 to 24 hours). Protein lysates were analysed by Western blot analysis followed by detection of Bim (upper panel) and ERK1 as a control for protein loading (lower panel). (B) Cells were stimulated by addition of 10 % serum (0 to 10 hours) and protein lysates subjected to Western Blotting, followed by the detection of phospho-Akt (upper panel) and actin as a control for protein loading (lower panel)



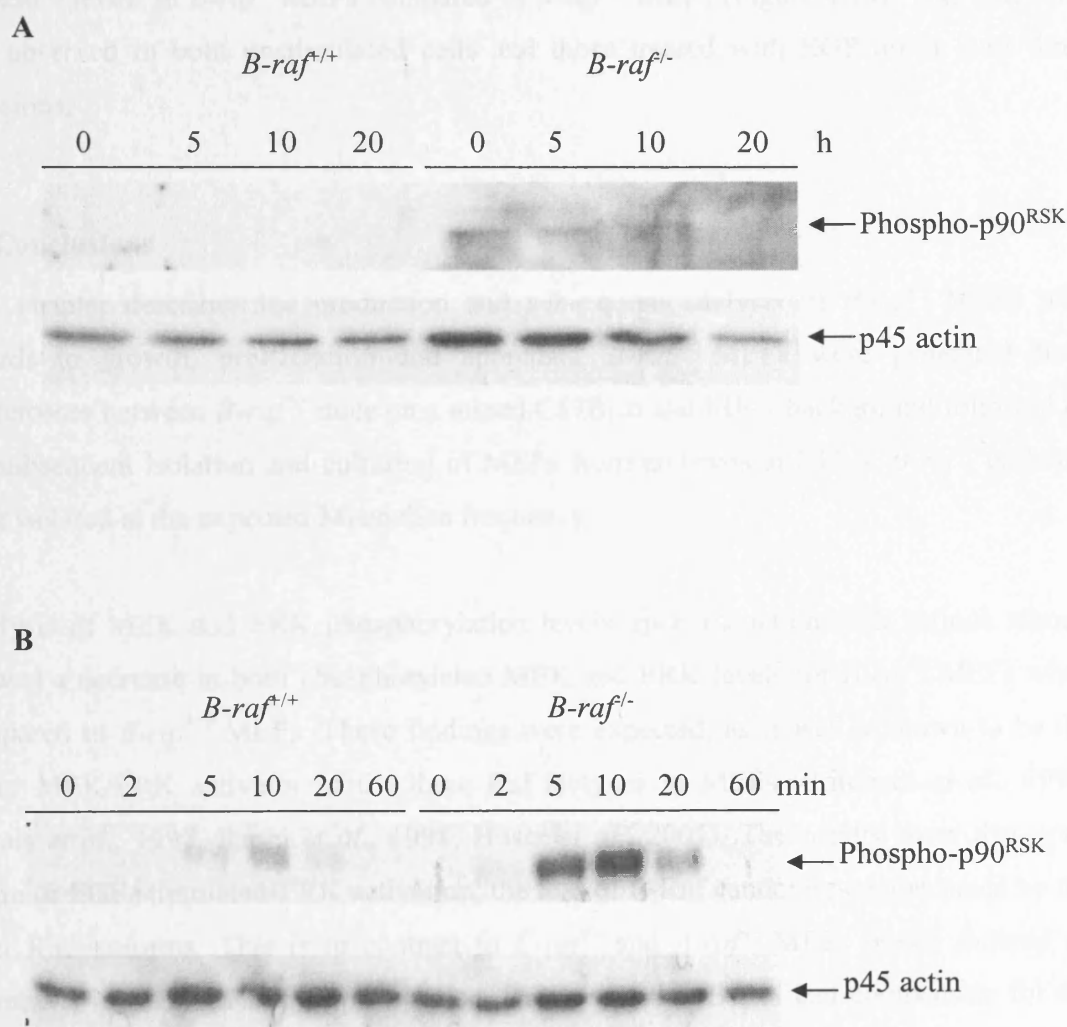
#### **4.3.11 Analysis of phospho-p90<sup>RSK</sup> levels upon serum withdrawal induced apoptosis of *B-raf* primary MEFs**

Inhibition of p90<sup>RSK</sup> was analysed by assessing the levels of phospho-p90<sup>RSK</sup> upon serum withdrawal induced apoptosis. Cells were plated in 6 cm dishes at a density of  $1.5 \times 10^6$  cells. Apoptosis was induced 24 hours after seeding by replacing the growth media with serum-free media. Cells were lysed in a suitable lysis buffer at time points of 0, 5, 10, and 20 hours after induction and protein lysates prepared. The lysates were used for SDS-PAGE followed by electro-transfer of the proteins onto nitrocellulose. The blots were incubated with an  $\alpha$ -phospho-p90<sup>RSK</sup> antibody to detect levels of phospho-p90<sup>RSK</sup>. An  $\alpha$ -actin antibody was used as a control for protein loading. Results showed no phospho-p90<sup>RSK</sup> was detected in *B-raf*<sup>+/+</sup> MEFs upon serum withdrawal. In contrast, the levels of phospho-p90<sup>RSK</sup> increased over the 20 hour time course in *B-raf*<sup>-/-</sup> MEFs (Figure 4.12A). Detection of phospho-p90<sup>RSK</sup> upon serum withdrawal proved difficult, and on a number of occasions the phospho-protein was not detected. Therefore, phospho-p90<sup>RSK</sup> levels were investigated upon PMA stimulation, which is known to strongly stimulate phosphorylation of p90<sup>RSK</sup>. Cells were seeded at  $1.5 \times 10^6$  cells in 6 cm dishes until confluent. Cells were stimulated with 10 ng/ml PMA and the cell lysed at 0, 2, 5, 10, 30 and 60 minutes of stimulation. SDS-PAGE of the protein lysates produced was carried out followed by electro-transfer of the proteins onto nitrocellulose. The blots were incubated with the phospho-P90<sup>RSK</sup> antibody and protein loading control as previously described. The results agreed with those observed upon serum withdrawal, showing there is an increase in phospho-p90<sup>RSK</sup> levels in the *B-raf*<sup>-/-</sup> MEFs when compared to the *B-raf*<sup>+/+</sup> MEFs (Figure 4.12B). Upon PMA stimulation, the levels of phospho-P90<sup>RSK</sup> rose after 5 minutes of stimulation and peaked at 10 minutes of stimulation. This pattern was observed for both *B-raf*<sup>+/+</sup> and *B-raf*<sup>-/-</sup> MEFs, although the levels were significantly higher for the *B-raf*<sup>-/-</sup> MEFs. Similar findings were observed a minimum of two times for two different cell lines of each genotype.

#### **4.3.12 Analysis of T125-phospho-specific caspase 9 levels upon serum withdrawal induced apoptosis of *B-raf* primary MEFs**

As none of the previously identified pathways appeared to account for the increase in apoptosis observed for the *B-raf*<sup>-/-</sup> MEFs, the role B-Raf plays in apoptosis via ERK phosphorylation of caspase 9 at threonine residue 125 was investigated. This was assessed

**Figure 4.12** Phospho-p90<sup>RSK</sup> levels in *B-raf*<sup>+/+</sup> and *B-raf*<sup>-/-</sup> primary MEFs over a time course of induction. **(A)** MEFs were induced to undergo apoptosis by serum withdrawal (0 to 20 hours). Protein lysates were analysed by Western blot analysis followed by detection of phospho-p90<sup>RSK</sup> (upper panel) and actin as a control for protein loading (lower panel). **(B)** MEFs were stimulated with phorbol 12-myristate 13-acetate (0 to 60 min). Protein lysates were analysed by Western blot analysis followed by detection of phospho-p90<sup>RSK</sup> (upper panel) and actin as a control for protein loading (lower panel).



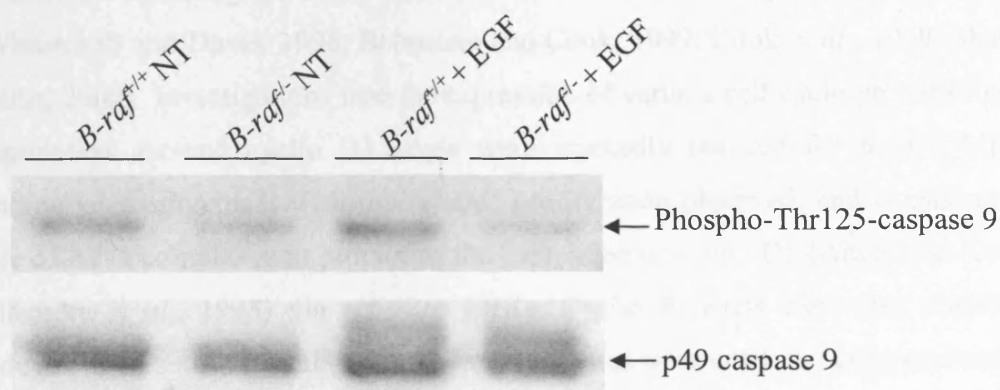
by performing an immuno-precipitation assay. Cells were grown in 10 cm plates until fully confluent and apoptosis was induced by placing in serum-free media for 48 hours. Cells were then left untreated or treated with 25 ng/ml EGF for 5 min. The cells were lysed and an immuno-precipitation assay performed using 1 mg of protein per sample and an  $\alpha$ -caspase 9 antibody. SDS-PAGE of the protein lysates produced was carried out followed by electro-transfer of the proteins onto nitrocellulose. The blots were incubated with an  $\alpha$ -T125-phospho-specific caspase 9 antibody. An  $\alpha$ -total caspase 9 antibody was used as a control for protein loading. The results showed a decrease in  $\alpha$ -T125-phospho-specific caspase 9 levels in *B-raf*<sup>-/-</sup> MEFs compared to *B-raf*<sup>+/+</sup> MEFs (Figure 4.13). This reduction was observed in both unstimulated cells and those treated with EGF on at least three occasions.

#### 4.4 Conclusions

This chapter describes the production and subsequent analysis of *B-raf*<sup>-/-</sup> MEFs with regards to growth, proliferation and apoptosis. *B-raf*<sup>-/-</sup> MEFs were generated from intercrosses between *B-raf*<sup>+/-</sup> mice on a mixed C57BL6 and MF-1 background followed by the subsequent isolation and culturing of MEFs from embryos at E12.5. *B-raf*<sup>-/-</sup> embryos were isolated at the expected Mendelian frequency.

Analysis of MEK and ERK phosphorylation levels upon induction with various stimuli showed a decrease in both phosphorylated MEK and ERK levels for *B-raf*<sup>-/-</sup> MEFs when compared to *B-raf*<sup>+/+</sup> MEFs. These findings were expected, as B-Raf is known to be the major MEK/ERK activator of the three Raf isotypes in MEFs (Pritchard *et al.*, 1995; Marais *et al.*, 1997; Papin *et al.*, 1998; Hüser *et al.*, 2001). The results show that upon serum or EGF stimulated-ERK activation, the loss of B-Raf cannot be compensated by the other Raf isoforms. This is in contrast to *C-raf*<sup>-/-</sup> and *A-raf*<sup>-/-</sup> MEFs which showed no alterations in MEK/ERK phosphorylation, suggesting that B-Raf can compensate for the effect that these other Raf isotypes have on controlling MEK/ERK activation (Hüser *et al.*, 2001; Mercer *et al.*, 2002). These results also suggest B-Raf is not a key activator in response to PMA, as phospho-ERK levels were not significantly reduced upon PMA stimulation of *B-raf*<sup>-/-</sup> MEFs.

**Figure 4.13** Phospho-Thr125-specific caspase 9 levels in *B-raf*<sup>+/+</sup> and *B-raf*<sup>-/-</sup> primary MEFs. MEFs were left untreated (NT) or stimulated by the addition of 25 ng/ml epidermal growth factor (EGF) for 5 min. Immunoprecipitated protein lysates were analysed by Western blot analysis followed by detection of phospho-Thr125-specific caspase 9 (upper panel) and total caspase 9 as a control for protein loading (lower panel).



Cells p49<sup>+</sup> and p27<sup>+</sup> levels were observed to be similar in *B-raf*<sup>+/+</sup> and *B-raf*<sup>-/-</sup> MEFs. This suggests that the role of B-raf in inhibiting the G1 to S phase by regulating cyclin D levels (Petrova et al., 1994; Harper et al., 1995; Lee et al., 1995). Figure 4.13 shows B-raf plays a role in suppressing apoptosis. Apoptosis is not inhibited in *B-raf*<sup>-/-</sup> MEFs at a concentration and time that is sufficient to increase levels of p49<sup>+</sup> and p27<sup>+</sup> in *B-raf*<sup>+/+</sup> MEFs.

Analysis of the apoptotic phenotype of the *B-raf*<sup>-/-</sup> MEFs revealed an increased susceptibility to apoptosis upon treatment with staurosporine. A three fold increase in the number of cells undergoing apoptosis was observed in *B-raf*<sup>-/-</sup> MEFs compared with *B-raf*<sup>+/+</sup> MEFs. This phenotype was partially rescued by treatment of *B-raf*<sup>-/-</sup> MEFs with a constitutively active form of *B-raf*, *B-raf*<sup>V600E</sup>. They also may partly account for the increased number of *B-raf*<sup>-/-</sup> MEFs at the end of the reduction in the number of cells surviving upon treatment with EGF. Cell cycle data shows B-raf plays a role in suppressing apoptosis. In *B-raf*<sup>-/-</sup> MEFs, apoptosis was not accompanied by a reduction in p49<sup>+</sup> and p27<sup>+</sup> levels. Western blot analysis showed reduced phospho-ERK and phospho-FAK, but not a reduction in total ERK suggesting that the role of B-raf in suppressing apoptosis may be mediated by the

Comparison of the growth profiles of the *B-raf*<sup>+/+</sup> and *B-raf*<sup>-/-</sup> MEFs showed that *B-raf*<sup>-/-</sup> MEFs grew much slower. As the balance between proliferation and apoptosis affects the rate of growth, both processes were investigated in *B-raf*<sup>-/-</sup> MEFs.

Investigations into the proliferation of *B-raf*<sup>-/-</sup> MEFs showed a significant reduction in the ability of *B-raf*<sup>-/-</sup> MEFs to undergo DNA synthesis. This finding is consistent with the role of ERK in regulating the G1 to S phase of the cell cycle via regulation of AP-1 complexes (Whitmarsh and Davis, 1996; Balmano and Cook, 1999; Cook *et al.*, 1999; Shaulian and Karin, 2002). Investigations into the expression of various cell cycle proteins upon serum stimulation showed cyclin D1 levels were markedly reduced for *B-raf*<sup>-/-</sup> MEFs. This finding is in agreement with the reduced proliferation observed, and consistent with the role of AP-1 complexes in promoting the expression of cyclin D1 (Angel and Karin, 1991; Albanese *et al.*, 1995) via activated ERKs. Cyclin E levels were also observed to be reduced upon serum stimulation of *B-raf*<sup>-/-</sup> MEFs, as were cdk4 and cdk6 expression levels. Both p21<sup>CIP1</sup> and p27<sup>KIP1</sup> levels were observed to be elevated up to one hour after serum stimulation of *B-raf*<sup>-/-</sup> MEFs. This agrees with the role of these CIP/KIP family members in inhibiting the G1 to S phase by targeting cyclin D-cdk4/6 and cyclin E-cdk2 complexes (Polylak *et al.*, 1994; Harper *et al.*, 1995; Lee *et al.*, 1995; Woods *et al.*, 1997). Overall the data shows B-Raf plays a role in cell growth and proliferation. In its absence, growth and proliferation occur at a slower rate and this is associated with reduced ERK activity, leading to reduced expression levels of cyclin D, cyclin E and cdk proteins, and elevated levels of p21<sup>CIP1</sup> and p27<sup>KIP1</sup>.

Analysis of the apoptotic phenotype of the *B-raf*<sup>-/-</sup> MEFs showed an increased susceptibility to apoptosis upon  $\alpha$ -CD95 antibody treatment or serum withdrawal. A more significant level of apoptosis was observed upon serum withdrawal. These findings are consistent with those observed by Wojnowski *et al.* (1997) that showed increased apoptosis of *B-raf*<sup>-/-</sup> embryos. They also may partly account for the reduced growth of the *B-raf*<sup>-/-</sup> MEFs, as well as the reduction in the number of cells passing from G1 to S phase of the cell cycle. Thus, B-Raf plays a role in suppressing apoptosis and increasing survival that is not compensated by C-Raf or A-Raf. Observation of MEK and ERK phosphorylation showed reduced phospho-MEK and phospho-ERK levels upon induction of apoptosis suggesting that the role of B-Raf in suppressing apoptosis may be mediated by the

MEK/ERK pathways. This is clearly different from the role of C-Raf in suppressing  $\alpha$ -CD95-induced apoptosis which is clearly independent of MEK/ERK (Chapter 3).

To further characterise the role of B-Raf in apoptosis upon serum withdrawal, a number of pathways known to be regulated by the ERKs were assessed. Analysis of the pro-apoptotic protein Bim showed expression levels were reduced for *B-raf*<sup>-/-</sup> MEFs when compared to *B-raf*<sup>+/+</sup> MEFs. This indicates Bim may not be responsible for the increased apoptosis observed, as B-Raf does not appear to repress Bim levels. These findings conflict with previous data in CC139 fibroblasts showing that ERK-regulated suppression of Bim levels may be an important mediator of survival during serum withdrawal. The reduced levels of Bim observed may have occurred due to an increase in the phospho-Akt levels in these cells, as Bim expression levels are also regulated via the PI3-K/Akt pathway (Kops *et al.*, 1999; Rena *et al.*, 1999; Dijkers *et al.*, 2000). Elevated phospho-Akt levels were observed for *B-raf*<sup>-/-</sup> MEFs 30 minutes after serum stimulation, but were undetectable upon serum withdrawal. Therefore, more analysis is required to confirm that the reduced Bim expression levels observed are due to increased phospho-Akt levels.

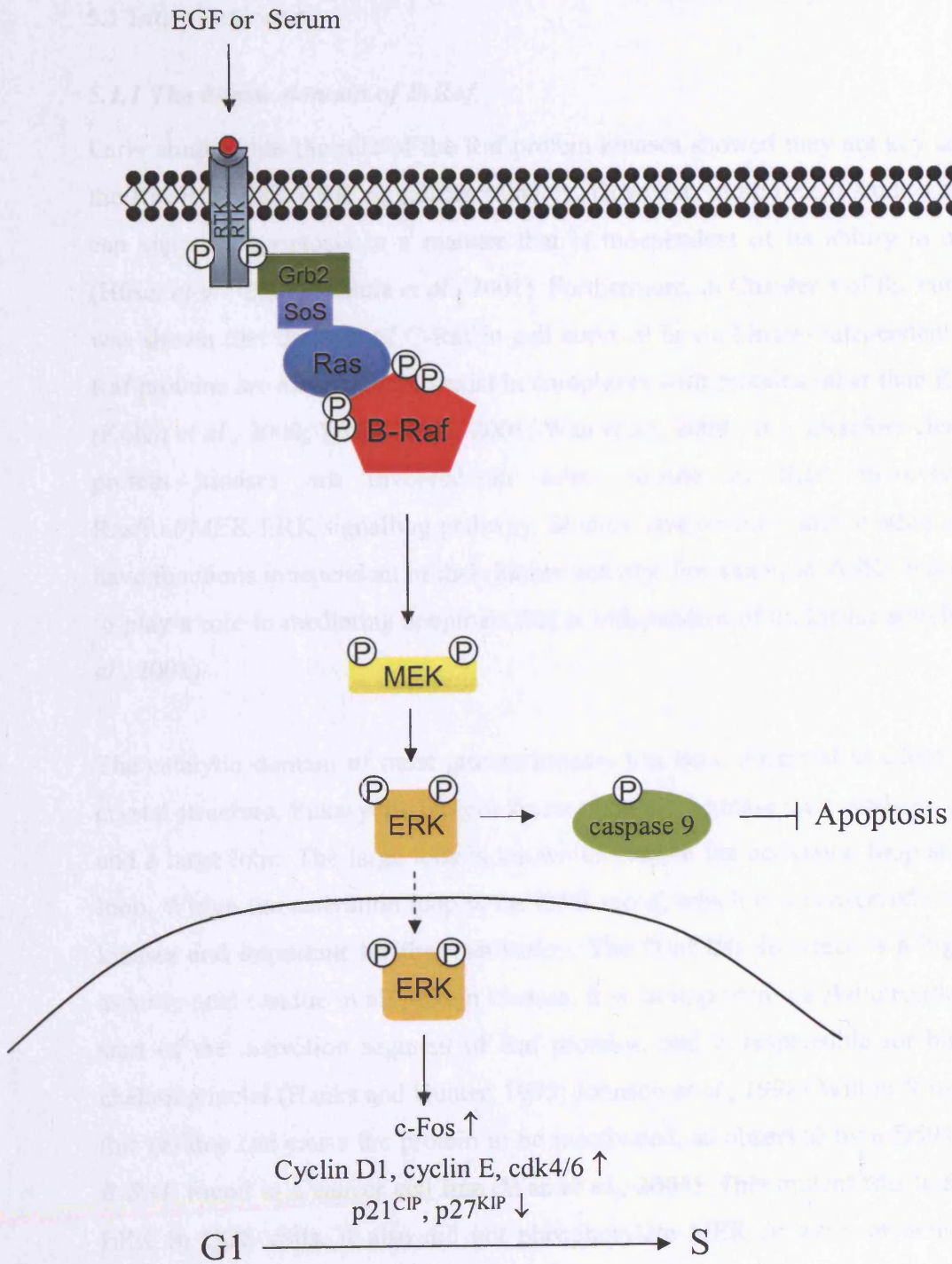
ERKs are also known to phosphorylate and activate the p90<sup>RSK</sup> proteins that promote cell survival (Sturgill *et al.*, 1988). However, phospho-p90<sup>RSK</sup> levels were found to be increased for *B-raf*<sup>-/-</sup> MEFs upon serum withdrawal and also when stimulated with PMA. Therefore p90<sup>RSK</sup> does not appear to be responsible for the increased susceptibility to apoptosis of the *B-raf*<sup>-/-</sup> MEFs. It is unclear as to the role of the elevated phospho-p90<sup>RSK</sup> levels observed for the *B-raf*<sup>-/-</sup> MEFs.

Analysis of phospho-Thr125-caspase 9 levels showed a decrease in the levels observed for *B-raf*<sup>-/-</sup> MEFs when compared to *B-raf*<sup>+/+</sup> MEFs. This was seen in untreated cells as well as those stimulated with EGF. Caspase 9 has been reported to be phosphorylated by ERKs on residue Thr125, thereby preventing caspase 9 processing and caspase 3 activation (Allen *et al.*, 2003). The current findings are consistent with these data. The results show that the increase in apoptosis observed for *B-raf*<sup>-/-</sup> MEFs is associated with a reduction in the phosphorylation of Thr125 of caspase 9, which in turn is likely to be occurring due to reduced ERK activity. Thus it would be interesting to assess whether this in turn leads to increased levels of processed caspase 9 in *B-raf*<sup>-/-</sup> MEFs, and subsequent cleavage of the effector pro-caspases 3 and 7, thereby leading to increased apoptosis. Due to time

limitations, efforts to rescue the increased susceptibility to apoptosis of the *B-raf*<sup>-/-</sup> MEFs were not concluded. Future investigations are required to confirm that rescuing the apoptotic phenotype restores phospho-Thr125-caspase 9 levels to those observed for *B-raf*<sup>+/+</sup> MEFs.

A summary of the findings of this Chapter are shown in Figure 4.14. The data show that, B-Raf, through the regulation of ERK, has multiple roles in the cell including regulation of proliferation, survival and also motility (Pritchard *et al.*, 2004). The *B-raf*<sup>-/-</sup> MEFs generated will be useful in further characterising these functions. This will be of increased importance given that B-Raf is an oncogene in numerous human cancers (Davies *et al.*, 2002).

**Figure 4.14** Summary of the findings of Chapter 4. Roles for B-Raf in proliferation and apoptosis.



## 5. GENERATION OF A CONDITIONAL B-RAF KINASE INACTIVE MOUSE

### 5.1 Introduction

#### 5.1.1 The kinase domain of B-Raf

Early studies into the role of the Raf protein kinases showed they are key components of the Ras/Raf/MEK/ERK signalling pathway. However, more recent studies showed C-Raf can suppress apoptosis in a manner that is independent of its ability to activate MEK (Hüser *et al.*, 2001; Mikula *et al.*, 2001). Furthermore, in Chapter 3 of the current project it was shown that the role of C-Raf in cell survival is via kinase-independent mechanisms. Raf proteins are also known to exist in complexes with proteins other than RAS and MEK (Kolch *et al.*, 2000; Weber *et al.*, 2001; Wan *et al.*, 2004). It is therefore clear that the Raf protein kinases are involved in roles outside of their involvement in the Ras/Raf/MEK/ERK signalling pathway. Studies have recently shown other protein kinases have functions independent of their kinase activity. For example, ASK1 has been observed to play a role in mediating apoptosis that is independent of its kinase activity (Charette *et al.*, 2001).

The catalytic domain of most protein kinases has been observed to adopt a similar core crystal structure. Eukaryotic protein kinases contain a kinase core made up of a small lobe and a large lobe. The large lobe is known to contain the activation loop and the catalytic loop. Within the activation loop is the DFG motif, which is a conserved region in protein kinases and important for their activation. The D of this sequence is a highly conserved aspartic acid residue in all protein kinases. It is an important catalytic residue found at the start of the activation segment of Raf proteins, and is responsible for binding an ATP chelating metal (Hanks and Hunter, 1995; Johnson *et al.*, 1998) Within *B-raf*, mutations of this residue can cause the protein to be inactivated, as observed by a D594V mutation of *B-RAF* found in a cancer cell line (Wan *et al.*, 2004). This mutant was unable to activate ERK in COS cells. It also did not phosphorylate MEK *in vitro*, or activate *C-RAF* or NF- $\kappa$ B (Ikenoue *et al.*, 2003; Wan *et al.*, 2004). Mutations at other residues of *B-RAF* in cancer cells were shown to lead to elevated ERK levels (Wan *et al.*, 2004). It is therefore unclear as to how this mutation is involved in the progression to malignancy.

### 5.1.2 *Cre/loxP* technology

Embryonic stem (ES) cell mediated gene targeting can be used to create mutations in a gene of interest. Conventionally, null mutations have been created by deleting part of the gene of interest and replacing it with an antibiotic resistance gene. This can be very useful, but is also limiting in the amount of information it can provide. The null mutation is constitutively expressed which may lead to compensatory effects and therefore the true phenotype may not be observed. Also, due to the mutation being present in the germline, if it results in an early lethal phenotype, later phenotypes can not be assessed. This problem can be overcome by combining transgenic technologies with the *Cre/loxP* site-specific recombination system. This allows the introduction of conditional genome alterations that are spatially and temporally restricted. Therefore the alteration can be expressed at later phenotypes, adult animals can be assessed, and the alteration can be restricted to one tissue or cell type, allowing more specific studies to take place. It also allows the phenotype to be assessed without the problems of adaptation.

Conventional *B-raf* null mutants die at mid-gestation, therefore only allowing analysis of MEFs and early embryonic phenotypes (Wojnowski *et al.*, 1997). As the mice being generated in the present project were thought likely to also be embryonically lethal, using the *Cre/loxP* site-specific recombination system would allow generation of mice that could be used for many further studies and permit the characterisation of later phenotypes.

Cre recombinase is a 38 KDa product of the *cre* (cyclization recombination) gene of bacteriophage P1. It recognises and mediates site-specific recombination between 34 bp *loxP* sequences. A *loxP* sequence consists of two 13 bp inverted repeats and an 8 bp non-palindromic spacer sequence. (Figure 5.1) If two *loxP* sites are placed in the same orientation on linear DNA, Cre will excise the region in between the *loxP* sequences, known as the floxed sequence. This will leave one *loxP* site on the linear DNA (Figure 5.2). Thus, incorporation of two such *loxP* sequences into a genomic locus, followed by treatment with Cre recombinase, will lead to the deletion of the intervening DNA sequence (Hoess *et al.*, 1982; Hoess and Abremski, 1984). Cre can be placed under the control of a range of promoters, thus allowing both spatial and temporal restriction of the Cre-mediated recombination event by the generation of Cre-mediated transgenic mice.



under the control of the *lck* proximal promoter ( $cre^{lck}$ ), leading to selective expression of Cre in T lineage cells. Assessment of homozygous  $pol\beta^{lox}$  mice harbouring  $cre^{lck}$  showed normal development. However, further investigation showed incomplete deletion of the  $pol\beta$  gene in the T cells. This may have occurred due to the *lck* proximal promoter only being transiently active during early T cell development and therefore there may not have been enough time for complete recombination (Gu *et al.*, 1994).

Another study utilised the homozygous  $pol\beta^{lox}$  mice to perform inducible inactivation of the  $pol\beta$  gene (Kühn *et al.*, 1995). Cre was placed under the control of the promoter of the *Mx1* gene. This gene is part of the defence to viral infections and is silent in healthy mice. Upon administration of interferon ( $\alpha$  or  $\beta$ ) the *Mx1* promoter is activated, leading to high transcription levels. Thus, by crossing  $pol\beta^{lox}$  mice with mice expressing Cre under the control of the *Mx1* promoter, mice were generated that were susceptible to excision of the floxed gene upon administering of interferon- $\alpha$ . The resulting offspring were analysed and it was found that excision of the floxed region of the gene had occurred in all organs. However, Southern blot analysis showed complete deletion had not occurred in all tissues. This may have been due to the inability of interferon- $\alpha$  to access certain organs, due to interferon- $\alpha$  leading to different cell responses or due to the difference in cell proliferation rates affecting the Cre-mediated recombination (Kühn *et al.*, 1995).

Cre has been engineered to be part of a ligand-activated fusion protein (Feil *et al.*, 1996). Cre recombinase was fused to a mutant ligand-binding domain of the human estrogen receptor (ER), and used to generate Cre-ER mice in which the fusion protein was placed under the control of a cytomegalovirus (CMV) promoter. These mice were crossed to mice harbouring a floxed target allele to allow excision of the floxed sequence. The gene that was floxed was a modified retinoid X receptor  $\alpha$  (RXR $\alpha$ ) allele carrying a floxed neomycin resistance gene integrated by homologous recombination. Addition of 4-hydroxytamoxifen to offspring led to Cre-mediated excision of the floxed target gene in all organs except the thymus. Subsequent PCR analysis indicated the degree of excision. 40-50 % excision was observed in skin, tail, kidney and spleen, with lesser amounts occurring in other tissues. The differences observed between tissues may have occurred due to the variation in expression of the CMV driven transgene between tissues, alterations

in 4-hydroxytamoxifen accessibility between tissues, or the difference in cell proliferation rates affecting the Cre-mediated recombination (Feil *et al.*, 1996).

Another study generated Cre transgenic mice harbouring several copies of the *Cre* gene under the control of the human CMV minimal promoter (Schwenk *et al.*, 1995). Upon crossing these mice with *polβ<sup>flox</sup>* mice, Southern blot analysis indicated homozygous offspring had undergone excision of the floxed target gene in all cells including germ cells. This showed Cre is ubiquitously expressed in all cell lines early in embryogenesis (Schwenk *et al.*, 1995). This deleter strain has subsequently been a useful tool for knocking out genes in the germline.

The numerous studies described indicate that excision of a floxed target gene can occur upon Cre-mediated excision. This can be engineered in such a way that it leads to ubiquitous deletion of a gene, or can be more restricted to occur in a specific cell type or at a particular point in development.

The Cre/*loxP* recombination system has also been used to investigate diseases involving chromosomal rearrangements via the generating of chromosomal translocations (Smith *et al.*, 1995; Van Deursen *et al.*, 1995). The Cre/*loxP* technology can also be used to generate conditional knockins, such as that described for oncogenic *K-Ras* (Jackson *et al.*, 2001; Meuwissen *et al.*, 2001).

## 5.2 Aims

To date there have been no reports in the literature of the production of *B-raf* kinase inactive mice or MEFs. It would be of great interest to discover the precise role that the *B-Raf* kinase activity plays in cellular processes, and if any kinase-independent mechanisms exist. Therefore, the initial aim of this chapter was to generate a floxed *B-raf* allele using the Cre/*loxP* site-specific recombination system. Homologous recombination in ES cells would allow the generation of the targeted allele, which would be used to generate *B-raf* kinase inactive conditional mice. The floxed allele would contain a site-specific mutation of B-Raf that would render it kinase inactive upon Cre-mediated excision of the floxed target gene at a later date.

### 5.3 Results

The generation of the *B-raf* kinase inactive conditional mice involved the initial construction of a targeting vector. This vector contained a left arm, a right arm and a central region between these arms, referred to as the middle arm. The left arm consisted of a 4 Kb fragment, containing exon 14 of the *B-raf* gene (Figure 5.3B). The middle arm contained one *loxP* site and a region named the minigene. This was made up of exons 15-18 of the wild type *B-raf* gene flanked by a strong splice acceptor and a poly-adenylation site to aid the strategy being used (Figure 5.3B). These two arms of the targeting vector were supplied by C. Pritchard. The remaining arm, the right arm, comprised a *neo*<sup>R</sup> gene flanked by two *loxP* sites, and a 5-Kb genomic DNA fragment containing exons 15 of *B-raf* (Figure 5.3B). Exon 15 within this arm contained a site-specific mutation of B-Raf, thought to render it kinase inactive. The mutation was of aspartic acid 594 to alanine (D594A). As previously stated this residue is important for kinase activity and mutating it has been shown to lead to no kinase activity (Wan *et al.*, 2004). The D594A site specific mutation had previously been carried out and a vector containing the mutation was provided by C. Pritchard. The construction of the right arm, and the subsequent construction of the final targeting vector incorporating the three arms, is part of the current chapter. Using Cre-mediated excision would allow removal of the *neo*<sup>R</sup> gene and the minigene containing wild type *B-raf* exons 15-18. This would then allow read-through to the mutated exon 15 and allow expression of D594A.

#### 5.3.1 Construction of the right arm of the targeting vector

The D594A mutation had been previously obtained by site directed mutagenesis of a 0.5 Kb fragment of *B-raf* and cloned into the pSP72 plasmid to give pSP *B-raf* AFG (Figure 5.4A; provided by C. Pritchard). To facilitate a subsequent cloning step, an additional *Spe* I site was added to the 5' end of the 0.5 Kb D594A fragment of *B-raf* by PCR. This was performed by linearising the plasmid by *Xho* I digestion, followed by PCR with primers T7 and Ocp129. The resulting PCR product was analysed by agarose gel electrophoresis and by DNA sequencing (data not shown).

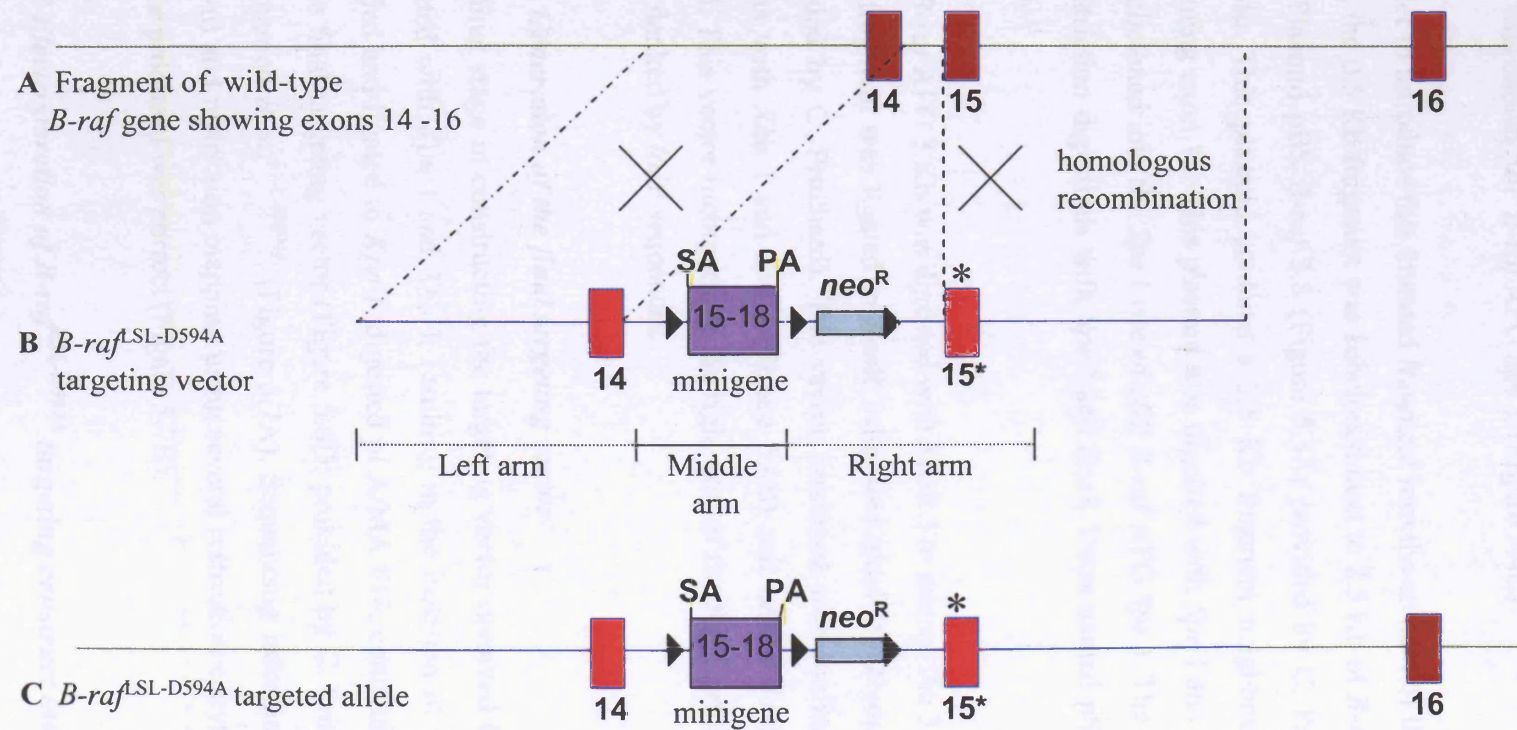


**Figure 5.3** *B-raf* targeting event to generate a conditional kinase inactivating mutation of D594A. (A) Exon-intron structure of wild type mouse *B-raf* gene. (B) Restriction map of *B-raf*<sup>LSL-D594A</sup> targeting vector. (C) *B-raf* targeted allele upon homologous recombination of *B-raf*<sup>LSL-D594A</sup> targeting vector with wild type *B-raf*. Abbreviations: Numbers indicate exon numbers, SA = splice acceptor, PA = polyadenylation site, 15\* = exon 15 containing D594A mutation.

The 0.5 Kb D594A *B-raf* PCR product with the additional *Spe* I site was gel purified and digested with *Sal* I and *Eco*R I and subcloned into pSP72 that had been digested with *Sal* I and *Eco*R I. The resulting vector, confirmed by *Spe* I restriction digestion analysis (Figure 5.4B) was named pSP *B-raf* AFG *Spe* I. (Figure 5.4C)

In order to introduce this mutated fragment into the context of the wild type *B-raf* genomic DNA, the 0.5 Kb fragment was subcloned next to 2.5 Kb of *B-raf* genomic DNA on the 3' side. Plasmid pBS *B-raf* 3.8 (Figure 5.5A; provided by C. Pritchard) was used for this purpose. This plasmid contains a 3.8 Kb fragment neighbouring the 0.5 Kb fragment containing exon 15. This plasmid was digested with *Spe* I and a 2.5 Kb fragment isolated and subcloned into the *Spe* I site of pSP *B-raf* AFG *Spe* I. The resulting vector, confirmed by restriction digestions with *Spe* I and *Eco*R I was named pSP *B-raf* AFG 3 Kb (Figure 5.5B).

pSP *B-raf* AFG 3 Kb was digested with *Eco*R I to release the 3 Kb D594A *B-raf* fragment. This fragment was ligated to *Eco*R I-digested *loxP*(pgkNeopA)*loxP*Salx2 (Figure 5.6A; provided by C. Pritchard). The vector produced was confirmed by separate restriction digests with *Xho* I and *Sac* I (Figure 5.6B) and named *loxP*neoloxP RA AFG (Figure 5.5C). This vector incorporated the right arm of the final targeting vector next to the *neo*<sup>R</sup> gene flanked by *loxP* sequences.

### 5.3.2 Generation of the final targeting vector

The final stage in constructing the targeting vector involved *loxP*neoloxP RA AFG being digested with *Kpn* I and *Xho* I, resulting in the isolation of the right arm. This was gel purified and ligated to *Kpn* I digested pLA/MA #18, containing the left and middle arms of the final targeting vector (Figure 5.6D; provided by C. Pritchard). The resulting vector was named *B-raf*<sup>LSL-D594A</sup> (Figure 5.7A). Sequencing information was obtained (data not shown) and restriction mapping using several restriction enzymes performed to ensure the vector produced was correct (Figure 5.7B).

### 5.3.3 Electroporation of *B-raf*<sup>LSL-D594A</sup> targeting construct into ES cells

60 µg of the *B-raf*<sup>LSL-D594A</sup> vector was linearised by restriction digest with *Not* I. The resulting linearised vector was electroporated into 1 x 10<sup>8</sup> E14.1a ES cells as described in

**Figure 5.4** Restriction maps of plasmids used in the construction of the *B-raf*<sup>LSL-D594A</sup> targeting vector. (A) pSP *B-raf* AFG with the *Xho* I site highlighted. (B) *Spe* I restriction digestion to confirm construction of pSP *B-raf* AFG *Spe* I. (C) pSP *B-raf* AFG *Spe* I with *Spe* I site highlighted. Abbreviation: 15\* = exon 15 containing D594A mutation.

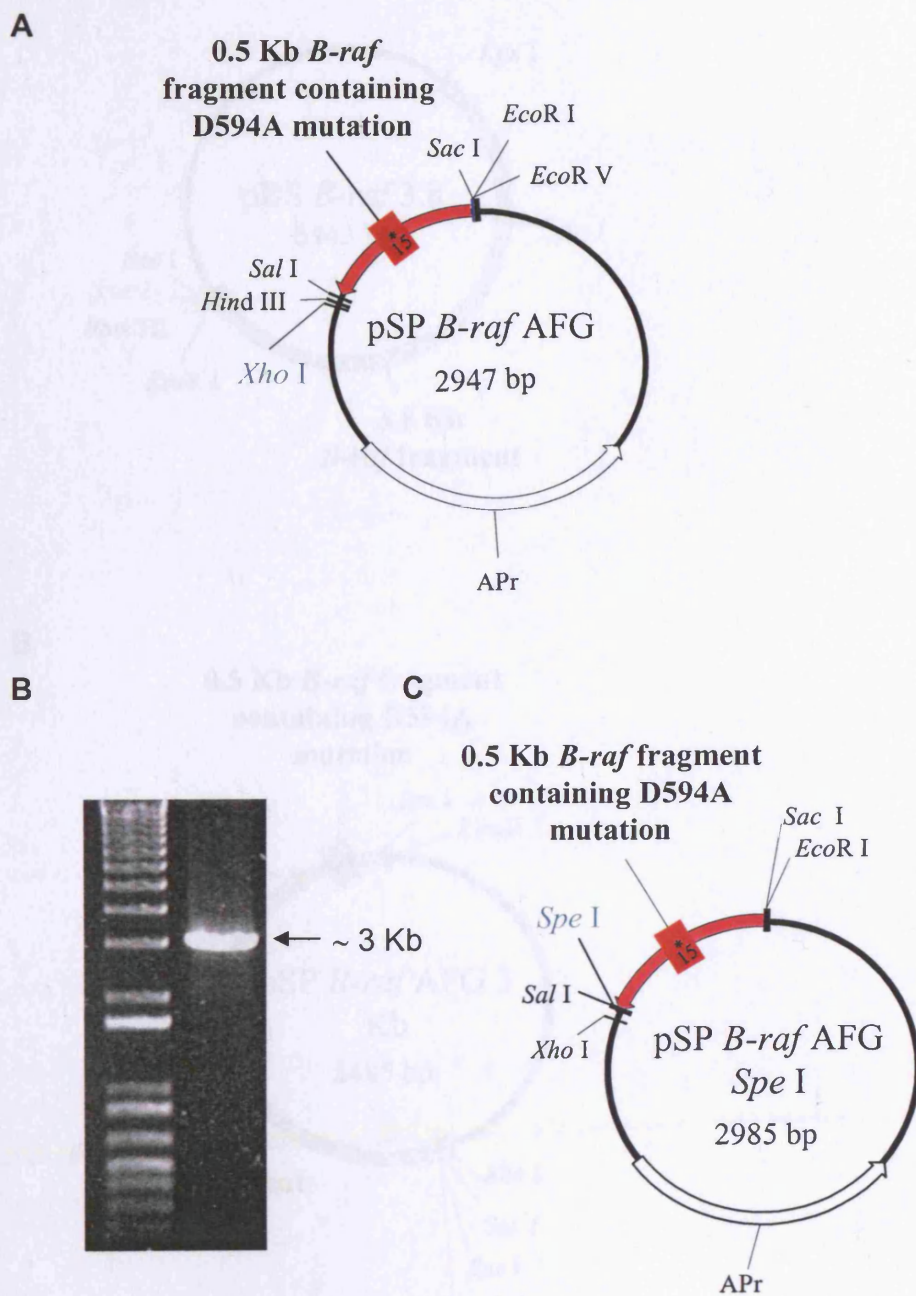


**Figure 5.5** Restriction maps of plasmids used in the construction of the *B-raf*<sup>LSL-D594A</sup> targeting vector. (A) pBS *B-raf* 3.8 with *Spe* I site highlighted. (B) pSP *B-raf* AFG 3 Kb with *Eco*R I sites highlighted. Abbreviation: 15\* = exon 15 containing D594A mutation.

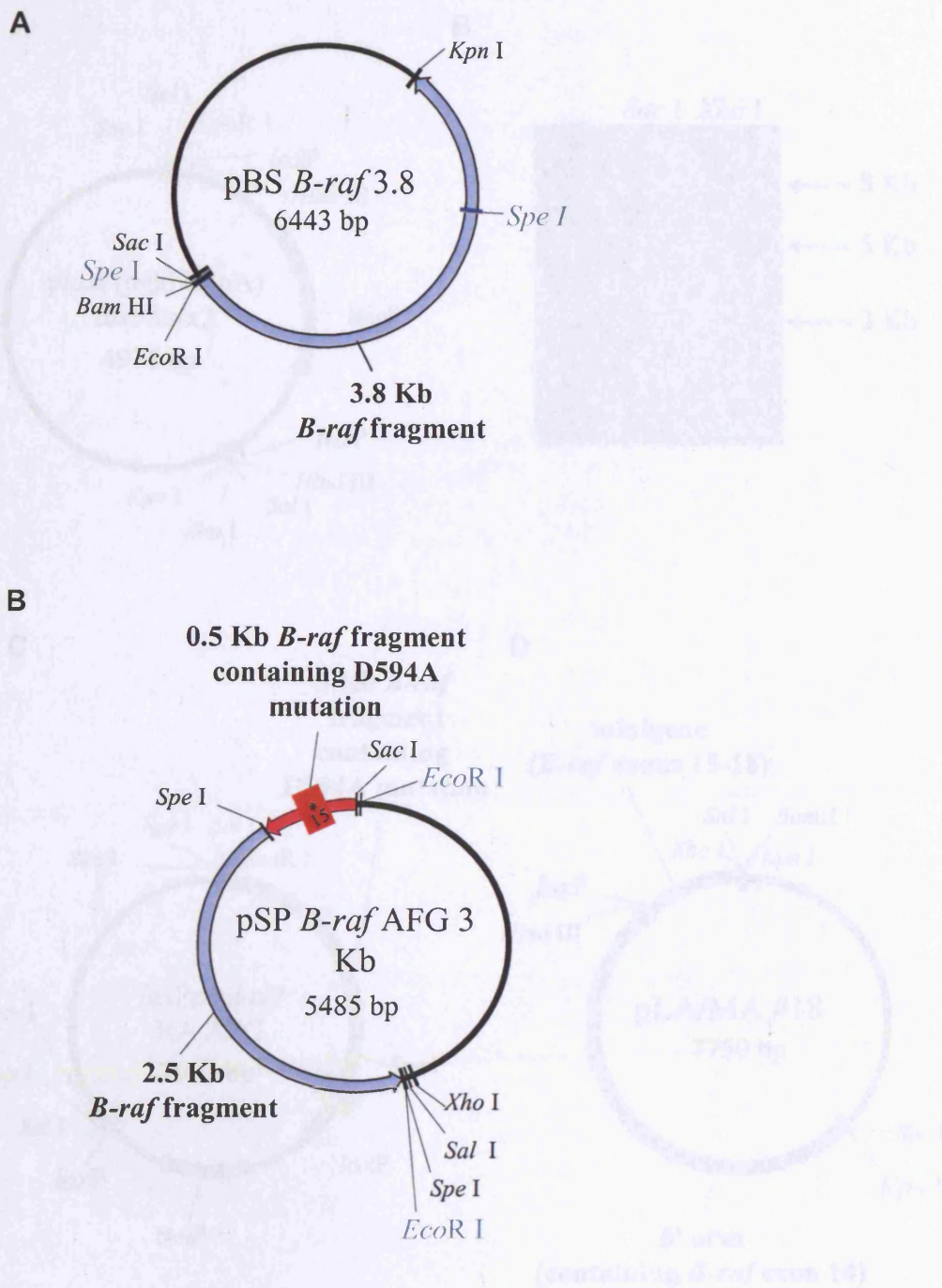


**Figure 5.6** Restriction maps of plasmids used in the construction of the *B-raf*<sup>LSL-D594A</sup> targeting vector. (A) *ploxP*(pgkNeopA)*loxP*Salx2 with *EcoR* I site highlighted. (B) Restriction digests of *loxP*Neo*loxP* RA AFG with *Sac* I or *Xho* I (C) *loxP*Neo*loxP* RA AFG with *Kpn* I and *Xho* I sites highlighted. (D) pLA/MA #18 with *Kpn* I site highlighted. Abbreviation: 15\* = exon 15 containing D594A mutation.

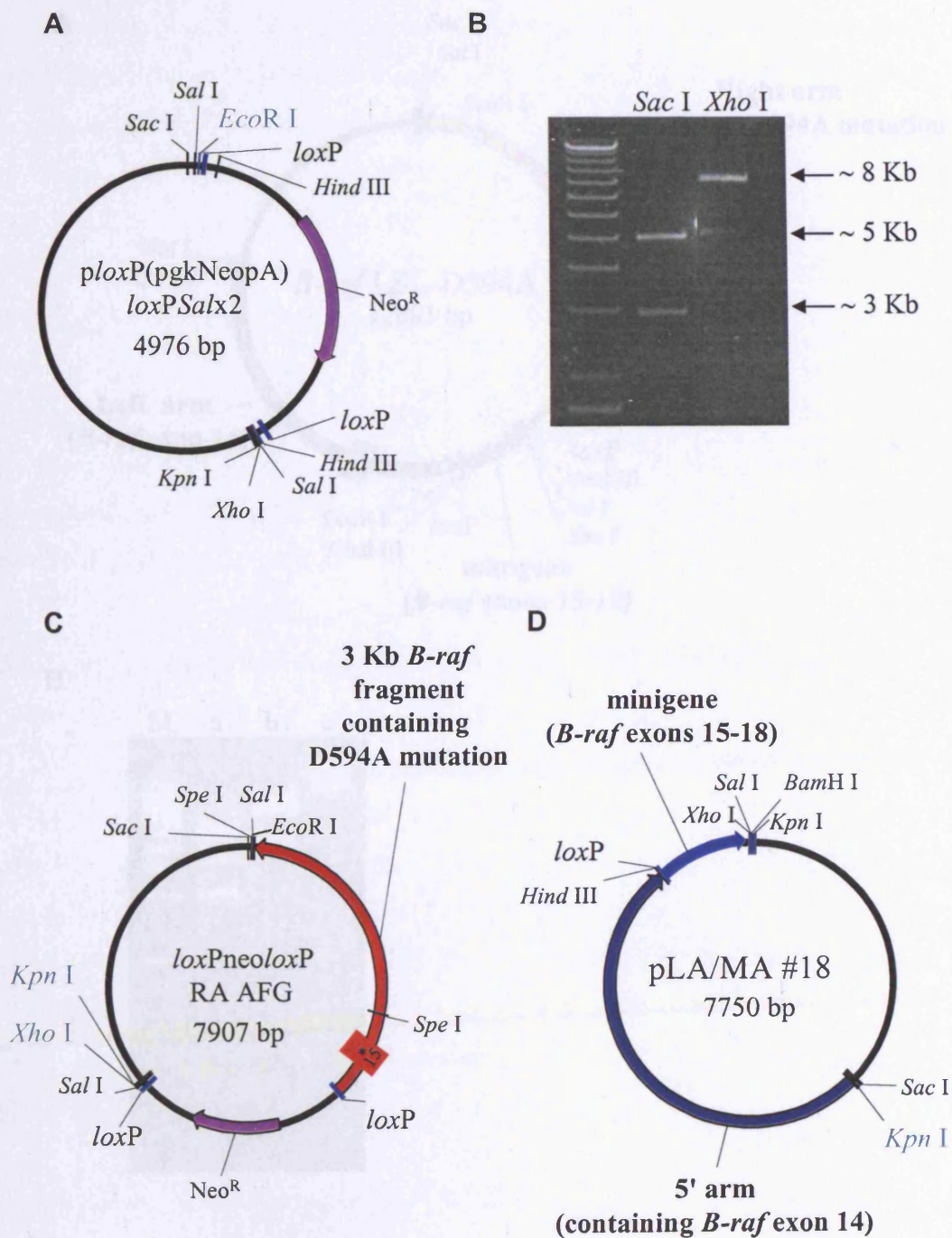
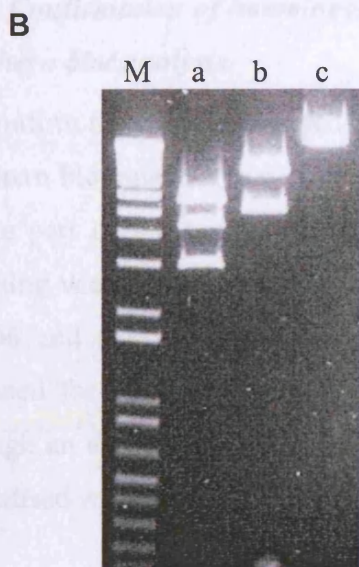
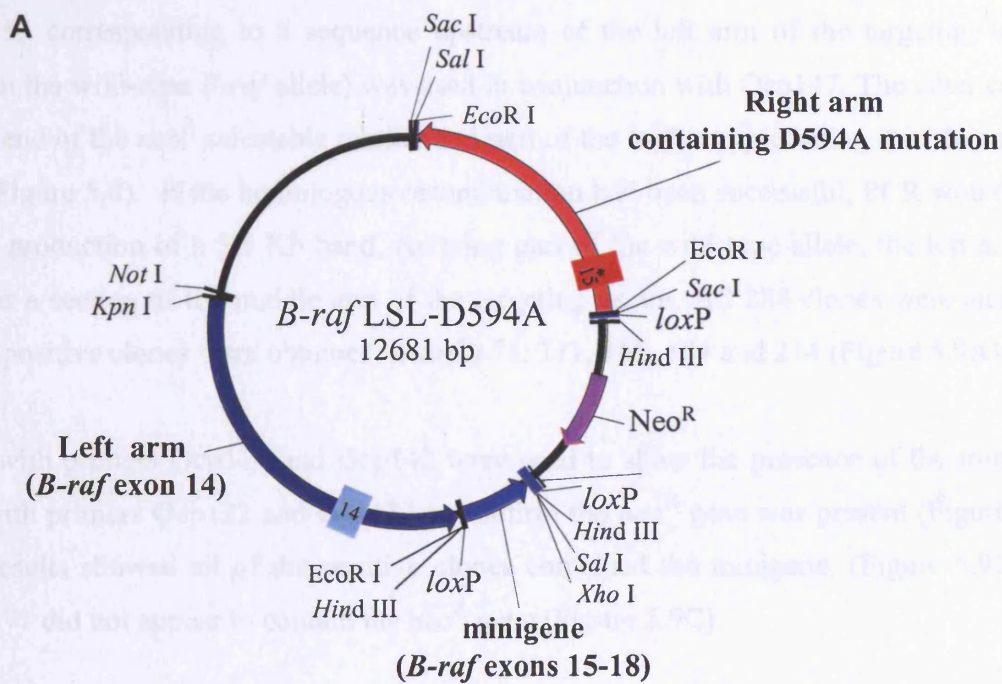


**Figure 5.7** *B-raf*<sup>LSL-D594A</sup> targeting vector (A) Restriction map of *B-raf*<sup>LSL-D594A</sup> targeting vector. (B) Result of restriction digests of *B-raf*<sup>LSL-D594A</sup> with various restriction enzymes; (a) *EcoR* I digest (b) *Sac* I digest (c) *Not* I digest. Abbreviations: 14 = exon 14; 15\* = exon 15 containing D594A mutation; M = 1 Kb DNA ladder.



Chapter 2. The ES cells were placed on G418 selection for seven days. 284 G418-resistant clones were picked and grown up. The majority of the cells from each clone were frozen and the remainder lysed for DNA analysis.

#### **5.3.4 Detection of homologous recombination with *B-raf*<sup>LSL-D594A</sup> by PCR**

Primers were designed to discover if ES cell homologous recombination with *B-raf*<sup>LSL-D594A</sup> had successfully occurred in the ES cells electroporated with the targeting vector. OCP153 corresponding to a sequence upstream of the left arm of the targeting vector (within the wild-type *B-raf* allele) was used in conjunction with Ocp147. The latter covers the 5' end of the *neo*<sup>R</sup> selectable marker and part of the *loxP* site preceding it in the middle arm (Figure 5.8). If the homologous recombination had been successful, PCR would lead to the production of a 5.5 Kb band, covering part of the wild type allele, the left arm, as well as a section of the middle arm of the targeting vector. All 284 clones were analysed and 5 positive clones were obtained, namely 71, 111, 166, 184 and 214 (Figure 5.9A).

PCR with primers Ocp114 and Ocp142 were used to show the presence of the minigene and with primers Ocp122 and Ocp137 to confirm the *neo*<sup>R</sup> gene was present (Figure 5.8). The results showed all of the positive clones contained the minigene, (Figure 5.9B) but clone 71 did not appear to contain the *neo*<sup>R</sup> gene (Figure 5.9C).

#### **5.3.5 Confirmation of homologous recombination with *B-raf*<sup>LSL-D594A</sup> targeting vector by Southern blot analysis**

To confirm the PCR results and to check for the number of copies of the targeting vector, Southern blot analysis was performed. A probe was designed by PCR. This corresponded to the part of the *neo*<sup>R</sup> gene in the middle arm and a section of the right arm of the targeting vector. This was constructed by PCR of the *B-raf*<sup>LSL-D594A</sup> targeting vector with Ocp66 and Ocp122, producing a 1.2 Kb fragment (Figure 5.10 and 5.11). The DNA obtained for the positive clones was digested with *Xba* I or *Hind* III, electrophoresed through an agarose gel and transferred onto a nylon membrane. The resulting blots were hybridised with the 1.2 Kb probe generated.

If homologous recombination of the ES cells with *B-raf*<sup>LSL-D594A</sup> had been successful, digestion with *Xba* I, followed by Southern blot analysis with the 1.2 Kb probe, would

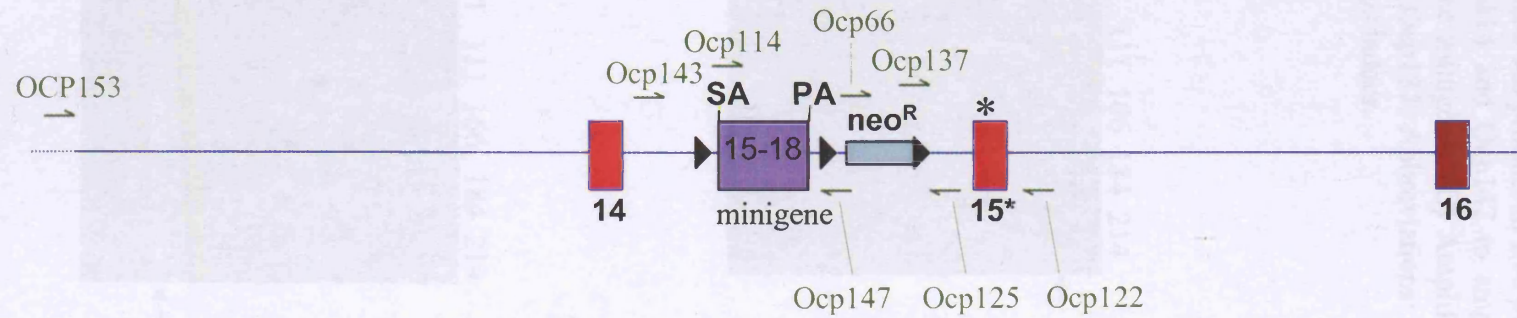
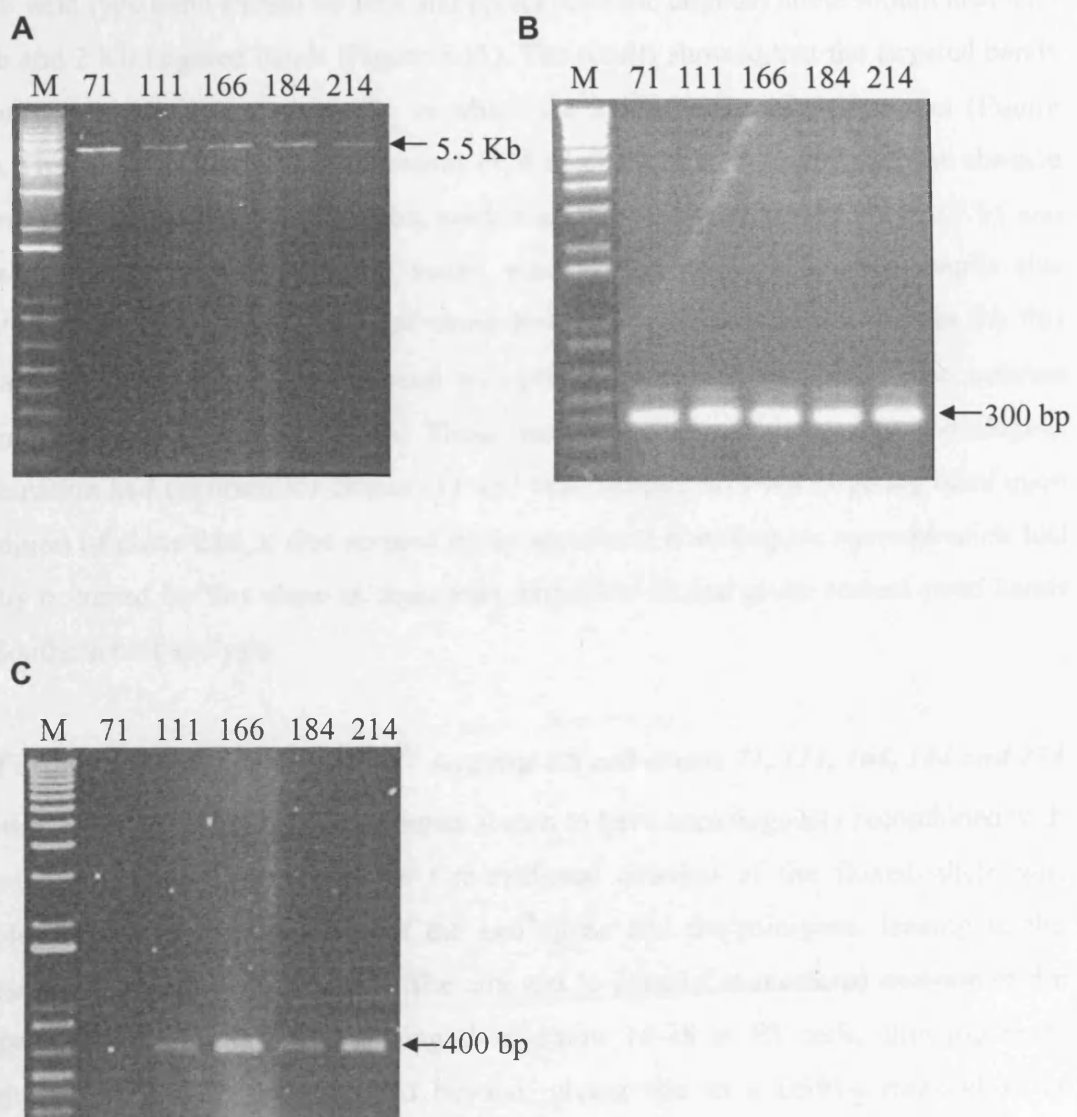


**Figure 5.8** *B-raf*<sup>LSL-D594A</sup> allele highlighting the positions of primers used in confirming the homologous recombination event. Abbreviations: Numbers in black correspond to exon numbers, SA = splice acceptor, PA = polyadenylation site, 15\* = exon 15 containing kinase inactivating mutation. Primer positions are shown in green.

**Figure 5.9** Screening for homologous recombination in ES cell clones electroporated with *B-raf*<sup>LSL-D594A</sup>. **(A)** PCR with primers Ocp147 and Ocp 153 amplifying a 5.5 Kb product in five positively identified clones. **(B)** PCR with primers Ocp114 and Ocp142 to amplify the region of the targeting vector containing the minigene. **(C)** Amplification of the neo<sup>R</sup> gene using primers Ocp122 and Ocp137. Abbreviations: Numbers correspond to clone numbers; M = 1 Kb plus ladder.



give a 12.7 Kb wild type band and an additional 7 Kb band, indicating the presence of the targeted allele (Figure 5.10). The results of this blot indicated a wild type band in all lanes, although this band was very faint for clones 111, 166 and 184 (Figure 5.12A). The 7 Kb targeted band was very clear for these three clones, but there was no 7 Kb band for clone 71, instead a ~ 5 Kb band was observed. In addition, no 7 Kb targeted band was observed for clone 214. This is thought to be due to the observation of strong wild type bands, suggesting incomplete *Xba* I digestion (Figure 5.12A).

Upon digestion with *Hind* III followed by Southern blot analysis with the 1.2 Kb probe, a 14.2 Kb wild type band should be seen and presence of the targeted allele should also lead to 5 Kb and 2 Kb targeted bands (Figure 5.11). The results showed that the targeted bands were present in all clones except 71 in which the 2 Kb band was not present (Figure 5.12B). This result agreed with the previous PCR results for clone 71, showing the absence of the region between the Neo selectable marker and the mutated exon 15 (Figure 5.9), and thus confirmed part of the targeting vector was missing in clone 71. The results also suggested partial *Hind* III digestion of clone 184, as the 2 Kb band was fainter for this clone and an additional ~ 2.5 Kb band was present, although this could also indicate random integrations (Figure 5.12B). These results suggested successful homologous recombination had occurred for clones 111 and 166. Despite no 7 Kb targeting band upon *Xba* I digest of clone 214, it also seemed likely successful homologous recombination had correctly occurred for this clone as digestions with *Hind* III had given correct sized bands upon Southern blot analysis.

### 5.3.6 Further analysis of *B-raf*<sup>LSL-D594A</sup> targeted ES cell clones 71, 111, 166, 184 and 214

To further characterise the 5 ES cell clones shown to have homologously recombined with the endogenous *B-raf* gene, *in vitro* Cre-mediated deletion of the floxed allele was attempted to confirm the deletion of the *neo*<sup>R</sup> gene and the minigene, leading to the expression of the mutant *B-raf* allele. The aim was to obtain Cre-mediated excision of the *neo*<sup>R</sup> gene and the minigene containing *B-raf* exons 15-18 in ES cells, allowing read-through to the mutated exon 15 and beyond, giving rise to a D594A mutated *B-raf* transcript. As Cre-mediated excision leads to one *loxP* site remaining, this additional *loxP* site would allow identification of the Cre-mediated deletion event, as it would add an extra 34 bp to the PCR product upon using primers Ocp125 and Ocp137 (Figure 5.13A).

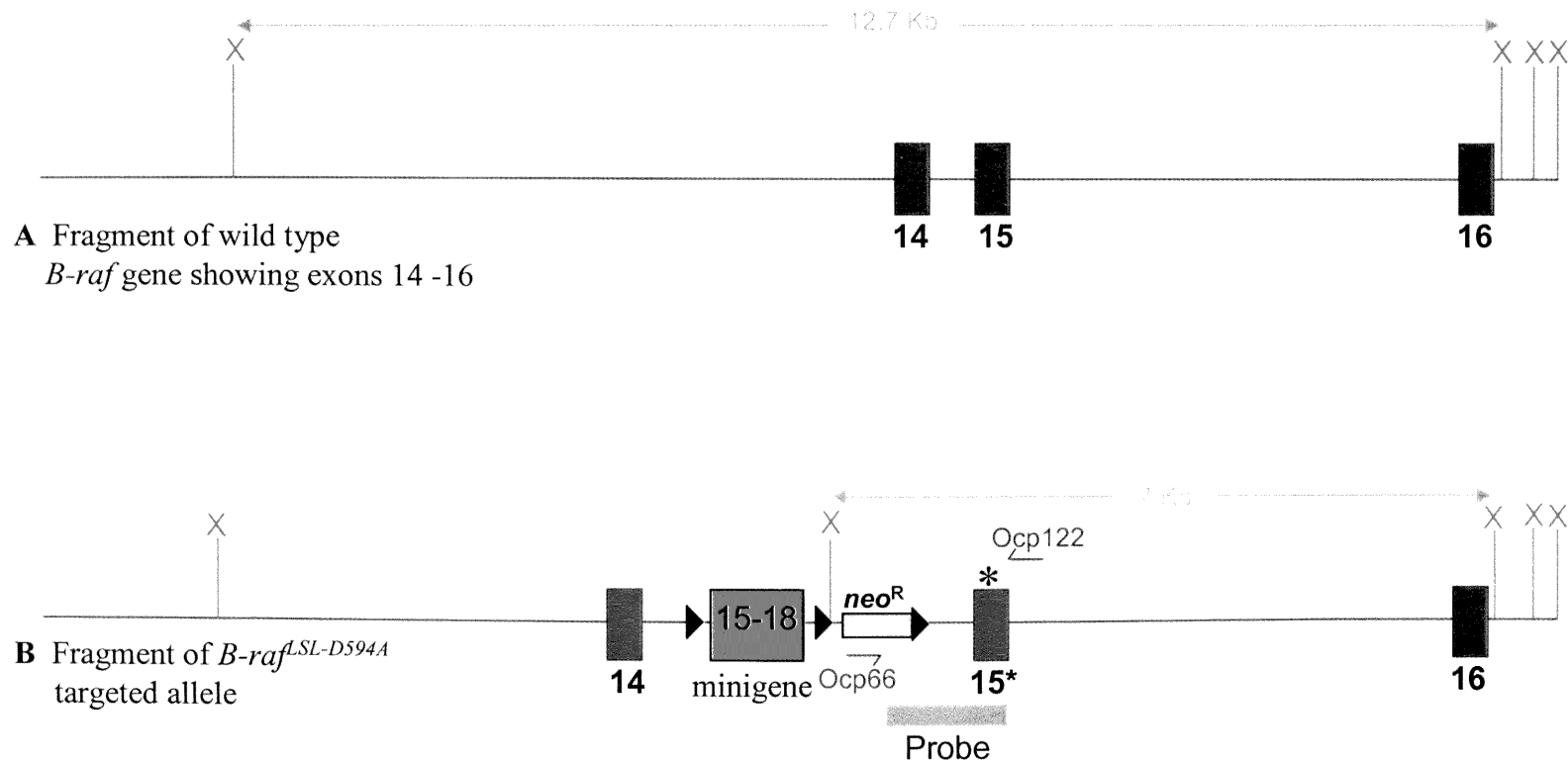
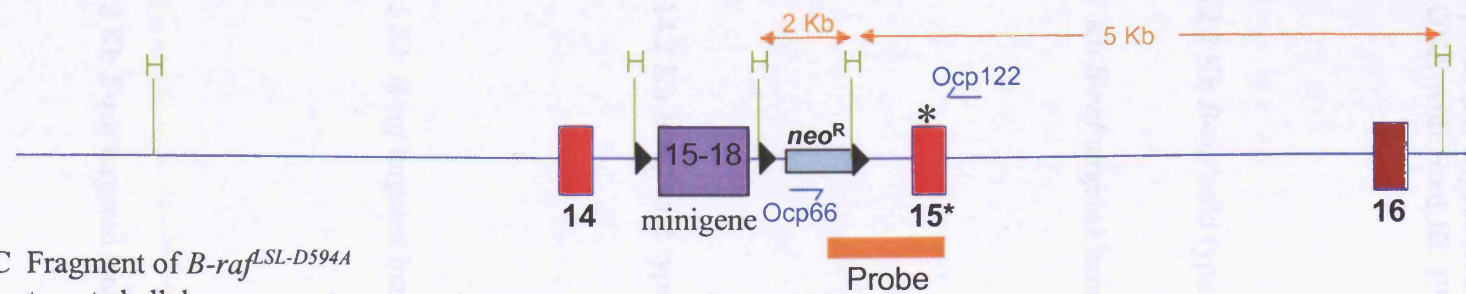


**Figure 5.10** *B-raf* wild type and *B-raf*<sup>f.SL-D594A</sup> targeted allele highlighting the positions of *Xba* I restriction enzymes sites (X), the positions of primers used to generate the probe for Southern blot analysis, the position of the probe and the size of the restriction fragments that hybridised to the probe. Abbreviations: Numbers in black correspond to exon numbers, 15\* = exon 15 containing D594A mutation. No *Xba* I restriction sites are located between exons 1-13 of *B-raf*.



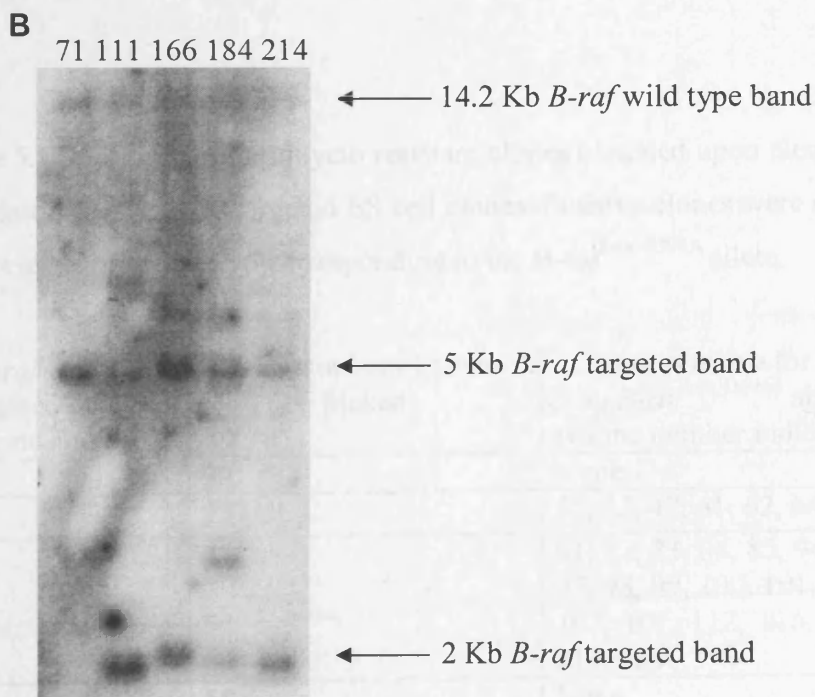
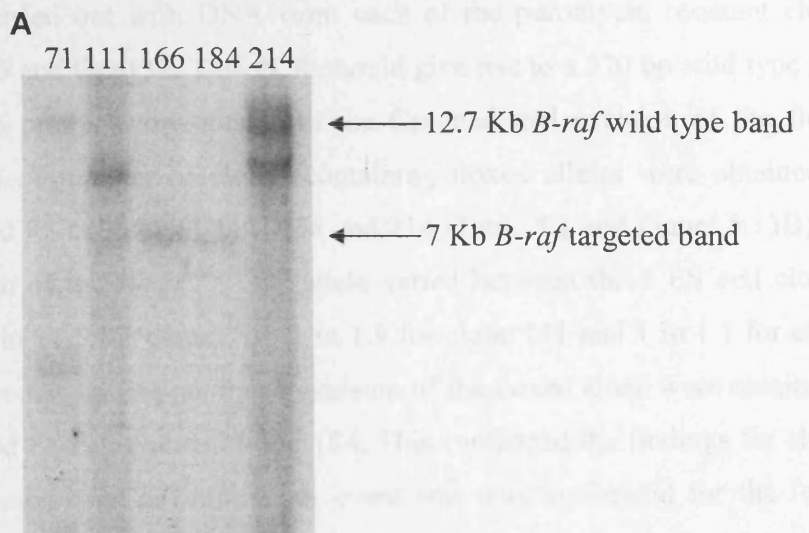
A Fragment of wild type  
*B-raf* gene showing exons 14-16



C Fragment of *B-raf*<sup>LSL-D594A</sup>  
targeted allele

**Figure 5.11** *B-raf* wild type and *B-raf*<sup>LSL-D594A</sup> targeted allele highlighting the positions of *Hind* III restriction enzymes sites (H), the positions of primers used to generate the probe for Southern blot analysis, the positions of the probe and the size of the restriction fragments that hybridised to the probe. Abbreviations: Numbers in black correspond to exon numbers, 15\* = exon 15 containing D594A mutation. No *Hind* III restriction sites are located between exons 1-13 of *B-raf*.

**Figure 5.12** Southern blot analysis for clones containing the *B-raf*<sup>LSL-D594A</sup> targeted event. Southern blots were hybridised with a 1.2 Kb *B-raf* probe amplified by PCR with Ocp66 and Ocp122. (A) Digestion of genomic DNA with *Xba* I (B) Digestion of genomic DNA with *Hind* III. ES clone numbers are indicated.



Cre-mediated excision can be achieved *in vitro* by transfecting ES cells with a vector expressing Cre under the control of a suitable promoter. pCre-PAC is a plasmid containing a Cre construct under the control of the MC1 promoter and also containing a puromycin selectable marker gene (Figure 2.1). 30 µg of pCre-Pac was electroporated into  $5 \times 10^6$  ES cells of clones 71, 111, 184, 166 and 214. After 7 days of puromycin selection a number of clones were picked from each cell line and DNA obtained for analysis. PCR was carried out with DNA from each of the puromycin resistant clones using primers Ocp125 and Ocp132. This PCR should give rise to a 570 bp wild type *B-raf* product and a 604 bp product corresponds to the Cre-mediated excision of the floxed allele (Figure 5.13A). A number of clones containing floxed alleles were obtained for *B-raf*<sup>LSL-D594A</sup> targeted ES cell clones 111, 166 and 214 (Table 5.1 and Figure 5.13B). The Cre-mediated deletion of the *B-raf*<sup>LSL-D594A</sup> allele varied between the 3 ES cell clones. The efficiency was 1 in 11.5 for clone 214, 1 in 1.9 for clone 111 and 1 in 1.1 for clone 166. No clones positive for the Cre-mediated excision of the floxed allele were obtained for *B-raf*<sup>LSL-D594A</sup> targeted ES cell clones 71 and 184. This confirmed the findings for clone 71 showing that the homologous recombination event was only successful for the left arm. The current results suggested complete homologous recombination had also not occurred for clone 184.

**Table 5.1** Summary of puromycin resistant clones obtained upon electroporation of pCre-PAC into *B-raf*<sup>LSL-D594A</sup> targeted ES cell clones. Positive clones were analysed by PCR for the presence of the 604 bp corresponding to the *B-raf*<sup>Lox-D594A</sup> allele.

<i>B-raf</i> <sup>LSL-D594A</sup> targeted ES cell clone number	Total number of clones picked	Clones positive for 604 bp <i>B-raf</i> <sup>Lox-D594A</sup> allele (Clone number indicated)	Efficiency
71	22	None	0
111	13	31, 32, 47, 61, 62, 64, 75	1:1.9
166	21	81, 82, 83, 84, 85, 94, 95, 97, 98, 99, 100, 101, 102, 103, 107, 112, 116, 117, 119, 122	1:1.1
184	18	None	0
214	23	16, 78	1:11.5

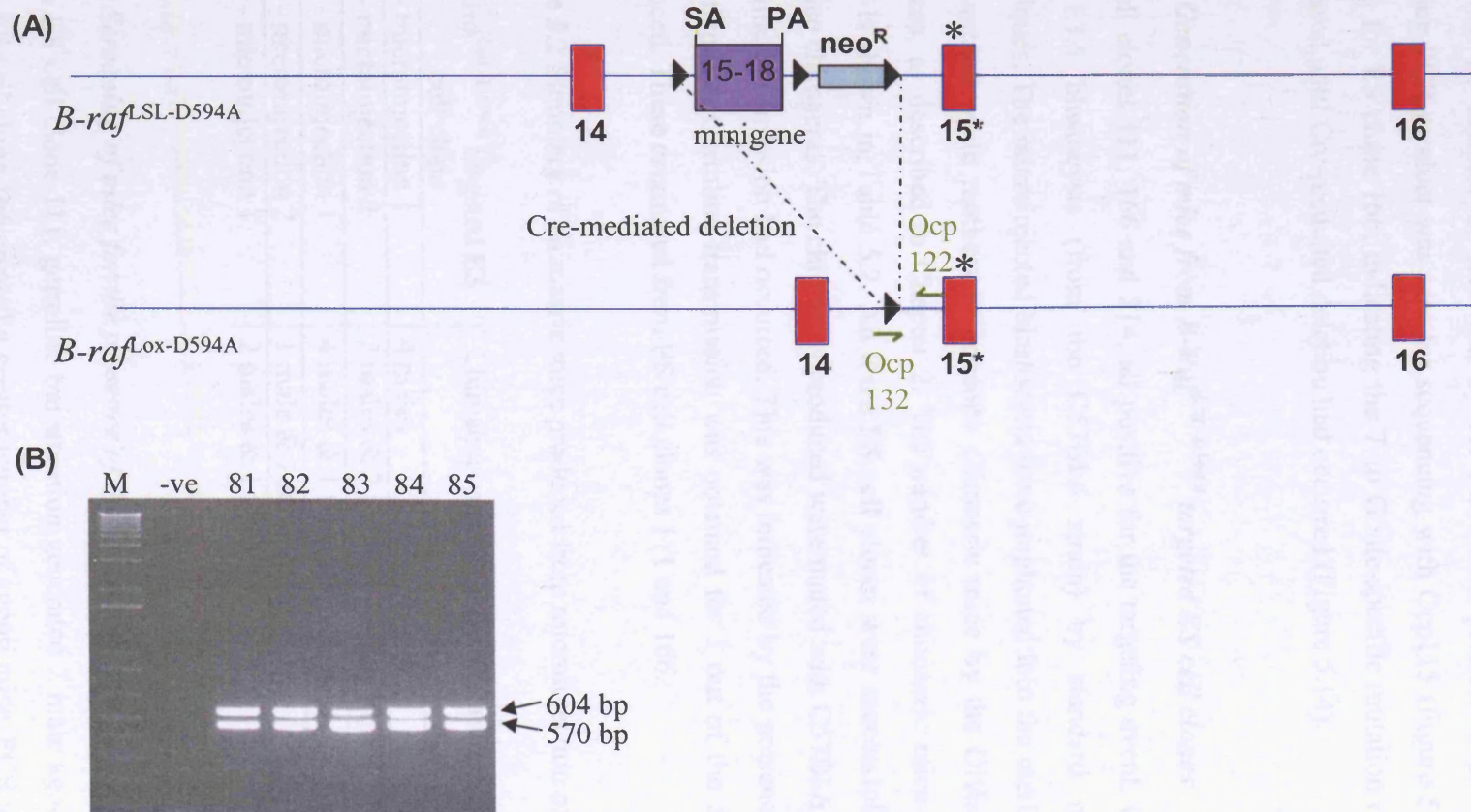


**Figure 5.13** Cre-mediated deletion of minigene and *neo*<sup>R</sup> to allow formation of *B-raf*<sup>Lox-D594A</sup> allele. (A) Diagram showing how Cre-mediated deletion of the *B-raf* targeted allele leads to the creation of an excised allele expressing the D594A mutation. Abbreviations: Numbers in black correspond to exon numbers, SA = splice acceptor, PA = polyadenylation site, 15\* = exon 15 containing D594A mutation. (B) Agarose gel showing PCR with primers Ocp125 and Ocp132 amplifying the *B-raf* wild-type allele and the Cre-mediated deletion of the floxed allele of five clones, originating from *B-raf*<sup>LSL-D594A</sup> clone 166, transfected with pCre-PAC. Numbers correspond to clone numbers, M = 1 Kb plus ladder, -ve = PCR reaction without DNA added.

To ensure the mutation was being expressed upon *in-vitro* Cre-mediated deletion of the ES clones, sequencing analysis was carried out. RNA was obtained for clones positive for the *B-raf*<sup>Lox-D594A</sup> allele originating from clones 111, and 166 and used to make cDNA as described in Chapter 2, followed by RT-PCR with primers Ocp3 and Ocp143. The resulting PCR product was sent for sequencing with Ocp115 (Figure 5.14A). Results are shown for ES clone 166, indicating the T to G site-specific mutation of D594A was not expressed until Cre-mediated deletion had occurred (Figure 5.14).

### 5.3.7 Generation of mice from *B-Raf*<sup>LSL-D594A</sup> targeted ES cell clones

ES cell clones 111, 166 and 214, all positive for the targeting event, were microinjected into E3.5 blastocysts (from the C57BL6 strain) by standard micro-manipulation techniques. The microinjected blastocysts were implanted into the uterine tract of pseudo-pregnant surrogate mothers to generate chimaeric mice by the Division of Biomedical Services, as described in Chapter 2. The number of chimaeric mice produced for each clone is shown in Table 5.2. All three ES cell clones were successfully microinjected to produce chimaeras. The chimaeras produced were mated with C57BL6 mice to discover if germline transmission had occurred. This was indicated by the presence of agouti mice in the offspring. Germline transmission was obtained for 3 out of the 5 sets of chimaeras produced. These originated from ES cell clones 111 and 166.

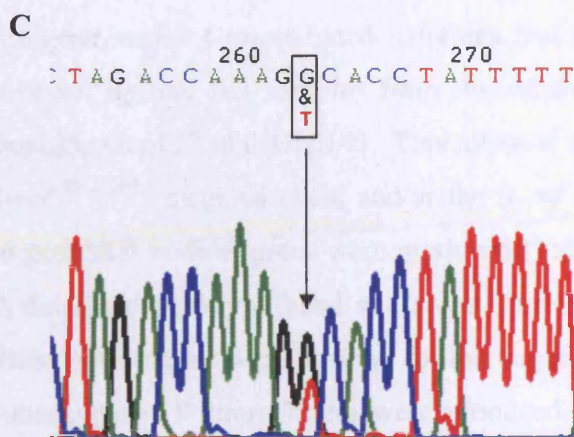
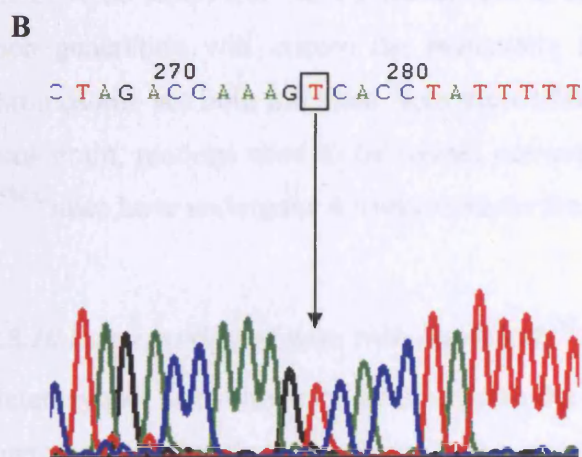
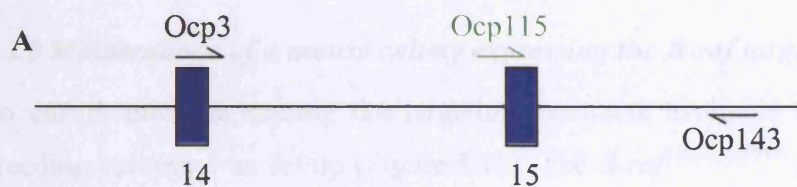
**Table 5.2** Summary of chimaeric mice produced from microinjection of blastocysts

<i>B-raf</i> <sup>LSL-D594A</sup> targeted ES cell clone	Chimaeras produced	Germline transmission achieved
111- microinjection 1	4 males	No
111- microinjection 2	2 males & 2 females	Yes
166 - microinjection 1	4 males & 1 female	Yes
166 - microinjection 2	1 male & 1 female	Yes
214 - microinjection 1	2 males & 1 female	No

### 5.3.8 Screening of mice for the presence of the targeting event

From ES cell clone 111, germline transmission generated 2 male agouti pups in the first litter. ES cell clone 166 created a greater number of agouti mice. PCR analysis was carried

**Figure 5.14** Sequencing analysis of cDNA *B-raf*<sup>LSL-D594A</sup> ES clone 166. (A) Diagram indicating positions of primers used for RT-PCR and sequencing. RT-PCR was carried out with primers Ocp3 and Ocp143 using cDNA originating from ES clone 166, and originating from an ES clone of 166 obtained after addition of Cre recombinase. Subsequent sequencing analysis was carried out with Ocp115. (B) Sequencing chromatogram showing the wild-type thymidine nucleotide is expressed in ES clone 166 (C) Sequencing chromatogram showing the expression of the D594A mutation by a T → G site-specific nucleotide mutation upon treatment of ES clone 166 with Cre. Two peaks are present due to the presence of the thymidine nucleotide representing the *B-raf* wild-type allele on the other non-targeted chromosome.



out to assess the presence of the targeting event in these mice, and in subsequent generations. Tail samples were obtained for each pup and lysed to obtain DNA. Primers Ocp125 and Ocp137 were used to check for the presence or absence of the targeting event (Figure 5.8). An example of the results obtained is shown in Figure 5.15A. 10 out of the 12 mice initially tested were positive for the targeted event. PCR with Ocp147 and Ocp153 amplifying a 5.5 Kb product to show successful homologous recombination, was also carried out. The results showed the 5.5 Kb band was present in the agouti mice tested (Figure 5.15B). Mice confirmed as being positive for the targeting event were mated to C57BL6 mice in order to increase the number of mice carrying the targeted event.

### **5.3.9 Maintenance of a mouse colony expressing the B-raf targeted event**

To ensure mice expressing the targeting event are available for future experiments, a breeding strategy was set up (Figure 5.16). The *B-raf*<sup>+/<sup>LSL-D594A</sup> mice were backcrossed to the C57BL6 strain and the sex was altered at each generation. Switching between sexes at each generation will ensure the maternally inherited mitochondrial DNA and the Y chromosome are both inherited from the C57BL6 strain. To obtain a virtually genetically pure strain, matings need to be carried out over 10 generations. Currently the *B-raf*<sup>+/<sup>LSL-D594A</sup> mice have undergone 6 backcrosses to the C57BL6 strain.</sup></sup>

### **5.3.10 Intercrossing of mice with the B-Raf<sup>LSL-D594A</sup> allele**

Heterozygote mice shown to be expressing the *B-raf* targeted allele (*B-raf*<sup>+/<sup>LSL-D594A</sup>) were intercrossed, with the aim of producing mice homozygous for the targeted allele. The offspring produced would be expressing wild type *B-raf* due to the presence of the minigene, as no Cre-mediated deletions had been performed. A number of intercrosses were set up and tail samples from the offspring produced were analysed with primers Ocp125, Ocp137 and Ocp143. This allowed analysis of whether the mice contained the *B-raf*<sup>LSL-D594A</sup> targeted event and/or the *B-raf* wild-type allele in one PCR. Unfortunately no postnatal homozygotes were produced (Table 5.4). All tail samples analysed gave rise to the *B-raf* wild-type band and some samples were heterozygous for the *B-raf*<sup>LSL-D594A</sup> allele. No samples were positive for the targeted allele only (Figure 5.17A and Table 5.4). Subsequently, 9 more litters were produced, but no homozygotes were obtained upon screening of the 87 offspring produced in total. The genotypes of the offspring generated</sup>

**Figure 5.15** Screening for the *B-raf*<sup>LSL-D594A</sup> targeted event in mice. (A) PCR with primers Ocp125 and Ocp137 amplifying a 150bp product confirming the presence or absence of the *B-raf*<sup>LSL-D594A</sup> targeted allele. (B) PCR with primers Ocp147 and Ocp153 amplifying a 5.5 Kb product confirming the correct homologous recombination event in mice. Abbreviations: Numbers correspond to litter mates; M = 1 Kb plus ladder.

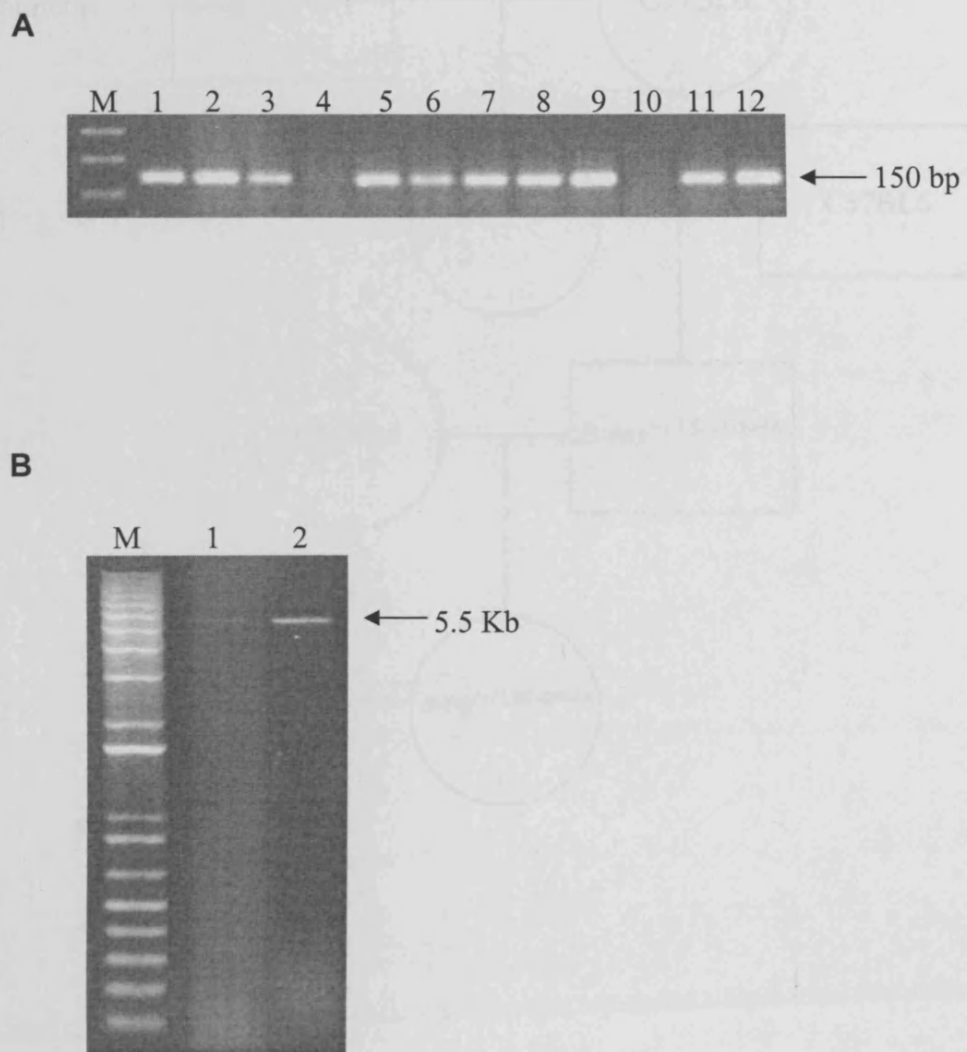
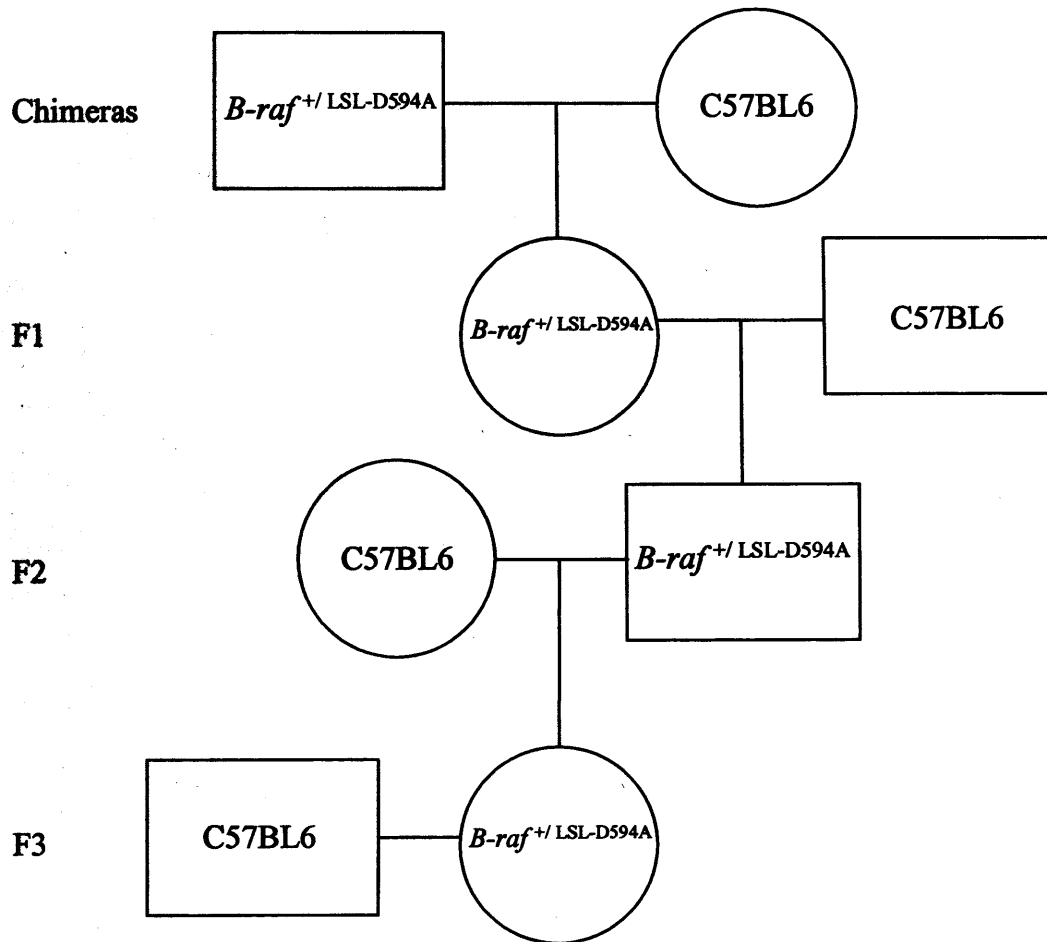
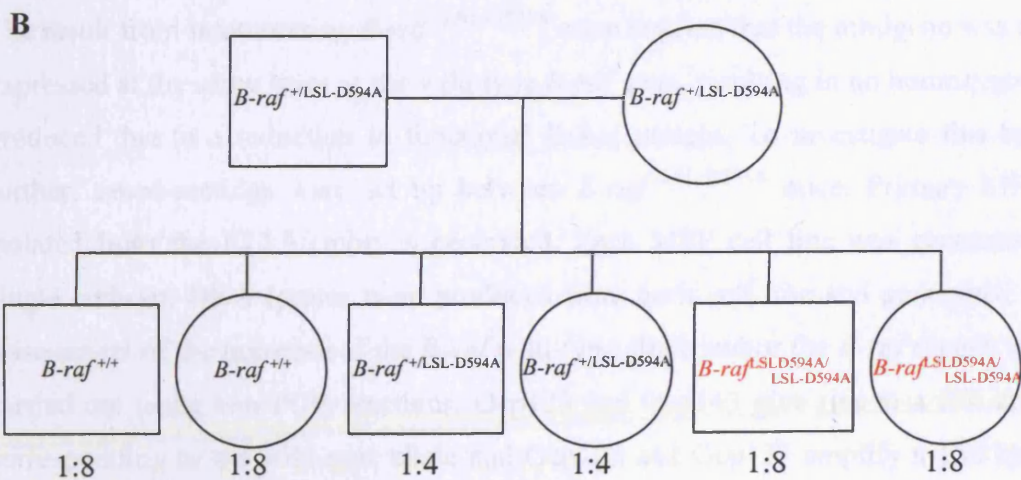
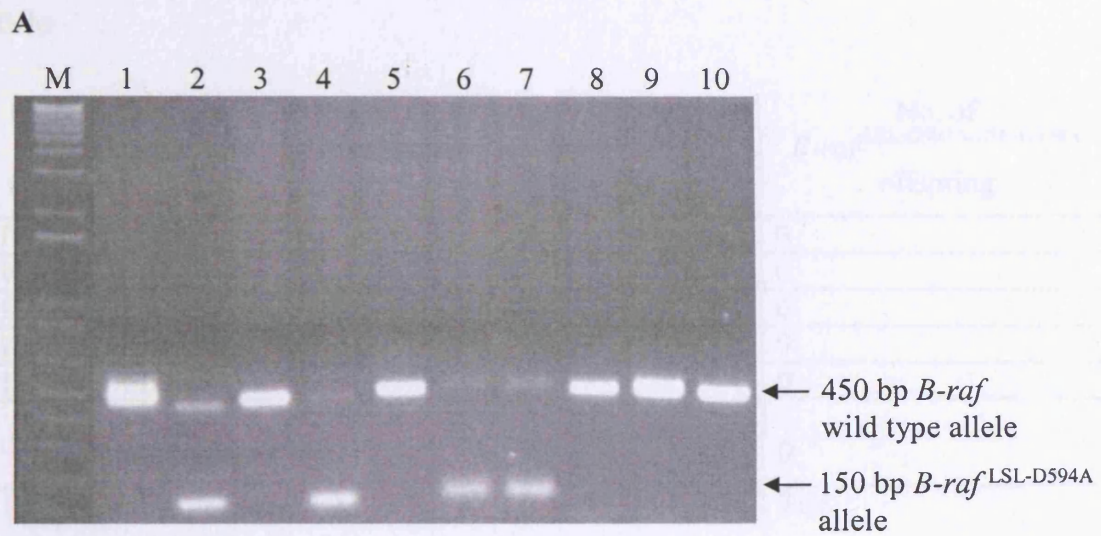


**Figure 5.16** Breeding strategy for the production of mice carrying the targeted event (containing the *B-raf* D594A kinase inactivating mutation) on the C57BL6 inbred strain. The mutation would not be expressed in these mice (*B-raf*<sup>+/LSL-D594A</sup>) until Cre was administered.



.....etc.

**Figure 5.17** Intercrossing of  $B\text{-raf}^{+/LSL\text{-D594A}}$  mice to obtain homozygous  $B\text{-raf}^{LSL\text{-D594A}/LSL\text{-D594A}}$  mice. (A) PCR analysis of tail DNA of the offspring. PCR with primers Ocp125, Ocp137 and Ocp143 amplify a 450 bp product corresponding to the wild type allele and a 150 bp product corresponding to the  $B\text{-raf}^{LSL\text{-D594A}}$  allele. Abbreviations: Numbers correspond to litter mates; M = 1 Kb plus ladder. (B) Genotypes of expected offspring from the intercross. Ratios indicate expected frequency based on Mendelian inheritance.



did not agree with the expected Mendelian frequency (Figure 5.17B), as a greater number of  $B\text{-raf}^{+/+}$  mice were generated than expected. As well as the lack of  $B\text{-raf}^{\text{LSL-D594A/LSL-D594A}}$  homozygous mice, the numbers of  $B\text{-raf}^{+/LSL-D594A}$  heterozygote mice were also reduced. These data suggest that mice homozygote for the targeted allele were dying *in utero*. It is therefore likely that there was some sort of problem with the expression of B-Raf in these mice, and suggested the minigene was not functioning as was hoped.

**Table 5.4** Summary of the first intercrosses of mice heterozygote for the  $B\text{-raf}^{\text{LSL-D594A}}$  allele

ES cell clone	Intercross number	No. of $B\text{-raf}^{+/+}$ offspring	No. of $B\text{-raf}^{+/LSL-D594A}$ offspring	No. of $B\text{-raf}^{\text{LSL-D594A/LSL-D594A}}$ offspring
166	IDA1	6	4	0
166	IDA2	2	2	0
166	IDA3	4	0	0
166	IDA4	7	0	0
111	IDA5	3	1	0
<b>Total obtained</b>		22	7	0
<b>Total expected</b>		7.25	14.5	7.25

### 5.3.11 Generation of embryos homozygous for the $B\text{-raf}^{\text{LSL-D594A}}$ targeted event

The result from intercrossing  $B\text{-raf}^{+/LSL-D594A}$  mice implied that the minigene was not being expressed at the same level as the wild type  $B\text{-raf}$  gene, resulting in no homozygotes being produced due to a reduction in functional B-Raf protein. To investigate this hypothesis further, timed-matings were set up between  $B\text{-raf}^{+/LSL-D594A}$  mice. Primary MEFs were isolated from the E12.5 embryos generated. Each MEF cell line was generated from a single embryo. DNA lysates were produced from each cell line and genotyped by PCR. Assessment of the presence of the  $B\text{-raf}$  wild-type allele and/or the  $B\text{-raf}$  mutant allele was carried out using two PCR reactions. Ocp125 and Ocp143 give rise to a 570 bp product corresponding to the wild-type allele and Ocp125 and Ocp137 amplify a 150 bp product indicating the presence of the  $B\text{-raf}$  targeted allele. A total of three timed-matings were carried out and the genotypes of the embryos generated are shown in Table 5.5. The PCR results obtained from the third timed mating is shown in Figure 5.18A. Overall, it was

observed that  $B\text{-raf}^{\text{LSL-D594A/LSL-D594A}}$  embryos at E12.5 were produced close to the expected Mendelian frequency.

**Table 5.5** Summary of the genotypes of E12.5 embryos arising from intercrossing  $B\text{-raf}^{\text{LSL-D594A}}$  mice.

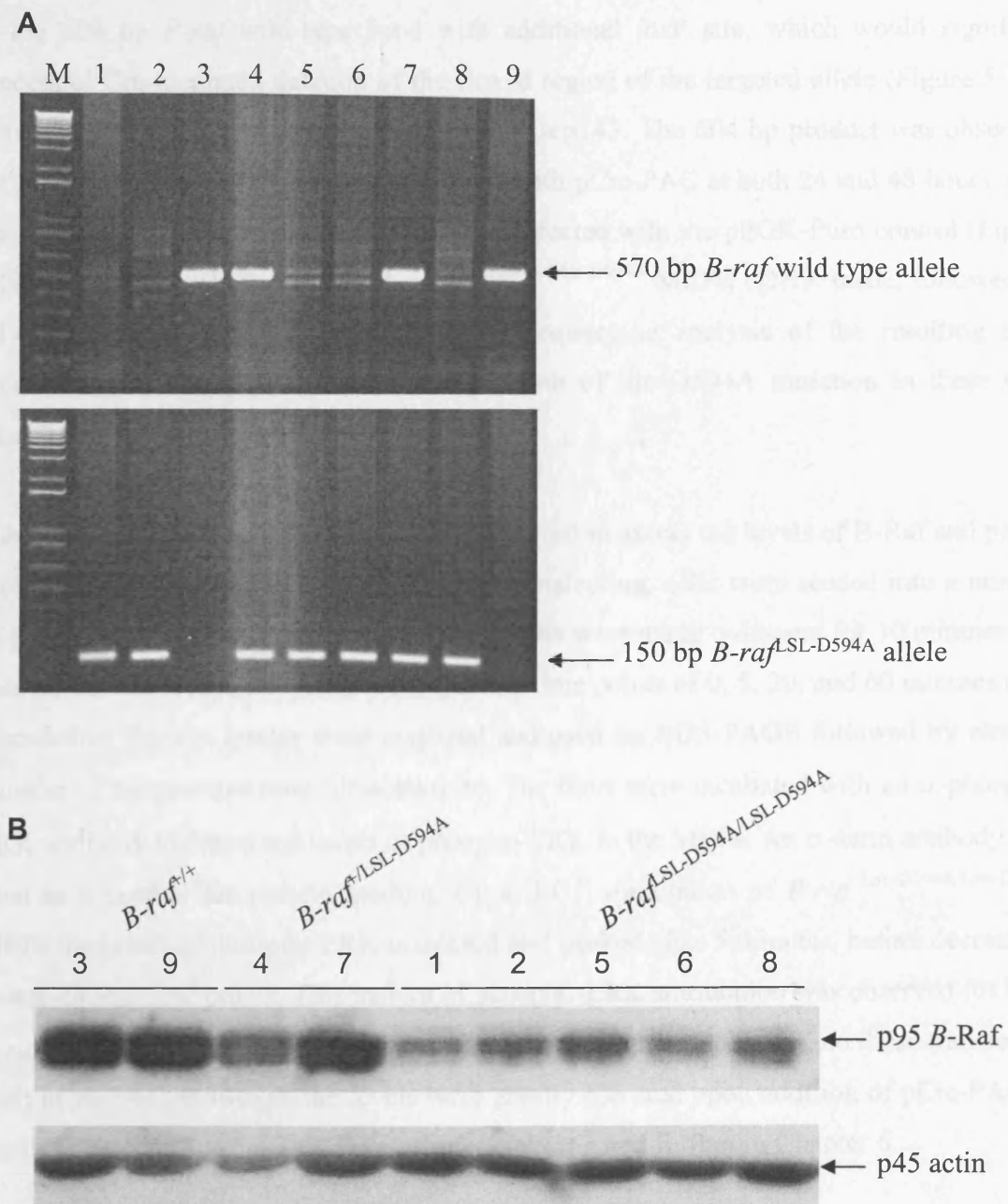
Time mating	No. of $B\text{-raf}^{+/+}$ embryos	No. of $B\text{-raf}^{+/LSL-D594A}$ embryos	No. of $B\text{-raf}^{\text{LSL-D594A/LSL-D594A}}$ embryos
1	4	3	2
2	2	6	2
3	2	2	5
<b>Total obtained</b>	8	11	9
<b>Total expected</b>	7	14	7

To discover if the  $B\text{-raf}^{\text{LSL-D594A/LSL-D594A}}$  MEFs produced were expressing B-Raf, MEFs of all genotypes were subject to Western blot analysis. Protein lysates were prepared from the MEFs and used for SDS-PAGE followed by electro-transfer of the proteins onto nitrocellulose. The blots were incubated with an  $\alpha$ -B-Raf antibody and an  $\alpha$ -actin antibody was used as a loading control. The results showed that the  $B\text{-raf}^{\text{LSL-D594A/LSL-D594A}}$  MEFs were expressing B-Raf, but at levels much lower than that observed for  $B\text{-raf}^{+/+}$  and  $B\text{-raf}^{+/LSL-D594A}$  cells (Figure 5.18B). It therefore appears that the minigene is functional, but B-Raf is produced at too low a level to allow survival postnatally in the homozygotes, but allows survival to at least E12.5.

### 5.3.12 *In vitro* Cre-mediated deletion of the $B\text{-raf}^{\text{LSL-D594A}}$ allele

Having discovered that the targeted allele was not fully functional, it was important to assess the ability of Cre-mediated deletion of the targeted allele, which would allow the expression of the kinase inactivating mutation. Transient transfections were performed using the Nucleofector<sup>TM</sup> electroporation technique. Initially experiments were carried out to discover if the technology would be suitable for the MEFs. Transfecting a GFP vector into  $B\text{-raf}^{\text{LSL-D594A/LSL-D594A}}$  cell lines using various transfection conditions resulted in a 61 % transfection rate (data not shown), thus showing it was possible to transfect a plasmid into these cells using this technique. Therefore,  $B\text{-raf}^{\text{LSL-D594A/LSL-D594A}}$  MEFs were seeded

**Figure 5.18** Screening of E12.5 embryos arising from *B-raf*<sup>f/LSL-D594A</sup> intercross. (A) PCR with primers Ocp125 and either Ocp143 and Ocp137 amplifying 570 bp and 150 bp products respectively. MEFs numbered 1, 2, 5, 6 and 8 were homozygotes. Abbreviations: M = 1 Kb DNA ladder; numbers correspond to embryo number. (B) Western blot analysis to detect B-Raf (upper panel) and actin (lower panel) in *B-raf*<sup>f/+</sup>, *B-raf*<sup>f/LSL-D594A</sup> and *B-raf*<sup>LSL-D594A/LSL-D594A</sup> primary MEFs.



in 15 cm culture dishes at  $4 \times 10^6$  cells, 24 hours prior to the transfection occurring. The following day,  $1 \times 10^6$  of the MEFs were harvested and used, along with 10  $\mu$ g DNA, per transfection. The vectors used for the transfections were pCre-PAC (Figure 2.1) to initiate Cre-mediated excision of the floxed allele, and pPGK-Puro (Figure 2.1) as a control. After transfecting, cells were seeded into a number of 6 well dishes.

DNA was harvested from the transiently transfected MEFs at 24 and 48 hours after the transfection. PCR was carried out on the DNA samples obtained to evaluate the presence of the 604 bp *B-raf* wild-type band with additional *loxP* site, which would signify a successful Cre-mediated deletion of the floxed region of the targeted allele (Figure 5.13). This was assessed using primers Ocp125 and Ocp143. The 604 bp product was observed for *B-raf*<sup>LSL-D594A/LSL-D594A</sup> MEFs transfected with pCre-PAC at both 24 and 48 hours after transfection. No band was seen for MEFs transfected with the pPGK-Puro control (Figure 5.19A). RNA was obtained from *B-raf*<sup>LSL-D594A/LSL-D594A</sup> MEFs, cDNA made, followed by RT-PCR with primers Ocp3 and Ocp143. Sequencing analysis of the resulting PCR product with Ocp115 confirmed the expression of the D594A mutation in these Cre-transfected MEFs (Figure 5.19B).

Subsequent transient transfections were carried out to assess the levels of B-Raf and pERK proteins upon Cre-mediated deletion. After transfecting, cells were seeded into a number of 6 well dishes. 24 hours after transfecting, cells were made quiescent for 30 minutes and then stimulated with EGF. Cells were lysed at time points of 0, 5, 20, and 60 minutes after stimulation. Protein lysates were prepared and used for SDS-PAGE followed by electro-transfer of the proteins onto nitrocellulose. The blots were incubated with an  $\alpha$ -phospho-ERK antibody to detect the levels of phospho-ERK in the MEFs. An  $\alpha$ -actin antibody was used as a control for protein loading. Upon EGF stimulation of *B-raf*<sup>Lox-D594A/Lox-D594A</sup> MEFs the levels of phospho-ERK increased and peaked after 5 minutes, before decreasing at subsequent time points. This pattern of phospho-ERK stimulation was observed for both *B-raf*<sup>LSL-D594A/LSL-D594A</sup> MEFs transiently transfected with pPGK-puro and those transfected with pCre-PAC. However, the levels were greatly elevated upon addition of pCre-PAC to the cells (Figure 5.19C). This observation is investigated further in Chapter 6.



These lysates were also used to produce blots that were incubated with an  $\alpha$ -B-Raf antibody. The levels of B-Raf increased upon Cre-mediated excision by pCre-PAC over the time course of 60 min when compared to cells transiently transfected with pPGK-puro (Figure 5.19C). This agreed with the findings of Sections 5.3.12, showing B-Raf levels increase upon cre-mediated deletion due to the likelihood that the minigene is not functioning efficiently.

## 5.4 Conclusions

This chapter describes the successful generation of a targeting vector involving numerous cloning steps, and the use of this targeting vector to generate mice with a conditional knockin mutation of *B-raf* D594A. The targeting vector produced consisted of three regions; a left arm and middle arm that had been previously cloned in the laboratory, and a right arm that was generated as part of the current project. The right arm was generated in 3 cloning steps and ligated to the remainder of the vector in a final cloning step. The 3 loxP sites within the final vector were located on either side of a *neo*<sup>R</sup> gene and/or a minigene containing exons 15-18 of wild type *B-raf*. The vector was designed in this manner so that the minigene would allow expression of wild type B-Raf in non-Cre-deleted cells. The aim was that upon Cre-mediated excision of this region, read-through transcription to the right arm containing a mutated *B-raf* exon 15 would occur. This exon contained the D594A mutation, thus creating a kinase inactive form of the B-Raf protein.

Gene targeting was performed and upon electroporation of the final targeting vector *B-raf*<sup>LSL-D594A</sup>, a targeting frequency of 1 in 57 was observed. Five out of a total of 284 ES clones analysed were shown to have successfully undergone homologous recombination with *B-raf*<sup>LSL-D594A</sup> upon PCR analysis for each clone. Upon further PCR and Southern blot analysis it was discovered that one of these clones (#71) was missing part of the targeting vector and thus was discarded. It was also unclear as to if the targeting vector had correctly integrated with the *B-raf* wild-type allele for a second clone (#184) and therefore this was also not used for further studies. The problems with these two clones were confirmed upon *in vitro* Cre-mediated deletion of the ES clones. No Cre-deleted clones originating from these two ES clones were positive for the 604 bp band corresponding to the *B-raf*<sup>Lox-D594A</sup> allele. *In vitro* Cre-mediated deletion of the *neo*<sup>R</sup> and minigene was successfully

performed for clones 111, 166 and 214. These ES clones were microinjected into blastocysts and 18 chimaeras were produced.

Germline transmission was achieved for ES clones 111 and 166. From ES cell clone 111, germline transmission generated 2 male agouti offspring from two chimaera matings. From ES cell clone 166, 4 male and 3 female agouti offspring were produced from three chimaera matings. PCR analysis was carried out to assess the presence of the targeted event in these mice and in subsequent generations. A breeding colony was subsequently set up using mice confirmed as being positive for the targeted allele to maintain a mouse colony of *B-raf*<sup>LSL-D594A</sup>.

The mice generated contained a wild-type *B-raf* allele and a targeted allele; *B-raf*<sup>+/LSL-D594A</sup> mice. In order to test whether the minigene was functional, intercrosses between the *B-raf*<sup>+/LSL-D594A</sup> mice were set up. PCR analysis of tails obtained from the resulting 87 offspring of various mating pairs showed no live mice containing the *B-raf*<sup>LSL-D594A</sup> integration on both alleles were generated. As these mice should express wild-type B-Raf, they should have been obtained at the expected Mendelian frequency. Given that none were obtained, this suggested there was a problem with the expression of the minigene.

To investigate why *B-raf*<sup>LSL-D594A/LSL-D594A</sup> mice expressing wild-type B-Raf were not produced, E12.5 embryos were obtained. Three matings were set up, which overall produced E12.5 *B-raf*<sup>LSL-D594A/LSL-D594A</sup> embryos at the expected Mendelian frequency. This indicated that any problems caused by the *B-raf*<sup>LSL-D594A</sup> allele were likely to be occurring at a later stage in embryogenesis. Subsequent analysis of these embryos showed that the *B-raf*<sup>LSL-D594A/LSL-D594A</sup> MEFs were expressing B-Raf, but at levels much lower than that observed for *B-raf*<sup>+/+</sup> and *B-raf*<sup>+/LSL-D594A</sup> cells. It therefore appears that the minigene is expressed, but inefficiently. This may possibly be due to the splice acceptor (SA) sequence in the targeted allele not giving rise to splicing between exons 14 and 15 as efficiently as the wild type allele, for unknown reasons.

Upon Cre-mediated excision of the *neo*<sup>R</sup> and minigene in ES cells by transient transfection of the *B-raf*<sup>LSL-D594A/LSL-D594A</sup> MEFs, expression of the D594A mutation was observed in

these cells. Subsequent analysis of these cells showed B-Raf protein levels increased upon Cre-mediated deletion and phospho-ERK levels also increased.

In conclusion, the *B-raf*<sup>LSL-D594A</sup> conditional allele was successfully generated and can be regulated by Cre delivery. Mice and MEFs expressing the D594A mutation are an extremely important resource for studying the role of the kinase activity of B-Raf, and in studying the effects of D594 mutations in the development of cancer.

## 6. CHARACTERISATION OF *B-raf* KINASE INACTIVE MICE AND MEFs

### 6.1 Introduction

#### 6.1.1 *B-Raf* kinase activity

The best characterised role of B-Raf is as a key component of the Ras/Raf/MEK/ERK signalling pathway. Within this pathway, B-Raf activates MEK via phosphorylation. B-Raf has been shown to be the strongest MEK activator of the three Raf proteins. This has been concluded for a number of cell types including fibroblasts, neuronal tissue and lymphocytes (Hüser *et al.*, 2001; Catling *et al.*, 1994; Reuter *et al.*, 1995; Jaiswal *et al.*, 1994; Eychene *et al.*, 1995; Jaiswal *et al.*, 1996; Kao *et al.*, 2001). B-Raf plays many roles in the cell via activation of ERK1/2 in this pathway. These include roles in the suppression of apoptosis and in proliferation as described in Chapter 4. It is now being observed that protein kinases including Raf isoforms may have roles outside of their function as protein kinases. Chapter 3 shows that C-Raf does not require its kinase activity for its role in suppressing apoptosis. A kinase independent role of C-Raf in suppressing apoptosis is supported by the findings that kinase inactive forms of C-Raf are able to inhibit ASK1 induced apoptosis (Chen *et al.*, 2001). It is therefore of interest to discover if and how B-Raf may function in cells without its kinase activity.

Recent studies have identified that B-Raf plays a role in the development of malignant melanomas. Davies *et al.* (2002) screened 923 cancer samples and reported *B-RAF* somatic mis-sense mutations in 66 % of human malignant melanomas and 15 % of colorectal cancers. Mutations were found at a lower frequency in gliomas, lung cancers, sarcomas, ovarian carcinomas, breast cancers and liver cancers. Numerous mutations were observed in these cancer samples, the most frequently occurring mutation was V600E, and was shown to lead to increased B-RAF kinase activity (Wan *et al.*, 2004). Mutations were also found that led to impaired B-RAF activity, but were found to activate ERK via the activation of C-RAF (Wan *et al.*, 2004). However, one mutation that led to impaired B-RAF kinase activity was unable to activate ERK in COS or *Xenopus* cells. This mutant also did not phosphorylate MEK *in vitro*, or activate C-RAF or NF- $\kappa$ B in COS cells (Ikenoue *et al.*, 2003; Wan *et al.*, 2004). This mutant was D594V. D594 is an important catalytic residue located in the activation segment of protein kinases (Hanks and Hunter,

1995; Johnson *et al.*, 1998). The incidence of mutations at this site in cancer samples analysed is low, however, other mis-sense mutations at this site have been observed. The D594V mutation has also been observed in colon cancer (Yuen *et al.*, 2002). A D594E mutation has been detected in an invasive melanoma sample (Thomas *et al.*, 2004). D594G mutations have been observed in samples of primary melanoma (Deichmann *et al.*, 2004), melanocytic nevus (Kumar *et al.*, 2004), stomach cancer (Lee *et al.*, 2003), non-Hodgkin's lymphoma (Lee *et al.*, 2003), and colon cancer (Yuen *et al.*, 2002; Wang *et al.*, 2003; Fransen *et al.*, 2004). A D594K mutation was observed in two colon cancer samples (Yamamoto *et al.*, 2003). The frequency of D594 mutations observed in cancer samples would suggest it is not a random polymorphism. Similar mutations at this site are not observed for C-RAF or A-RAF. The role of D594 mutants in cancer is still unclear. It is possible that they may convey a dominant-negative effect on RAS to prevent a high level of ERK activity, as a number of these mutants have been observed in coincidence with RAS mutations (Yuen *et al.*, 2002; Houben *et al.*, 2004). Alternatively, D594 mutants may be involved in cancer via a yet undiscovered mechanism. Thus investigating the role of B-Raf in cells upon mutation of this residue is of added interest due to the discovery of D594 mutations in cancer samples.

## 6.2 Aims

Having generated mice carrying the D594A mutation in Chapter 5 (i.e. *B-raf*<sup>+/LSL-D594A</sup> mice), the aim of this chapter was to generate mice expressing this mutation by intercrossing these mice with mice from a Cre transgenic mouse strain, namely the deleter Cre strain. The resulting mice and MEFs generated could then be examined. Following on from the findings of chapter 4, which investigated the involvement of B-Raf in apoptosis and proliferation, the second aim of this chapter was to characterise the role of the kinase inactive mutant of B-Raf with respect to both proliferation and apoptosis using *B-raf*<sup>Lox-D594A/Lox-D594A</sup> MEFs. Cell growth and proliferation upon serum stimulation were analysed. The apoptotic phenotype was also assessed upon  $\alpha$ -CD95 antibody and serum withdrawal induced apoptosis.

## 6.3 Results

### 6.3.1 Generation of *B-raf*<sup>+/*Lox-D594A*</sup> mice

In order to examine the effects of permanent expression of D594A, deleter Cre mice were crossed with *B-raf*<sup>+/*LSL-D594A*</sup> mice, with the aim of Cre-mediated deletion producing mice heterozygote for expressing the mutation (*B-raf*<sup>+/*Lox-D594A*</sup> mice). It would then be possible to intercross the resulting mice to discover the phenotype of *B-raf*<sup>*Lox-D594A/Lox-D594A*</sup> offspring, homozygous for expressing the D594A kinase inactivating mutation. This would also allow the generation of *B-raf*<sup>*Lox-D594A/Lox-D594A*</sup> MEFs.

### 6.3.2 Preliminary evaluation of *B-raf*<sup>+/*LSL-D594A*</sup> + Cre mice

After a number of crosses between deleter Cre and *B-raf*<sup>+/*LSL-D594A*</sup> mice, it soon became apparent that the number of *B-raf*<sup>*LSL-D594A*</sup> + Cre offspring being produced was below the expected Mendelian frequency of 1 in 4 (Figure 6.1A). The frequency obtained for *B-raf*<sup>*LSL-D594A*</sup> Cre/+ mice (F1) was 1 in 13, from the 92 offspring produced in total (Table 6.1). Since the *B-raf*<sup>*LSL-D594A*</sup> Cre/+ mice would contain the *B-raf*<sup>*Lox-D594A*</sup> allele and be expressing *B-raf* D594A in many cells, these results suggest the mutated protein has detrimental effects on survival.

**Table 6.1** Summary of the genotype of the offspring produced from matings of deleter Cre mice and *B-raf*<sup>+/*LSL-D594A*</sup> mice.

Genotype	Number of offspring observed	Number of offspring expected
<i>B-raf</i> <sup>+/+</sup>	35	23
<i>B-raf</i> <sup>+/+</sup> Cre/+	32	23
<i>B-raf</i> <sup>+/<i>LSL-D594A</i></sup>	18	23
<i>B-raf</i> <sup>+/<i>LSL-D594A</i></sup> Cre/+	7	23
Total	92	92

Backcrossing of *B-raf*<sup>*LSL-D594A*</sup> Cre/+ mice led to the generation of mice regarded as expressing the D594A mutation in all cells, i.e. *B-raf*<sup>*Lox-D594A*</sup> mice (F2). Upon backcrossing of *B-raf*<sup>*LSL-D594A*</sup> Cre/+ mice with wild-type mice of the C57BL6 or MF-1 background strains, 16 *B-raf*<sup>*Lox-D594A*</sup> offspring were produced, this was below the expected Mendelian frequency (Table 6.2).

**Table 6.2** Summary of the genotype of the offspring produced from matings of wild type C57BL6 or MF-1 mice and *B-raf*<sup>+/*LSL-D594A*</sup> Cre/+ mice.

Genotype	Number of offspring observed	Number of offspring expected
<i>B-raf</i> <sup>+/+</sup>	28	22
<i>B-raf</i> <sup>+/<i>Lox-D594A</i></sup>	16	22
Total	44	44

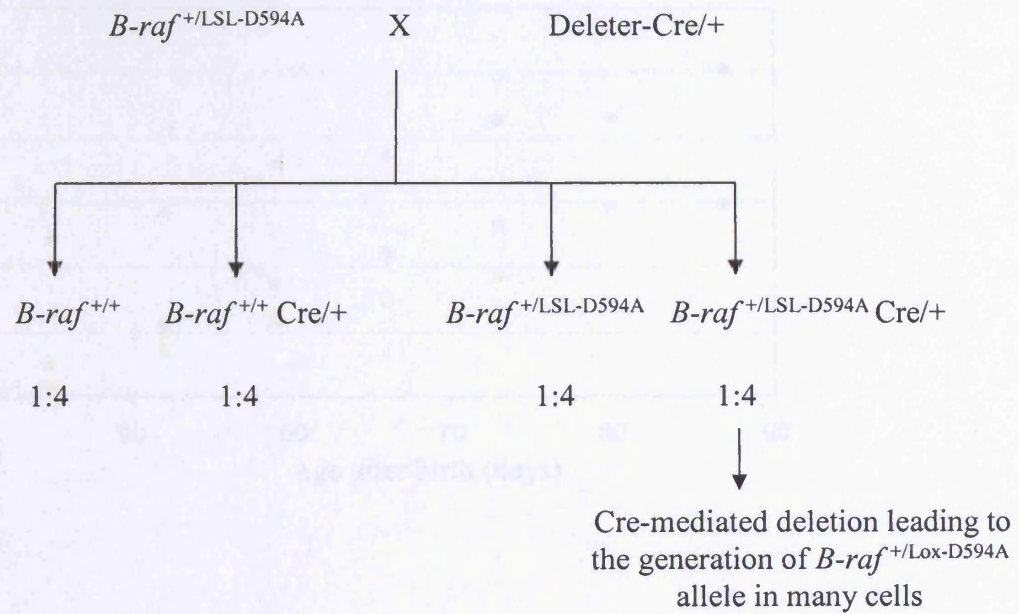
It was observed that many of the *B-raf*<sup>+/*Lox-D594A*</sup> mice appeared smaller than their *B-raf*<sup>+/+</sup> littermates within the early weeks after birth. This was more apparent for the male offspring (Figure 6.1B). Evaluation of the weights of *B-raf*<sup>+/*Lox-D594A*</sup> mice over time was carried out for two litters, one on the C57BL6 background and a second on the MF-1 background. The data obtained showed *B-raf*<sup>+/*Lox-D594A*</sup> male mice were significantly smaller than their *B-raf*<sup>+/+</sup> male littermates on both the C57BL6 and MF-1 backgrounds (Figure 6.2). The difference in weight of the female offspring was less pronounced (Figure 6.2).

Further evaluation of *B-raf*<sup>+/*Lox-D594A*</sup> mice showed that many died within 5 months of birth (Figure 6.3A). No significant differences were observed between strains. At the conclusion of this study the oldest living *B-raf*<sup>+/*Lox-D594A*</sup> mouse was 168 days old. Of all the *B-raf*<sup>+/*Lox-D594A*</sup> mice produced during this period, 48 % died (n=23). This strongly suggested the expression of the D594A mutation on one allele was having a detrimental effect on the *B-raf*<sup>+/*Lox-D594A*</sup> mice being generated. A reduced life-span was also observed for *B-raf*<sup>+/*LSL-D594A*</sup> Cre/+ (F1) mice, for which 54 % (n=11) died within 6 months of birth.

Further evaluation of the sick *B-raf*<sup>+/*Lox-D594A*</sup> mice showed some common abnormalities in their phenotype. Many were found to have sore eyes and a prolapsed rear end. Two *B-raf*<sup>+/*Lox-D594A*</sup> male mice had an abscess around the testes and one female mouse had a growth under the chin. A further female initially developed a prolapsed rear end, but this soon developed into paralysis of the hind legs. Post-mortems of 7 of the *B-raf*<sup>+/*Lox-D594A*</sup> mice that had died were carried out. It was observed that the mice had pale livers and some also had pale lungs and kidneys. Many had enlarged hearts. The major observation was that upon post-mortems all animals showed a significant enlargement of the spleen (Figure 6.4A).

**Figure 6.1** Generation of  $B\text{-raf}^{+/Lox-D594A}$  mice. **(A)** Genotypes of expected offspring from the intercross of  $B\text{-raf}^{+/LSL-D594A}$  and deleter-Cre mice. Ratios indicate expected frequency based on Mendelian inheritance. **(B)** Observation of the size comparison of  $B\text{-raf}^{+/Lox-D594A}$  mice with  $B\text{-raf}^{+/+}$  mice. Photograph showing a  $B\text{-raf}^{+/Lox-D594A}$  male mouse with a  $B\text{-raf}^{+/+}$  male littermate at 19 days old, on the MF-1 background. Actual weights of mice are indicated.

**A**



**B**



**Figure 6.2** Evaluation of the weights of *B-raf*<sup>f/Lox-D594A</sup> and *B-raf*<sup>f/+</sup> mice. Weights of *B-raf*<sup>f/Lox-D594A</sup> and *B-raf*<sup>f/+</sup> mice were recorded over a 90 day period for (A) mice on the C57BL6 background and (B) mice on the MF-1 background.

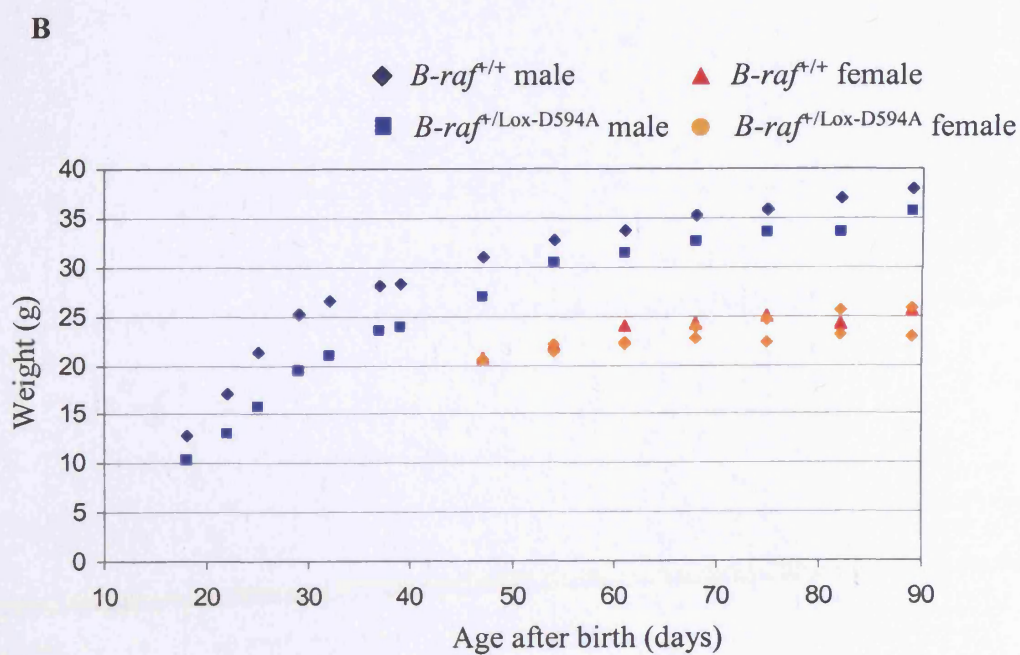
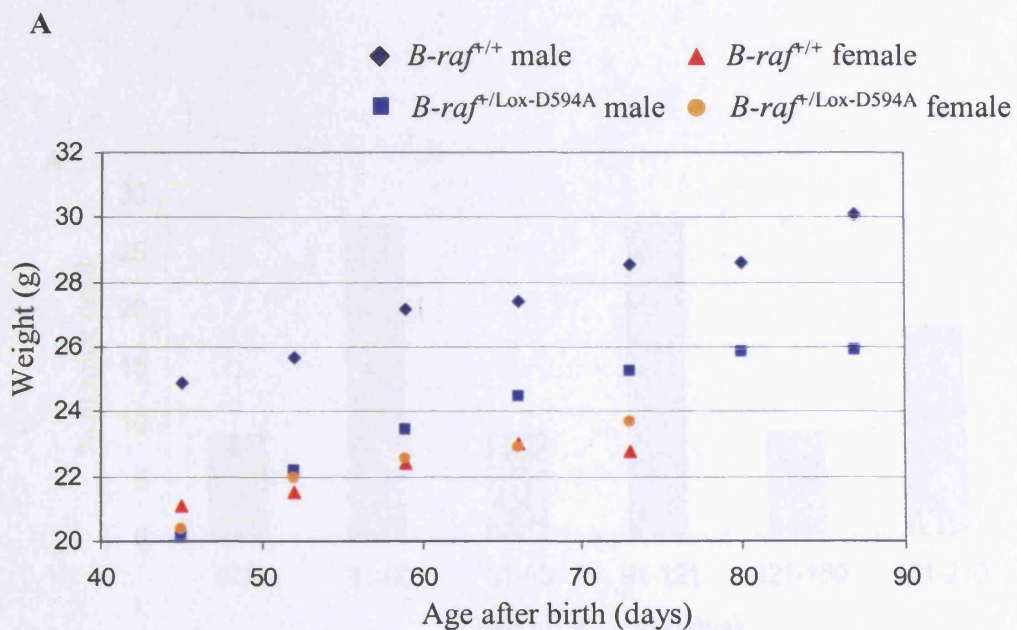


**Figure 6.3** Evaluation of deaths of *B-raf*<sup>f/Lox-D594A</sup> mice. Graph showing age groups at which *B-raf*<sup>f/Lox-D594A</sup> mice died.

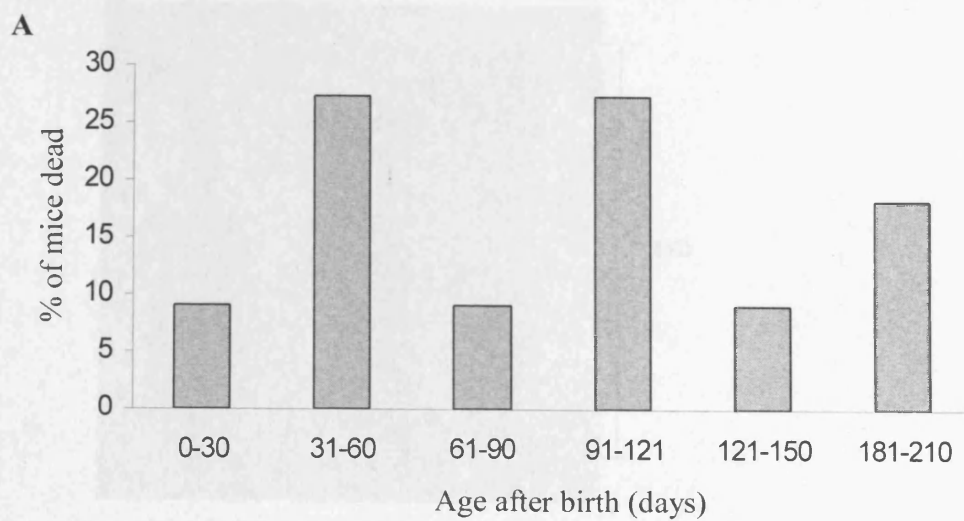
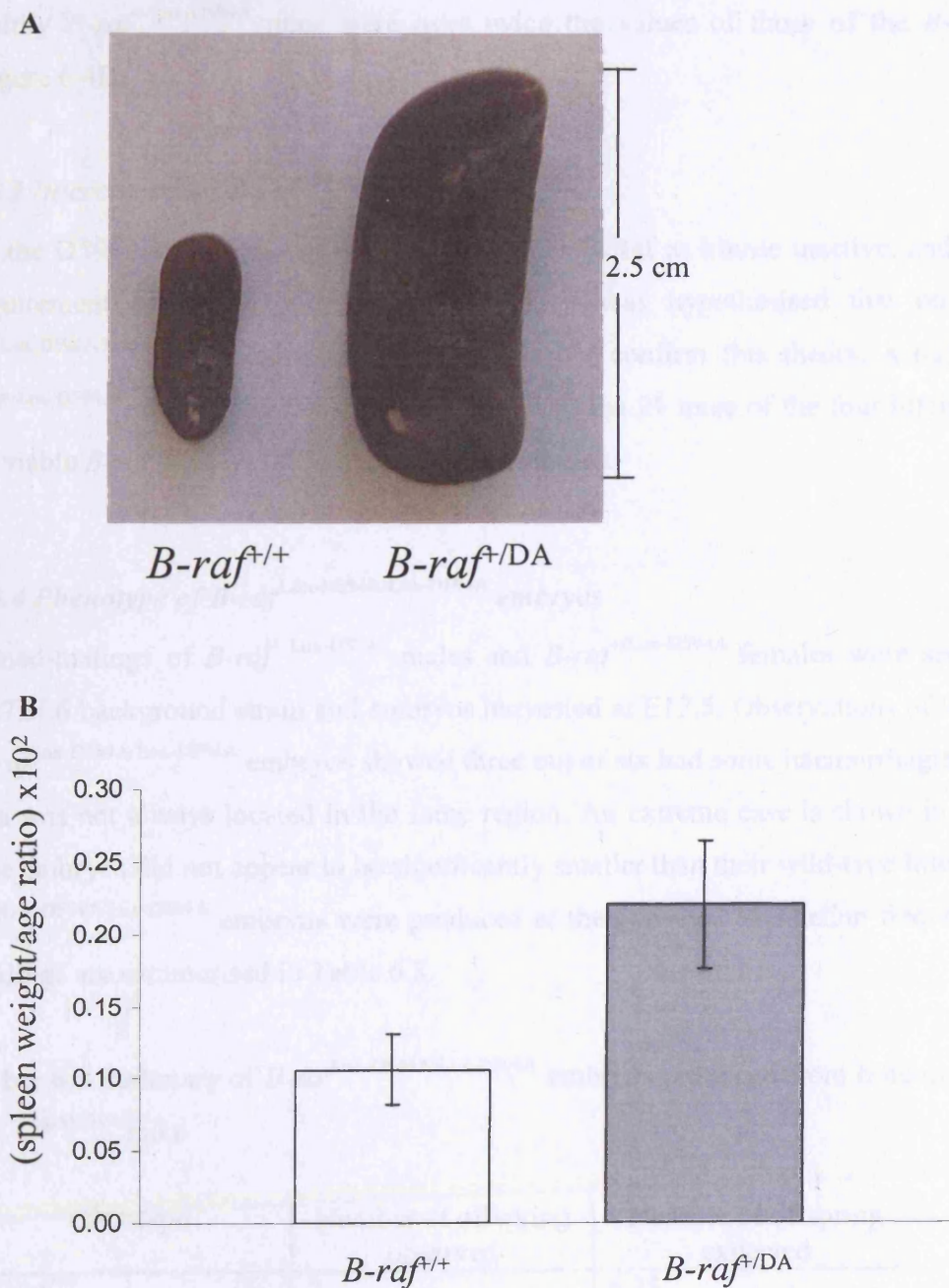


**Figure 6.4** Evaluation of spleens of  $B\text{-raf}^{\Delta/Lox-D594A}$  and  $B\text{-raf}^{\Delta/+}$  mice. (A) Photograph of spleens (following post-mortem and fixing in paraformaldehyde) from an unwell  $B\text{-raf}^{\Delta/Lox-D594A}$  mouse and a healthy  $B\text{-raf}^{\Delta/+}$  mouse (B) Graph showing the spleen weight/age ratios of spleens following post mortem of healthy  $B\text{-raf}^{\Delta/Lox-D594A}$  mice and their  $B\text{-raf}^{\Delta/+}$  littermates. Standard error bars are shown.



Due to the abnormal phenotype of the *B-raf*<sup>+/*Lox-D594A*</sup> mice, the remaining healthy mice were culled at the end of the project before showing any signs of illness. At this point, the spleen weights of all *B-raf*<sup>+/*Lox-D594A*</sup> mice and *B-raf*<sup>+/+</sup> littermates were recorded. Due to the wide range in ages of these mice, weight/age ratios were calculated to allow direct comparison of all the mice. These values were calculated for 9 *B-raf*<sup>+/*Lox-D594A*</sup> mice and 8 *B-raf*<sup>+/+</sup> mice. Pooled ratios for each genotype showed that the spleen weights of the healthy *B-raf*<sup>+/*Lox-D594A*</sup> mice were over twice the values of those of the *B-raf*<sup>+/+</sup> mice (Figure 6.4B).

### 6.3.3 Intercrosses of *B-raf*<sup>+/*Lox-D594A*</sup> mice

As the D594A mutation was expected to render B-Raf as kinase inactive, and due to the requirement of B-Raf during development, it was hypothesised that no viable *B-raf*<sup>*Lox-D594A*/*Lox-D594A*</sup> mice would be obtained. To confirm this theory, a number of *B-raf*<sup>+/*Lox-D594A*</sup> mice intercrosses were set up. From the 21 mice of the four litters produced, no viable *B-raf*<sup>*Lox-D594A*/*Lox-D594A*</sup> mice were obtained.

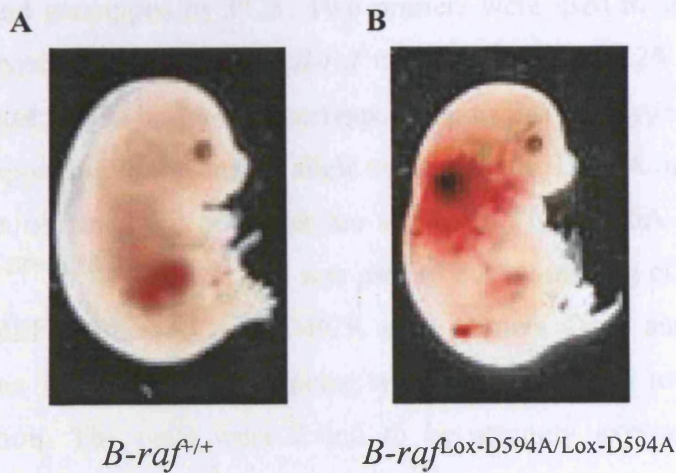
### 6.3.4 Phenotype of *B-raf*<sup>*Lox-D594A*/*Lox-D594A*</sup> embryos

Timed-matings of *B-raf*<sup>+/*Lox-D594A*</sup> males and *B-raf*<sup>+/*Lox-D594A*</sup> females were set up on the C57BL6 background strain and embryos harvested at E12.5. Observations of the resulting *B-raf*<sup>*Lox-D594A*/*Lox-D594A*</sup> embryos showed three out of six had some haemorrhaging, although this was not always located in the same region. An extreme case is shown in Figure 6.5. The embryos did not appear to be significantly smaller than their wild-type litter mates. *B-raf*<sup>*Lox-D594A*/*Lox-D594A*</sup> embryos were produced at the expected Mendelian frequency. These findings are summarised in Table 6.3.

**Table 6.3** Summary of *B-raf*<sup>*Lox-D594A*/*Lox-D594A*</sup> embryos produced from time-matings of *B-raf*<sup>+/*Lox-D594A*</sup> mice

Genotype	Number of offspring observed	Number of offspring expected
<i>B-raf</i> <sup>+/+</sup>	7	6.25
<i>B-raf</i> <sup>+/<i>Lox-D594A</i></sup>	12	12.5
<i>B-raf</i> <sup><i>Lox-D594A</i>/<i>Lox-D594A</i></sup>	6	6.25
<b>Total</b>	25	25

**Figure 6.5** Comparison of the phenotype of (A) *B-raf*<sup>f/+</sup> and (B) *B-raf*<sup>lox-D594A/Lox-D594A</sup> E12.5 embryos



#### 6.5.5 Analysis of *B-raf* expression levels in *B-raf*<sup>lox-D594A/Lox-D594A</sup> primary MEFs

To analyze the expression of the *B-raf*<sup>lox-D594A</sup> mutation had not had an effect on protein expression levels, a number of proteins were analyzed. Cytochrome c was lysed and lysates prepared and used for SDS-PAGE followed by electro-transfer to the nitrocellulose membrane. The blots were incubated with an anti-*B-raf*, an anti-*β-actin* or anti-*α-tubulin* antibody. Anti-*β-actin* antibody was used as a control for protein loading. The results showed no difference in *B-raf* protein expression levels between *B-raf*<sup>f/+</sup> and *B-raf*<sup>lox-D594A/Lox-D594A</sup> MEFs (Figure 6.5).

#### 6.5.6 Analysis of MEK and ERK phosphorylation in *B-raf*<sup>lox-D594A/Lox-D594A</sup> primary MEFs

To analyze if there was any difference in the phosphorylation of MEK and ERK, the *B-raf*<sup>lox-D594A/Lox-D594A</sup> MEFs were compared to *B-raf*<sup>f/+</sup> MEFs. The MEFs were cultured in DMEM supplemented with 10% fetal bovine serum (FBS) and treated with 100 ng/ml of PDGF or PDGF + FBS for 10, 30 and 60 minutes after induction. Protein lysates were analyzed for MEK and ERK phosphorylation by SDS-PAGE followed by electro-transfer to the nitrocellulose membrane.

### 6.3.5 Derivation of *B-raf*<sup>Lox-D594A/Lox-D594A</sup> primary MEFs

Primary MEFs were isolated from the *B-raf*<sup>Lox-D594A/Lox-D594A</sup> E12.5 embryos. Each MEF cell line was generated from a single embryo. DNA lysates were produced from each cell line and genotyped by PCR. Two primers were used to assess the presence of the *B-raf* wild-type allele and/or the *B-raf* mutant allele. Ocp125 and Ocp143 give rise to two products; a 570 bp product corresponding to the wild type allele and/or a 604 bp product corresponding to the mutant allele expressing the D594A mutation (Figure 5.13). The PCR results obtained for one litter are shown in Figure 6.6A Sequencing analysis of the *B-raf*<sup>Lox-D594A/Lox-D594A</sup> cell line was carried out by making cDNA from RNA extracted from the MEFs, followed by RT-PCR with primers Ocp3 and Ocp143. The resulting PCR product was sent for sequencing with primer Ocp115 to confirm the expression of the mutation. The cells were found to be strongly expressing the site-specific T to G nucleotide mutation targeted to exon 15 (Figure 6.6B).

### 6.3.6 Analysis of Raf protein expression levels in *B-Raf*<sup>Lox-D594A/Lox-D594A</sup> primary MEFs

To ensure the expression of the *B-raf* D594A mutation had not had an effect on protein expression levels, a number of proteins were assessed. Cycling cells were lysed, protein lysates prepared, and used for SDS-PAGE followed by electro-transfer of the proteins onto nitrocellulose. The blots were incubated with an  $\alpha$ -B-Raf, an  $\alpha$ -C-Raf, or an  $\alpha$ -A-Raf antibody. An  $\alpha$ -actin antibody was used as a control for protein loading. The results showed no differences in Raf protein expression levels between *B-raf*<sup>+/+</sup> and *B-raf*<sup>Lox-D594A/Lox-D594A</sup> MEFs (Figure 6.7).

### 6.3.7 Analysis of MEK and ERK phosphorylation in *B-Raf*<sup>Lox-D594A/Lox-D594A</sup> primary MEFs

To discover if there was any difference in the phosphorylation of MEK and ERK for *B-raf*<sup>Lox-D594A/Lox-D594A</sup> MEFs when compared to *B-raf*<sup>+/+</sup> MEFs, the MEFs were treated with different stimuli and the levels of phosphorylated proteins assessed. Cells were seeded at  $1.5 \times 10^6$  cells in 6 cm dishes until confluent. The cells were made quiescent for 30 minutes and stimulated with serum, EGF or PDGA. Cells were lysed at time points of 0, 2, 5, 10, 30 and 60 minutes after stimulation. Protein lysates were prepared and used for SDS-PAGE followed by electro-transfer of the proteins onto nitrocellulose. The blots were

**Figure 6.6** Analysis of MEFs arising from *B-raf*<sup>f/Lox-D594A</sup> intercross (A) PCR with primers Ocp125, and Ocp143 amplifying 570 bp and 604 bp products. Four of the MEF cell lines are positive for the 570 bp band, indicating they are *B-raf*<sup>f/+</sup>. Both bands are present for three cell lines, genotyping them as *B-raf*<sup>f/Lox-D594A</sup> and one cell line is identified as *B-raf*<sup>Lox-D594A/Lox-D594A</sup>, as only the 604 bp product corresponding to the mutant allele is present. Abbreviations: M = 1 Kb DNA ladder; numbers correspond to embryo number. (B) Sequencing results of *B-raf*<sup>Lox-D594A/Lox-D594A</sup> embryo number 5 to show the expression of the T → G nucleotide mutation. Mutated nucleotide is highlighted.

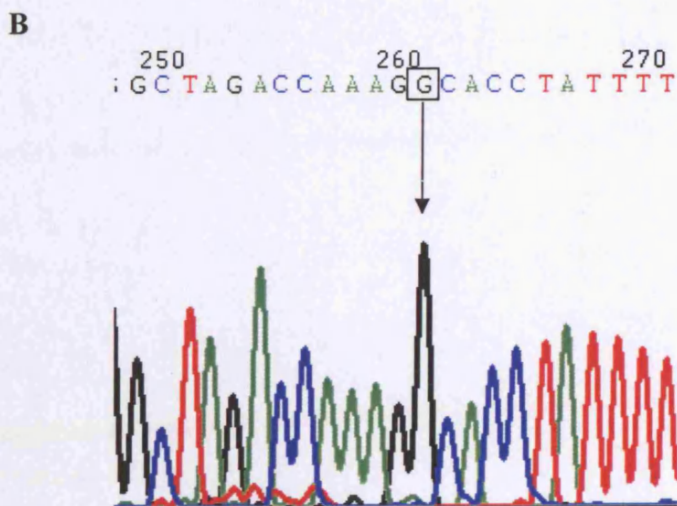
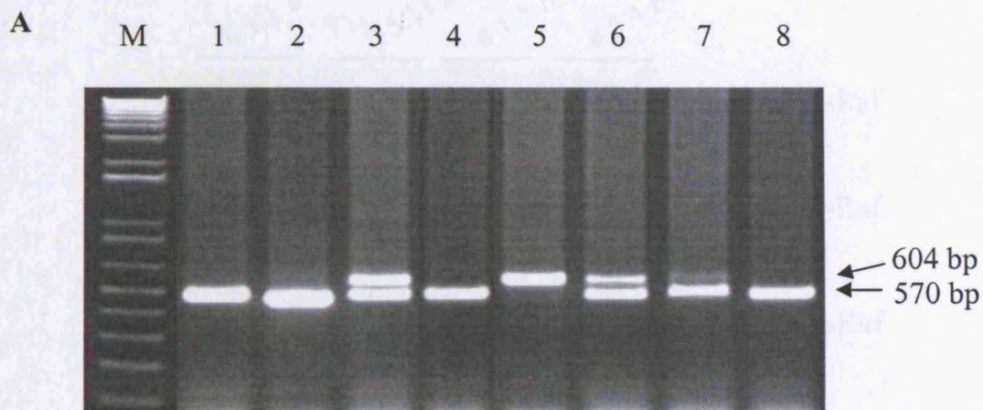
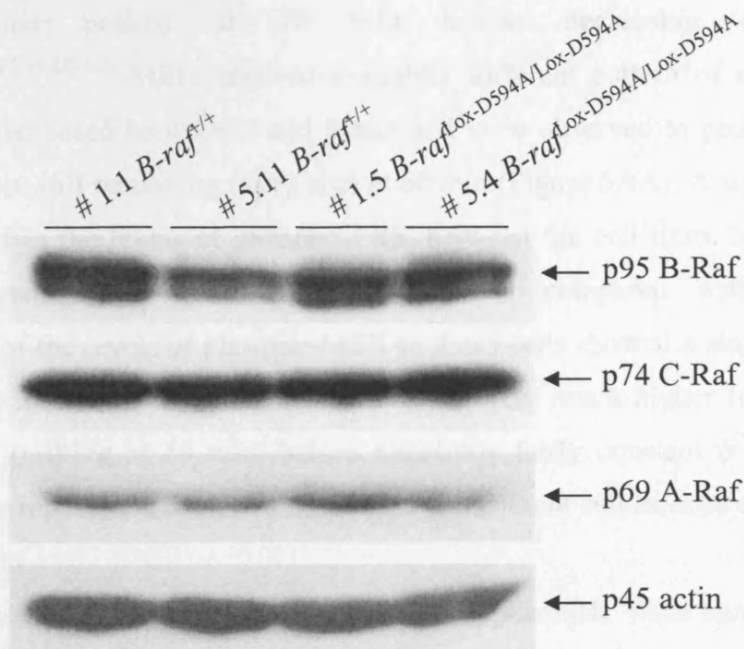


**Figure 6.7** Raf protein expression levels in *B-raf*<sup>f/+</sup> and *B-raf*<sup>Lox-D594A/Lox-D594A</sup> primary MEFs. Protein lysates were subject to Western blot analysis followed by detection of B-Raf, C-Raf, or A-Raf, and actin as a control for protein loading (lower panel).



incubated with an  $\alpha$ -phospho-ERK antibody to detect the levels of phospho-ERK in the MEFs. Serum stimulated MEFs were also incubated with an  $\alpha$ -phospho-MEK antibody to detect the levels of phospho-MEK. An  $\alpha$ -vinculin antibody was used as a control for protein loading.

Upon serum stimulation of the cells, levels of phospho-ERK in *B-raf*<sup>+/+</sup> MEFs gradually increased and peaked at 20 min before decreasing at 60 minutes. *B-raf*<sup>Lox-D594A/Lox-D594A</sup> MEFs showed a slightly different pattern of response; phospho-ERK levels increased between 2 and 5 min and were observed to peak at 10 min before decreasing, but still remaining fairly high at 60 min (Figure 6.8A). A significant difference was observed in the levels of phospho-ERK between the cell lines. Much greater levels were observed for *B-raf*<sup>Lox-D594A/Lox-D594A</sup> MEFs compared with *B-raf*<sup>+/+</sup> MEFs. Observation of the levels of phospho-MEK in these cells showed a similar pattern. Levels peaked at 20 min for *B-raf*<sup>+/+</sup> MEFs. The levels were much higher for *B-raf*<sup>Lox-D594A/Lox-D594A</sup> MEFs, peaking at 10 min, before remaining fairly constant (Figure 6.8A). These findings were repeated at least two times for two different cell lines of each genotype.

Upon treatment with EGF, higher levels of phospho-ERK were again observed for *B-raf*<sup>Lox-D594A/Lox-D594A</sup> MEFs when compared to *B-raf*<sup>+/+</sup> MEFs (Figure 6.8B). PDGF stimulation led to a slightly different outcome. The levels peaked at 10 min after stimulation for *B-raf*<sup>+/+</sup> MEFs, and for *B-raf*<sup>Lox-D594A/Lox-D594A</sup> MEFs, peaked at 2 min after treatment and remained at this level until reducing slightly at the 60 min time point (Figure 6.8C). Overall, the increase in the phospho-ERK levels observed for *B-raf*<sup>Lox-D594A/Lox-D594A</sup> MEFs was more significant upon PDGF treatment than upon treatment with EGF.

### 6.3.8 Analysis of *B-raf*<sup>+Lox-D594A</sup> primary MEFs

As shown above, analysis of *B-raf*<sup>Lox-D594A/Lox-D594A</sup> MEFs homozygous for the expression of the D594A mutation, showed an elevated level of phospho-ERK in these cells. To discover if this was also the case for *B-raf*<sup>+Lox-D594A</sup> heterozygous MEFs, *B-raf*<sup>+/+</sup> and *B-raf*<sup>+Lox-D594A</sup> MEFs were treated with serum and the levels of phospho-ERK assessed. Cells were grown until confluent, made quiescent and stimulated with 10 % serum. Cells were lysed at time points of 0, 2, 5, 10, 30 and 60 minutes after stimulation. Protein lysates were prepared, SDS-PAGE performed, followed by electro-transfer of the proteins onto

nitrocellulose. The blots were incubated with an  $\alpha$ -phospho-ERK antibody to detect the levels of phospho-ERK in the MEFs. An  $\alpha$ -ERK2 antibody was used as a control for protein loading. Upon serum stimulation of the cells, levels of phospho-ERK in *B-raf*<sup>+/+</sup> MEFs gradually increased and peaked at 20 min before decreasing at 60 minutes. *B-raf*<sup>+/*Lox-D594A*</sup> MEFs showed a slightly different pattern of response; phospho-ERK levels were observed to peak at 10 min before decreasing, but still remaining fairly high at 60 min (Figure 6.8B). A significant difference was observed in the overall levels of phospho-ERK between the two cell lines. Much greater levels being observed for *B-raf*<sup>+/*Lox-D594A*</sup> MEFs compared to *B-raf*<sup>+/+</sup> MEFs.

### 6.3.9 Analysis of the growth characteristics of *B-raf*<sup>*Lox-D594A/Lox-D594A*</sup> primary MEFs

The growth of the *B-raf*<sup>*Lox-D594A/Lox-D594A*</sup> MEFs was analysed by daily measurements of the number of cells present. *B-raf*<sup>+/+</sup> and *B-raf*<sup>*Lox-D594A/Lox-D594A*</sup> MEFs were seeded at  $1 \times 10^4$  cells per well in 24 well plates. 48 hour after seeding the number of cells present per well was counted using a haemocytometer. This was carried out in triplicate and recorded. Counting was repeated for the subsequent 6 days. The values obtained were used to produce growth curves for *B-raf*<sup>+/+</sup> (1.1, 5.6 and 5.11) and *B-raf*<sup>*Lox-D594A/Lox-D594A*</sup> MEFs (1.5, 5.3 and 5.4). The growth curves obtained showed that *B-raf*<sup>*Lox-D594A/Lox-D594A*</sup> MEFs grew at a faster rate than *B-raf*<sup>+/+</sup> MEFs (n=12; p=0.003; Figure 6.9). The rate of growth increased steadily over the time course for *B-raf*<sup>*Lox-D594A/Lox-D594A*</sup> MEFs, but appears to plateau after 7 days for *B-raf*<sup>+/+</sup> MEFs. The data represents pooled data for each genotype from 6 data sets. The increase in growth observed could be due to a decrease in apoptosis, an increase in proliferation, or a combination of both.

### 6.3.10 Analysis of ERK phosphorylation upon serum stimulation for 20 hours in *B-Raf*<sup>*Lox-D594A/Lox-D594A*</sup> primary MEFs

Sustained ERK activation were measured upon serum stimulation by assessing levels of phospho-ERK in the *B-raf*<sup>+/+</sup> and *B-raf*<sup>*Lox-D594A/Lox-D594A*</sup> MEFs. Cells were seeded at  $1.5 \times 10^6$  in 6 cm dishes. Cells were made quiescent for 24 hours, followed by the addition of serum. Cells were lysed at time points of 0, 0.5, 1, 3, 5, 10 and 20 hours after stimulation. Protein lysates were prepared and SDS-PAGE carried out followed by electro-transfer of

**Figure 6.8** MEK and ERK phosphorylation in *B-raf*<sup>Lox-D594A</sup> homozygous and heterozygous primary MEFs over a time course of stimulation (0 to 60 min). **(A)** Protein lysates from *B-raf*<sup>+/+</sup> and *B-raf*<sup>Lox-D594A/Lox-D594A</sup> MEFs were analysed by Western blot analysis followed by stimulation with 10 % serum and detection of phospho-ERK and phospho-MEK. Phospho-ERK was also analysed upon stimulation with 10 ng/ml epidermal growth factor and 50 ng/ml platelet-derived growth factor. Vinculin was used as a control for protein loading (lower panel). **(B)** *B-raf*<sup>+/+</sup> and *B-raf*<sup>+/Lox-D594A</sup> primary MEFs over a time course of stimulation (0 to 60 min) Protein lysates from *B-raf*<sup>+/+</sup> and *B-raf*<sup>+/Lox-D594A</sup> MEFs were analysed by Western blot analysis followed by stimulation with 10 % serum and detection of phospho-ERK (upper panel) and total ERK as a control for protein loading (lower panel).

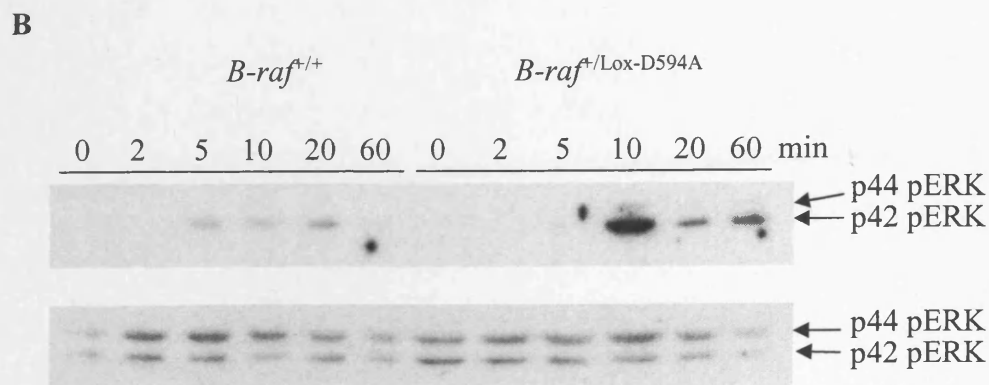
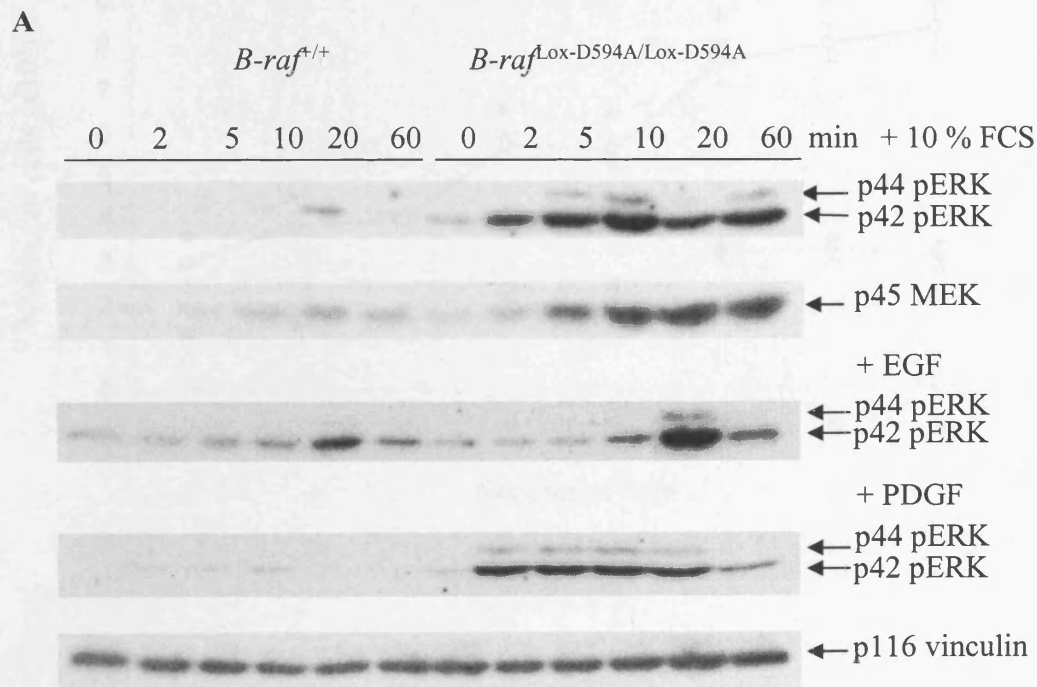
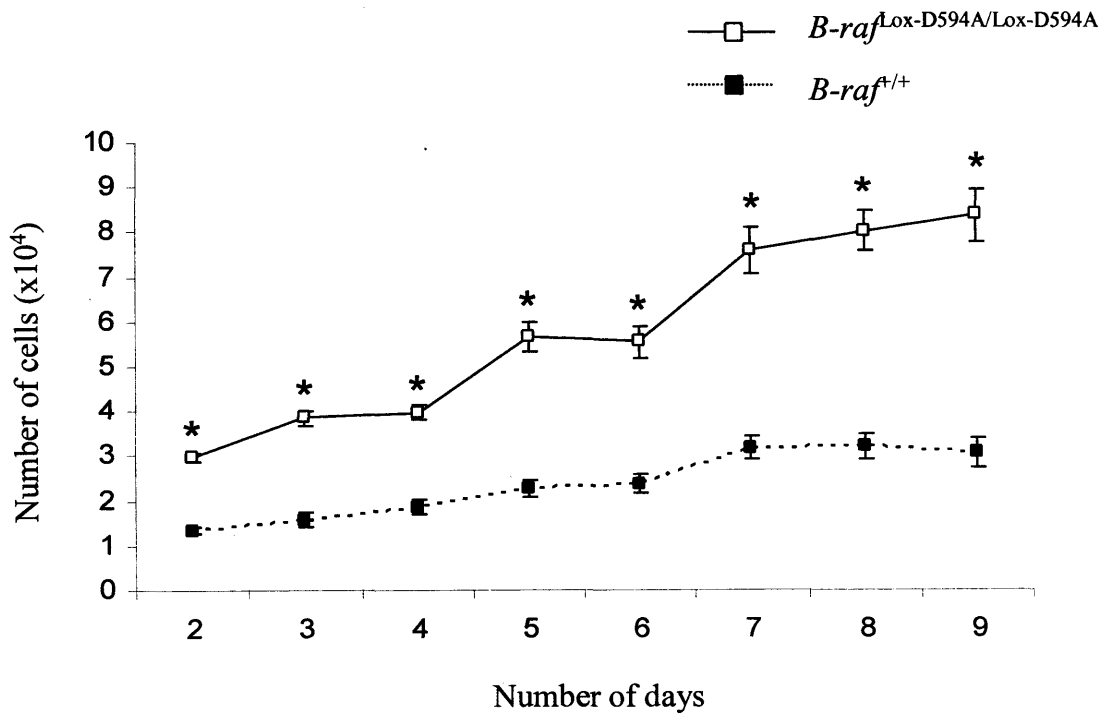


**Figure 6.9** Analysis of the growth characteristics of *B-raf*<sup>+/+</sup> and *B-raf*<sup>Lox-D594A/Lox-D594A</sup> primary MEFs. Cell counts were performed over a period of 8 days and growth profiles produced. Pooled data for *B-raf*<sup>+/+</sup> (closed squares) and *B-raf*<sup>Lox-D594A/Lox-D594A</sup> (opened squares) are indicated. Standard error bars are shown. A *P* value was generated for the overall growth rate of *B-raf*<sup>Lox-D594A/Lox-D594A</sup> MEFs via a paired t-Test against *B-raf*<sup>+/+</sup> MEFs. (\* = *P* ≤ 0.05).



the proteins onto nitrocellulose. The blots were incubated with an  $\alpha$ -phospho-ERK antibody to observe the levels of phospho-ERK in the MEFs. An  $\alpha$ -actin antibody was used as a control for protein loading. The results show that for *B-raf*<sup>Lox-D594A/Lox-D594A</sup> MEFs the phospho-ERK levels increased upon stimulation and peaked at 0.5 h, before decreasing back to basal levels by 5 h after stimulating. However, phospho-ERK levels were much lower for *B-raf*<sup>+/+</sup> MEFs (Figure 6.10).

### **6.3.11 Analysis of proteins involved in the G1 to S phase of the cell cycle in *B-Raf*<sup>Lox-D594A/Lox-D594A</sup> primary MEFs**

To investigate what may be leading to the differences in the rate of cell growth observed for *B-raf*<sup>Lox-D594A/Lox-D594A</sup> and *B-raf*<sup>+/+</sup> MEFs, some of the proteins known to be involved in the G1 to S phase of the cell cycle were analysed. This was carried out due to findings in Chapter 4, showing that the rate of cell growth in *B-raf*<sup>-/-</sup> MEFs may have been affected by the levels of some of these proteins. Cells were seeded at  $1.5 \times 10^6$  cells in 6 cm dishes. At 60 % confluency, cells were made quiescent by placing in reduced serum media for 24 hours. Cells were stimulated by the addition of serum and the cell lysed at 0, 0.5, 1, 3, 5, 10 and 20 hours after stimulating. SDS-PAGE of the protein lysates produced was carried out followed by electro-transfer of the proteins onto nitrocellulose. A number of blots were produced using this method, each used to investigation the presence of proteins involved in the G1 to S phase of the cell cycle. Each set of findings were repeated at least two times for two different cell lines of each genotype.

$\alpha$ -cyclin D1 antibody was used to discover levels of cyclin D1 upon serum stimulation, an  $\alpha$ -cdk4 antibody for cdk4 levels, and an  $\alpha$ -p27<sup>KIP1</sup> antibody for p27<sup>KIP1</sup> levels. An  $\alpha$ -actin antibody was used as a control for protein loading. The results showed the highest levels of cyclin D1 were observed after 20 h of serum stimulation for both cell lines. However, the levels observed for *B-raf*<sup>Lox-D594A/Lox-D594A</sup> MEFs over the time course were markedly elevated when compared to *B-raf*<sup>+/+</sup> MEFs (Figure 6.10) Low levels of cdk4 protein were detected for *B-raf*<sup>+/+</sup> MEFs between 1 and 3 hours of serum stimulation. The levels decreased over the remainder of the time course. The levels observed for *B-raf*<sup>Lox-D594A/Lox-D594A</sup> MEFs appeared to remain constant over the time course of serum stimulation, and were significantly higher to those observed for *B-raf*<sup>+/+</sup> MEFs (Figure 6.10). Investigations



into the protein levels of p27<sup>KIP1</sup> showed the levels of p27<sup>KIP1</sup> proteins were barely detectable for *B-raf*<sup>+/+</sup> MEFs. In contrast, for *B-raf*<sup>Lox-D594A/Lox-D594A</sup> MEFs, p27<sup>KIP1</sup> protein levels increased after 3 hours of serum stimulation, the levels subsequently decrease, before peaking at 20 hours (Figure 6.10).

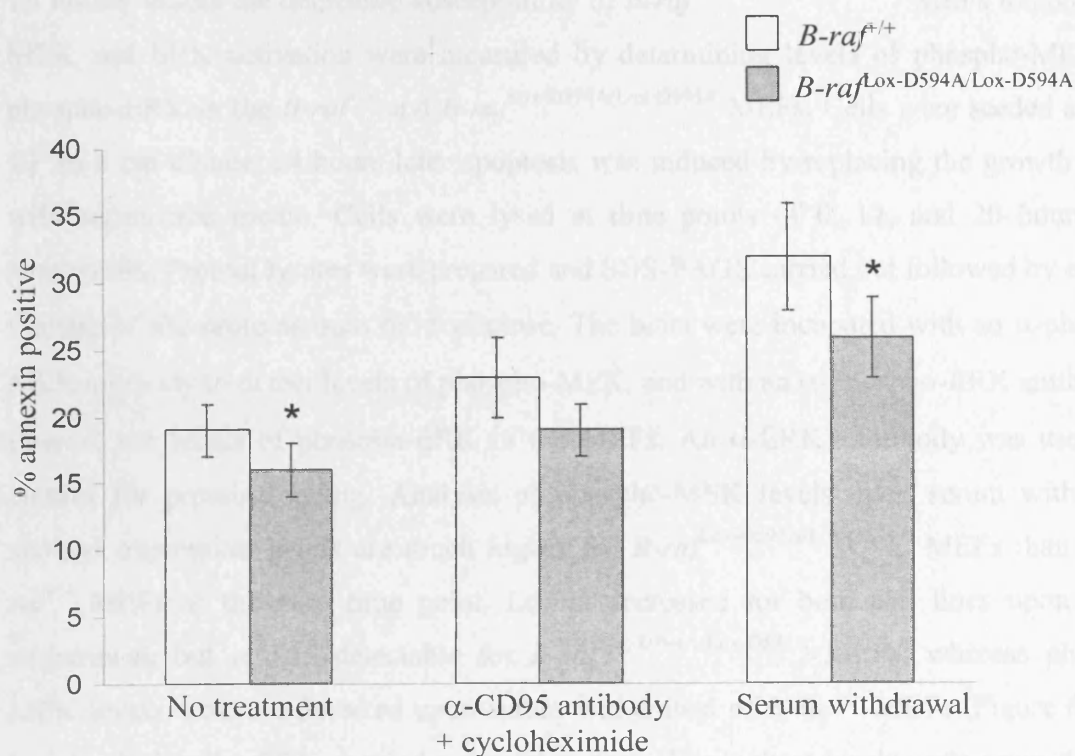
### **6.3.12 Analysis of the apoptotic phenotype of *B-raf*<sup>Lox-D594A/Lox-D594A</sup> primary MEFs upon $\alpha$ -CD95 induction**

To assess apoptosis upon  $\alpha$ -CD95 antibody treatment, *B-raf*<sup>+/+</sup> and *B-raf*<sup>Lox-D594A/Lox-D594A</sup> MEFs were plated at a density of  $1.5 \times 10^6$  cells onto 6 cm dishes. The cells were fed with growth media 24 hours after plating. Apoptosis was induced 24 hours later by the addition of 50 ng/ml anti-CD95 antibody and 0.5  $\mu$ M cycloheximide for 20 hours. Suspended and attached cells were collected, annexin V FITC staining performed and PI added, followed by FACS analysis. The experiment was performed on three separate occasions. The results show there is a trend towards a decrease in apoptosis for *B-raf*<sup>Lox-D594A/Lox-D594A</sup> MEFs (1.5, 5.3 and 5.4) when compared with *B-raf*<sup>+/+</sup> MEFs (1.1, 5.6 and 5.11). The decrease in apoptosis is seen for *B-raf*<sup>Lox-D594A/Lox-D594A</sup> MEFs in both untreated cells and cells treated with  $\alpha$ -CD95 antibody. Pooling the data from each cell line and each experiment gave an average percentage of apoptosis for the untreated *B-raf*<sup>+/+</sup> MEFs of 19 %  $\pm$  2 and this decreased to 16 %  $\pm$  2 (n=12;  $P=0.07$ ) in the untreated *B-raf*<sup>Lox-D594A/Lox-D594A</sup> MEFs. Upon  $\alpha$ -CD95 induction apoptosis levels of 19 %  $\pm$  2 were observed for *B-raf*<sup>Lox-D594A/Lox-D594A</sup> MEFs whereas for *B-raf*<sup>+/+</sup> MEFs a value of 23 %  $\pm$  3 (n=12;  $P=0.46$ ) was obtained (Figure 6.11). Although overall these values are not significant, they show a trend towards a reduction in apoptosis.

### **6.3.13 Analysis of the apoptotic phenotype of *B-raf*<sup>Lox-D594A/Lox-D594A</sup> and *B-raf*<sup>+/+</sup> primary MEFs upon serum withdrawal**

To investigate the phenotype of the *B-raf*<sup>Lox-D594A/Lox-D594A</sup> MEFs upon serum withdrawal, MEFs were plated at a density of  $1.5 \times 10^6$  cells onto 6 cm dishes and the media changed 24 hours after plating. After a further 24 hours, apoptosis was induced by placing cells into serum-free media for 20 hours. Cells were harvested and annexin V FITC staining and FACS analysis performed as described previously. The results showed there was a significant decrease in apoptosis for *B-raf*<sup>Lox-D594A/Lox-D594A</sup> MEFs (1.5, 5.3 and 5.4) compared with *B-raf*<sup>+/+</sup> MEFs (1.1, 5.6 and 5.11). Upon serum withdrawal the pooled

**Figure 6.11** Apoptotic analysis of *B-raf*<sup>f/+</sup> and *B-raf*<sup>Lox-D594A/Lox-D594A</sup> primary MEFs. MEFs were induced to undergo apoptosis by treating with 50 ng/ml  $\alpha$ -CD95 antibody plus 0.5  $\mu$ M cycloheximide, or by serum withdrawal, or left untreated. Apoptosis was determined using annexin V FITC staining followed by flow cytometric analysis. Graph represents pooled data for *B-raf*<sup>f/+</sup> and *B-raf*<sup>Lox-D594A/Lox-D594A</sup> MEFs (n=12). Standard error bars are shown. *P* values were generated for *B-raf*<sup>Lox-D594A/Lox-D594A</sup> MEFs via paired t-Tests against *B-raf*<sup>f/+</sup> MEFs for both treated and untreated cells. (\* = *P*≤0.05).



percentage of apoptosis observed was  $32 \% \pm 3$  for *B-raf*<sup>+/+</sup> MEFs and this value decreased to  $26 \% \pm 6$  for *B-raf*<sup>Lox-D594A/Lox-D594A</sup> MEFs (n=12; *P*=0.01; Figure 6.11). The results show that B-Raf cells are significantly more prone to apoptosis induced by serum withdrawal than via  $\alpha$ -CD95 antibody, and that *B-raf*<sup>Lox-D594A/Lox-D594A</sup> MEFs show a reduced susceptibility to apoptosis when compared to *B-raf*<sup>+/+</sup> MEFs for both treatments.

#### **6.3.14 Analysis of MEK and ERK phosphorylation of *B-raf*<sup>Lox-D594A/Lox-D594A</sup> primary MEFs upon induction of apoptosis by serum withdrawal**

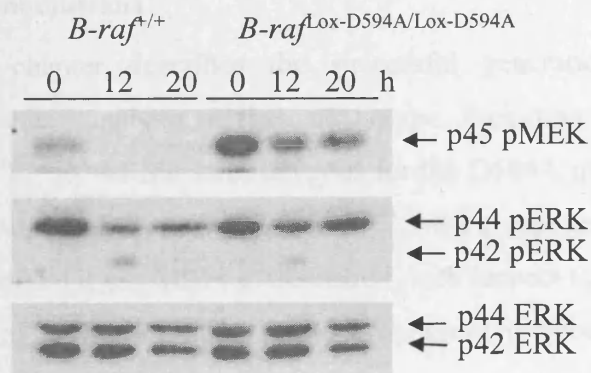
To further assess the decreased susceptibility of *B-raf*<sup>Lox-D594A/Lox-D594A</sup> MEFs to apoptosis, MEK and ERK activation were measured by determining levels of phospho-MEK and phospho-ERK in the *B-raf*<sup>+/+</sup> and *B-raf*<sup>Lox-D594A/Lox-D594A</sup> MEFs. Cells were seeded at  $1.5 \times 10^6$  in 6 cm dishes. 24 hours later apoptosis was induced by replacing the growth media with serum-free media. Cells were lysed at time points of 0, 12, and 20 hours after stimulation. Protein lysates were prepared and SDS-PAGE carried out followed by electro-transfer of the proteins onto nitrocellulose. The blots were incubated with an  $\alpha$ -phospho-MEK antibody to detect levels of phospho-MEK, and with an  $\alpha$ -phospho-ERK antibody to observe the levels of phospho-ERK in the MEFs. An  $\alpha$ -ERK1 antibody was used as a control for protein loading. Analysis of phospho-MEK levels upon serum withdrawal showed expression levels are much higher for *B-raf*<sup>Lox-D594A/Lox-D594A</sup> MEFs than for *B-raf*<sup>+/+</sup> MEFs at the zero time point. Levels decreased for both cell lines upon serum withdrawal, but remain detectable for *B-raf*<sup>Lox-D594A/Lox-D594A</sup> MEFs, whereas phospho-MEK levels were not detected upon serum withdrawal of *B-raf*<sup>+/+</sup> MEFs (Figure 6.12A). Levels of phospho-ERK showed a similar pattern. The highest levels were again detected at the zero time point for both cell lines and appeared slightly higher for *B-raf*<sup>Lox-D594A/Lox-D594A</sup> MEFs. Upon serum withdrawal levels decreased, but remained detectable for both cell lines. However, phospho-ERK levels for *B-raf*<sup>Lox-D594A/Lox-D594A</sup> MEFs were significantly elevated when compared to *B-raf*<sup>+/+</sup> MEFs (Figure 6.12A).

#### **6.3.15 Analysis of Thr125-phospho-specific caspase 9 levels upon EGF stimulation of *B-Raf*<sup>Lox-D594A/Lox-D594A</sup> primary MEFs**

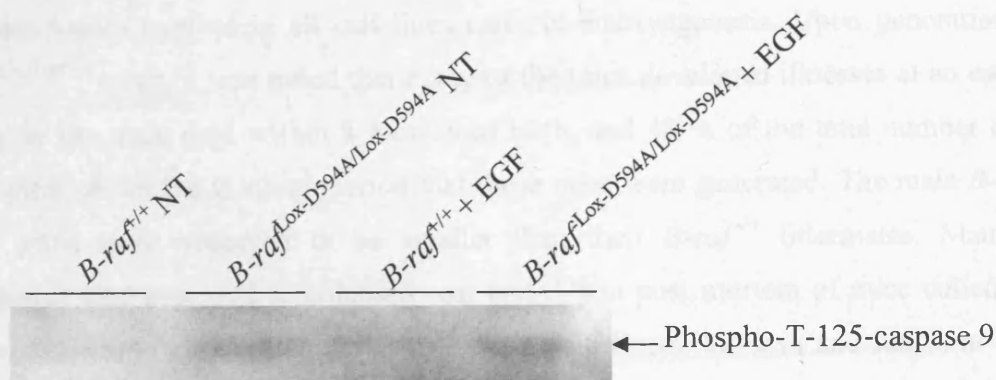
In Chapter 4 it was shown that the increase in apoptosis observed for *B-raf*<sup>-/-</sup> cells strongly correlated with the phosphorylation of Thr-125 caspase 9 levels. To assess if the levels of phospho-Thr-125 caspase 9 were altered in *B-raf*<sup>Lox-D594A/Lox-D594A</sup> MEFs, cells were

**Figure 6.12** ERK and T-125 caspase 9 phosphorylation in *B-raf*<sup>+/+</sup> and *B-raf*<sup>Lox-D594A/Lox-D594A</sup> primary MEFs upon stimulation. (A) MEK and ERK phosphorylation of *B-raf*<sup>+/+</sup> and *B-raf*<sup>Lox-D594A/Lox-D594A</sup> primary MEFs over a time course of induced apoptosis by serum withdrawal (0 to 20 hours). Protein lysates were analysed by Western blot analysis followed by detection of phospho-MEK (upper panel), phospho-ERK (middle panel) and ERK1 as a control for protein loading (lower panel) (B) *B-raf*<sup>+/+</sup> and *B-raf*<sup>Lox-D594A/Lox-D594A</sup> MEFs were left untreated (NT) or stimulated by the addition of 25 ng/ml epidermal growth factor (EGF) for 5 min. Immunoprecipitated protein lysates were analysed by Western blot analysis followed by detection of phospho-Thr125-specific caspase 9. 0.25mg of protein was loaded per well of the SDS PAGE gel.

A



B



seeded in 10 cm plates until fully confluent and apoptosis induced by placing in serum-free media for 48 hours. MEFs were then left untreated or treated with 25 ng/ml EGF for 5 min. The cells were lysed and an immuno-precipitation assay performed using 1 mg of protein per sample and an  $\alpha$ -caspase 9 antibody. SDS-PAGE of 0.25 mg of protein lysate/cell line was carried out followed by electro-transfer of the proteins onto nitrocellulose. The blots were incubated with an  $\alpha$ -Thr125-phospho-specific caspase 9 antibody. The results showed that there was an increase in phospho-Thr-125 caspase 9 levels in *B-raf*<sup>Lox-D594A/Lox-D594A</sup> MEFs when compared to *B-raf*<sup>+/+</sup> MEFs (Figure 6.12B). Due to time constraints this experiment was only undertaken once and therefore needs to be repeated to confirm these initial findings.

## 6.4 Conclusions

This chapter describes the successful generation of *B-raf*<sup>+/Lox-D594A</sup> mice and the subsequent analysis of their phenotype. Preliminary analysis was also carried out for *B-raf*<sup>+/Lox-D594A</sup> MEFs, heterozygous for the D594A mutation. Also detailed is the successful generation of *B-raf*<sup>Lox-D594A/Lox-D594A</sup> MEFs expressing the D594A mutation. Subsequent analysis of these MEFs is described, with respect to the role of the D594A mutation in cell growth, proliferation and the suppression of apoptosis.

To aid in the production of *B-raf*<sup>Lox-D594A/Lox-D594A</sup> MEFs, *B-raf*<sup>+/Lox-D594A</sup> mice were produced by crossing *B-raf*<sup>+/LSL-D594A</sup> mice with deleter-Cre transgenic mice in which Cre is ubiquitously expressed in all cell lines early in embryogenesis. Upon generation of *B-raf*<sup>+/Lox-D594A</sup> mice, it was noted that many of the mice developed illnesses at an early age. Many of the mice died within 5 months of birth, and 48 % of the total number of these mice died within the 9 month period that these mice were generated. The male *B-raf*<sup>+/Lox-D594A</sup> mice were observed to be smaller than their *B-raf*<sup>+/+</sup> littermates. Many mice developed sore eyes and a prolapsed rear end. Upon post mortem of mice culled due to illness, the majority were observed as having pale livers, kidneys and lungs, as well as enlarged hearts and spleens. The enlargement of the spleen, known as splenomegaly, was the most prominent feature upon post mortem. The spleens were significantly larger than their wild type littermates, even for mice that physically appeared healthy.

The phenotypic characteristics observed for the *B-raf*<sup>+/*Lox*-D594A</sup> mice relate to those characterised for spontaneous lymphomas. The Bethesda proposal for classification of lymphoid neoplasms in mice (Morse III *et al.*, 2002) states the characteristics of a precursor B cell lymphoblastic lymphoma/leukaemia (Pre-B LBL) are “splenomegaly, generalized lymphadenopathy, usually with extensive spread to liver, kidney, and lungs, sometimes to meninges with skull exostoses and hind limb paralysis”. Many of these characteristics were observed for the *B-raf*<sup>+/*Lox*-D594A</sup> mice. Within the literature, one study found a D594G mutation in human *B-RAF* upon screening of non-Hodgkin’s lymphoma tumours (Lee *et al.*, 2003c). Unfortunately it was not within the scope of this project to further characterise the *B-raf*<sup>+/*Lox*-D594A</sup> mice to establish whether they had a form of lymphoma. If more time had been available it would have been of great interest to carry out further analysis of these mice to confirm that they are subject to spontaneous lymphomas. During the project a number of organs were fixed upon post-mortem. It would be of interest to carry out histological studies on these fixed organs to characterise the cells and discover if the results agreed with the potential diagnosis of spontaneous lymphoma. Upon firm diagnosis of the symptoms observed for the *B-raf*<sup>+/*Lox*-D594A</sup> mice, studies could then be carried out to discover the exact role the B-Raf D594A mutation is playing in the development of neoplasia in these mice.

Intercrossing of *B-raf*<sup>+/*Lox*-D594A</sup> mice led to the generation of *B-raf*<sup>*Lox*-D594A/*Lox*-D594A</sup> E12.5 embryos occurred at the expected Mendelian frequency, although haemorrhaging of a number of these embryos was noted. This suggests that although *B-raf*<sup>*Lox*-D594A/*Lox*-D594A</sup> embryos were successfully obtained at this stage in development, they may not have been obtained at a slightly later stage. Indeed, viable *B-raf*<sup>*Lox*-D594A/*Lox*-D594A</sup> pups were not produced. This shows that the kinase activity of B-Raf is essential during embryonic development and cannot be compensated by the other Raf isoforms.

Although haemorrhaging was observed for three out of six of the *B-raf*<sup>*Lox*-D594A/*Lox*-D594A</sup> embryos, no other abnormal phenotypes were observed. A previous study reported *B-raf*<sup>-/-</sup> embryos as having haemorrhaging in the ventral region, enlarged and irregularly shaped large blood vessels and rupturing of the endothelial cell layers of the vessels leading to extravasation of blood. *B-raf*<sup>-/-</sup> embryos were also smaller than their wild-type counterparts (Wojnowski *et al.*, 1997). Detailed analysis of the *B-raf*<sup>*Lox*-D594A/*Lox*-D594A</sup> embryos was not carried out, although no differences in size were observed when compared to *B-raf*<sup>+/+</sup>

embryos. Therefore more analysis would be required to discover if the phenotype of the *B-raf*<sup>Lox-D594A/Lox-D594A</sup> embryos is similar to that of the *B-raf*<sup>-/-</sup> embryos.

Assessment of the phospho-MEK levels of *B-raf*<sup>Lox-D594A/Lox-D594A</sup> MEFs showed the levels were significantly elevated when compared to *B-raf*<sup>+/+</sup> MEFs upon stimulation with various growth factors. As MEK is responsible for activating ERK, the elevated levels of phospho-ERK observed confirmed this finding. Since the D594A mutation was thought to render B-Raf kinase inactive, these findings are surprising. Previous findings have stated that mutation of this conserved residue is known to render protein kinases inactive (Johnson *et al.*, 1998). Indeed, a mutation of this residue found in cancer cells was shown to have impaired B-RAF kinase activity and was unable to activate ERK in COS cells. This mutant was also unable to phosphorylate MEK *in vitro*, or activate C-RAF or NF-κB in cells (Ikenoue *et al.*, 2003; Wan *et al.*, 2004). Sequencing analysis of the *B-raf*<sup>Lox-D594A/Lox-D594A</sup> MEFs had confirmed the mutation was being expressed in the cells and therefore the increased activity of MEK and ERK was unclear, given that B-Raf is known to be a major MEK/ERK activator in MEFs (Hüser *et al.*, 2001; Pritchard *et al.*, 2004). Due to the abnormal characteristics of the *B-raf*<sup>+/Lox-D594A</sup> mice, *B-raf*<sup>+/Lox-D594A</sup> MEFs were generated. *B-raf*<sup>+/Lox-D594A</sup> MEFs showed elevated phospho-ERK levels upon serum stimulation. These observations agreed with those observed for *B-raf*<sup>Lox-D594A/Lox-D594A</sup> MEFs. These data suggests that the B-Raf D594A may be a dominant mutation.

Investigating the growth rates of *B-raf*<sup>Lox-D594A/Lox-D594A</sup> MEFs showed that they grew at a faster rate than *B-raf*<sup>+/+</sup> MEFs. This could be due to a decrease in apoptosis or an increase in proliferation, or a combination of both. Although the increased growth rate observed can be partly explained by the decreased apoptosis, investigations in our laboratory have also shown that these cells have increased proliferation (see Figure A.1 in Appendix).

Activated ERK is known to be involved in the activation of a number of cell cycle proteins. A reduction in phospho-ERK of *B-raf*<sup>-/-</sup> MEFs was shown to lead to a delay in G1 to S phase of the cell cycle in Chapter 4 and affected levels of various cell cycle proteins. Therefore a number of G1 to S phase proteins were assessed upon serum stimulation of *B-raf*<sup>Lox-D594A/Lox-D594A</sup> MEFs. Cyclin D1 and cdk4 levels were shown to be elevated in *B-raf*<sup>Lox-D594A/Lox-D594A</sup> MEFs. As these proteins are involved in promoting the

G1 to S phase of the cell cycle (Sherr, 1994), their elevated levels correspond to the increased proliferation rate observed for the *B-raf*<sup>Lox-D594A/Lox-D594A</sup> MEFs. p27<sup>KIP1</sup> was also found to be elevated for *B-raf*<sup>Lox-D594A/Lox-D594A</sup> MEFs. This protein is known to inactivate cyclin-cdk complexes (Polyak *et al.*, 1994; Harper *et al.*, 1995; Lee *et al.*, 1995). However, it is also been shown to play a role in tumourigenesis and may promote proliferation under some circumstances (Nho and Sheaff *et al.*, 2003). Therefore, more detailed analysis would be required to evaluate the exact role of p27<sup>KIP1</sup> for *B-raf*<sup>Lox-D594A/Lox-D594A</sup> MEFs.

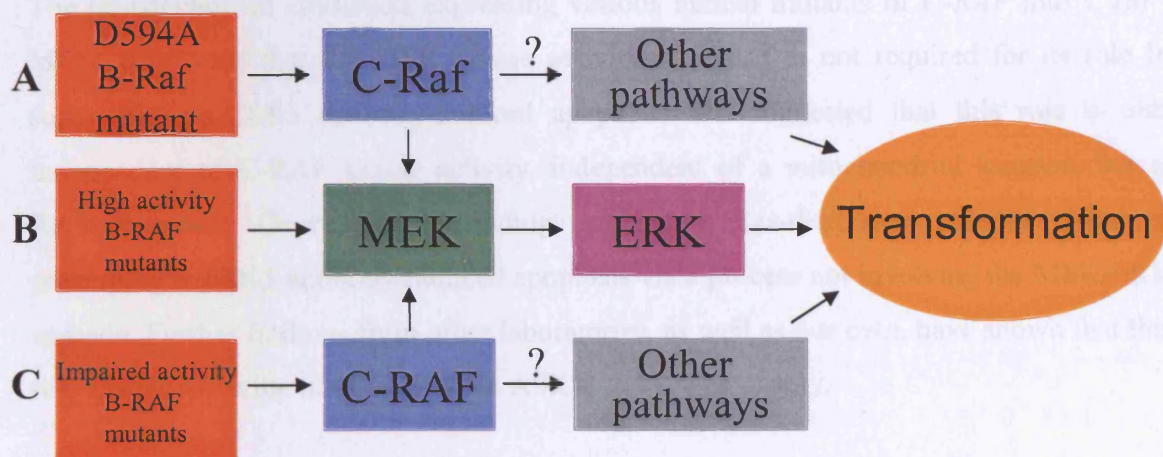
*B-raf*<sup>Lox-D594A/Lox-D594A</sup> MEFs were found to be less susceptible to apoptosis compared to *B-raf*<sup>+/+</sup> MEFs upon serum withdrawal and  $\alpha$ -CD95 antibody induced apoptosis. Phospho-ERK levels were elevated upon serum withdrawal of *B-raf*<sup>Lox-D594A/Lox-D594A</sup> MEFs and may account for the reduced susceptibility to apoptosis upon serum withdrawal, as decreased phospho-ERK levels observed for *B-raf*<sup>-/-</sup> MEKs were associated with increased susceptibility to apoptosis as discussed in Chapter 4. This increased susceptibility of the *B-raf*<sup>-/-</sup> MEFs was shown to associate with decreased phosphorylation of caspase 9 on Thr125. In accordance with these findings, initial analysis of the levels of phosph-Thr-125 caspase 9 were shown to be increased in *B-raf*<sup>Lox-D594A/Lox-D594A</sup> MEFs when compared to *B-raf*<sup>+/+</sup> cells. These results potentially identify an important survival pathway through which B-Raf oncogenes such as D594 may mediate their effects. Overall the results obtained concur with the roles of B-Raf in apoptosis and proliferation via ERK that were observed in Chapter 4 and show that D594A may induce its oncogenic effects by inducing decreased apoptosis and increased proliferation.

In order to try and clarify what may account for the increased ERK activity in the *B-raf*<sup>Lox-D594A/Lox-D594A</sup> MEFs, immunoprecipitation kinase cascade assays were carried out on these cells by R.Marais's laboratory (ICR, London). The results showed that the B-Raf expressed in these cells is indeed inactive in the *B-raf*<sup>Lox-D594A/Lox-D594A</sup> MEFs (See Figure A.2 in Appendix). However, the C-Raf kinase activity was increased in the *B-raf*<sup>Lox-D594A/Lox-D594A</sup> MEFs when compared to *B-raf*<sup>+/+</sup> MEFs. Previous findings have observed that B-Raf and C-Raf coimmunoprecipitate (Wan *et al.*, 2004). It is therefore possible that the elevated MEK and ERK activity observed is due to the increased kinase activity of C-Raf. A number of B-Raf mutants with impaired kinase activity have been shown to

activate MEK and ERK via C-Raf forming a complex with B-Raf (Wan *et al.*, 2004). However, expression of a D594V in COS or *Xenopus* cells does not induce ERK or C-Raf activity. The difference between this system and the current system observed for D594A is unclear. It may be that the observations for D594V were seen due to the over-expression of the mutant form in COS cells, rather than being due to endogenous levels, as observed for this D594A knockin mutation. It will therefore be important to confirm if the increased phospho-ERK levels observed for *B-raf*<sup>Lox-D594A/Lox-D594A</sup> MEFs are indeed occurring due to increased C-Raf kinase activity. This could be discovered via silencing the C-Raf gene using RNA interference techniques, investigating ERK kinase activity, and by studying the interactions of B-Raf and C-Raf in these cells.

In summary, the phenotype observed for *B-raf*<sup>+/Lox-D594A</sup> mice appears to be a form of neoplasia. The D594A mutation does not appear to lead to a phenotype similar to that observed for *B-raf*<sup>-/-</sup> MEFs. It appears to be more consistent to that seen for B-Raf impaired activity mutants, as observed in a number of cancer cell lines (Wan *et al.*, 2004). Upon kinase inactivation of B-Raf, due to the D594A mutation, C-Raf activity is increased and this may possibly account for the elevated levels of MEK and ERK phosphorylation being observed. This is likely to be contributing to the neoplasia observed for the *B-raf*<sup>+/Lox-D594A</sup> mice. In light of these data, a proposed role of the various *B-RAF* mutants in cancer is shown in Figure 6.13.

**Figure 6.13** Proposed model of B-Raf signalling for B-Raf D594A mutants in comparison to signalling of other B-RAF mutants found in human cancer cell lines (Wan *et al.*, 2004).



The results of this analysis help to further demonstrate the role of C-Raf in apoptosis, and in particular shows that this role is dependent on Ras binding. The data agree with results published by others, suggesting a MEK/ERK independent role of C-Raf in suppressing apoptosis that could involve the inhibition of the ASK1 pathway (Montopoli *et al.*, 2004). However, as ASK1 can be activated by both TRP and  $\alpha$ -CD95 antibody, whereas previous findings have shown C-Raf is only involved in  $\alpha$ -CD95 antibody induced apoptosis (Hsieh *et al.*, 2001; Ichihara *et al.*, 2003), it is likely that other pathways are involved. It may be that Mad2 plays a major role in mediating the effects of C-Raf, as these two proteins have been shown to interact and C-Raf has been shown to inhibit the activity of Mad2 by direct phosphorylation of Thr160 (O'Neill *et al.*, 2005). It would therefore be interesting if future studies compared the analysis of Mad2 expression levels, activity and phosphorylation status in C-Raf<sup>+</sup> MEFs compared to wild-type MEFs following  $\alpha$ -CD95 antibody treatment. Also, by overexpressing mRNA of Mad2 in the C-Raf<sup>+</sup> MEFs, it would be possible to investigate if this would rescue the increase in apoptosis observed in these cells.

Further studies to clarify the requirement for Ras in the suppression of  $\alpha$ -CD95 antibody induced apoptosis by C-Raf would be of interest. It remains unclear as to whether Ras is simply required to activate C-Raf at the plasma membrane, or whether it plays a role in subsequent interactions. If expression of SAP-CALX in the C-Raf<sup>+</sup> MEFs was

## 7. SUMMARY AND DISCUSSION

### 7.1 Characterisation of the role of C-Raf in the suppression of $\alpha$ -CD95 antibody-induced apoptosis

The transfection of constructs expressing various human mutants of *C-RAF* into *C-raf*<sup>-/-</sup> MEFs confirmed that the MEK kinase activity of C-Raf is not required for its role in suppressing  $\alpha$ -CD95 antibody-induced apoptosis and suggested that this role is also independent of C-RAF kinase activity, independent of a mitochondrial location, but is RAS-dependent. Overall, these findings suggest a Ras-dependent role of C-Raf in preventing  $\alpha$ -CD95 antibody-induced apoptosis via a process not involving the MEK/ERK cascade. Further findings from other laboratories, as well as our own, have shown that this role may involve the inhibition of the ASK1/ p38<sup>MAPK</sup> pathway.

The results of this chapter help to further characterise the role of C-Raf in apoptosis, and in particular shows this role is dependent on Ras binding. The data agree with results published by others, suggesting a MEK/ERK independent role of C-Raf in suppressing apoptosis that could involve the inhibition of the ASK1 pathway (Yamaguchi *et al.*, 2004). However, as ASK1 can be activated by both TNF and  $\alpha$ -CD95 antibody, whereas previous findings have shown C-Raf is only involved in  $\alpha$ -CD95 antibody-induced apoptosis (Hüser *et al.*, 2001; Mikula *et al.*, 2001), it is likely that other pathways are involved. It may be that Mst2 plays a major role in mediating the effects of C-Raf, as these two proteins have been shown to interact and C-Raf has been shown to inhibit the activity of Mst2 by direct phosphorylation on Thr160 (O'Neill *et al.*, 2004). It would therefore be interesting if future studies involved the analysis of Mst2 expression levels, activity and phosphorylation status in *C-raf*<sup>-/-</sup> MEFs compared to wild-type MEFs following  $\alpha$ -CD95 antibody treatment. Also, by performing siRNA of Mst2 in the *C-raf*<sup>-/-</sup> MEFs, it would be possible to investigate if this would relieve the increase in apoptosis observed in these cells.

Further studies to clarify the requirement for Ras in the suppression of  $\alpha$ -CD95 antibody-induced apoptosis by C-Raf would be of interest. It remains unclear as to whether Ras is only required to localise C-Raf at the plasma membrane, or whether it plays a role in subsequent interactions. If expression of RAF-CAAX in the *C-raf*<sup>-/-</sup> MEFs was

investigated, and found to overcome the increase in apoptosis, this would indicate that the role of Ras is purely for localisation of C-Raf at the plasma membrane. However, as Ras has been shown to interact with ASK1 (Du *et al.*, 2004) and may also influence Mst2 activity (O'Neill *et al.*, 2005), studies to look at the effects on ASK1 and Mst2 activities could be carried out. It is possible that a Ras/C-Raf complex may work together to suppress the pro-apoptotic functions of ASK1, and this could be investigated by looking at Ras/ASK1 complexes in the *C-raf*<sup>-/-</sup> MEFs.

## 7.2 Characterisation of cell growth, proliferation and apoptosis in *B-raf*<sup>-/-</sup> primary MEFs

The role of B-Raf in cell growth and survival was investigated using primary MEFs lacking B-Raf. Cell growth and proliferation were found to be reduced and this coincided with alterations in the expression levels of various proteins involved in the G1 to S phase transition of the cell cycle. Analysis of *B-raf*<sup>-/-</sup> cells upon serum withdrawal-induced apoptosis showed this was associated with decreased phosphorylation levels of phospho-T125-caspase 9. These findings help to support previous findings showing roles for B-RAF in the regulation of the cell cycle, and the observation that ERK1/2 can phosphorylate caspase 9 on residue Thr125, preventing caspase 9 processing and caspase 3 activation (Allen *et al.*, 2003).

A number of further studies would be of interest to follow on from the data obtained in this chapter. It would be useful to confirm the defect in proliferation observed in *B-raf*<sup>-/-</sup> cells was occurring due to the observed changes in the expression levels of various cell cycle proteins. This could be achieved by attempting to rescue the reduced levels of proliferation, by transfecting cDNA expression vectors for B-RAF, active MEK or cyclin D1 into the *B-raf*<sup>-/-</sup> cells, and/or using siRNA to remove p21<sup>CIP1</sup> from the cells.

An interesting outcome from this chapter was the observation that serum withdrawal of *B-raf*<sup>-/-</sup> cells led to reduced levels of phospho-ERK and reduced levels of Bim expression, as this contradicts previous data showing ERK suppresses Bim levels upon serum withdrawal (Ley *et al.*, 2003). As the present study used primary cells and all previous reported studies took place using immortalised cells, this may have contributed to the varying observations. It would be interesting for studies to be carried out to knock out Bim

from the *B-raf*<sup>-/-</sup> cells via siRNA of Bim. This would confirm whether Bim is playing a role in apoptosis in these cells, as the present data does not rule out a post-translation role in the suppression of Bim by ERK.

To confirm that the observed decreased levels of phospho-T125-caspase 9 are contributing to the increased level of serum withdrawal-induced apoptosis, it would be of interest to investigate proteins downstream of caspase 9, such as caspase 3, as well as to investigate the levels of cytochrome c released. Furthermore, it would be ideal to obtain rescue data to show that the addition of wild-type B-RAF to the *B-raf*<sup>-/-</sup> cells leads to increased levels of phospho-T125-caspase 9, in conjunction with decreased apoptosis upon serum withdrawal. This would prove that the observed effects on caspase 9 in the *B-raf*<sup>-/-</sup> cells were truly attributed to the lack of B-RAF and not due to some other factor.

### **7.3 Generation of a floxed *B-raf* kinase inactive allele by homologous recombination and the subsequent generation of *B-raf*<sup>+/*Lox*-D594A</sup> mice expressing the *B-raf* kinase inactive mutation**

A *B-raf* allele containing a conditional kinase inactivating D594A mutation was generated. Upon gene targeting, ES clones produced were used to generate chimaeric mice. Mice carrying the mutation were mated with Cre-expressing mice, allowing the generation of mice heterozygous for the D594A mutation; *B-raf*<sup>+/*Lox*-D594A</sup> mice. These mice were shown to have neoplasia due to splenomegaly and this was attributed to the elevated phospho-ERK levels observed.

The generation of these *B-raf*<sup>+/*Lox*-D594A</sup> mice is very significant, as they provide an *in-vivo* model to allow analysis of the suggested roles of B-RAF in inducing cancer. Numerous organs were collected from various *B-raf*<sup>+/*Lox*-D594A</sup> mice and it would be of great interest to analyse these organs further using histopathological approaches. In addition, the mice could be used to investigate the roles B-RAF and C-RAF may play together in regulating cancer, as discussed in more detail below.

#### 7.4 Production and characterisation of *B-raf*<sup>+/*Lox-D594A*</sup> MEFs expressing the *B-raf* kinase inactive mutation

Analysis of *B-raf*<sup>*Lox-D594A/Lox-D594A*</sup> primary MEFs showed their phenotype differed from *B-raf*<sup>-/-</sup> cells. In *B-raf*<sup>*Lox-D594A/Lox-D594A*</sup> MEFs, phospho-MEK and phospho-ERK levels were significantly elevated. This may be attributed to the increased C-Raf kinase activity observed within these cells. This could be confirmed via siRNA to C-RAF in these cells to test whether this leads to a decrease in MEK/ERK activity. Further analysis of *B-raf*<sup>*Lox-D594A/Lox-D594A*</sup> MEFs indicated increased survival and increased cell growth and proliferation in these cells, suggesting that the mutation was acting as an oncogene, consistent with the description of B-Raf D594 mutations in human cancers.

These findings are again significant, as previous studies did not show an increase in ERK activity upon transfection of COS cells with an expression vector expression the B-RAF<sup>D594V</sup> mutation. This D593V mutant was shown to have impaired ERK activity, and was unable to phosphorylate MEK *in vitro* or activate C-RAF (Wan *et al.*, 2004). Given these contradictory results, it is therefore extremely important to further analyse the molecular basis of the increased ERK activity observed in the cells and tissues expressing B-RAF<sup>D594A</sup> generated in this study. Furthermore, the possible linkage in elevated ERK activity to increased C-Raf kinase activity in these cells, provides a model to investigate the suggested B-RAF/C-RAF interactions observed in numerous human cancer cells. It is thought that B-RAF/C-RAF heterodimers convey greater kinase activity than the individual homodimers alone, and that 14-3-3 plays a role in this association. Thus, the mice and cells generated in the present studies can be used with the aim of isolating B-Raf/C-Raf heterodimers, allowing more detailed analysis of the kinase activity of various B-Raf/C-Raf heterodimers, and to investigate the role 14-3-3 may play in this interaction. Studies could also investigate if, and possibly which, other proteins may be involved, whether C-Raf is responsible for activating MEK in this situation, and how C-RAF is involved in determining the tumour phenotype of cancers with B-RAF mutations.

#### 7.5 Conclusion

This study has further characterised the roles of C-Raf and B-Raf signalling pathways associated with survival and proliferation. The use of a conditional gene targeting system has allowed the generation and analysis of mice carrying a D594A kinase inactive

mutation of B-Raf. As D594 B-RAF mutations have been found in numerous cancer samples, further characterisation of these mice and MEFs may help gain significant insight into the role of this *B-RAF* oncogene in human cancers.

**RERERENCES**

- Abdel-Hafiz, H.A., Heasley, L.E., Kyriakis, J.M., Avruch, J., Kroll, D.J., Johnson, G.L. and Hoeffler, J.P. (1992) Activating transcription factor-2 DNA-binding activity is stimulated by phosphorylation catalyzed by p42 and p54 microtubule-associated protein kinases. *Mol Endocrinol*, **6**, 2079-2089.
- Abe, J., Kusuvara, M., Ulevitch, R.J., Berk, B.C. and Lee, J.D. (1996) Big mitogen-activated protein kinase 1 (BMK1) is a redox-sensitive kinase. *J Biol Chem*, **271**, 16586-16590.
- Abraham, D., Podar, K., Pacher, M., Kubicek, M., Welzel, N., Hemmings, B.A., Dilworth, S.M., Mischak, H., Kolch, W. and Baccarini, M. (2000) Raf-1-associated protein phosphatase 2A as a positive regulator of kinase activation. *J Biol Chem*, **275**, 22300-22304.
- Acehan, D., Jiang, X., Morgan, D.G., Heuser, J.E., Wang, X. and Akey, C.W. (2002) Three-dimensional structure of the apoptosome: implications for assembly, procaspase-9 binding, and activation. *Mol Cell*, **9**, 423-432.
- Albanese, C., Johnson, J., Watanabe, G., Eklund, N., Vu, D., Arnold, A. and Pestell, R.G. (1995) Transforming p21ras mutants and c-Ets-2 activate the cyclin D1 promoter through distinguishable regions. *J Biol Chem*, **270**, 23589-23597.
- Alessi, D.R., James, S.R., Downes, C.P., Holmes, A.B., Gaffney, P.R., Reese, C.B. and Cohen, P. (1997) Characterization of a 3-phosphoinositide-dependent protein kinase which phosphorylates and activates protein kinase Balpha. *Curr Biol*, **7**, 261-269.
- Alessi, D.R., Saito, Y., Campbell, D.G., Cohen, P., Sithanandam, G., Rapp, U., Ashworth, A., Marshall, C.J. and Cowley, S. (1994) Identification of the sites in MAP kinase kinase-1 phosphorylated by p74raf-1. *Embo J*, **13**, 1610-1619.
- Allan, L.A., Morrice, N., Brady, S., Magee, G., Pathak, S. and Clarke, P.R. (2003) Inhibition of caspase-9 through phosphorylation at Thr 125 by ERK MAPK. *Nat Cell Biol*, **5**, 647-654.
- Altschuler, D. and Lapetina, E.G. (1993) Mutational analysis of the cAMP-dependent protein kinase-mediated phosphorylation site of Rap1b. *J Biol Chem*, **268**, 7527-7531.
- Alvarez, E., Northwood, I.C., Gonzalez, F.A., Latour, D.A., Seth, A., Abate, C., Curran, T. and Davis, R.J. (1991) Pro-Leu-Ser/Thr-Pro is a consensus primary sequence for substrate protein phosphorylation. Characterization of the phosphorylation of c-myc

- and c-jun proteins by an epidermal growth factor receptor threonine 669 protein kinase. *J Biol Chem*, **266**, 15277-15285.
- Ambrosio, L., Mahowald, A.P. and Perrimon, N. (1989) Requirement of the *Drosophila* raf homologue for torso function. *Nature*, **342**, 288-291.
- Anderson, N.G., Li, P., Marsden, L.A., Williams, N., Roberts, T.M. and Sturgill, T.W. (1991) Raf-1 is a potential substrate for mitogen-activated protein kinase in vivo. *Biochem J*, **277** ( Pt 2), 573-576.
- Andjelkovic, M., Alessi, D.R., Meier, R., Fernandez, A., Lamb, N.J., Frech, M., Cron, P., Cohen, P., Lucocq, J.M. and Hemmings, B.A. (1997) Role of translocation in the activation and function of protein kinase B. *J Biol Chem*, **272**, 31515-31524.
- Andjelkovic, M., Maira, S.M., Cron, P., Parker, P.J. and Hemmings, B.A. (1999) Domain swapping used to investigate the mechanism of protein kinase B regulation by 3-phosphoinositide-dependent protein kinase 1 and Ser473 kinase. *Mol Cell Biol*, **19**, 5061-5072.
- Angel, P. and Karin, M. (1991) The role of Jun, Fos and the AP-1 complex in cell-proliferation and transformation. *Biochim Biophys Acta*, **1072**, 129-157.
- Anselmo, A.N., Bumeister, R., Thomas, J.M. and White, M.A. (2002) Critical contribution of linker proteins to Raf kinase activation. *J Biol Chem*, **277**, 5940-5943.
- Arcoleo, J.P. and Weinstein, I.B. (1985) Activation of protein kinase C by tumor promoting phorbol esters, teleocidin and aplysiatoxin in the absence of added calcium. *Carcinogenesis*, **6**, 213-217.
- Aronheim, A., Engelberg, D., Li, N., al-Alawi, N., Schlessinger, J. and Karin, M. (1994) Membrane targeting of the nucleotide exchange factor Sos is sufficient for activating the Ras signaling pathway. *Cell*, **78**, 949-961.
- Balmano, K. and Cook, S.J. (1999) Sustained MAP kinase activation is required for the expression of cyclin D1, p21Cip1 and a subset of AP-1 proteins in CCL39 cells. *Oncogene*, **18**, 3085-3097.
- Balmano, K., Millar, T., McMahon, M. and Cook, S.J. (2003) DeltaRaf-1:ER\* bypasses the cyclic AMP block of extracellular signal-regulated kinase 1 and 2 activation but not CDK2 activation or cell cycle reentry. *Mol Cell Biol*, **23**, 9303-9317.
- Barnard, D., Diaz, B., Clawson, D. and Marshall, M. (1998) Oncogenes, growth factors and phorbol esters regulate Raf-1 through common mechanisms. *Oncogene*, **17**, 1539-1547.

- Barnier, J.V., Papin, C., Eychene, A., Lecoq, O. and Calothy, G. (1995) The mouse B-raf gene encodes multiple protein isoforms with tissue-specific expression. *J Biol Chem*, **270**, 23381-23389.
- Bar-Sagi, D. (1994) The Sos (Son of Sevenless) protein. *Trends Endocrinol Metab*, **5**, 165-169.
- Baumann, B., Weber, C.K., Troppmair, J., Whiteside, S., Israel, A., Rapp, U.R. and Wirth, T. (2000) Raf induces NF-kappaB by membrane shuttle kinase MEKK1, a signaling pathway critical for transformation. *Proc Natl Acad Sci U S A*, **97**, 4615-4620.
- Beck, T.W., Huleihel, M., Gunnell, M., Bonner, T.I. and Rapp, U.R. (1987) The complete coding sequence of the human A-raf-1 oncogene and transforming activity of a human A-raf carrying retrovirus. *Nucleic Acids Res*, **15**, 595-609.
- Beg, A.A. and Baltimore, D. (1996) An essential role for NF-kappaB in preventing TNF-alpha-induced cell death. *Science*, **274**, 782-784.
- Beier, F., Taylor, A.C. and LuValle, P. (1999) The Raf-1/MEK/ERK pathway regulates the expression of the p21(Cip1/Waf1) gene in chondrocytes. *J Biol Chem*, **274**, 30273-30279.
- Berger, D.H., Jardines, L.A., Chang, H. and Ruggeri, B. (1997) Activation of Raf-1 in human pancreatic adenocarcinoma. *J Surg Res*, **69**, 199-204.
- Bhatt, K.V., Spofford, L.S., Aram, G., McMullen, M., Pumiglia, K. and Aplin, A.E. (2005) Adhesion control of cyclin D1 and p27Kip1 levels is deregulated in melanoma cells through BRAF-MEK-ERK signaling. *Oncogene*, **24**, 3459-3471.
- Bird, T.A., Kyriakis, J.M., Tyshler, L., Gayle, M., Milne, A. and Virca, G.D. (1994) Interleukin-1 activates p54 mitogen-activated protein (MAP) kinase/stress-activated protein kinase by a pathway that is independent of p21ras, Raf-1, and MAP kinase kinase. *J Biol Chem*, **269**, 31836-31844.
- Boldyreff, B. and Issinger, O.G. (1997) A-Raf kinase is a new interacting partner of protein kinase CK2 beta subunit. *FEBS Lett*, **403**, 197-199.
- Bonizzi, G. and Karin, M. (2004) The two NF-kappaB activation pathways and their role in innate and adaptive immunity. *Trends Immunol*, **25**, 280-288.
- Bonner, T.I., Kerby, S.B., Sutrave, P., Gunnell, M.A., Mark, G. and Rapp, U.R. (1985) Structure and biological activity of human homologs of the raf/mil oncogene. *Mol Cell Biol*, **5**, 1400-1407.

- Bonni, A., Brunet, A., West, A.E., Datta, S.R., Takasu, M.A. and Greenberg, M.E. (1999) Cell survival promoted by the Ras-MAPK signaling pathway by transcription-dependent and -independent mechanisms. *Science*, **286**, 1358-1362.
- Boriack-Sjodin, P.A., Margarit, S.M., Bar-Sagi, D. and Kuriyan, J. (1998) The structural basis of the activation of Ras by Sos. *Nature*, **394**, 337-343.
- Borner, C. (2003) The Bcl-2 protein family: sensors and checkpoints for life-or-death decisions. *Mol Immunol*, **39**, 615-647.
- Bos, J.L. (1989) ras oncogenes in human cancer: a review. *Cancer Res*, **49**, 4682-4689.
- Bost, F., Aouadi, M., Caron, L., Even, P., Belmonte, N., Prot, M., Dani, C., Hofman, P., Pages, G., Pouyssegur, J., Le Marchand-Brustel, Y. and Binetruy, B. (2005) The extracellular signal-regulated kinase isoform ERK1 is specifically required for in vitro and in vivo adipogenesis. *Diabetes*, **54**, 402-411.
- Bourne, H.R., Sanders, D.A. and McCormick, F. (1990) The GTPase superfamily: a conserved switch for diverse cell functions. *Nature*, **348**, 125-132.
- Bradley, A., Evans, M., Kaufman, M.H. and Robertson, E. (1984) Formation of germ-line chimaeras from embryo-derived teratocarcinoma cell lines. *Nature*, **309**, 255-256.
- Brehm, A., Miska, E.A., McCance, D.J., Reid, J.L., Bannister, A.J. and Kouzarides, T. (1998) Retinoblastoma protein recruits histone deacetylase to repress transcription. *Nature*, **391**, 597-601.
- Brose, M.S., Volpe, P., Feldman, M., Kumar, M., Rishi, I., Gerrero, R., Einhorn, E., Herlyn, M., Minna, J., Nicholson, A., Roth, J.A., Albelda, S.M., Davies, H., Cox, C., Brignell, G., Stephens, P., Futreal, P.A., Wooster, R., Stratton, M.R. and Weber, B.L. (2002) BRAF and RAS mutations in human lung cancer and melanoma. *Cancer Res*, **62**, 6997-7000.
- Brtva, T.R., Drugan, J.K., Ghosh, S., Terrell, R.S., Campbell-Burk, S., Bell, R.M. and Der, C.J. (1995) Two distinct Raf domains mediate interaction with Ras. *J Biol Chem*, **270**, 9809-9812.
- Brummer, T., Naegele, H., Reth, M. and Misawa, Y. (2003) Identification of novel ERK-mediated feedback phosphorylation sites at the C-terminus of B-Raf. *Oncogene*, **22**, 8823-8834.
- Brummer, T., Shaw, P.E., Reth, M. and Misawa, Y. (2002) Inducible gene deletion reveals different roles for B-Raf and Raf-1 in B-cell antigen receptor signalling. *Embo J*, **21**, 5611-5622.

- Buchkovich, K., Duffy, L.A. and Harlow, E. (1989) The retinoblastoma protein is phosphorylated during specific phases of the cell cycle. *Cell*, **58**, 1097-1105.
- Buday, L. and Downward, J. (1993) Epidermal growth factor regulates p21ras through the formation of a complex of receptor, Grb2 adapter protein, and Sos nucleotide exchange factor. *Cell*, **73**, 611-620.
- Burgering, B.M., Pronk, G.J., van Weeren, P.C., Chardin, P. and Bos, J.L. (1993) cAMP antagonizes p21ras-directed activation of extracellular signal-regulated kinase 2 and phosphorylation of mSos nucleotide exchange factor. *Embo J*, **12**, 4211-4220.
- Buschmann, T., Potapova, O., Bar-Shira, A., Ivanov, V.N., Fuchs, S.Y., Henderson, S., Fried, V.A., Minamoto, T., Alarcon-Vargas, D., Pincus, M.R., Gaarde, W.A., Holbrook, N.J., Shiloh, Y. and Ronai, Z. (2001) Jun NH2-terminal kinase phosphorylation of p53 on Thr-81 is important for p53 stabilization and transcriptional activities in response to stress. *Mol Cell Biol*, **21**, 2743-2754.
- Cacace, A.M., Michaud, N.R., Therrien, M., Mathes, K., Copeland, T., Rubin, G.M. and Morrison, D.K. (1999) Identification of constitutive and ras-inducible phosphorylation sites of KSR: implications for 14-3-3 binding, mitogen-activated protein kinase binding, and KSR overexpression. *Mol Cell Biol*, **19**, 229-240.
- Calipel, A., Lefevre, G., Pouponnot, C., Mouriaux, F., Eychene, A. and Mascarelli, F. (2003) Mutation of B-Raf in human choroidal melanoma cells mediates cell proliferation and transformation through the MEK/ERK pathway. *J Biol Chem*, **278**, 42409-42418.
- Cameron, S.J., Abe, J., Malik, S., Che, W. and Yang, J. (2004) Differential role of MEK5alpha and MEK5beta in BMK1/ERK5 activation. *J Biol Chem*, **279**, 1506-1512.
- Cantley, L.C. (2002) The phosphoinositide 3-kinase pathway. *Science*, **296**, 1655-1657.
- Carey, K.D., Watson, R.T., Pessin, J.E. and Stork, P.J. (2003) The requirement of specific membrane domains for Raf-1 phosphorylation and activation. *J Biol Chem*, **278**, 3185-3196.
- Carnero, A. and Hannon, G.J. (1998) The INK4 family of CDK inhibitors. *Curr Top Microbiol Immunol*, **227**, 43-55.
- Carroll, M.P. and May, W.S. (1994) Protein kinase C-mediated serine phosphorylation directly activates Raf-1 in murine hematopoietic cells. *J Biol Chem*, **269**, 1249-1256.
- Catling, A.D., Reuter, C.W., Cox, M.E., Parsons, S.J. and Weber, M.J. (1994) Partial purification of a mitogen-activated protein kinase kinase activator from bovine brain.

- Identification as B-Raf or a B-Raf-associated activity. *J Biol Chem*, **269**, 30014-30021.
- Catling, A.D., Schaeffer, H.J., Reuter, C.W., Reddy, G.R. and Weber, M.J. (1995) A proline-rich sequence unique to MEK1 and MEK2 is required for raf binding and regulates MEK function. *Mol Cell Biol*, **15**, 5214-5225.
- Cavigelli, M., Dolfi, F., Claret, F.X. and Karin, M. (1995) Induction of c-fos expression through JNK-mediated TCF/Elk-1 phosphorylation. *Embo J*, **14**, 5957-5964.
- Chao, T.H., Hayashi, M., Tapping, R.I., Kato, Y. and Lee, J.D. (1999) MEKK3 directly regulates MEK5 activity as part of the big mitogen-activated protein kinase 1 (BMK1) signaling pathway. *J Biol Chem*, **274**, 36035-36038.
- Charette, S.J., Lambert, H. and Landry, J. (2001) A kinase-independent function of Ask1 in caspase-independent cell death. *J Biol Chem*, **276**, 36071-36074.
- Chen, C., Edelstein, L.C. and Gelinas, C. (2000) The Rel/NF-kappaB family directly activates expression of the apoptosis inhibitor Bcl-x(L). *Mol Cell Biol*, **20**, 2687-2695.
- Chen, J., Fujii, K., Zhang, L., Roberts, T. and Fu, H. (2001) Raf-1 promotes cell survival by antagonizing apoptosis signal-regulating kinase 1 through a MEK-ERK independent mechanism. *Proc Natl Acad Sci U S A*, **98**, 7783-7788.
- Chen, R.H., Abate, C. and Blenis, J. (1993) Phosphorylation of the c-Fos transrepression domain by mitogen-activated protein kinase and 90-kDa ribosomal S6 kinase. *Proc Natl Acad Sci U S A*, **90**, 10952-10956.
- Chen, R.H., Juo, P.C., Curran, T. and Blenis, J. (1996) Phosphorylation of c-Fos at the C-terminus enhances its transforming activity. *Oncogene*, **12**, 1493-1502.
- Chen, R.H., Sarnecki, C. and Blenis, J. (1992) Nuclear localization and regulation of erk- and rsk-encoded protein kinases. *Mol Cell Biol*, **12**, 915-927.
- Chen, Z., Hagler, J., Palombella, V.J., Melandri, F., Scherer, D., Ballard, D. and Maniatis, T. (1995) Signal-induced site-specific phosphorylation targets I kappa B alpha to the ubiquitin-proteasome pathway. *Genes Dev*, **9**, 1586-1597.
- Chiloeches, A., Mason, C.S. and Marais, R. (2001) S338 phosphorylation of Raf-1 is independent of phosphatidylinositol 3-kinase and Pak3. *Mol Cell Biol*, **21**, 2423-2434.
- Chong, H., Lee, J. and Guan, K.L. (2001) Positive and negative regulation of Raf kinase activity and function by phosphorylation. *Embo J*, **20**, 3716-3727.

- Chu, Z.L., McKinsey, T.A., Liu, L., Gentry, J.J., Malim, M.H. and Ballard, D.W. (1997) Suppression of tumor necrosis factor-induced cell death by inhibitor of apoptosis c-IAP2 is under NF-kappaB control. *Proc Natl Acad Sci U S A*, **94**, 10057-10062.
- Chuang, E., Barnard, D., Hettich, L., Zhang, X.F., Avruch, J. and Marshall, M.S. (1994) Critical binding and regulatory interactions between Ras and Raf occur through a small, stable N-terminal domain of Raf and specific Ras effector residues. *Mol Cell Biol*, **14**, 5318-5325.
- Cioffi, C.L., Garay, M., Johnston, J.F., McGraw, K., Boggs, R.T., Hreniuk, D. and Monia, B.P. (1997) Selective inhibition of A-Raf and C-Raf mRNA expression by antisense oligodeoxynucleotides in rat vascular smooth muscle cells: role of A-Raf and C-Raf in serum-induced proliferation. *Mol Pharmacol*, **51**, 383-389.
- Clark, G.J., Drugan, J.K., Rossman, K.L., Carpenter, J.W., Rogers-Graham, K., Fu, H., Der, C.J. and Campbell, S.L. (1997) 14-3-3 zeta negatively regulates raf-1 activity by interactions with the Raf-1 cysteine-rich domain. *J Biol Chem*, **272**, 20990-20993.
- Cleveland, J.L., Troppmair, J., Packham, G., Askew, D.S., Lloyd, P., Gonzalez-Garcia, M., Nunez, G., Ihle, J.N. and Rapp, U.R. (1994) v-raf suppresses apoptosis and promotes growth of interleukin-3-dependent myeloid cells. *Oncogene*, **9**, 2217-2226.
- Cohen, G.M. (1997) Caspases: the executioners of apoptosis. *Biochem J*, **326** ( Pt 1), 1-16.
- Cohen, Y., Rosenbaum, E., Clark, D.P., Zeiger, M.A., Umbricht, C.B., Tufano, R.P., Sidransky, D. and Westra, W.H. (2004) Mutational analysis of BRAF in fine needle aspiration biopsies of the thyroid: a potential application for the preoperative assessment of thyroid nodules. *Clin Cancer Res*, **10**, 2761-2765.
- Cook, S.J., Aziz, N. and McMahon, M. (1999) The repertoire of fos and jun proteins expressed during the G1 phase of the cell cycle is determined by the duration of mitogen-activated protein kinase activation. *Mol Cell Biol*, **19**, 330-341.
- Cook, S.J. and McCormick, F. (1993) Inhibition by cAMP of Ras-dependent activation of Raf. *Science*, **262**, 1069-1072.
- Cook, S.J., Rubinfeld, B., Albert, I. and McCormick, F. (1993) RapV12 antagonizes Ras-dependent activation of ERK1 and ERK2 by LPA and EGF in Rat-1 fibroblasts. *Embo J*, **12**, 3475-3485.
- Corbit, K.C., Trakul, N., Eves, E.M., Diaz, B., Marshall, M. and Rosner, M.R. (2003) Activation of Raf-1 signaling by protein kinase C through a mechanism involving Raf kinase inhibitory protein. *J Biol Chem*, **278**, 13061-13068.

- Cowley, S., Paterson, H., Kemp, P. and Marshall, C.J. (1994) Activation of MAP kinase is necessary and sufficient for PC12 differentiation and for transformation of NIH 3T3 cells. *Cell*, **77**, 841-852.
- Crews, C.M. and Erikson, R.L. (1992) Purification of a murine protein-tyrosine/threonine kinase that phosphorylates and activates the Erk-1 gene product: relationship to the fission yeast byr1 gene product. *Proc Natl Acad Sci U S A*, **89**, 8205-8209.
- Cutler, R.E., Jr., Stephens, R.M., Saracino, M.R. and Morrison, D.K. (1998) Autoregulation of the Raf-1 serine/threonine kinase. *Proc Natl Acad Sci U S A*, **95**, 9214-9219.
- Darragh, J., Soloaga, A., Beardmore, V.A., Wingate, A.D., Wiggin, G.R., Peggie, M. and Arthur, J.S. (2005) MSKs are required for the transcription of the nuclear orphan receptors Nur77, Nurr1 and Nor1 downstream of MAPK signalling. *Biochem J*, **390**, 749-759.
- Dasgupta, P., Sun, J., Wang, S., Fusaro, G., Betts, V., Padmanabhan, J., Sebti, S.M. and Chellappan, S.P. (2004) Disruption of the Rb--Raf-1 interaction inhibits tumor growth and angiogenesis. *Mol Cell Biol*, **24**, 9527-9541.
- Datta, S.R., Dudek, H., Tao, X., Masters, S., Fu, H., Gotoh, Y. and Greenberg, M.E. (1997) Akt phosphorylation of BAD couples survival signals to the cell-intrinsic death machinery. *Cell*, **91**, 231-241.
- Daum, G., Eisenmann-Tappe, I., Fries, H.W., Troppmair, J. and Rapp, U.R. (1994) The ins and outs of Raf kinases. *Trends Biochem Sci*, **19**, 474-480.
- Davies, H., Bignell, G.R., Cox, C., Stephens, P., Edkins, S., Clegg, S., Teague, J., Woffendin, H., Garnett, M.J., Bottomley, W., Davis, N., Dicks, E., Ewing, R., Floyd, Y., Gray, K., Hall, S., Hawes, R., Hughes, J., Kosmidou, V., Menzies, A., Mould, C., Parker, A., Stevens, C., Watt, S., Hooper, S., Wilson, R., Jayatilake, H., Gusterson, B.A., Cooper, C., Shipley, J., Hargrave, D., Pritchard-Jones, K., Maitland, N., Chenevix-Trench, G., Riggins, G.J., Bigner, D.D., Palmieri, G., Cossu, A., Flanagan, A., Nicholson, A., Ho, J.W., Leung, S.Y., Yuen, S.T., Weber, B.L., Seigler, H.F., Darrow, T.L., Paterson, H., Marais, R., Marshall, C.J., Wooster, R., Stratton, M.R. and Futreal, P.A. (2002) Mutations of the BRAF gene in human cancer. *Nature*, **417**, 949-954.
- Daya-Grosjean, L., Dumaz, N. and Sarasin, A. (1995) The specificity of p53 mutation spectra in sunlight induced human cancers. *J Photochem Photobiol B*, **28**, 115-124.

- De Smaele, E., Zazzeroni, F., Papa, S., Nguyen, D.U., Jin, R., Jones, J., Cong, R. and Franzoso, G. (2001) Induction of gadd45beta by NF-kappaB downregulates proapoptotic JNK signalling. *Nature*, **414**, 308-313.
- de Vries-Smits, A.M., Burgering, B.M., Leervers, S.J., Marshall, C.J. and Bos, J.L. (1992) Involvement of p21ras in activation of extracellular signal-regulated kinase 2. *Nature*, **357**, 602-604.
- Deak, M., Clifton, A.D., Lucocq, L.M. and Alessi, D.R. (1998) Mitogen- and stress-activated protein kinase-1 (MSK1) is directly activated by MAPK and SAPK2/p38, and may mediate activation of CREB. *Embo J*, **17**, 4426-4441.
- DeChant, A.K., Dee, K. and Weyman, C.M. (2002) Raf-induced effects on the differentiation and apoptosis of skeletal myoblasts are determined by the level of Raf signaling: abrogation of apoptosis by Raf is downstream of caspase 3 activation. *Oncogene*, **21**, 5268-5279.
- Deichmann, M., Thome, M., Benner, A. and Naher, H. (2004) B-raf exon 15 mutations are common in primary melanoma resection specimens but not associated with clinical outcome. *Oncology*, **66**, 411-419.
- Dent, P., Haser, W., Haystead, T.A., Vincent, L.A., Roberts, T.M. and Sturgill, T.W. (1992) Activation of mitogen-activated protein kinase kinase by v-Raf in NIH 3T3 cells and in vitro. *Science*, **257**, 1404-1407.
- Dent, P. and Sturgill, T.W. (1994) Activation of (His)6-Raf-1 in vitro by partially purified plasma membranes from v-Ras-transformed and serum-stimulated fibroblasts. *Proc Natl Acad Sci U S A*, **91**, 9544-9548.
- Derijard, B., Hibi, M., Wu, I.H., Barrett, T., Su, B., Deng, T., Karin, M. and Davis, R.J. (1994) JNK1: a protein kinase stimulated by UV light and Ha-Ras that binds and phosphorylates the c-Jun activation domain. *Cell*, **76**, 1025-1037.
- Derijard, B., Raingeaud, J., Barrett, T., Wu, I.H., Han, J., Ulevitch, R.J. and Davis, R.J. (1995) Independent human MAP-kinase signal transduction pathways defined by MEK and MKK isoforms. *Science*, **267**, 682-685.
- Deveraux, Q.L. and Reed, J.C. (1999) IAP family proteins--suppressors of apoptosis. *Genes Dev*, **13**, 239-252.
- Dhillon, A.S., Meikle, S., Yazici, Z., Eulitz, M. and Kolch, W. (2002a) Regulation of Raf-1 activation and signalling by dephosphorylation. *Embo J*, **21**, 64-71.

- Dhillon, A.S., Pollock, C., Steen, H., Shaw, P.E., Mischak, H. and Kolch, W. (2002b) Cyclic AMP-dependent kinase regulates Raf-1 kinase mainly by phosphorylation of serine 259. *Mol Cell Biol*, **22**, 3237-3246.
- Diaz, B., Barnard, D., Filson, A., MacDonald, S., King, A. and Marshall, M. (1997) Phosphorylation of Raf-1 serine 338-serine 339 is an essential regulatory event for Ras-dependent activation and biological signaling. *Mol Cell Biol*, **17**, 4509-4516.
- Dickson, B., Sprenger, F. and Hafen, E. (1992) Prepattern in the developing Drosophila eye revealed by an activated torso--sevenless chimeric receptor. *Genes Dev*, **6**, 2327-2339.
- Dougherty, M.K., Muller, J., Ritt, D.A., Zhou, M., Zhou, X.Z., Copeland, T.D., Conrads, T.P., Veenstra, T.D., Lu, K.P. and Morrison, D.K. (2005) Regulation of Raf-1 by direct feedback phosphorylation. *Mol Cell*, **17**, 215-224.
- Drugan, J.K., Khosravi-Far, R., White, M.A., Der, C.J., Sung, Y.J., Hwang, Y.W. and Campbell, S.L. (1996) Ras interaction with two distinct binding domains in Raf-1 may be required for Ras transformation. *J Biol Chem*, **271**, 233-237.
- Du, K. and Montminy, M. (1998) CREB is a regulatory target for the protein kinase Akt/PKB. *J Biol Chem*, **273**, 32377-32379.
- Dumaz, N., Light, Y. and Marais, R. (2002) Cyclic AMP blocks cell growth through Raf-1-dependent and Raf-1-independent mechanisms. *Mol Cell Biol*, **22**, 3717-3728.
- Dumaz, N. and Marais, R. (2003) Protein kinase A blocks Raf-1 activity by stimulating 14-3-3 binding and blocking Raf-1 interaction with Ras. *J Biol Chem*, **278**, 29819-29823.
- Earnshaw, W.C., Martins, L.M. and Kaufmann, S.H. (1999) Mammalian caspases: structure, activation, substrates, and functions during apoptosis. *Annu Rev Biochem*, **68**, 383-424.
- Egan, S.E., Giddings, B.W., Brooks, M.W., Buday, L., Sizeland, A.M. and Weinberg, R.A. (1993) Association of Sos Ras exchange protein with Grb2 is implicated in tyrosine kinase signal transduction and transformation. *Nature*, **363**, 45-51.
- English, J.M., Vanderbilt, C.A., Xu, S., Marcus, S. and Cobb, M.H. (1995) Isolation of MEK5 and differential expression of alternatively spliced forms. *J Biol Chem*, **270**, 28897-28902.
- Erhardt, P., Schremser, E.J. and Cooper, G.M. (1999) B-Raf inhibits programmed cell death downstream of cytochrome c release from mitochondria by activating the MEK/Erk pathway. *Mol Cell Biol*, **19**, 5308-5315.

- Esteban, L.M., Vicario-Abejon, C., Fernandez-Salguero, P., Fernandez-Medarde, A., Swaminathan, N., Yienger, K., Lopez, E., Malumbres, M., McKay, R., Ward, J.M., Pellicer, A. and Santos, E. (2001) Targeted genomic disruption of H-ras and N-ras, individually or in combination, reveals the dispensability of both loci for mouse growth and development. *Mol Cell Biol*, **21**, 1444-1452.
- Evans, M.J. and Kaufman, M.H. (1981) Establishment in culture of pluripotential cells from mouse embryos. *Nature*, **292**, 154-156.
- Ewanowich, C., Brynes, R.K., Medeiros, L., McCourty, A. and Lai, R. (2001) Cyclin D1 expression in dysplastic nevi: an immunohistochemical study. *Arch Pathol Lab Med*, **125**, 208-210.
- Eychene, A., Dusanter-Fourt, I., Barnier, J.V., Papin, C., Charon, M., Gisselbrecht, S. and Calothy, G. (1995) Expression and activation of B-Raf kinase isoforms in human and murine leukemia cell lines. *Oncogene*, **10**, 1159-1165.
- Fabian, J.R., Daar, I.O. and Morrison, D.K. (1993) Critical tyrosine residues regulate the enzymatic and biological activity of Raf-1 kinase. *Mol Cell Biol*, **13**, 7170-7179.
- Fantl, W.J., Muslin, A.J., Kikuchi, A., Martin, J.A., MacNicol, A.M., Gross, R.W. and Williams, L.T. (1994) Activation of Raf-1 by 14-3-3 proteins. *Nature*, **371**, 612-614.
- Feil, R., Brocard, J., Mascrez, B., LeMeur, M., Metzger, D. and Chambon, P. (1996) Ligand-activated site-specific recombination in mice. *Proc Natl Acad Sci U S A*, **93**, 10887-10890.
- Feramisco, J.R., Gross, M., Kamata, T., Rosenberg, M. and Sweet, R.W. (1984) Microinjection of the oncogene form of the human H-ras (T-24) protein results in rapid proliferation of quiescent cells. *Cell*, **38**, 109-117.
- Foltz, I.N., Lee, J.C., Young, P.R. and Schrader, J.W. (1997) Hemopoietic growth factors with the exception of interleukin-4 activate the p38 mitogen-activated protein kinase pathway. *J Biol Chem*, **272**, 3296-3301.
- Franke, T.F., Kaplan, D.R., Cantley, L.C. and Toker, A. (1997) Direct regulation of the Akt proto-oncogene product by phosphatidylinositol-3,4-bisphosphate. *Science*, **275**, 665-668.
- Fransen, K., Klintenas, M., Osterstrom, A., Dimberg, J., Monstein, H.J. and Soderkvist, P. (2004) Mutation analysis of the BRAF, ARAF and RAF-1 genes in human colorectal adenocarcinomas. *Carcinogenesis*, **25**, 527-533.

- Freed, E., Symons, M., Macdonald, S.G., McCormick, F. and Ruggieri, R. (1994) Binding of 14-3-3 proteins to the protein kinase Raf and effects on its activation. *Science*, **265**, 1713-1716.
- Freshney, N., Rawlinson, L., Guesdon, F., Jones, E., Cowley, S., Hsuan, J. and Saklatvala, J. (1994) Interleukin-1 activates a novel protein kinase cascade that results in the phosphorylation of Hsp27. *Cell*, **78**, 1039-1049.
- Fu, H., Xia, K., Pallas, D.C., Cui, C., Conroy, K., Narsimhan, R.P., Mamon, H., Collier, R.J. and Roberts, T.M. (1994) Interaction of the protein kinase Raf-1 with 14-3-3 proteins. *Science*, **266**, 126-129.
- Fujita, N., Sato, S. and Tsuruo, T. (2003) Phosphorylation of p27Kip1 at threonine 198 by p90 ribosomal protein S6 kinases promotes its binding to 14-3-3 and cytoplasmic localization. *J Biol Chem*, **278**, 49254-49260.
- Fukuhara, S., Marinissen, M.J., Chiariello, M. and Gutkind, J.S. (2000) Signaling from G protein-coupled receptors to ERK5/Big MAPK 1 involves Galpha q and Galpha 12/13 families of heterotrimeric G proteins. Evidence for the existence of a novel Ras AND Rho-independent pathway. *J Biol Chem*, **275**, 21730-21736.
- Fukui, M., Yamamoto, T., Kawai, S., Maruo, K. and Toyoshima, K. (1985) Detection of a raf-related and two other transforming DNA sequences in human tumors maintained in nude mice. *Proc Natl Acad Sci U S A*, **82**, 5954-5958.
- Fukushima, T., Suzuki, S., Mashiko, M., Ohtake, T., Endo, Y., Takebayashi, Y., Sekikawa, K., Hagiwara, K. and Takenoshita, S. (2003) BRAF mutations in papillary carcinomas of the thyroid. *Oncogene*, **22**, 6455-6457.
- Galcheva-Gargova, Z., Derijard, B., Wu, I.H. and Davis, R.J. (1994) An osmosensing signal transduction pathway in mammalian cells. *Science*, **265**, 806-808.
- Garcia, J., de Gunzburg, J., Eychene, A., Gisselbrecht, S. and Porteu, F. (2001) Thrombopoietin-mediated sustained activation of extracellular signal-regulated kinase in UT7-Mpl cells requires both Ras-Raf-1- and Rap1-B-Raf-dependent pathways. *Mol Cell Biol*, **21**, 2659-2670.
- Gartel, A.L., Ye, X., Goufman, E., Shianov, P., Hay, N., Najmabadi, F. and Tyner, A.L. (2001) Myc represses the p21(WAF1/CIP1) promoter and interacts with Sp1/Sp3. *Proc Natl Acad Sci U S A*, **98**, 4510-4515.
- Gast, A., Forsti, A., Soderberg, M., Hemminki, K. and Kumar, R. (2005) B-RAF mutations in tumors from melanoma-breast cancer families. *Int J Cancer*, **113**, 336-337.

- Geng, Y., Yu, Q., Sicinska, E., Das, M., Schneider, J.E., Bhattacharya, S., Rideout, W.M., Bronson, R.T., Gardner, H. and Sicinski, P. (2003) Cyclin E ablation in the mouse. *Cell*, **114**, 431-443.
- Georgieva, J., Sinha, P. and Schadendorf, D. (2001) Expression of cyclins and cyclin dependent kinases in human benign and malignant melanocytic lesions. *J Clin Pathol*, **54**, 229-235.
- Gerwins, P., Blank, J.L. and Johnson, G.L. (1997) Cloning of a novel mitogen-activated protein kinase kinase kinase, MEKK4, that selectively regulates the c-Jun amino terminal kinase pathway. *J Biol Chem*, **272**, 8288-8295.
- Ghosh, S., Xie, W.Q., Quest, A.F., Mabrouk, G.M., Strum, J.C. and Bell, R.M. (1994) The cysteine-rich region of raf-1 kinase contains zinc, translocates to liposomes, and is adjacent to a segment that binds GTP-ras. *J Biol Chem*, **269**, 10000-10007.
- Gille, H., Kortenjann, M., Thomae, O., Moomaw, C., Slaughter, C., Cobb, M.H. and Shaw, P.E. (1995) ERK phosphorylation potentiates Elk-1-mediated ternary complex formation and transactivation. *Embo J*, **14**, 951-962.
- Gille, H., Sharrocks, A.D. and Shaw, P.E. (1992) Phosphorylation of transcription factor p62TCF by MAP kinase stimulates ternary complex formation at c-fos promoter. *Nature*, **358**, 414-417.
- Gille, H. and Downward, J. (1999) Multiple ras effector pathways contribute to G(1) cell cycle progression. *J Biol Chem*, **274**, 22033-22040.
- Giroux, S., Tremblay, M., Bernard, D., Cardin-Girard, J.F., Aubry, S., Larouche, L., Rousseau, S., Huot, J., Landry, J., Jeannotte, L. and Charron, J. (1999) Embryonic death of Mek1-deficient mice reveals a role for this kinase in angiogenesis in the labyrinthine region of the placenta. *Curr Biol*, **9**, 369-372.
- Glading, A., Chang, P., Lauffenburger, D.A. and Wells, A. (2000) Epidermal growth factor receptor activation of calpain is required for fibroblast motility and occurs via an ERK/MAP kinase signaling pathway. *J Biol Chem*, **275**, 2390-2398.
- Gomez, N. and Cohen, P. (1991) Dissection of the protein kinase cascade by which nerve growth factor activates MAP kinases. *Nature*, **353**, 170-173.
- Gottlieb, T.M., Leal, J.F., Seger, R., Taya, Y. and Oren, M. (2002) Cross-talk between Akt, p53 and Mdm2: possible implications for the regulation of apoptosis. *Oncogene*, **21**, 1299-1303.
- Gotz, R., Kramer, B.W., Camarero, G. and Rapp, U.R. (2004) BAG-1 haplo-insufficiency impairs lung tumorigenesis. *BMC Cancer*, **4**, 85.

- Grammatikakis, N., Lin, J.H., Grammatikakis, A., Tsihchlis, P.N. and Cochran, B.H. (1999) p50(cdc37) acting in concert with Hsp90 is required for Raf-1 function. *Mol Cell Biol*, **19**, 1661-1672.
- Gross, A., Yin, X.M., Wang, K., Wei, M.C., Jockel, J., Milliman, C., Erdjument-Bromage, H., Tempst, P. and Korsmeyer, S.J. (1999) Caspase cleaved BID targets mitochondria and is required for cytochrome c release, while BCL-XL prevents this release but not tumor necrosis factor-R1/Fas death. *J Biol Chem*, **274**, 1156-1163.
- Gu, H., Marth, J.D., Orban, P.C., Mossmann, H. and Rajewsky, K. (1994) Deletion of a DNA polymerase beta gene segment in T cells using cell type-specific gene targeting. *Science*, **265**, 103-106.
- Guan, K.L., Figueroa, C., Brtva, T.R., Zhu, T., Taylor, J., Barber, T.D. and Vojtek, A.B. (2000) Negative regulation of the serine/threonine kinase B-Raf by Akt. *J Biol Chem*, **275**, 27354-27359.
- Gupta, S., Barrett, T., Whitmarsh, A.J., Cavanagh, J., Sluss, H.K., Derijard, B. and Davis, R.J. (1996) Selective interaction of JNK protein kinase isoforms with transcription factors. *Embo J*, **15**, 2760-2770.
- Gupta, S., Campbell, D., Derijard, B. and Davis, R.J. (1995) Transcription factor ATF2 regulation by the JNK signal transduction pathway. *Science*, **267**, 389-393.
- Gupta, S., Seth, A. and Davis, R.J. (1993) Transactivation of gene expression by Myc is inhibited by mutation at the phosphorylation sites Thr-58 and Ser-62. *Proc Natl Acad Sci USA*, **90**, 3216-3220.
- Hafner, S., Adler, H.S., Mischak, H., Janosch, P., Heidecker, G., Wolfman, A., Pippig, S., Lohse, M., Ueffing, M. and Kolch, W. (1994) Mechanism of inhibition of Raf-1 by protein kinase A. *Mol Cell Biol*, **14**, 6696-6703.
- Hallberg, B., Rayter, S.I. and Downward, J. (1994) Interaction of Ras and Raf in intact mammalian cells upon extracellular stimulation. *J Biol Chem*, **269**, 3913-3916.
- Han, J., Lee, J.D., Bibbs, L. and Ulevitch, R.J. (1994) A MAP kinase targeted by endotoxin and hyperosmolarity in mammalian cells. *Science*, **265**, 808-811.
- Han, J., Lee, J.D., Jiang, Y., Li, Z., Feng, L. and Ulevitch, R.J. (1996) Characterization of the structure and function of a novel MAP kinase kinase (MKK6). *J Biol Chem*, **271**, 2886-2891.
- Hanks, S.K. and Hunter, T. (1995) Protein kinases 6. The eukaryotic protein kinase superfamily: kinase (catalytic) domain structure and classification. *Faseb J*, **9**, 576-596.

- Harper, J.W., Elledge, S.J., Keyomarsi, K., Dynlacht, B., Tsai, L.H., Zhang, P., Dobrowolski, S., Bai, C., Connell-Crowley, L., Swindell, E. and et al. (1995) Inhibition of cyclin-dependent kinases by p21. *Mol Biol Cell*, **6**, 387-400.
- Hase, T., Muller, U., Riezman, H. and Schatz, G. (1984) A 70-kd protein of the yeast mitochondrial outer membrane is targeted and anchored via its extreme amino terminus. *Embo J*, **3**, 3157-3164.
- Hatai, T., Matsuzawa, A., Inoshita, S., Mochida, Y., Kuroda, T., Sakamaki, K., Kuida, K., Yonehara, S., Ichijo, H. and Takeda, K. (2000) Execution of apoptosis signal-regulating kinase 1 (ASK1)-induced apoptosis by the mitochondria-dependent caspase activation. *J Biol Chem*, **275**, 26576-26581.
- Heckman, C.A., Mehew, J.W. and Boxer, L.M. (2002) NF-kappaB activates Bcl-2 expression in t(14;18) lymphoma cells. *Oncogene*, **21**, 3898-3908.
- Heldin, C.H. (1995) Dimerization of cell surface receptors in signal transduction. *Cell*, **80**, 213-223.
- Hengartner, M.O. and Horvitz, H.R. (1994) Programmed cell death in *Caenorhabditis elegans*. *Curr Opin Genet Dev*, **4**, 581-586.
- Hermeking, H., Rago, C., Schuhmacher, M., Li, Q., Barrett, J.F., Obaya, A.J., O'Connell, B.C., Mateyak, M.K., Tam, W., Kohlhuber, F., Dang, C.V., Sedivy, J.M., Eick, D., Vogelstein, B. and Kinzler, K.W. (2000) Identification of CDK4 as a target of c-MYC. *Proc Natl Acad Sci U S A*, **97**, 2229-2234.
- Hingorani, S.R., Jacobetz, M.A., Robertson, G.P., Herlyn, M. and Tuveson, D.A. (2003a) Suppression of BRAF(V599E) in human melanoma abrogates transformation. *Cancer Res*, **63**, 5198-5202.
- Hingorani, S.R., Petricoin, E.F., Maitra, A., Rajapakse, V., King, C., Jacobetz, M.A., Ross, S., Conrads, T.P., Veenstra, T.D., Hitt, B.A., Kawaguchi, Y., Johann, D., Liotta, L.A., Crawford, H.C., Putt, M.E., Jacks, T., Wright, C.V., Hruban, R.H., Lowy, A.M. and Tuveson, D.A. (2003b) Preinvasive and invasive ductal pancreatic cancer and its early detection in the mouse. *Cancer Cell*, **4**, 437-450.
- Hoess, R.H. and Abremski, K. (1984) Interaction of the bacteriophage P1 recombinase Cre with the recombining site loxP. *Proc Natl Acad Sci U S A*, **81**, 1026-1029.
- Hoess, R.H., Ziese, M. and Sternberg, N. (1982) P1 site-specific recombination: nucleotide sequence of the recombining sites. *Proc Natl Acad Sci U S A*, **79**, 3398-3402.

- Hoppe, J., Schafer, R., Hoppe, V. and Sachinidis, A. (1999) ATP and adenosine prevent via different pathways the activation of caspases in apoptotic AKR-2B fibroblasts. *Cell Death Differ*, **6**, 546-556.
- Hoshino, R., Chatani, Y., Yamori, T., Tsuruo, T., Oka, H., Yoshida, O., Shimada, Y., Ari-i, S., Wada, H., Fujimoto, J. and Kohno, M. (1999) Constitutive activation of the 41-/43-kDa mitogen-activated protein kinase signaling pathway in human tumors. *Oncogene*, **18**, 813-822.
- Houben, R., Becker, J.C., Kappel, A., Terheyden, P., Brocker, E.B., Goetz, R. and Rapp, U.R. (2004) Constitutive activation of the Ras-Raf signaling pathway in metastatic melanoma is associated with poor prognosis. *J Carcinog*, **3**, 6.
- Howe, L.R., Leever, S.J., Gomez, N., Nakielny, S., Cohen, P. and Marshall, C.J. (1992) Activation of the MAP kinase pathway by the protein kinase raf. *Cell*, **71**, 335-342.
- Hsu, V., Zobel, C.L., Lambie, E.J., Schedl, T. and Kornfeld, K. (2002) *Caenorhabditis elegans* lin-45 raf is essential for larval viability, fertility and the induction of vulval cell fates. *Genetics*, **160**, 481-492.
- Hu, C.D., Kariya, K., Tamada, M., Akasaka, K., Shirouzu, M., Yokoyama, S. and Kataoka, T. (1995) Cysteine-rich region of Raf-1 interacts with activator domain of post-translationally modified Ha-Ras. *J Biol Chem*, **270**, 30274-30277.
- Hughes, P.E., Renshaw, M.W., Pfaff, M., Forsyth, J., Keivens, V.M., Schwartz, M.A. and Ginsberg, M.H. (1997) Suppression of integrin activation: a novel function of a Ras/Raf-initiated MAP kinase pathway. *Cell*, **88**, 521-530.
- Huleihel, M., Goldsborough, M., Cleveland, J., Gunnell, M., Bonner, T. and Rapp, U.R. (1986) Characterization of murine A-raf, a new oncogene related to the v-raf oncogene. *Mol Cell Biol*, **6**, 2655-2662.
- Huser, M., Luckett, J., Chiloeches, A., Mercer, K., Iwobi, M., Giblett, S., Sun, X.M., Brown, J., Marais, R. and Pritchard, C. (2001) MEK kinase activity is not necessary for Raf-1 function. *Embo J*, **20**, 1940-1951.
- Ichijo, H., Nishida, E., Irie, K., ten Dijke, P., Saitoh, M., Moriguchi, T., Takagi, M., Matsumoto, K., Miyazono, K. and Gotoh, Y. (1997) Induction of apoptosis by ASK1, a mammalian MAPKKK that activates SAPK/JNK and p38 signaling pathways. *Science*, **275**, 90-94.
- Ikawa, S., Fukui, M., Ueyama, Y., Tamaoki, N., Yamamoto, T. and Toyoshima, K. (1988) B-raf, a new member of the raf family, is activated by DNA rearrangement. *Mol Cell Biol*, **8**, 2651-2654.

- Ikenoue, T., Hikiba, Y., Kanai, F., Aragaki, J., Tanaka, Y., Imamura, J., Imamura, T., Ohta, M., Ijichi, H., Tateishi, K., Kawakami, T., Matsumura, M., Kawabe, T. and Omata, M. (2004) Different effects of point mutations within the B-Raf glycine-rich loop in colorectal tumors on mitogen-activated protein/extracellular signal-regulated kinase kinase/extracellular signal-regulated kinase and nuclear factor kappaB pathway and cellular transformation. *Cancer Res*, **64**, 3428-3435.
- Ikenoue, T., Hikiba, Y., Kanai, F., Tanaka, Y., Imamura, J., Imamura, T., Ohta, M., Ijichi, H., Tateishi, K., Kawakami, T., Aragaki, J., Matsumura, M., Kawabe, T. and Omata, M. (2003) Functional analysis of mutations within the kinase activation segment of B-Raf in human colorectal tumors. *Cancer Res*, **63**, 8132-8137.
- Irie, K., Gotoh, Y., Yashar, B.M., Errede, B., Nishida, E. and Matsumoto, K. (1994) Stimulatory effects of yeast and mammalian 14-3-3 proteins on the Raf protein kinase. *Science*, **265**, 1716-1719.
- Ise, K., Nakamura, K., Nakao, K., Shimizu, S., Harada, H., Ichise, T., Miyoshi, J., Gondo, Y., Ishikawa, T., Aiba, A. and Katsuki, M. (2000) Targeted deletion of the H-ras gene decreases tumor formation in mouse skin carcinogenesis. *Oncogene*, **19**, 2951-2956.
- Jackson, E.L., Willis, N., Mercer, K., Bronson, R.T., Crowley, D., Montoya, R., Jacks, T. and Tuveson, D.A. (2001) Analysis of lung tumor initiation and progression using conditional expression of oncogenic K-ras. *Genes Dev*, **15**, 3243-3248.
- Jaiswal, R.K., Moodie, S.A., Wolfman, A. and Landreth, G.E. (1994) The mitogen-activated protein kinase cascade is activated by B-Raf in response to nerve growth factor through interaction with p21ras. *Mol Cell Biol*, **14**, 6944-6953.
- Jaiswal, R.K., Weissinger, E., Kolch, W. and Landreth, G.E. (1996) Nerve growth factor-mediated activation of the mitogen-activated protein (MAP) kinase cascade involves a signaling complex containing B-Raf and HSP90. *J Biol Chem*, **271**, 23626-23629.
- Janosch, P., Schellerer, M., Seitz, T., Reim, P., Eulitz, M., Brielmeier, M., Kolch, W., Sedivy, J.M. and Mischak, H. (1996) Characterization of IkappaB kinases. IkappaB-alpha is not phosphorylated by Raf-1 or protein kinase C isozymes, but is a casein kinase II substrate. *J Biol Chem*, **271**, 13868-13874.
- Jansen-Durr, P., Meichle, A., Steiner, P., Pagano, M., Finke, K., Botz, J., Wessbecher, J., Draetta, G. and Eilers, M. (1993) Differential modulation of cyclin gene expression by MYC. *Proc Natl Acad Sci U S A*, **90**, 3685-3689.

- Jat, P.S. and Sharp, P.A. (1989) Cell lines established by a temperature-sensitive simian virus 40 large-T-antigen gene are growth restricted at the nonpermissive temperature. *Mol Cell Biol*, **9**, 1672-1681.
- Jaumot, M. and Hancock, J.F. (2001) Protein phosphatases 1 and 2A promote Raf-1 activation by regulating 14-3-3 interactions. *Oncogene*, **20**, 3949-3958.
- Jesenberger, V., Procyk, K.J., Ruth, J., Schreiber, M., Theussl, H.C., Wagner, E.F. and Baccarini, M. (2001) Protective role of Raf-1 in Salmonella-induced macrophage apoptosis. *J Exp Med*, **193**, 353-364.
- Jiang, Y., Chen, C., Li, Z., Guo, W., Gegner, J.A., Lin, S. and Han, J. (1996) Characterization of the structure and function of a new mitogen-activated protein kinase (p38beta). *J Biol Chem*, **271**, 17920-17926.
- Johnson, L., Greenbaum, D., Cichowski, K., Mercer, K., Murphy, E., Schmitt, E., Bronson, R.T., Umanoff, H., Edelman, W., Kucherlapati, R. and Jacks, T. (1997) K-ras is an essential gene in the mouse with partial functional overlap with N-ras. *Genes Dev*, **11**, 2468-2481.
- Johnson, L.N., Lowe, E.D., Noble, M.E. and Owen, D.J. (1998) The Eleventh Datta Lecture. The structural basis for substrate recognition and control by protein kinases. *FEBS Lett*, **430**, 1-11.
- Kamakura, S., Moriguchi, T. and Nishida, E. (1999) Activation of the protein kinase ERK5/BMK1 by receptor tyrosine kinases. Identification and characterization of a signaling pathway to the nucleus. *J Biol Chem*, **274**, 26563-26571.
- Kao, S., Jaiswal, R.K., Kolch, W. and Landreth, G.E. (2001) Identification of the mechanisms regulating the differential activation of the mapk cascade by epidermal growth factor and nerve growth factor in PC12 cells. *J Biol Chem*, **276**, 18169-18177.
- Karasarides, M., Chiloehes, A., Hayward, R., Niculescu-Duvaz, D., Scanlon, I., Friedlos, F., Ogilvie, L., Hedley, D., Martin, J., Marshall, C.J., Springer, C.J. and Marais, R. (2004) B-RAF is a therapeutic target in melanoma. *Oncogene*, **23**, 6292-6298.
- Kato, J., Matsushime, H., Hiebert, S.W., Ewen, M.E. and Sherr, C.J. (1993) Direct binding of cyclin D to the retinoblastoma gene product (pRb) and pRb phosphorylation by the cyclin D-dependent kinase CDK4. *Genes Dev*, **7**, 331-342.
- Kato, Y., Kravchenko, V.V., Tapping, R.I., Han, J., Ulevitch, R.J. and Lee, J.D. (1997) BMK1/ERK5 regulates serum-induced early gene expression through transcription factor MEF2C. *Embo J*, **16**, 7054-7066.

- Kauffmann-Zeh, A., Rodriguez-Viciana, P., Ulrich, E., Gilbert, C., Coffey, P., Downward, J. and Evan, G. (1997) Suppression of c-Myc-induced apoptosis by Ras signalling through PI(3)K and PKB. *Nature*, **385**, 544-548.
- Kerkhoff, E. and Rapp, U.R. (1997) Induction of cell proliferation in quiescent NIH 3T3 cells by oncogenic c-Raf-1. *Mol Cell Biol*, **17**, 2576-2586.
- Kerkhoff, E. and Rapp, U.R. (1998) High-intensity Raf signals convert mitotic cell cycling into cellular growth. *Cancer Res*, **58**, 1636-1640.
- Khwaja, A., Rodriguez-Viciana, P., Wennstrom, S., Warne, P.H. and Downward, J. (1997) Matrix adhesion and Ras transformation both activate a phosphoinositide 3-OH kinase and protein kinase B/Akt cellular survival pathway. *Embo J*, **16**, 2783-2793.
- Kimura, E.T., Nikiforova, M.N., Zhu, Z., Knauf, J.A., Nikiforov, Y.E. and Fagin, J.A. (2003) High prevalence of BRAF mutations in thyroid cancer: genetic evidence for constitutive activation of the RET/PTC-RAS-BRAF signaling pathway in papillary thyroid carcinoma. *Cancer Res*, **63**, 1454-1457.
- King, A.J., Sun, H., Diaz, B., Barnard, D., Miao, W., Bagrodia, S. and Marshall, M.S. (1998) The protein kinase Pak3 positively regulates Raf-1 activity through phosphorylation of serine 338. *Nature*, **396**, 180-183.
- Klemke, R.L., Cai, S., Giannini, A.L., Gallagher, P.J., de Lanerolle, P. and Cheresch, D.A. (1997) Regulation of cell motility by mitogen-activated protein kinase. *J Cell Biol*, **137**, 481-492.
- Kluck, R.M., Bossy-Wetzel, E., Green, D.R. and Newmeyer, D.D. (1997) The release of cytochrome c from mitochondria: a primary site for Bcl-2 regulation of apoptosis. *Science*, **275**, 1132-1136.
- Koide, H., Satoh, T., Nakafuku, M. and Kaziro, Y. (1993) GTP-dependent association of Raf-1 with Ha-Ras: identification of Raf as a target downstream of Ras in mammalian cells. *Proc Natl Acad Sci U S A*, **90**, 8683-8686.
- Kolbus, A., Pilat, S., Husak, Z., Deiner, E.M., Stengl, G., Beug, H. and Baccarini, M. (2002) Raf-1 antagonizes erythroid differentiation by restraining caspase activation. *J Exp Med*, **196**, 1347-1353.
- Kolch, W. (2000) Meaningful relationships: the regulation of the Ras/Raf/MEK/ERK pathway by protein interactions. *Biochem J*, **351 Pt 2**, 289-305.
- Kolch, W., Heidecker, G., Kochs, G., Hummel, R., Vahidi, H., Mischak, H., Finkenzeller, G., Marme, D. and Rapp, U.R. (1993) Protein kinase C alpha activates RAF-1 by direct phosphorylation. *Nature*, **364**, 249-252.

- Kolch, W., Heidecker, G., Lloyd, P. and Rapp, U.R. (1991) Raf-1 protein kinase is required for growth of induced NIH/3T3 cells. *Nature*, **349**, 426-428.
- Kolch, W., Philipp, A., Mischak, H., Dutil, E.M., Mullen, T.M., Feramisco, J.R., Meinkoth, J.L. and Rose, D.W. (1996) Inhibition of Raf-1 signaling by a monoclonal antibody, which interferes with Raf-1 activation and with Mek substrate binding. *Oncogene*, **13**, 1305-1314.
- Korsmeyer, S.J., Wei, M.C., Saito, M., Weiler, S., Oh, K.J. and Schlesinger, P.H. (2000) Pro-apoptotic cascade activates BID, which oligomerizes BAK or BAX into pores that result in the release of cytochrome c. *Cell Death Differ*, **7**, 1166-1173.
- Kozar, K., Ciemerych, M.A., Rebel, V.I., Shigematsu, H., Zagozdzon, A., Sicinska, E., Geng, Y., Yu, Q., Bhattacharya, S., Bronson, R.T., Akashi, K. and Sicinski, P. (2004) Mouse development and cell proliferation in the absence of D-cyclins. *Cell*, **118**, 477-491.
- Kramer, R.M., Roberts, E.F., Um, S.L., Borsch-Haubold, A.G., Watson, S.P., Fisher, M.J. and Jakubowski, J.A. (1996) p38 mitogen-activated protein kinase phosphorylates cytosolic phospholipase A2 (cPLA2) in thrombin-stimulated platelets. Evidence that proline-directed phosphorylation is not required for mobilization of arachidonic acid by cPLA2. *J Biol Chem*, **271**, 27723-27729.
- Krimpenfort, P., Quon, K.C., Mooi, W.J., Loonstra, A. and Berns, A. (2001) Loss of p16Ink4a confers susceptibility to metastatic melanoma in mice. *Nature*, **413**, 83-86.
- Kubicek, M., Pacher, M., Abraham, D., Podar, K., Eulitz, M. and Baccarini, M. (2002) Dephosphorylation of Ser-259 regulates Raf-1 membrane association. *J Biol Chem*, **277**, 7913-7919.
- Kuhn, R., Schwenk, F., Aguet, M. and Rajewsky, K. (1995) Inducible gene targeting in mice. *Science*, **269**, 1427-1429.
- Kumar, R., Angelini, S., Czene, K., Sauroja, I., Hahka-Kemppinen, M., Pyrhonen, S. and Hemminki, K. (2003) BRAF mutations in metastatic melanoma: a possible association with clinical outcome. *Clin Cancer Res*, **9**, 3362-3368.
- Kumar, R., Angelini, S., Snellman, E. and Hemminki, K. (2004) BRAF mutations are common somatic events in melanocytic nevi. *J Invest Dermatol*, **122**, 342-348.
- Kyriakis, J., Woodgett, J. and Avruch, J. (1995) The stress-activated protein kinases. A novel ERK subfamily responsive to cellular stress and inflammatory cytokines. *Ann N Y Acad Sci*, **766**, 303-319.

- Kyriakis, J.M., App, H., Zhang, X.F., Banerjee, P., Brautigan, D.L., Rapp, U.R. and Avruch, J. (1992) Raf-1 activates MAP kinase-kinase. *Nature*, **358**, 417-421.
- LaBaer, J., Garrett, M.D., Stevenson, L.F., Slingerland, J.M., Sandhu, C., Chou, H.S., Fattaey, A. and Harlow, E. (1997) New functional activities for the p21 family of CDK inhibitors. *Genes Dev*, **11**, 847-862.
- Lange-Carter, C.A., Pleiman, C.M., Gardner, A.M., Blumer, K.J. and Johnson, G.L. (1993) A divergence in the MAP kinase regulatory network defined by MEK kinase and Raf. *Science*, **260**, 315-319.
- Le Gall, M., Chambard, J.C., Breittmayer, J.P., Grall, D., Pouyssegur, J. and Van Obberghen-Schilling, E. (2000) The p42/p44 MAP kinase pathway prevents apoptosis induced by anchorage and serum removal. *Mol Biol Cell*, **11**, 1103-1112.
- Le Guellec, R., Couturier, A., Le Guellec, K., Paris, J., Le Fur, N. and Philippe, M. (1991) Xenopus c-raf proto-oncogene: cloning and expression during oogenesis and early development. *Biol Cell*, **72**, 39-45.
- Le Mellay, V., Troppmair, J., Benz, R. and Rapp, U.R. (2002) Negative regulation of mitochondrial VDAC channels by C-Raf kinase. *BMC Cell Biol*, **3**, 14.
- Lee, C.W., Nam, J.S., Park, Y.K., Choi, H.K., Lee, J.H., Kim, N.H., Cho, J., Song, D.K., Suh, H.W., Lee, J., Kim, Y.H. and Huh, S.O. (2003a) Lysophosphatidic acid stimulates CREB through mitogen- and stress-activated protein kinase-1. *Biochem Biophys Res Commun*, **305**, 455-461.
- Lee, J.D., Ulevitch, R.J. and Han, J. (1995a) Primary structure of BMK1: a new mammalian map kinase. *Biochem Biophys Res Commun*, **213**, 715-724.
- Lee, J.H., Cho, K.S., Lee, J., Kim, D., Lee, S.B., Yoo, J., Cha, G.H. and Chung, J. (2002) Drosophila PDZ-GEF, a guanine nucleotide exchange factor for Rap1 GTPase, reveals a novel upstream regulatory mechanism in the mitogen-activated protein kinase signaling pathway. *Mol Cell Biol*, **22**, 7658-7666.
- Lee, J.W., Yoo, N.J., Soung, Y.H., Kim, H.S., Park, W.S., Kim, S.Y., Lee, J.H., Park, J.Y., Cho, Y.G., Kim, C.J., Ko, Y.H., Kim, S.H., Nam, S.W., Lee, J.Y. and Lee, S.H. (2003c) BRAF mutations in non-Hodgkin's lymphoma. *Br J Cancer*, **89**, 1958-1960.
- Lee, M.H., Reynisdottir, I. and Massague, J. (1995b) Cloning of p57KIP2, a cyclin-dependent kinase inhibitor with unique domain structure and tissue distribution. *Genes Dev*, **9**, 639-649.

- Lee, S.H., Lee, J.W., Soung, Y.H., Kim, H.S., Park, W.S., Kim, S.Y., Lee, J.H., Park, J.Y., Cho, Y.G., Kim, C.J., Nam, S.W., Kim, S.H., Lee, J.Y. and Yoo, N.J. (2003b) BRAF and KRAS mutations in stomach cancer. *Oncogene*, **22**, 6942-6945.
- Leevers, S.J. and Marshall, C.J. (1992) Activation of extracellular signal-regulated kinase, ERK2, by p21ras oncoprotein. *Embo J*, **11**, 569-574.
- Leevers, S.J., Paterson, H.F. and Marshall, C.J. (1994) Requirement for Ras in Raf activation is overcome by targeting Raf to the plasma membrane. *Nature*, **369**, 411-414.
- Lei, K. and Davis, R.J. (2003) JNK phosphorylation of Bim-related members of the Bcl2 family induces Bax-dependent apoptosis. *Proc Natl Acad Sci U S A*, **100**, 2432-2437.
- Lei, K., Nimmual, A., Zong, W.X., Kennedy, N.J., Flavell, R.A., Thompson, C.B., Bar-Sagi, D. and Davis, R.J. (2002) The Bax subfamily of Bcl2-related proteins is essential for apoptotic signal transduction by c-Jun NH(2)-terminal kinase. *Mol Cell Biol*, **22**, 4929-4942.
- Ley, R., Balmanno, K., Hadfield, K., Weston, C. and Cook, S.J. (2003) Activation of the ERK1/2 signaling pathway promotes phosphorylation and proteasome-dependent degradation of the BH3-only protein, Bim. *J Biol Chem*, **278**, 18811-18816.
- Ley, R., Ewings, K.E., Hadfield, K., Howes, E., Balmanno, K. and Cook, S.J. (2004) Extracellular signal-regulated kinases 1/2 are serum-stimulated "Bim(EL) kinases" that bind to the BH3-only protein Bim(EL) causing its phosphorylation and turnover. *J Biol Chem*, **279**, 8837-8847.
- Li, H., Zhu, H., Xu, C.J. and Yuan, J. (1998) Cleavage of BID by caspase 8 mediates the mitochondrial damage in the Fas pathway of apoptosis. *Cell*, **94**, 491-501.
- Li, S., Janosch, P., Tanji, M., Rosenfeld, G.C., Waymire, J.C., Mischak, H., Kolch, W. and Sedivy, J.M. (1995) Regulation of Raf-1 kinase activity by the 14-3-3 family of proteins. *Embo J*, **14**, 685-696.
- Li, S. and Sedivy, J.M. (1993) Raf-1 protein kinase activates the NF-kappa B transcription factor by dissociating the cytoplasmic NF-kappa B-I kappa B complex. *Proc Natl Acad Sci U S A*, **90**, 9247-9251.
- Li, W., Han, M. and Guan, K.L. (2000) The leucine-rich repeat protein SUR-8 enhances MAP kinase activation and forms a complex with Ras and Raf. *Genes Dev*, **14**, 895-900.
- Lin, A., Minden, A., Martinetto, H., Claret, F.X., Lange-Carter, C., Mercurio, F., Johnson, G.L. and Karin, M. (1995) Identification of a dual specificity kinase that activates the Jun kinases and p38-Mpk2. *Science*, **268**, 286-290.

- Lin, L.L., Wartmann, M., Lin, A.Y., Knopf, J.L., Seth, A. and Davis, R.J. (1993) cPLA2 is phosphorylated and activated by MAP kinase. *Cell*, **72**, 269-278.
- Liscovitch, M., Ben-Av, P., Danin, M., Faiman, G., Eldar, H. and Livneh, E. (1993) Phospholipase D-mediated hydrolysis of phosphatidylcholine: role in cell signalling. *J Lipid Mediat*, **8**, 177-182.
- Liu, X., Kim, C.N., Yang, J., Jemmerson, R. and Wang, X. (1996) Induction of apoptotic program in cell-free extracts: requirement for dATP and cytochrome c. *Cell*, **86**, 147-157.
- Lloyd, A.C., Obermuller, F., Staddon, S., Barth, C.F., McMahon, M. and Land, H. (1997) Cooperating oncogenes converge to regulate cyclin/cdk complexes. *Genes Dev*, **11**, 663-677.
- Lowenstein, E.J., Daly, R.J., Batzer, A.G., Li, W., Margolis, B., Lammers, R., Ullrich, A., Skolnik, E.Y., Bar-Sagi, D. and Schlessinger, J. (1992) The SH2 and SH3 domain-containing protein GRB2 links receptor tyrosine kinases to ras signaling. *Cell*, **70**, 431-442.
- Lowy, D.R., Zhang, K., DeClue, J.E. and Willumsen, B.M. (1991) Regulation of p21ras activity. *Trends Genet*, **7**, 346-351.
- Luckett, J.C., Huser, M.B., Giagtzoglou, N., Brown, J.E. and Pritchard, C.A. (2000) Expression of the A-raf proto-oncogene in the normal adult and embryonic mouse. *Cell Growth Differ*, **11**, 163-171.
- Luo, Z., Diaz, B., Marshall, M.S. and Avruch, J. (1997) An intact Raf zinc finger is required for optimal binding to processed Ras and for ras-dependent Raf activation in situ. *Mol Cell Biol*, **17**, 46-53.
- Luo, Z., Tzivion, G., Belshaw, P.J., Vavvas, D., Marshall, M. and Avruch, J. (1996) Oligomerization activates c-Raf-1 through a Ras-dependent mechanism. *Nature*, **383**, 181-185.
- MacNicol, A.M., Muslin, A.J. and Williams, L.T. (1993) Raf-1 kinase is essential for early *Xenopus* development and mediates the induction of mesoderm by FGF. *Cell*, **73**, 571-583.
- Manser, E., Leung, T., Salihuddin, H., Zhao, Z.S. and Lim, L. (1994) A brain serine/threonine protein kinase activated by Cdc42 and Rac1. *Nature*, **367**, 40-46.
- Marais, R., Light, Y., Mason, C., Paterson, H., Olson, M.F. and Marshall, C.J. (1998) Requirement of Ras-GTP-Raf complexes for activation of Raf-1 by protein kinase C. *Science*, **280**, 109-112.

- Marais, R., Light, Y., Paterson, H.F. and Marshall, C.J. (1995) Ras recruits Raf-1 to the plasma membrane for activation by tyrosine phosphorylation. *Embo J*, **14**, 3136-3145.
- Marais, R., Light, Y., Paterson, H.F., Mason, C.S. and Marshall, C.J. (1997) Differential regulation of Raf-1, A-Raf, and B-Raf by oncogenic ras and tyrosine kinases. *J Biol Chem*, **272**, 4378-4383.
- Marais, R., Wynne, J. and Treisman, R. (1993) The SRF accessory protein Elk-1 contains a growth factor-regulated transcriptional activation domain. *Cell*, **73**, 381-393.
- Marani, M., Hancock, D., Lopes, R., Tenev, T., Downward, J. and Lemoine, N.R. (2004) Role of Bim in the survival pathway induced by Raf in epithelial cells. *Oncogene*, **23**, 2431-2441.
- Marani, M., Tenev, T., Hancock, D., Downward, J. and Lemoine, N.R. (2002) Identification of novel isoforms of the BH3 domain protein Bim which directly activate Bax to trigger apoptosis. *Mol Cell Biol*, **22**, 3577-3589.
- Mark, G.E., MacIntyre, R.J., Digan, M.E., Ambrosio, L. and Perrimon, N. (1987) *Drosophila melanogaster* homologs of the raf oncogene. *Mol Cell Biol*, **7**, 2134-2140.
- Martin, G.R. (1981) Isolation of a pluripotent cell line from early mouse embryos cultured in medium conditioned by teratocarcinoma stem cells. *Proc Natl Acad Sci U S A*, **78**, 7634-7638.
- Marx, M., Eychene, A., Laugier, D., Bechade, C., Crisanti, P., Dezelee, P., Pessac, B. and Calothy, G. (1988) A novel oncogene related to c-mil is transduced in chicken neuroretina cells induced to proliferate by infection with an avian lymphomatosis virus. *Embo J*, **7**, 3369-3373.
- Mason, C.S., Springer, C.J., Cooper, R.G., Superti-Furga, G., Marshall, C.J. and Marais, R. (1999) Serine and tyrosine phosphorylations cooperate in Raf-1, but not B-Raf activation. *Embo J*, **18**, 2137-2148.
- Matsuda, S., Gotoh, Y. and Nishida, E. (1993) Phosphorylation of Xenopus mitogen-activated protein (MAP) kinase kinase by MAP kinase kinase kinase and MAP kinase. *J Biol Chem*, **268**, 3277-3281.
- Matsuda, S., Kosako, H., Takenaka, K., Moriyama, K., Sakai, H., Akiyama, T., Gotoh, Y. and Nishida, E. (1992) Xenopus MAP kinase activator: identification and function as a key intermediate in the phosphorylation cascade. *Embo J*, **11**, 973-982.

- Mayo, L.D. and Donner, D.B. (2001) A phosphatidylinositol 3-kinase/Akt pathway promotes translocation of Mdm2 from the cytoplasm to the nucleus. *Proc Natl Acad Sci U S A*, **98**, 11598-11603.
- McCarthy, S.A., Chen, D., Yang, B.S., Garcia Ramirez, J.J., Cherwinski, H., Chen, X.R., Klagsbrun, M., Hauser, C.A., Ostrowski, M.C. and McMahon, M. (1997) Rapid phosphorylation of Ets-2 accompanies mitogen-activated protein kinase activation and the induction of heparin-binding epidermal growth factor gene expression by oncogenic Raf-1. *Mol Cell Biol*, **17**, 2401-2412.
- McKnight, G.S. (1991) Cyclic AMP second messenger systems. *Curr Opin Cell Biol*, **3**, 213-217.
- Melnick, M.B., Perkins, L.A., Lee, M., Ambrosio, L. and Perrimon, N. (1993) Developmental and molecular characterization of mutations in the Drosophila-raf serine/threonine protein kinase. *Development*, **118**, 127-138.
- Mercer, K., Chiloeches, A., Huser, M., Kiernan, M., Marais, R. and Pritchard, C. (2002) ERK signalling and oncogene transformation are not impaired in cells lacking A-Raf. *Oncogene*, **21**, 347-355.
- Mercer, K., Giblett, S., Oakden, A., Brown, J., Marais, R. and Pritchard, C. (2005) A-Raf and Raf-1 work together to influence transient ERK phosphorylation and G1/S cell cycle progression. *Oncogene*, **24**, 5207-5217.
- Mercer, K.E. and Pritchard, C.A. (2003) Raf proteins and cancer: B-Raf is identified as a mutational target. *Biochim Biophys Acta*, **1653**, 25-40.
- Mercurio, F., DiDonato, J.A., Rosette, C. and Karin, M. (1993) p105 and p98 precursor proteins play an active role in NF-kappa B-mediated signal transduction. *Genes Dev*, **7**, 705-718.
- Meuwissen, R., Linn, S.C., van der Valk, M., Mooi, W.J. and Berns, A. (2001) Mouse model for lung tumorigenesis through Cre/lox controlled sporadic activation of the K-Ras oncogene. *Oncogene*, **20**, 6551-6558.
- Michaud, N.R., Fabian, J.R., Mathes, K.D. and Morrison, D.K. (1995) 14-3-3 is not essential for Raf-1 function: identification of Raf-1 proteins that are biologically activated in a 14-3-3- and Ras-independent manner. *Mol Cell Biol*, **15**, 3390-3397.
- Micheau, O., Lens, S., Gaide, O., Alevizopoulos, K. and Tschopp, J. (2001) NF-kappaB signals induce the expression of c-FLIP. *Mol Cell Biol*, **21**, 5299-5305.

- Mikula, M., Schreiber, M., Husak, Z., Kucerova, L., Ruth, J., Wieser, R., Zatloukal, K., Beug, H., Wagner, E.F. and Baccarini, M. (2001) Embryonic lethality and fetal liver apoptosis in mice lacking the c-raf-1 gene. *Embo J*, **20**, 1952-1962.
- Mineo, C., Anderson, R.G. and White, M.A. (1997) Physical association with ras enhances activation of membrane-bound raf (RafCAAX). *J Biol Chem*, **272**, 10345-10348.
- Mirza, A.M., Gysin, S., Malek, N., Nakayama, K., Roberts, J.M. and McMahon, M. (2004) Cooperative regulation of the cell division cycle by the protein kinases RAF and AKT. *Mol Cell Biol*, **24**, 10868-10881.
- Mischak, H., Seitz, T., Janosch, P., Eulitz, M., Steen, H., Schellerer, M., Philipp, A. and Kolch, W. (1996) Negative regulation of Raf-1 by phosphorylation of serine 621. *Mol Cell Biol*, **16**, 5409-5418.
- Miyashita, T., Shikama, Y., Tadokoro, K. and Yamada, M. (2001) Molecular cloning and characterization of six novel isoforms of human Bim, a member of the proapoptotic Bcl-2 family. *FEBS Lett*, **509**, 135-141.
- Moelling, K., Schad, K., Bosse, M., Zimmermann, S. and Schweneker, M. (2002) Regulation of Raf-Akt Cross-talk. *J Biol Chem*, **277**, 31099-31106.
- Moodie, S.A., Paris, M., Villafranca, E., Kirshmeier, P., Willumsen, B.M. and Wolfman, A. (1995) Different structural requirements within the switch II region of the Ras protein for interactions with specific downstream targets. *Oncogene*, **11**, 447-454.
- Moriguchi, T., Kuroyanagi, N., Yamaguchi, K., Gotoh, Y., Irie, K., Kano, T., Shirakabe, K., Muro, Y., Shibuya, H., Matsumoto, K., Nishida, E. and Hagiwara, M. (1996) A novel kinase cascade mediated by mitogen-activated protein kinase kinase 6 and MKK3. *J Biol Chem*, **271**, 13675-13679.
- Morrison, D.K. (1995) Mechanisms regulating Raf-1 activity in signal transduction pathways. *Mol Reprod Dev*, **42**, 507-514.
- Morrison, D.K., Heidecker, G., Rapp, U.R. and Copeland, T.D. (1993) Identification of the major phosphorylation sites of the Raf-1 kinase. *J Biol Chem*, **268**, 17309-17316.
- Morrison, D.K., Kaplan, D.R., Rapp, U. and Roberts, T.M. (1988) Signal transduction from membrane to cytoplasm: growth factors and membrane-bound oncogene products increase Raf-1 phosphorylation and associated protein kinase activity. *Proc Natl Acad Sci U S A*, **85**, 8855-8859.
- Morse, H.C.r., Anver, M.R., Fredrickson, T.N., Haines, D.C., Harris, A.W., Harris, N.L., Jaffe, E.S., Kogan, S.C., MacLennan, I.C., Pattengale, P.K. and Ward, J.M. (2002)

- Bethesda proposals for classification of lymphoid neoplasms in mice. *Blood*, **100**, 246-258.
- Mott, H.R., Carpenter, J.W., Zhong, S., Ghosh, S., Bell, R.M. and Campbell, S.L. (1996) The solution structure of the Raf-1 cysteine-rich domain: a novel ras and phospholipid binding site. *Proc Natl Acad Sci U S A*, **93**, 8312-8317.
- Movilla, N., Crespo, P. and Bustelo, X.R. (1999) Signal transduction elements of TC21, an oncogenic member of the R-Ras subfamily of GTP-binding proteins. *Oncogene*, **18**, 5860-5869.
- Muller, J., Ory, S., Copeland, T., Piwnica-Worms, H. and Morrison, D.K. (2001) C-TAK1 regulates Ras signaling by phosphorylating the MAPK scaffold, KSR1. *Mol Cell*, **8**, 983-993.
- Murai, H., Ikeda, M., Kishida, S., Ishida, O., Okazaki-Kishida, M., Matsuura, Y. and Kikuchi, A. (1997) Characterization of Ral GDP dissociation stimulator-like (RGL) activities to regulate c-fos promoter and the GDP/GTP exchange of Ral. *J Biol Chem*, **272**, 10483-10490.
- Murphy, L.O., Smith, S., Chen, R.H., Fingar, D.C. and Blenis, J. (2002) Molecular interpretation of ERK signal duration by immediate early gene products. *Nat Cell Biol*, **4**, 556-564.
- Muslin, A.J. and Xing, H. (2000) 14-3-3 proteins: regulation of subcellular localization by molecular interference. *Cell Signal*, **12**, 703-709.
- Muszynski, K.W., Ruscetti, F.W., Heidecker, G., Rapp, U., Troppmair, J., Gooya, J.M. and Keller, J.R. (1995) Raf-1 protein is required for growth factor-induced proliferation of hematopoietic cells. *J Exp Med*, **181**, 2189-2199.
- Nakielny, S., Cohen, P., Wu, J. and Sturgill, T. (1992) MAP kinase activator from insulin-stimulated skeletal muscle is a protein threonine/tyrosine kinase. *Embo J*, **11**, 2123-2129.
- Nho, R.S. and Sheaff, R.J. (2003) p27kip1 contributes to cancer. *Prog Cell Cycle Res*, **5**, 249-259.
- Nimnual, A. and Bar-Sagi, D. (2002) The two hats of SOS. *Sci STKE*, **2002**, PE36.
- Norris, J.L. and Baldwin, A.S., Jr. (1999) Oncogenic Ras enhances NF-kappaB transcriptional activity through Raf-dependent and Raf-independent mitogen-activated protein kinase signaling pathways. *J Biol Chem*, **274**, 13841-13846.
- Northwood, I.C., Gonzalez, F.A., Wartmann, M., Raden, D.L. and Davis, R.J. (1991) Isolation and characterization of two growth factor-stimulated protein kinases that

- phosphorylate the epidermal growth factor receptor at threonine 669. *J Biol Chem*, **266**, 15266-15276.
- O'Connor, L., Strasser, A., O'Reilly, L.A., Hausmann, G., Adams, J.M., Cory, S. and Huang, D.C. (1998) Bim: a novel member of the Bcl-2 family that promotes apoptosis. *Embo J*, **17**, 384-395.
- Ohmachi, M., Rocheleau, C.E., Church, D., Lambie, E., Schedl, T. and Sundaram, M.V. (2002) *C. elegans* ksr-1 and ksr-2 have both unique and redundant functions and are required for MPK-1 ERK phosphorylation. *Curr Biol*, **12**, 427-433.
- Ohtsubo, M., Theodoras, A.M., Schumacher, J., Roberts, J.M. and Pagano, M. (1995) Human cyclin E, a nuclear protein essential for the G1-to-S phase transition. *Mol Cell Biol*, **15**, 2612-2624.
- Ohtsuka, T., Shimizu, K., Yamamori, B., Kuroda, S. and Takai, Y. (1996) Activation of brain B-Raf protein kinase by Rap1B small GTP-binding protein. *J Biol Chem*, **271**, 1258-1261.
- Okada, T., Hu, C.D., Jin, T.G., Kariya, K., Yamawaki-Kataoka, Y. and Kataoka, T. (1999) The strength of interaction at the Raf cysteine-rich domain is a critical determinant of response of Raf to Ras family small GTPases. *Mol Cell Biol*, **19**, 6057-6064.
- Oliveira, C., Pinto, M., Duval, A., Brennetot, C., Domingo, E., Espin, E., Armengol, M., Yamamoto, H., Hamelin, R., Seruca, R. and Schwartz, S., Jr. (2003) BRAF mutations characterize colon but not gastric cancer with mismatch repair deficiency. *Oncogene*, **22**, 9192-9196.
- Olivier, R., Otter, I., Monney, L., Wartmann, M. and Borner, C. (1997) Bcl-2 does not require Raf kinase activity for its death-protective function. *Biochem J*, **324** ( Pt 1), 75-83.
- O'Neill, E., Matallanas, D. and Kolch, W. (2005) Mammalian sterile 20-like kinases in tumor suppression: an emerging pathway. *Cancer Res*, **65**, 5485-5487.
- O'Neill, E., Rushworth, L., Baccarini, M. and Kolch, W. (2004) Role of the kinase MST2 in suppression of apoptosis by the proto-oncogene product Raf-1. *Science*, **306**, 2267-2270.
- Orita, S., Kaibuchi, K., Kuroda, S., Shimizu, K., Nakanishi, H. and Takai, Y. (1993) Comparison of kinetic properties between two mammalian ras p21 GDP/GTP exchange proteins, ras guanine nucleotide-releasing factor and smg GDP dissociation stimulation. *J Biol Chem*, **268**, 25542-25546.

- Ory, S., Zhou, M., Conrads, T.P., Veenstra, T.D. and Morrison, D.K. (2003) Protein phosphatase 2A positively regulates Ras signaling by dephosphorylating KSR1 and Raf-1 on critical 14-3-3 binding sites. *Curr Biol*, **13**, 1356-1364.
- Pages, G., Guerin, S., Grall, D., Bonino, F., Smith, A., Anjuere, F., Auberger, P. and Pouyssegur, J. (1999) Defective thymocyte maturation in p44 MAP kinase (Erk 1) knockout mice. *Science*, **286**, 1374-1377.
- Papin, C., Denouel, A., Calothy, G. and Eychene, A. (1996) Identification of signalling proteins interacting with B-Raf in the yeast two-hybrid system. *Oncogene*, **12**, 2213-2221.
- Papin, C., Denouel-Galy, A., Laugier, D., Calothy, G. and Eychene, A. (1998) Modulation of kinase activity and oncogenic properties by alternative splicing reveals a novel regulatory mechanism for B-Raf. *J Biol Chem*, **273**, 24939-24947.
- Park, S., Yeung, M.L., Beach, S., Shields, J.M. and Yeung, K.C. (2005) RKIP downregulates B-Raf kinase activity in melanoma cancer cells. *Oncogene*, **24**, 3535-3540.
- Payne, D.M., Rossomando, A.J., Martino, P., Erickson, A.K., Her, J.H., Shabanowitz, J., Hunt, D.F., Weber, M.J. and Sturgill, T.W. (1991) Identification of the regulatory phosphorylation sites in pp42/mitogen-activated protein kinase (MAP kinase). *Embo J*, **10**, 885-892.
- Pende, M., Fisher, T.L., Simpson, P.B., Russell, J.T., Blenis, J. and Gallo, V. (1997) Neurotransmitter- and growth factor-induced cAMP response element binding protein phosphorylation in glial cell progenitors: role of calcium ions, protein kinase C, and mitogen-activated protein kinase/ribosomal S6 kinase pathway. *J Neurosci*, **17**, 1291-1301.
- Perez-Roger, I., Solomon, D.L., Sewing, A. and Land, H. (1997) Myc activation of cyclin E/Cdk2 kinase involves induction of cyclin E gene transcription and inhibition of p27(Kip1) binding to newly formed complexes. *Oncogene*, **14**, 2373-2381.
- Peruzzi, F., Prisco, M., Dews, M., Salomoni, P., Grassilli, E., Romano, G., Calabretta, B. and Baserga, R. (1999) Multiple signaling pathways of the insulin-like growth factor 1 receptor in protection from apoptosis. *Mol Cell Biol*, **19**, 7203-7215.
- Petosa, C., Masters, S.C., Bankston, L.A., Pohl, J., Wang, B., Fu, H. and Liddington, R.C. (1998) 14-3-3zeta binds a phosphorylated Raf peptide and an unphosphorylated peptide via its conserved amphipathic groove. *J Biol Chem*, **273**, 16305-16310.

- Pham, C.D., Arlinghaus, R.B., Zheng, C.F., Guan, K.L. and Singh, B. (1995) Characterization of MEK1 phosphorylation by the v-Mos protein. *Oncogene*, **10**, 1683-1688.
- Polakis, P. and McCormick, F. (1993) Structural requirements for the interaction of p21ras with GAP, exchange factors, and its biological effector target. *J Biol Chem*, **268**, 9157-9160.
- Pollock, P.M., Harper, U.L., Hansen, K.S., Yudt, L.M., Stark, M., Robbins, C.M., Moses, T.Y., Hostetter, G., Wagner, U., Kakareka, J., Salem, G., Pohida, T., Heenan, P., Duray, P., Kallioniemi, O., Hayward, N.K., Trent, J.M. and Meltzer, P.S. (2003) High frequency of BRAF mutations in nevi. *Nat Genet*, **33**, 19-20.
- Polyak, K., Kato, J.Y., Solomon, M.J., Sherr, C.J., Massague, J., Roberts, J.M. and Koff, A. (1994) p27Kip1, a cyclin-Cdk inhibitor, links transforming growth factor-beta and contact inhibition to cell cycle arrest. *Genes Dev*, **8**, 9-22.
- Potenza, N., Vecchione, C., Notte, A., De Rienzo, A., Rosica, A., Bauer, L., Affuso, A., De Felice, M., Russo, T., Poulet, R., Cifelli, G., De Vita, G., Lembo, G. and Di Lauro, R. (2005) Replacement of K-Ras with H-Ras supports normal embryonic development despite inducing cardiovascular pathology in adult mice. *EMBO Rep*, **6**, 432-437.
- Price, M., Cruzalegui, F. and Treisman, R. (1996) The p38 and ERK MAP kinase pathways cooperate to activate Ternary Complex Factors and c-fos transcription in response to UV light. *EMBO J*, **15**, 6552-6563.
- Prisco, M., Romano, G., Peruzzi, F., Valentini, B. and Baserga, R. (1999) Insulin and IGF-I receptors signaling in protection from apoptosis. *Horm Metab Res*, **31**, 80-89.
- Pritchard, C.A., Bolin, L., Slattery, R., Murray, R. and McMahon, M. (1996) Post-natal lethality and neurological and gastrointestinal defects in mice with targeted disruption of the A-Raf protein kinase gene. *Curr Biol*, **6**, 614-617.
- Pritchard, C.A., Hayes, L., Wojnowski, L., Zimmer, A., Marais, R.M. and Norman, J.C. (2004) B-Raf acts via the ROCKII/LIMK/cofilin pathway to maintain actin stress fibers in fibroblasts. *Mol Cell Biol*, **24**, 5937-5952.
- Pritchard, C.A., Samuels, M.L., Bosch, E. and McMahon, M. (1995) Conditionally oncogenic forms of the A-Raf and B-Raf protein kinases display different biological and biochemical properties in NIH 3T3 cells. *Mol Cell Biol*, **15**, 6430-6442.
- Pulverer, B.J., Kyriakis, J.M., Avruch, J., Nikolakaki, E. and Woodgett, J.R. (1991) Phosphorylation of c-jun mediated by MAP kinases. *Nature*, **353**, 670-674.

- Qureshi, S.A., Joseph, C.K., Hendrickson, M., Song, J., Gupta, R., Bruder, J., Rapp, U. and Foster, D.A. (1993) A dominant negative Raf-1 mutant prevents v-Src-induced transformation. *Biochem Biophys Res Commun*, **192**, 969-975.
- Raingeaud, J., Whitmarsh, A.J., Barrett, T., Derijard, B. and Davis, R.J. (1996) MKK3- and MKK6-regulated gene expression is mediated by the p38 mitogen-activated protein kinase signal transduction pathway. *Mol Cell Biol*, **16**, 1247-1255.
- Rajagopalan, H., Bardelli, A., Lengauer, C., Kinzler, K.W., Vogelstein, B. and Velculescu, V.E. (2002) Tumorigenesis: RAF/RAS oncogenes and mismatch-repair status. *Nature*, **418**, 934.
- Rana, A., Gallo, K., Godowski, P., Hirai, S., Ohno, S., Zon, L., Kyriakis, J. and Avruch, J. (1996) The mixed lineage kinase SPRK phosphorylates and activates the stress-activated protein kinase activator, SEK-1. *J Biol Chem*, **271**, 19025-19028.
- Rapp, U.R., Cleveland, J.L., Fredrickson, T.N., Holmes, K.L., Morse, H.C., 3rd, Jansen, H.W., Patschinsky, T. and Bister, K. (1985) Rapid induction of hemopoietic neoplasms in newborn mice by a raf(mil)/myc recombinant murine retrovirus. *J Virol*, **55**, 23-33.
- Rapp, U.R., Goldsborough, M.D., Mark, G.E., Bonner, T.I., Groffen, J., Reynolds, F.H., Jr. and Stephenson, J.R. (1983) Structure and biological activity of v-raf, a unique oncogene transduced by a retrovirus. *Proc Natl Acad Sci U S A*, **80**, 4218-4222.
- Rapp, U.R., Rennefahrt, U. and Troppmair, J. (2004) Bcl-2 proteins: master switches at the intersection of death signaling and the survival control by Raf kinases. *Biochim Biophys Acta*, **1644**, 149-158.
- Ravi, R.K., Weber, E., McMahon, M., Williams, J.R., Baylin, S., Mal, A., Harter, M.L., Dillehay, L.E., Claudio, P.P., Giordano, A., Nelkin, B.D. and Mabry, M. (1998) Activated Raf-1 causes growth arrest in human small cell lung cancer cells. *J Clin Invest*, **101**, 153-159.
- Regan, C.P., Li, W., Boucher, D.M., Spatz, S., Su, M.S. and Kuida, K. (2002) Erk5 null mice display multiple extraembryonic vascular and embryonic cardiovascular defects. *Proc Natl Acad Sci U S A*, **99**, 9248-9253.
- Reiss, M., Jastreboff, M.M., Bertino, J.R. and Narayanan, R. (1986) DNA-mediated gene transfer into epidermal cells using electroporation. *Biochem Biophys Res Commun*, **137**, 244-249.

- Reusch, H.P., Zimmermann, S., Schaefer, M., Paul, M. and Moelling, K. (2001) Regulation of Raf by Akt controls growth and differentiation in vascular smooth muscle cells. *J Biol Chem*, **276**, 33630-33637.
- Reuter, C.W., Catling, A.D. and Weber, M.J. (1995) Immune complex kinase assays for mitogen-activated protein kinase and MEK. *Methods Enzymol*, **255**, 245-256.
- Reynolds, C.H., Nebreda, A.R., Gibb, G.M., Utton, M.A. and Anderton, B.H. (1997) Reactivating kinase/p38 phosphorylates tau protein in vitro. *J Neurochem*, **69**, 191-198.
- Rivera, V.M., Miranti, C.K., Misra, R.P., Ginty, D.D., Chen, R.H., Blenis, J. and Greenberg, M.E. (1993) A growth factor-induced kinase phosphorylates the serum response factor at a site that regulates its DNA-binding activity. *Mol Cell Biol*, **13**, 6260-6273.
- Rizos, H., Darmanian, A.P., Indsto, J.O., Shannon, J.A., Kefford, R.F. and Mann, G.J. (1999) Multiple abnormalities of the p16INK4a-pRb regulatory pathway in cultured melanoma cells. *Melanoma Res*, **9**, 10-19.
- Robertson, E., Bradley, A., Kuehn, M. and Evans, M. (1986) Germ-line transmission of genes introduced into cultured pluripotential cells by retroviral vector. *Nature*, **323**, 445-448.
- Rodriguez-Viciano, P., Sabatier, C. and McCormick, F. (2004) Signaling specificity by Ras family GTPases is determined by the full spectrum of effectors they regulate. *Mol Cell Biol*, **24**, 4943-4954.
- Rodriguez-Viciano, P., Warne, P.H., Dhand, R., Vanhaesebroeck, B., Gout, I., Fry, M.J., Waterfield, M.D. and Downward, J. (1994) Phosphatidylinositol-3-OH kinase as a direct target of Ras. *Nature*, **370**, 527-532.
- Rodriguez-Viciano, P., Warne, P.H., Vanhaesebroeck, B., Waterfield, M.D. and Downward, J. (1996) Activation of phosphoinositide 3-kinase by interaction with Ras and by point mutation. *Embo J*, **15**, 2442-2451.
- Rordorf-Nikolic, T., Van Horn, D.J., Chen, D., White, M.F. and Backer, J.M. (1995) Regulation of phosphatidylinositol 3'-kinase by tyrosyl phosphoproteins. Full activation requires occupancy of both SH2 domains in the 85-kDa regulatory subunit. *J Biol Chem*, **270**, 3662-3666.
- Rosario, M., Paterson, H.F. and Marshall, C.J. (1999) Activation of the Raf/MAP kinase cascade by the Ras-related protein TC21 is required for the TC21-mediated transformation of NIH 3T3 cells. *Embo J*, **18**, 1270-1279.

- Rouse, J., Cohen, P., Trigon, S., Morange, M., Alonso-Llamazares, A., Zamanillo, D., Hunt, T. and Nebreda, A.R. (1994) A novel kinase cascade triggered by stress and heat shock that stimulates MAPKAP kinase-2 and phosphorylation of the small heat shock proteins. *Cell*, **78**, 1027-1037.
- Roy, F., Laberge, G., Douziech, M., Ferland-McCollough, D. and Therrien, M. (2002) KSR is a scaffold required for activation of the ERK/MAPK module. *Genes Dev*, **16**, 427-438.
- Roy, S., Lane, A., Yan, J., McPherson, R. and Hancock, J.F. (1997) Activity of plasma membrane-recruited Raf-1 is regulated by Ras via the Raf zinc finger. *J Biol Chem*, **272**, 20139-20145.
- Roy, S., McPherson, R.A., Apolloni, A., Yan, J., Lane, A., Clyde-Smith, J. and Hancock, J.F. (1998) 14-3-3 facilitates Ras-dependent Raf-1 activation in vitro and in vivo. *Mol Cell Biol*, **18**, 3947-3955.
- Ruas, M. and Peters, G. (1998) The p16INK4a/CDKN2A tumor suppressor and its relatives. *Biochim Biophys Acta*, **1378**, F115-177.
- Saba-El-Leil, M.K., Vella, F.D., Vernay, B., Voisin, L., Chen, L., Labrecque, N., Ang, S.L. and Meloche, S. (2003) An essential function of the mitogen-activated protein kinase Erk2 in mouse trophoblast development. *EMBO Rep*, **4**, 964-968.
- Salmeron, A., Ahmad, T.B., Carlile, G.W., Pappin, D., Narsimhan, R.P. and Ley, S.C. (1996) Activation of MEK-1 and SEK-1 by Tpl-2 proto-oncoprotein, a novel MAP kinase kinase kinase. *Embo J*, **15**, 817-826.
- Salomoni, P., Wasik, M.A., Riedel, R.F., Reiss, K., Choi, J.K., Skorski, T. and Calabretta, B. (1998) Expression of constitutively active Raf-1 in the mitochondria restores antiapoptotic and leukemogenic potential of a transformation-deficient BCR/ABL mutant. *J Exp Med*, **187**, 1995-2007.
- Samuels, M.L., Weber, M.J., Bishop, J.M. and McMahon, M. (1993) Conditional transformation of cells and rapid activation of the mitogen-activated protein kinase cascade by an estradiol-dependent human raf-1 protein kinase. *Mol Cell Biol*, **13**, 6241-6252.
- Sanchez, I., Hughes, R.T., Mayer, B.J., Yee, K., Woodgett, J.R., Avruch, J., Kyriakis, J.M. and Zon, L.I. (1994) Role of SAPK/ERK kinase-1 in the stress-activated pathway regulating transcription factor c-Jun. *Nature*, **372**, 794-798.
- Sanghera, J.S., Peter, M., Nigg, E.A. and Pelech, S.L. (1992) Immunological characterization of avian MAP kinases: evidence for nuclear localization. *Mol Biol Cell*, **3**, 775-787.

- Sarbassov, D.D., Guertin, D.A., Ali, S.M. and Sabatini, D.M. (2005) Phosphorylation and regulation of Akt/PKB by the rictor-mTOR complex. *Science*, **307**, 1098-1101.
- Savill, J. and Fadok, V. (2000) Corpse clearance defines the meaning of cell death. *Nature*, **407**, 784-788.
- Scheffler, J.E., Waugh, D.S., Bekesi, E., Kiefer, S.E., LoSardo, J.E., Neri, A., Prinzo, K.M., Tsao, K.L., Wegrzynski, B., Emerson, S.D. and et al. (1994) Characterization of a 78-residue fragment of c-Raf-1 that comprises a minimal binding domain for the interaction with Ras-GTP. *J Biol Chem*, **269**, 22340-22346.
- Schmitz, I., Kirchhoff, S. and Krammer, P.H. (2000) Regulation of death receptor-mediated apoptosis pathways. *Int J Biochem Cell Biol*, **32**, 1123-1136.
- Schonwasser, D.C., Marais, R.M., Marshall, C.J. and Parker, P.J. (1998) Activation of the mitogen-activated protein kinase/extracellular signal-regulated kinase pathway by conventional, novel, and atypical protein kinase C isotypes. *Mol Cell Biol*, **18**, 790-798.
- Schulte, T.W., An, W.G. and Neckers, L.M. (1997) Geldanamycin-induced destabilization of Raf-1 involves the proteasome. *Biochem Biophys Res Commun*, **239**, 655-659.
- Schulte, T.W., Blagosklonny, M.V., Ingui, C. and Neckers, L. (1995) Disruption of the Raf-1-Hsp90 molecular complex results in destabilization of Raf-1 and loss of Raf-1-Ras association. *J Biol Chem*, **270**, 24585-24588.
- Schwenk, F., Baron, U. and Rajewsky, K. (1995) A cre-transgenic mouse strain for the ubiquitous deletion of loxP-flanked gene segments including deletion in germ cells. *Nucleic Acids Res*, **23**, 5080-5081.
- Seger, R., Ahn, N.G., Posada, J., Munar, E.S., Jensen, A.M., Cooper, J.A., Cobb, M.H. and Krebs, E.G. (1992) Purification and characterization of mitogen-activated protein kinase activator(s) from epidermal growth factor-stimulated A431 cells. *J Biol Chem*, **267**, 14373-14381.
- Sewing, A., Wiseman, B., Lloyd, A.C. and Land, H. (1997) High-intensity Raf signal causes cell cycle arrest mediated by p21Cip1. *Mol Cell Biol*, **17**, 5588-5597.
- Sharpless, N.E., Bardeesy, N., Lee, K.H., Carrasco, D., Castrillon, D.H., Aguirre, A.J., Wu, E.A., Horner, J.W. and DePinho, R.A. (2001) Loss of p16Ink4a with retention of p19Arf predisposes mice to tumorigenesis. *Nature*, **413**, 86-91.
- Shaulian, E. and Karin, M. (2002) AP-1 as a regulator of cell life and death. *Nat Cell Biol*, **4**, E131-136.

- Sherr, C.J. (1994) Growth factor-regulated G1 cyclins. *Stem Cells*, **12 Suppl 1**, 47-55; discussion 55-47.
- Sherr, C.J. and Roberts, J.M. (1995) Inhibitors of mammalian G1 cyclin-dependent kinases. *Genes Dev*, **9**, 1149-1163.
- Sherr, C.J. and Roberts, J.M. (1999) CDK inhibitors: positive and negative regulators of G1-phase progression. *Genes Dev*, **13**, 1501-1512.
- Sherr, C.J. and Roberts, J.M. (2004) Living with or without cyclins and cyclin-dependent kinases. *Genes Dev*, **18**, 2699-2711.
- Sidovar, M.F., Kozlowski, P., Lee, J.W., Collins, M.A., He, Y. and Graves, L.M. (2000) Phosphorylation of serine 43 is not required for inhibition of c-Raf kinase by the cAMP-dependent protein kinase. *J Biol Chem*, **275**, 28688-28694.
- Sieburth, D.S., Sun, Q. and Han, M. (1998) SUR-8, a conserved Ras-binding protein with leucine-rich repeats, positively regulates Ras-mediated signaling in *C. elegans*. *Cell*, **94**, 119-130.
- Silverstein, A.M., Grammatikakis, N., Cochran, B.H., Chinkers, M. and Pratt, W.B. (1998) p50(cdc37) binds directly to the catalytic domain of Raf as well as to a site on hsp90 that is topologically adjacent to the tetratricopeptide repeat binding site. *J Biol Chem*, **273**, 20090-20095.
- Sluss, H.K., Barrett, T., Derijard, B. and Davis, R.J. (1994) Signal transduction by tumor necrosis factor mediated by JNK protein kinases. *Mol Cell Biol*, **14**, 8376-8384.
- Smeal, T., Binetruy, B., Mercola, D.A., Birrer, M. and Karin, M. (1991) Oncogenic and transcriptional cooperation with Ha-Ras requires phosphorylation of c-Jun on serines 63 and 73. *Nature*, **354**, 494-496.
- Smith, A.G., Heath, J.K., Donaldson, D.D., Wong, G.G., Moreau, J., Stahl, M. and Rogers, D. (1988) Inhibition of pluripotential embryonic stem cell differentiation by purified polypeptides. *Nature*, **336**, 688-690.
- Smith, A.J., De Sousa, M.A., Kwabi-Addo, B., Heppell-Parton, A., Impey, H. and Rabbitts, P. (1995) A site-directed chromosomal translocation induced in embryonic stem cells by Cre-loxP recombination. *Nat Genet*, **9**, 376-385.
- Sohn, S.J., Sarvis, B.K., Cado, D. and Winoto, A. (2002) ERK5 MAPK regulates embryonic angiogenesis and acts as a hypoxia-sensitive repressor of vascular endothelial growth factor expression. *J Biol Chem*, **277**, 43344-43351.

- Soloaga, A., Thomson, S., Wiggin, G.R., Pampersaud, N., Dyson, M.H., Hazzalin, C.A., Mahadevan, L.C. and Arther, J.S. (2003) MSK2 and MSK1 mediate the mitogen- and stress-induced phosphorylation of histone H3 and HMG-14. *Embo J*, **22**, 2788-2797.
- Stancato, L.F., Chow, Y.H., Hutchison, K.A., Perdew, G.H., Jove, R. and Pratt, W.B. (1993) Raf exists in a native heterocomplex with hsp90 and p50 that can be reconstituted in a cell-free system. *J Biol Chem*, **268**, 21711-21716.
- Stewart, S., Sundaram, M., Zhang, Y., Lee, J., Han, M. and Guan, K.L. (1999) Kinase suppressor of Ras forms a multiprotein signaling complex and modulates MEK localization. *Mol Cell Biol*, **19**, 5523-5534.
- Stokoe, D., Macdonald, S.G., Cadwallader, K., Symons, M. and Hancock, J.F. (1994) Activation of Raf as a result of recruitment to the plasma membrane. *Science*, **264**, 1463-1467.
- Stokoe, D. and McCormick, F. (1997) Activation of c-Raf-1 by Ras and Src through different mechanisms: activation in vivo and in vitro. *Embo J*, **16**, 2384-2396.
- Stokoe, D., Stephens, L.R., Copeland, T., Gaffney, P.R., Reese, C.B., Painter, G.F., Holmes, A.B., McCormick, F. and Hawkins, P.T. (1997) Dual role of phosphatidylinositol-3,4,5-trisphosphate in the activation of protein kinase B. *Science*, **277**, 567-570.
- Storm, S.M., Cleveland, J.L. and Rapp, U.R. (1990) Expression of raf family proto-oncogenes in normal mouse tissues. *Oncogene*, **5**, 345-351.
- Sturgill, T.W., Ray, L.B., Erikson, E. and Maller, J.L. (1988) Insulin-stimulated MAP-2 kinase phosphorylates and activates ribosomal protein S6 kinase II. *Nature*, **334**, 715-718.
- Suen, K.L., Bustelo, X.R. and Barbacid, M. (1995) Lack of evidence for the activation of the Ras/Raf mitogenic pathway by 14-3-3 proteins in mammalian cells. *Oncogene*, **11**, 825-831.
- Sun, H., King, A.J., Diaz, H.B. and Marshall, M.S. (2000) Regulation of the protein kinase Raf-1 by oncogenic Ras through phosphatidylinositol 3-kinase, Cdc42/Rac and Pak. *Curr Biol*, **10**, 281-284.
- Sun, W., Kesavan, K., Schaefer, B.C., Garrington, T.P., Ware, M., Johnson, N.L., Gelfand, E.W. and Johnson, G.L. (2001) MEKK2 associates with the adapter protein Lad/RIBP and regulates the MEK5-BMK1/ERK5 pathway. *J Biol Chem*, **276**, 5093-5100.

- Sutrave, P., Bonner, T.I., Rapp, U.R., Jansen, H.W., Patschinsky, T. and Bister, K. (1984) Nucleotide sequence of avian retroviral oncogene v-mil: homologue of murine retroviral oncogene v-raf. *Nature*, **309**, 85-88.
- Szewczyk, N.J., Peterson, B.K. and Jacobson, L.A. (2002) Activation of Ras and the mitogen-activated protein kinase pathway promotes protein degradation in muscle cells of *Caenorhabditis elegans*. *Mol Cell Biol*, **22**, 4181-4188.
- Takayama, S. and Reed, J.C. (2001) Molecular chaperone targeting and regulation by BAG family proteins. *Nat Cell Biol*, **3**, E237-241.
- Takayama, S., Sato, T., Krajewski, S., Kochel, K., Irie, S., Millan, J.A. and Reed, J.C. (1995) Cloning and functional analysis of BAG-1: a novel Bcl-2-binding protein with anti-cell death activity. *Cell*, **80**, 279-284.
- Takishima, K., Griswold-Prenner, I., Ingebritsen, T. and Rosner, M.R. (1991) Epidermal growth factor (EGF) receptor T669 peptide kinase from 3T3-L1 cells is an EGF-stimulated "MAP" kinase. *Proc Natl Acad Sci U S A*, **88**, 2520-2524.
- Tan, Y., Ruan, H., Demeter, M.R. and Comb, M.J. (1999) p90(RSK) blocks bad-mediated cell death via a protein kinase C-dependent pathway. *J Biol Chem*, **274**, 34859-34867.
- Terasawa, K., Okazaki, K. and Nishida, E. (2003) Regulation of c-Fos and Fra-1 by the MEK5-ERK5 pathway. *Genes Cells*, **8**, 263-273.
- Thomas, K.R. and Capecchi, M.R. (1987) Site-directed mutagenesis by gene targeting in mouse embryo-derived stem cells. *Cell*, **51**, 503-512.
- Thomas, N.E., Alexander, A., Edmiston, S.N., Parrish, E., Millikan, R.C., Berwick, M., Groben, P., Ollila, D.W., Mattingly, D. and Conway, K. (2004) Tandem BRAF mutations in primary invasive melanomas. *J Invest Dermatol*, **122**, 1245-1250.
- Thomas, S.M., DeMarco, M., D'Arcangelo, G., Halegoua, S. and Brugge, J.S. (1992) Ras is essential for nerve growth factor- and phorbol ester-induced tyrosine phosphorylation of MAP kinases. *Cell*, **68**, 1031-1040.
- Thorson, J.A., Yu, L.W., Hsu, A.L., Shih, N.Y., Graves, P.R., Tanner, J.W., Allen, P.M., Piwnicka-Worms, H. and Shaw, A.S. (1998) 14-3-3 proteins are required for maintenance of Raf-1 phosphorylation and kinase activity. *Mol Cell Biol*, **18**, 5229-5238.
- Tobiome, K., Matsuzawa, A., Takahashi, T., Nishitoh, H., Morita, K., Takeda, K., Minowa, O., Miyazono, K., Noda, T. and Ichijo, H. (2001) ASK1 is required for sustained activations of JNK/p38 MAP kinases and apoptosis. *EMBO Rep*, **2**, 222-228.

- Townsend, P.A., Stephanou, A., Packham, G. and Latchman, D.S. (2005) BAG-1: a multi-functional pro-survival molecule. *Int J Biochem Cell Biol*, **37**, 251-259.
- Traenckner, E.B., Pahl, H.L., Henkel, T., Schmidt, K.N., Wilk, S. and Baeuerle, P.A. (1995) Phosphorylation of human I kappa B-alpha on serines 32 and 36 controls I kappa B-alpha proteolysis and NF-kappa B activation in response to diverse stimuli. *Embo J*, **14**, 2876-2883.
- Trakul, N. and Rosner, M.R. (2005) Modulation of the MAP kinase signaling cascade by Raf kinase inhibitory protein. *Cell Res*, **15**, 19-23.
- Tran, N.H. and Frost, J.A. (2003) Phosphorylation of Raf-1 by p21-activated kinase 1 and Src regulates Raf-1 autoinhibition. *J Biol Chem*, **278**, 11221-11226.
- Tran, N.H., Wu, X. and Frost, J.A. (2005) B-Raf and Raf-1 are regulated by distinct autoregulatory mechanisms. *J Biol Chem*, **280**, 16244-16253.
- Traverse, S., Cohen, P., Paterson, H., Marshall, C., Rapp, U. and Grand, R.J. (1993) Specific association of activated MAP kinase kinase kinase (Raf) with the plasma membranes of ras-transformed retinal cells. *Oncogene*, **8**, 3175-3181.
- Trotter, M.J., Tang, L. and Tron, V.A. (1997) Overexpression of the cyclin-dependent kinase inhibitor p21(WAF1/CIP1) in human cutaneous malignant melanoma. *J Cutan Pathol*, **24**, 265-271.
- Tuveson, D.A., Shaw, A.T., Willis, N.A., Silver, D.P., Jackson, E.L., Chang, S., Mercer, K.L., Grochow, R., Hock, H., Crowley, D., Hingorani, S.R., Zaks, T., King, C., Jacobetz, M.A., Wang, L., Bronson, R.T., Orkin, S.H., DePinho, R.A. and Jacks, T. (2004) Endogenous oncogenic K-ras(G12D) stimulates proliferation and widespread neoplastic and developmental defects. *Cancer Cell*, **5**, 375-387.
- Umanoff, H., Edelman, W., Pellicer, A. and Kucherlapati, R. (1995) The murine N-ras gene is not essential for growth and development. *Proc Natl Acad Sci U S A*, **92**, 1709-1713.
- Urano, T., Emkey, R. and Feig, L.A. (1996) Ral-GTPases mediate a distinct downstream signaling pathway from Ras that facilitates cellular transformation. *Embo J*, **15**, 810-816.
- Van Aelst, L., Barr, M., Marcus, S., Polverino, A. and Wigler, M. (1993) Complex formation between RAS and RAF and other protein kinases. *Proc Natl Acad Sci U S A*, **90**, 6213-6217.
- Van Antwerp, D.J., Martin, S.J., Kafri, T., Green, D.R. and Verma, I.M. (1996) Suppression of TNF-alpha-induced apoptosis by NF-kappaB. *Science*, **274**, 787-789.

- van der Geer, P. and Pawson, T. (1995) The PTB domain: a new protein module implicated in signal transduction. *Trends Biochem Sci*, **20**, 277-280.
- Van Deursen, J., Fornerod, M., Van Rees, B. and Grosveld, G. (1995) Cre-mediated site-specific translocation between nonhomologous mouse chromosomes. *Proc Natl Acad Sci U S A*, **92**, 7376-7380.
- Voice, J.K., Klemke, R.L., Le, A. and Jackson, J.H. (1999) Four human ras homologs differ in their abilities to activate Raf-1, induce transformation, and stimulate cell motility. *J Biol Chem*, **274**, 17164-17170.
- Vojtek, A.B., Hollenberg, S.M. and Cooper, J.A. (1993) Mammalian Ras interacts directly with the serine/threonine kinase Raf. *Cell*, **74**, 205-214.
- von Gise, A., Lorenz, P., Wellbrock, C., Hemmings, B., Berberich-Siebelt, F., Rapp, U.R. and Troppmair, J. (2001) Apoptosis suppression by Raf-1 and MEK1 requires MEK- and phosphatidylinositol 3-kinase-dependent signals. *Mol Cell Biol*, **21**, 2324-2336.
- Vossler, M.R., Yao, H., York, R.D., Pan, M.G., Rim, C.S. and Stork, P.J. (1997) cAMP activates MAP kinase and Elk-1 through a B-Raf- and Rap1-dependent pathway. *Cell*, **89**, 73-82.
- Wan, P.T., Garnett, M.J., Roe, S.M., Lee, S., Niculescu-Duvaz, D., Good, V.M., Jones, C.M., Marshall, C.J., Springer, C.J., Barford, D. and Marais, R. (2004) Mechanism of activation of the RAF-ERK signaling pathway by oncogenic mutations of B-RAF. *Cell*, **116**, 855-867.
- Wang, C., Deng, L., Hong, M., Akkaraju, G.R., Inoue, J. and Chen, Z.J. (2001) TAK1 is a ubiquitin-dependent kinase of MKK and IKK. *Nature*, **412**, 346-351.
- Wang, C.Y., Mayo, M.W., Korneluk, R.G., Goeddel, D.V. and Baldwin, A.S., Jr. (1998b) NF-kappaB antiapoptosis: induction of TRAF1 and TRAF2 and c-IAP1 and c-IAP2 to suppress caspase-8 activation. *Science*, **281**, 1680-1683.
- Wang, H.G., Miyashita, T., Takayama, S., Sato, T., Torigoe, T., Krajewski, S., Tanaka, S., Hovey, L., 3rd, Troppmair, J., Rapp, U.R. and et al. (1994) Apoptosis regulation by interaction of Bcl-2 protein and Raf-1 kinase. *Oncogene*, **9**, 2751-2756.
- Wang, H.G., Rapp, U.R. and Reed, J.C. (1996a) Bcl-2 targets the protein kinase Raf-1 to mitochondria. *Cell*, **87**, 629-638.
- Wang, H.G., Takayama, S., Rapp, U.R. and Reed, J.C. (1996b) Bcl-2 interacting protein, BAG-1, binds to and activates the kinase Raf-1. *Proc Natl Acad Sci U S A*, **93**, 7063-7068.

- Wang, L., Cunningham, J.M., Winters, J.L., Guenther, J.C., French, A.J., Boardman, L.A., Burgart, L.J., McDonnell, S.K., Schaid, D.J. and Thibodeau, S.N. (2003) BRAF mutations in colon cancer are not likely attributable to defective DNA mismatch repair. *Cancer Res*, **63**, 5209-5212.
- Wang, S., Ghosh, R.N. and Chellappan, S.P. (1998a) Raf-1 physically interacts with Rb and regulates its function: a link between mitogenic signaling and cell cycle regulation. *Mol Cell Biol*, **18**, 7487-7498.
- Warne, P.H., Viciano, P.R. and Downward, J. (1993) Direct interaction of Ras and the amino-terminal region of Raf-1 in vitro. *Nature*, **364**, 352-355.
- Wartmann, M. and Davis, R.J. (1994) The native structure of the activated Raf protein kinase is a membrane-bound multi-subunit complex. *J Biol Chem*, **269**, 6695-6701.
- Waskiewicz, A.J., Flynn, A., Proud, C.G. and Cooper, J.A. (1997) Mitogen-activated protein kinases activate the serine/threonine kinases Mnk1 and Mnk2. *Embo J*, **16**, 1909-1920.
- Weber, C.K., Slupsky, J.R., Kalmes, H.A. and Rapp, U.R. (2001) Active Ras induces heterodimerization of cRaf and B Raf. *Cancer Res*, **61**, 3595-3598.
- Wei, M.C., Zong, W.X., Cheng, E.H., Lindsten, T., Panoutsakopoulou, V., Ross, A.J., Roth, K.A., MacGregor, G.R., Thompson, C.B. and Korsmeyer, S.J. (2001) Proapoptotic BAX and BAK: a requisite gateway to mitochondrial dysfunction and death. *Science*, **292**, 727-730.
- Weiwad, M., Kullertz, G., Schutkowski, M. and Fischer, G. (2000) Evidence that the substrate backbone conformation is critical to phosphorylation by p42 MAP kinase. *FEBS Lett*, **478**, 39-42.
- Wellbrock, C., Ogilvie, L., Hedley, D., Karasarides, M., Martin, J., Niculescu-Duvaz, D., Springer, C.J. and Marais, R. (2004) V599EB-RAF is an oncogene in melanocytes. *Cancer Res*, **64**, 2338-2342.
- Weston, C.R., Balmanno, K., Chalmers, C., Hadfield, K., Molton, S.A., Ley, R., Wagner, E.F. and Cook, S.J. (2003) Activation of ERK1/2 by deltaRaf-1:ER\* represses Bim expression independently of the JNK or PI3K pathways. *Oncogene*, **22**, 1281-1293.
- Whitmarsh, A.J. and Davis, R.J. (1996) Transcription factor AP-1 regulation by mitogen-activated protein kinase signal transduction pathways. *J Mol Med*, **74**, 589-607.
- Whitmarsh, A.J., Yang, S.H., Su, M.S., Sharrocks, A.D. and Davis, R.J. (1997) Role of p38 and JNK mitogen-activated protein kinases in the activation of ternary complex factors. *Mol Cell Biol*, **17**, 2360-2371.

- Wiggin, G.R., Soloaga, A., Foster, J.M., Murray-Tait, V., Cohen, P. and Arthur, J.S. (2002) MSK1 and MSK2 are required for the mitogen- and stress-induced phosphorylation of CREB and ATF1 in fibroblasts. *Mol Cell Biol*, **22**, 2871-2881.
- Williams, N.G., Roberts, T.M. and Li, P. (1992) Both p21ras and pp60v-src are required, but neither alone is sufficient, to activate the Raf-1 kinase. *Proc Natl Acad Sci U S A*, **89**, 2922-2926.
- Wojnowski, L., Stancato, L.F., Zimmer, A.M., Hahn, H., Beck, T.W., Larner, A.C., Rapp, U.R. and Zimmer, A. (1998) Craf-1 protein kinase is essential for mouse development. *Mech Dev*, **76**, 141-149.
- Wojnowski, L., Zimmer, A.M., Beck, T.W., Hahn, H., Bernal, R., Rapp, U.R. and Zimmer, A. (1997) Endothelial apoptosis in Braf-deficient mice. *Nat Genet*, **16**, 293-297.
- Wolthuis, R.M., de Ruiter, N.D., Cool, R.H. and Bos, J.L. (1997) Stimulation of gene induction and cell growth by the Ras effector Rlf. *Embo J*, **16**, 6748-6761.
- Wolthuis, R.M., Zwartkruis, F., Moen, T.C. and Bos, J.L. (1998) Ras-dependent activation of the small GTPase Ral. *Curr Biol*, **8**, 471-474.
- Wood, K.W., Sarnecki, C., Roberts, T.M. and Blenis, J. (1992) ras mediates nerve growth factor receptor modulation of three signal-transducing protein kinases: MAP kinase, Raf-1, and RSK. *Cell*, **68**, 1041-1050.
- Woods, D., Parry, D., Cherwinski, H., Bosch, E., Lees, E. and McMahon, M. (1997) Raf-induced proliferation or cell cycle arrest is determined by the level of Raf activity with arrest mediated by p21Cip1. *Mol Cell Biol*, **17**, 5598-5611.
- Wu, J., Dent, P., Jelinek, T., Wolfman, A., Weber, M.J. and Sturgill, T.W. (1993a) Inhibition of the EGF-activated MAP kinase signaling pathway by adenosine 3',5'-monophosphate. *Science*, **262**, 1065-1069.
- Wu, J., Harrison, J.K., Dent, P., Lynch, K.R., Weber, M.J. and Sturgill, T.W. (1993b) Identification and characterization of a new mammalian mitogen-activated protein kinase kinase, MKK2. *Mol Cell Biol*, **13**, 4539-4548.
- Xia, Z., Dickens, M., Raingeaud, J., Davis, R.J. and Greenberg, M.E. (1995) Opposing effects of ERK and JNK-p38 MAP kinases on apoptosis. *Science*, **270**, 1326-1331.
- Xing, J., Ginty, D.D. and Greenberg, M.E. (1996) Coupling of the RAS-MAPK pathway to gene activation by RSK2, a growth factor-regulated CREB kinase. *Science*, **273**, 959-963.
- Xing, J., Kornhauser, J.M., Xia, Z., Thiele, E.A. and Greenberg, M.E. (1998) Nerve growth factor activates extracellular signal-regulated kinase and p38 mitogen-activated

- protein kinase pathways to stimulate CREB serine 133 phosphorylation. *Mol Cell Biol*, **18**, 1946-1955.
- Yamaguchi, O., Watanabe, T., Nishida, K., Kashiwase, K., Higuchi, Y., Takeda, T., Hikoso, S., Hirotsu, S., Asahi, M., Taniike, M., Nakai, A., Tsujimoto, I., Matsumura, Y., Miyazaki, J., Chien, K.R., Matsuzawa, A., Sadamitsu, C., Ichijo, H., Baccarini, M., Hori, M. and Otsu, K. (2004) Cardiac-specific disruption of the c-raf-1 gene induces cardiac dysfunction and apoptosis. *J Clin Invest*, **114**, 937-943.
- Yamamori, B., Kuroda, S., Shimizu, K., Fukui, K., Ohtsuka, T. and Takai, Y. (1995) Purification of a Ras-dependent mitogen-activated protein kinase kinase kinase from bovine brain cytosol and its identification as a complex of B-Raf and 14-3-3 proteins. *J Biol Chem*, **270**, 11723-11726.
- Yan, M., Dai, T., Deak, J.C., Kyriakis, J.M., Zon, L.I., Woodgett, J.R. and Templeton, D.J. (1994) Activation of stress-activated protein kinase by MEKK1 phosphorylation of its activator SEK1. *Nature*, **372**, 798-800.
- Yan, M. and Templeton, D.J. (1994) Identification of 2 serine residues of MEK-1 that are differentially phosphorylated during activation by raf and MEK kinase. *J Biol Chem*, **269**, 19067-19073.
- Yang, J., Liu, X., Bhalla, K., Kim, C.N., Ibrado, A.M., Cai, J., Peng, T.I., Jones, D.P. and Wang, X. (1997) Prevention of apoptosis by Bcl-2: release of cytochrome c from mitochondria blocked. *Science*, **275**, 1129-1132.
- Yeung, K., Seitz, T., Li, S., Janosch, P., McFerran, B., Kaiser, C., Fee, F., Katsanakis, K.D., Rose, D.W., Mischak, H., Sedivy, J.M. and Kolch, W. (1999) Suppression of Raf-1 kinase activity and MAP kinase signalling by RKIP. *Nature*, **401**, 173-177.
- Yeung, K., Janosch, P., McFerran, B., Rose, D.W., Mischak, H., Sedivy, J.M. and Kolch, W. (2000) Mechanism of suppression of the Raf/MEK/extracellular signal-regulated kinase pathway by the raf kinase inhibitor protein. *Mol Cell Biol*, **20**, 3079-3085.
- Yin, X.M., Wang, K., Gross, A., Zhao, Y., Zinkel, S., Klocke, B., Roth, K.A. and Korsmeyer, S.J. (1999) Bid-deficient mice are resistant to Fas-induced hepatocellular apoptosis. *Nature*, **400**, 886-891.
- Yip-Schneider, M.T., Miao, W., Lin, A., Barnard, D.S., Tzivion, G. and Marshall, M.S. (2000) Regulation of the Raf-1 kinase domain by phosphorylation and 14-3-3 association. *Biochem J*, **351**, 151-159.

- York, R.D., Yao, H., Dillon, T., Ellig, C.L., Eckert, S.P., McCleskey, E.W. and Stork, P.J. (1998) Rap1 mediates sustained MAP kinase activation induced by nerve growth factor. *Nature*, **392**, 622-626.
- Yuen, S.T., Davies, H., Chan, T.L., Ho, J.W., Bignell, G.R., Cox, C., Stephens, P., Edkins, S., Tsui, W.W., Chan, A.S., Futreal, P.A., Stratton, M.R., Wooster, R. and Leung, S.Y. (2002) Similarity of the phenotypic patterns associated with BRAF and KRAS mutations in colorectal neoplasia. *Cancer Res*, **62**, 6451-6455.
- Yuryev, A., Ono, M., Goff, S.A., Macaluso, F. and Wennogle, L.P. (2000) Isoform-specific localization of A-RAF in mitochondria. *Mol Cell Biol*, **20**, 4870-4878.
- Zandi, E., Chen, Y. and Karin, M. (1998) Direct phosphorylation of I $\kappa$ B by IKK $\alpha$  and IKK $\beta$ : discrimination between free and NF- $\kappa$ B-bound substrate. *Science*, **281**, 1360-1363.
- Zha, J., Harada, H., Yang, E., Jockel, J. and Korsmeyer, S.J. (1996) Serine phosphorylation of death agonist BAD in response to survival factor results in binding to 14-3-3 not BCL-X(L). *Cell*, **87**, 619-628.
- Zhang, B.H. and Guan, K.L. (2000) Activation of B-Raf kinase requires phosphorylation of the conserved residues Thr598 and Ser601. *Embo J*, **19**, 5429-5439.
- Zhang, B.H., Tang, E.D., Zhu, T., Greenberg, M.E., Vojtek, A.B. and Guan, K.L. (2001) Serum- and glucocorticoid-inducible kinase SGK phosphorylates and negatively regulates B-Raf. *J Biol Chem*, **276**, 31620-31626.
- Zhang, H., Wu, W., Du, Y., Santos, S.J., Conrad, S.E., Watson, J.T., Grammatikakis, N. and Gallo, K.A. (2004) Hsp90/p50cdc37 is required for mixed-lineage kinase (MLK) 3 signaling. *J Biol Chem*, **279**, 19457-19463.
- Zhang, X.F., Settleman, J., Kyriakis, J.M., Takeuchi-Suzuki, E., Elledge, S.J., Marshall, M.S., Bruder, J.T., Rapp, U.R. and Avruch, J. (1993) Normal and oncogenic p21ras proteins bind to the amino-terminal regulatory domain of c-Raf-1. *Nature*, **364**, 308-313.
- Zheng, C.F. and Guan, K.L. (1993) Cloning and characterization of two distinct human extracellular signal-regulated kinase activator kinases, MEK1 and MEK2. *J Biol Chem*, **268**, 11435-11439.
- Zheng, C.F. and Guan, K.L. (1994) Activation of MEK family kinases requires phosphorylation of two conserved Ser/Thr residues. *Embo J*, **13**, 1123-1131.
- Zhong, J., Troppmair, J. and Rapp, U.R. (2001) Independent control of cell survival by Raf-1 and Bcl-2 at the mitochondria. *Oncogene*, **20**, 4807-4816.

- 
- Zhou, G., Bao, Z.Q. and Dixon, J.E. (1995) Components of a new human protein kinase signal transduction pathway. *J Biol Chem*, **270**, 12665-12669.
- Zimmermann, S. and Moelling, K. (1999) Phosphorylation and regulation of Raf by Akt (protein kinase B). *Science*, **286**, 1741-1744.
- Zou, H., Li, Y., Liu, X. and Wang, X. (1999) An APAF-1.cytochrome c multimeric complex is a functional apoptosome that activates procaspase-9. *J Biol Chem*, **274**, 11549-11556.
- Zuo, L., Weger, J., Yang, Q., Goldstein, A.M., Tucker, M.A., Walker, G.J., Hayward, N. and Dracopoli, N.C. (1996) Germline mutations in the p16INK4a binding domain of CDK4 in familial melanoma. *Nat Genet*, **12**, 97-99.

## APPENDIX

***B-Raf amino acid sequence***

When the B-Raf sequence was originally deposited onto the NCBI web site a codon (encoding in the region containing amino acids 31 and 32) was missing. The correct sequence is therefore one amino acid longer, with all amino acids after amino acid 33 being displaced by one position. The amino acid numbers cited in the majority of the published literature refer to the original sequence, whereas those used in this project correspond to the correct amino acid sequence.

**Figure A.1** Analysis of the proliferation in *B-raf*<sup>+/+</sup> and *B-raf*<sup>Lox-D594A/Lox-D594A</sup> primary MEFs. DNA synthesis analysis was carried out via BrdU staining. Cells were left untreated or stimulated with 10 % serum for 16 hours. Graph represents pooled data for BrdU positive *B-raf*<sup>+/+</sup> MEFs compared to BrdU positive *B-raf*<sup>Lox-D594A/Lox-D594A</sup> MEFs. Standard error bars are shown. Data obtained from C. Pritchard.

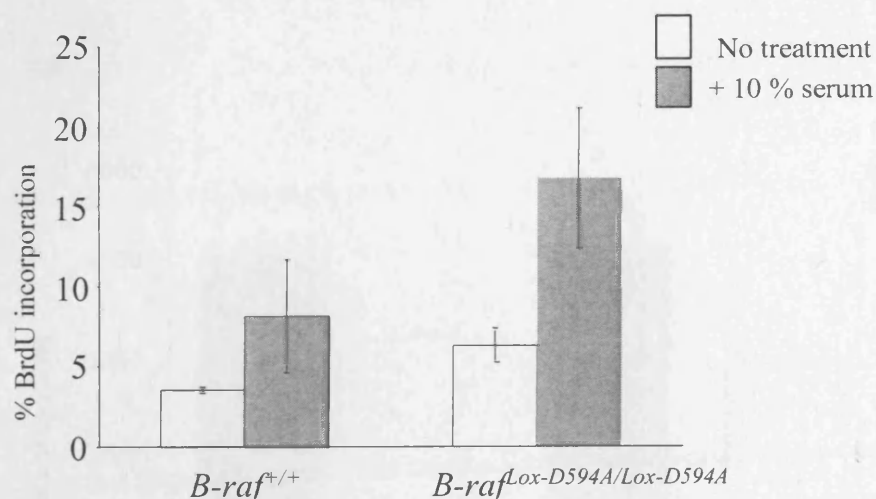


**Figure A.2** Immunoprecipitation Raf kinase assays of *B-raf*<sup>Lox-D594A/Lox-D594A</sup> MEFs. Proteins were immunoprecipitated from *B-raf*<sup>Lox-D594A/Lox-D594A</sup> and *B-raf*<sup>+/+</sup> MEF extracts that had previously been stimulated with 0.5 % or 10 % serum, and this was followed by a kinase assay with MEK1, ERK1 and MBP as substrates. **(A)** Immunoprecipitation of B-Raf. **(B)** Immunoprecipitation of C-Raf. Assays were carried out by R. Marais's laboratory, Institute of Cancer, London. Standard error bars are shown. For detailed methodology refer to Marais *et al.*, 1997).

